DECRETION

LARAMIDE CORDILLERAN TECTONICS IN THE TUCSON REGION

by

Stanley B. Keith

and

Jan C. Wilt

ARIZONA GEOLOGICAL SOCIETY

1983 SPRING FIELD TRIP

April 16-17, 1983

[Section 1]

Road Log

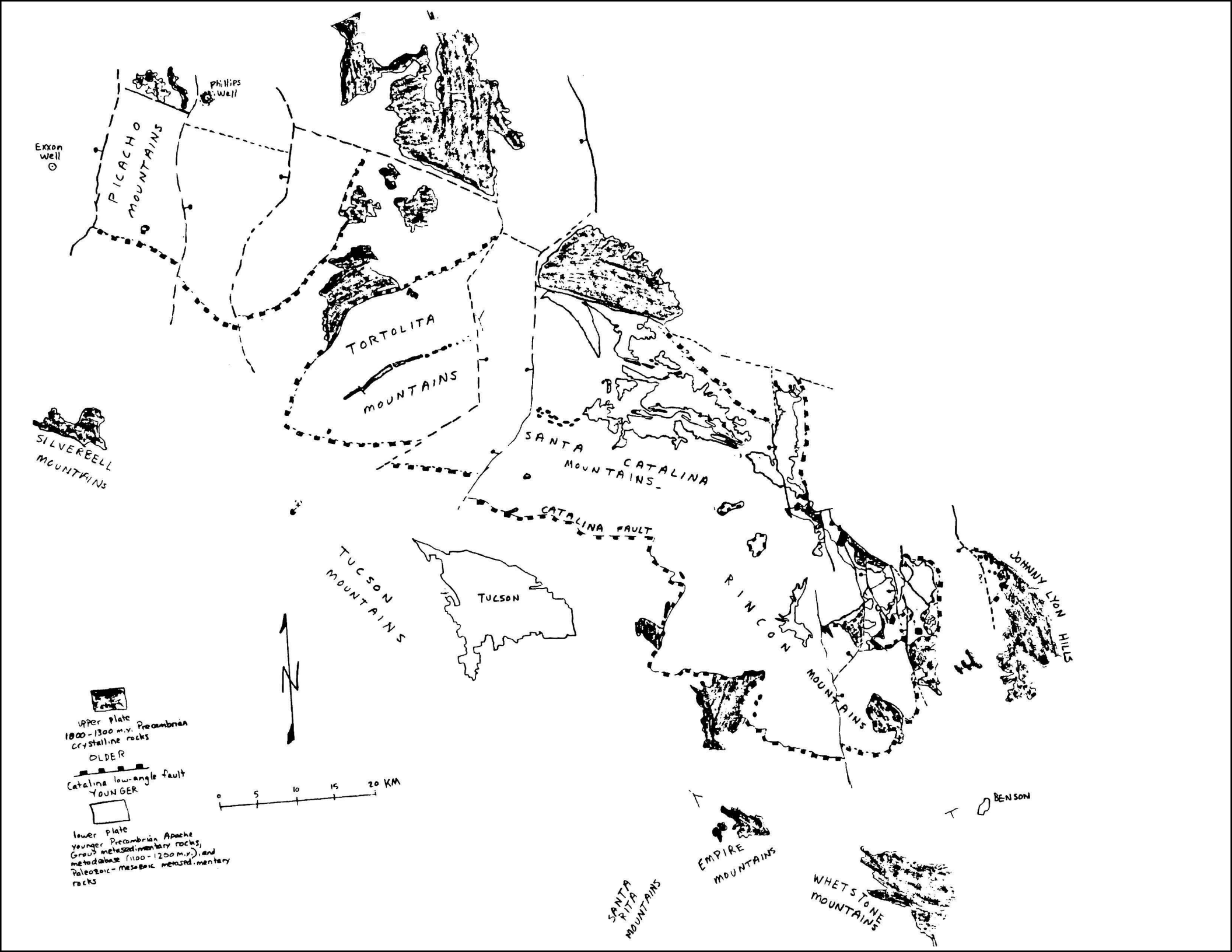
Phillips Well
Exxon well
PICACHO MOUNTAINS
TORTOLITA MOUNTAINS
SILVERBELL MOUNTAINS
SANTA CATALINA MOUNTAINS
CATALINA FAULT
TUCSON MOUNTAINS
TUCSON
RINCON MOUNTAINS
JOHNNY LYON HILLS
BENSON
EMPIRE MOUNTAINS
SANTA RITA MOUNTAINS
WHETSTONE MOUNTAINS
N
0 5 10 15 20 KM
Upper Plate
1800-1300 m.y. Precambrian crystalline rocks
OLDER
Catalina low-angle fault
YOUNGER
lower Plate
younger Precambrian Apache Group metasedimentary rocks, metadiabase (1100-1200 m.y.), and Paleozoic-mesozoic metasedimentary rocks

Keith & Wilt, 1978, Santa Rita part of Day 2 road log:
New Mexico Geol. Soc. Guidebook, Land of Cochise.

entrenched flood plain. Compare these soils with the older Pleistocene soils which contain bright-red argillic (B) horizons and white petrocalcic (Cca) or "caliche" horizons, which cap the early Pleistocene surface throughout the Sonoita area. The flood-plain soils are possibly no older than 10,000 years (Holocene). Some have assigned a Sangamon interglacial age to the red paleosol (Melton, 1965a, b).

2.7

94.5 Pavement begins—yea!

0.3

94.8 Low roadcuts contain a thick petrocalcic (Cca) horizon; here the red argillic horizon has been stripped.

0.6

95.4 Milepost 25. Low roadcuts ahead contain excellent examples of the red argillic (B) horizon.

0.7

96.1 Mount Fagin in the northern Santa Rita Mountains is at 12:00. Empire Mountains are at 12:30 in middle distance, backed by Rincon and Santa Catalina massif in far distance.

1.5

97.6 Dirt road to Elgin on right. Whetstone Mountains from 1:00 to 2:00; Mustang Mountains from 2:00 to 3:00, with Mount Bruce at 2:30 and Mustang Peak at 3:00. The Mustang Mountains are separated from the central Whetstone Mountains on the north by the Mescal Spring fault and from the low valley south of the Mustangs by an east-west striking fault along the Babocomari River. Rocks within the Mustang Mountain block are mostly upper Paleozoic rocks (Horquilla through Rain Valley formations) and Triassic-Jurassic volcanics and sediments, which are probable Canelo Hills Volcanics equivalents. These rocks have been broadly flexed around northwest-plunging fold axes. Local bedding-plane faults resulting from this folding were mapped by Hayes and Raup (1968) in the southern Mustang Mountains. The Mustang Mountains are the type locality for the Rain Valley Formation, the youngest Paleozoic formation (late Early Permian) in southeastern Arizona.

0.6

98.2 Milepost 28. Note buried soils on right for next 0.2 mi. Underlying soil layer was probably buried by road construction fill.

0.5

98.7 Cattleguard. Just ahead road to Elgin on right. Abandoned railroad grade ahead on right after left turn.

2.8

101.5 Entering Sonoita (Papago meaning: "place where corn will grow"). The scenic qualities of the Sonoita area have attracted film makers for such movies as *Duel In The Sun, Oklahoma,* and more recently, *A Star is Born.* A popular annual quarter horse race held here at the race track on the left attracts racing fans from all over the Southwest. Sonoita at an elevation of 4,865 ft has an average annual precipitation of approximately 17 inches, sustaining the area's lush, rolling plains grasslands (see **Dunham, this guidebook**).

In 1859 a traveler noted that the entire Sonoita Valley was golden with grain and that one field alone contained one hundred and fifty acres of corn. Hinton noted that corn grew as high and as lushly in the Sonoita Valley as it did in Missouri bottomlands and that the Sonoita River rose to the ground and disappeared several times within twelve miles of Camp Crittenden. In 1856 Col. Gray referred to the stream as the "Sonoita or Clover Creek."

Like other areas in southern Arizona, the Sonoita Valley because of trouble with Apaches in the period 1861-1876 was nearly uninhabited by white men.

The present day community of Sonoita is of relatively recent origin, having come into existence in 1882 when it was established on the newly constructed railroad line. When the newer community of Sonoita was established on the railroad to the east of the old Sobaipuri rancheria, a post office was established.

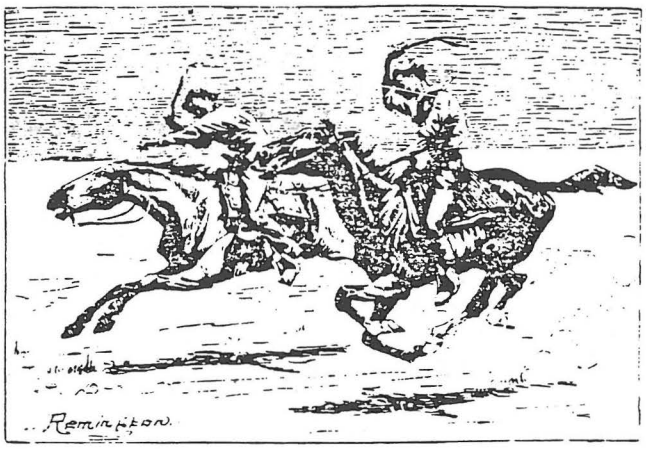

Figure 101.5. Early Arizona horse racing scene as sketched by Remington (1887).

P.O. est. May 8, 1912. Clara L. Hummel, p.m. (Barnes, 1960).

0.3

101.8 Junction of Arizona 83 with Arizona 82. **Continue straight ahead** (north) on Arizona 83. **(Note: Supplemental Road Log No. 1 intersects here.)** The original name for Sonoita was Sonydag or Sonoydak which means "spring-field" in Sobaipuri-Pima. This was the range land for mission cattle belonging to Kino's rancheria at Los Santos Reyes (Polzer, pers. comm.).

0.9

102.7 We are now on the high grassland of Sonoita basin. The highway has ascended onto the highest Pleistocene surface in the region. This surface was created before Sonoita Creek (to the southwest), slopes northeast and is gently graded to the Babocomari River at the south end of the Mustang Mountains. Drainage related to this surface has been progressively captured by headward erosion of drainage systems such as Sonoita Creek.

Roadcuts are in Plio-Pleistocene valley-fill gravels. Thickness of basin fill is geophysically estimated at about 5,000 ft (Bittson, 1976). From geophysical profiling the Sonoita basin in general trends northwest; it is bounded on the south by the Sawmill Canyon zone, which may connect to the southeast with Kino Spring fault zone in the northern Huachuca Mountains. To the west the basin is bounded by a north-trending fault at the west edge of the central Santa Rita Mountains.

Bedrock pediments extend far up into the Santa Rita Mountain block; thus the present mountain edge is not the structural edge of the block. The pedimentation process related to backwearing of mountain blocks adjacent to the Sonoita basin is no longer active due to the downcutting episodes which have captured drainages related to the mid-Pleistocene surface.

Basin-Range faulting (since 15 m.y. ago) initially formed Sonoita basin, which filled up with alluvium while the mountain fronts retreated by pedimentation from the initial, mountain-bounding faults. Sonoita basin then filled at a much slower rate and gravels onlapped onto the extensive pediment surfaces until mid-Pleistocene time. At that time a fall in the regional base level in the Gila-Santa Cruz River system induced downcutting in the upper reaches of the system and progressive capture of drainage systems.

The post-1880 gully cutting episode merely reflects the latest in a series of downcutting cycles which began in mid-Pleistocene time. Changes in climate and man-made perturbations have been superimposed on a more regional, geologically pre-determined tendency for net downcutting since mid-Pleistocene time throughout the upper Gila drainage system. Climatic changes, possibly related to glacial cycles, could have promoted cyclic backfilling and downcutting events, which produced numerous sets of terraces in entrenched drainage basins. Thus, entrenchment in many stream systems in southeastern Arizona is not necessarily indicative of tectonic activity. Perhaps the regional base-level fall could be attributed to integration events in the lower Gila River system, with resulting downcutting in the upper reaches. As demonstrated by Sonoita and Cienega creeks, the amount of downcutting and drainage divide migration in Quaternary time has been very impressive.

1.0

103.7 The west-northwest-striking Mescal Spring fault zone (3:00) separates the central Whetstone Mountain block, on the north, from the Mustang Mountain block, which includes the lower, southern Whetstones and the Mustangs. Mescal Spring fault zone is regarded by some as an element of the notorious Texas lineament.

The Whetstone Mountains are the least structurally disturbed mountain range in southern Arizona. From the Mescal Spring fault zone northward past Apache Peak (1:30), the entire Phanerozoic section from Bolsa Quartzite through Bisbee Group is homoclinally tilted southwestward. The lower Bisbee Group contains concordant bodies of rhyolite which Creasey (1967) indicated to include both extrusive and intrusive rocks. The rhyolite-Bisbee Group section is intruded by the 74 m.y. Mine Camp stock (Creasey, 1967) near Granite Peak (2:30) north of the Mescal Spring fault zone.

0.7

104.4 Road ahead descends into Gardner Canyon, which has numerous Pleistocene surfaces related to long term downcutting and backfilling cycles in the Gardner Canyon drainage. The red argillic horizon at top of roadcut on left displays A, B and C soil horizons.

1.0

105.4 Pima County line. Terrace alluvium on both sides of road ahead is dissected below the

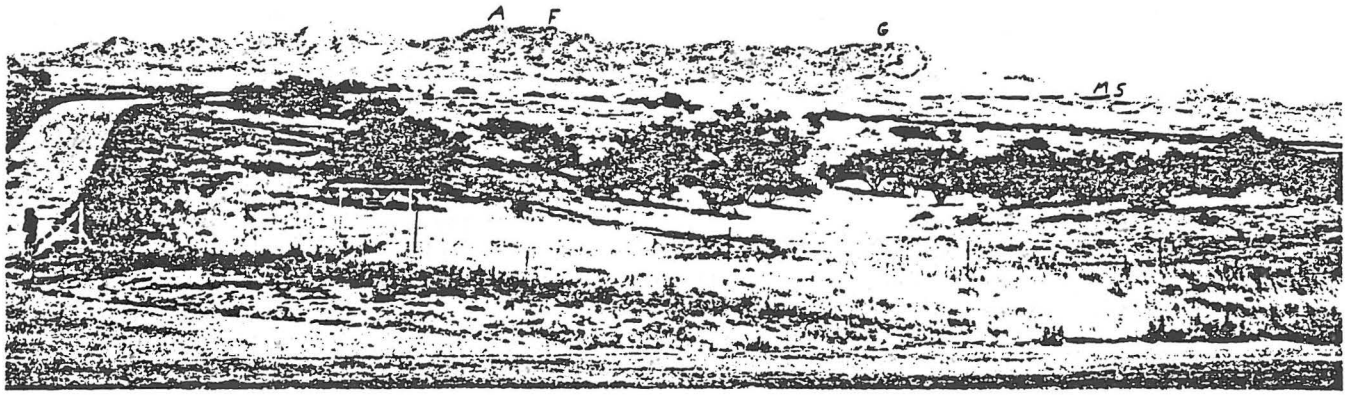

Figure 103.7. West side of Whetstone Mountains. Apache Peak (A), French Joe Peak (F), Granite Peak (G), Mine Camp stock(s) and Mescal Spring fault zone (MS) (R. Mortimer photo).

upper surface. Observe several sets of surfaces including that produced by the post-1880 downcutting event.

0.2

105.6 Milepost 37. Roadcuts in fine-grained valley fill capped by coarse, rounded, cobble-boulder alluvium on a surface below the high, early Pleistocene, aggradational surface. Note excellent channel at base of terrace gravels. The surface is also present ahead on the north side of Gardner Canyon. Finer-grained sediments represent bank overflow and flood-plain deposits in the wider flood plain of an earlier Gardner Canyon. This proto-Gardner Canyon surface in turn has been entrenched by the modern Gardner Canyon, which is currently entrenching its own flood plain. Similar valley fill is exposed in roadcuts for next 7 mi.

0.2

105.8 Gardner Canyon bridge.

0.1

105.9 Gardner Canyon road on left.

0.7

106.6 Mount Wrightson at 9:00. Central Santa Rita Mountains (8:30 to 9:30) are separated from northern Santa Rita Mountains (9:30 to 11:00) by the complex Sawmill Canyon fault zone, which passes through the low saddle at 9:30.

Sawmill Canyon was so named because Henry Lazard and Sam Hughes maintained a sawmill here in 1869, employing 24 teams to haul lumber. Lazard, who was a small, excitable and totally deaf man and therefore a very loud talker, lived extremely well, importing French wine by the barrel for the sake of his health (Barnes, 1960).

The east slopes of the central Santa Rita Mountains are composed mostly of Mt. Wrightson Formation, a series of interbedded andesitic, rhyolitic and latitic flows with a subordinate amount of aeolian sandstone, which is intercalated with volcanics in the upper part of the formation (Drewes, 1971a, b). The aeolian sandstones, well-exposed on the ridges just south of Sawmill Canyon, are of particular interest because they resemble sandstones on the Colorado Plateau. The middle member of the Mt. Wrightson Formation has yielded a lead-alpha age on zircons of 220 m.y. (Drewes, 1971a).

The Mt. Wrightson Formation has been intruded by northwest-trending Piper Gulch Monzonite pluton which yielded radiometric ages of 184 and 180 m.y. In turn, the Piper Gulch Monzonite was intruded by the large, northwest-trending Squaw Gulch Granite pluton which yielded ages of 160 and 145 m.y. (Drewes, 1971a).

The Triassic-Jurassic volcanic-plutonic complex is unconformably overlain by the Temporal and Bathtub formations, which have been assigned an Early Cretaceous age by Drewes (1971a). These formations may have equivalents in the Glance Conglomerate of the Bisbee Group farther east (see Bilodeau, this guidebook). The Bathtub and Temporal formations in the lower slopes from 8:30 to 9:00 contain fanglomerate wedges which thin southward from the Sawmill Canyon fault zone and are intercalated

with rhyolite welded tuff and tuff breccia, tuffaceous sandstone, latite and rhyolite flows and andesitic flow breccia. If the correlations are valid the Glance progressively contains more of a volcanic component to the west. The fanglomerate wedges contain clasts of Precambrian Continental Granodiorite and Pinal Schist and indicate a major period of upward movement of the block north of the Sawmill Canyon fault zone before the end of the Early Cretaceous(?).

The Triassic through Lower Cretaceous(?) strata are separated from Upper Cretaceous Fort Crittenden Formation by a northwest-trending fault in the low pedimented area (9:00 to 9:30). This is the type area for the Fort Crittenden Formation, which here overlies Turney Ranch Formation, the uppermost member of the Bisbee Group. The Fort Crittenden Formation has been sharply folded around northwest-trending, low-plunging fold axes and intruded by a Tertiary rhyolite stock and associated dike swarms striking northeast. These intrusive rocks yielded lead-alpha dates of 26 and 40 m.y. (Drewes, 1971c). The dikes intrude the Sawmill Canyon fault zone without being deformed and therefore place a minimum age of 26 m.y. on the last movement on the Sawmill Canyon fault in the central Santa Rita Mountains.

1.7

108.3 Empire ranch road on right. The Empire ranch was purchased by Anamax Mining Company for the water rights to develop the Helvetia-Rosemont deposits in the northern Santa Rita Mountains near the skyline ridge at 9:30.

1.3

Figure 108.3. View west of, east flank of Santa Rita Mountains. Knobs along ridge crest are Bolsa Quartzite. Rosemont deposit (R) near center just below crest (R. Mortimer photo).

109.6 Madera Canyon-Greaterville road via Box Canyon is just ahead on left.

Greaterville developed after the discovery of placer gold in 1874. The mining district was organized in March, 1875. Scarcity of water made it necessary to work placers by rocker and long tom. Water was brought in canvas or goatskin bags from Gardner Canyon, four miles away. By 1881 the gold had nearly played out and miners began to desert the camp. Others left because of Indian attacks. From 1886 to 1900 Greaterville was dead on its feet. (Barnes, 1960).

The great depression of 1929 supplied incentive to revive its popularity for weekend dry gold panners.

2.4

112.0 Road crosses major drainage divide. Gently tilted Plio-Pleistocene valley fill is exposed in roadcuts ahead.

0.5

112.5 Empire Mountains (1:00) are separated from the northern Santa Rita Mountains (9:00 to 12:00) by Davidson Canyon. A conspicuous change in geomorphic style at drainage divide 0.5 mi ahead illustrates headward erosion and progressive stream capture by Davidson Canyon of the high Pleistocene surfaces in the Sonoita area that were formerly graded to the Babocomari River. The higher gradients of streams such as Davidson Canyon, Cienega Creek to the east, and Box Canyon and Sonoita Creek are related to the considerably lower base level of the Santa Cruz River system to the west, which is as much as 1,600 ft lower than the San Pedro-Babocomari system to the east. The difference between geomorphic styles of the headcutting streams and the former, low-relief, low-gradient, mid-Pleistocene drainage is particularly well displayed at this drainage divide.

Roadcuts ahead are in gently tilted, Plio-Pleistocene valley fill, which rests on an extensive, now exhumed topography of pre-Pliocene(?) age in the Empire and northern Santa Rita mountains.

1.0

113.5 Empire Mountains at 11:00 to 12:00; northern Whetstones at 1:00. Southern Empire Mountains in view are a southeast-dipping homocline of Paleozoic through Mesozoic rocks. They are intruded in the core of the range by the Sycamore Canyon quartz monzonite, known informally as the Sycamore stock, which has yielded dates of 71.9 and 80 m.y. (Marvin and others, 1973). Next to the Whetstone Mountains, the southern Empire

Mountains contain the second most complete Naco section exposed in southeastern Arizona and have a different nomenclature from the Mule Mountains. A good Bisbee group section is also exposed **(see Hayes and Drewes, this guidebook).**

Mount Fagin (9:00 to 9:30) in the northern Santa Rita Mountains is composed of Late Cretaceous pyroclastic volcanics of the Salero Formation. On the west side of Mount Fagin these volcanics rest with angular discordance upon Bisbee Group, which is tightly folded about east-west, low-plunging fold axes. In Davidson Canyon Salero Formation laps across the Empire thrust fault (Drewes and Finnell, 1968). Roadcuts ahead continue in gently tilted, Plio-Pleistocene valley-fill alluvium.

0.9

114.4 Roadcut on right contains a well-exposed angular unconformity between Plio-Pleistocene valley fill and underlying Pantano Formation, which here is moderately to steeply tilted, red boulder conglomerate. Dacite intercalated in the Pantano Formation has yielded a date of 28.7 m.y. (Finnell, 1970b). Roadcuts ahead are in poorly-sorted, poorly-bedded, red boulder conglomerates of Pantano Formation, named by Brennan (1962) for exposures along Pantano Wash about 12 mi north-northeast of here.

0.1

114.5 Milepost 46. Roadcuts ahead are in extremely jumbled, unbedded Pantano Formation. Note size and diversity of some blocks; neither matrix nor clasts are well indurated. Perhaps this chaotic assemblage represents a landslide or debris-flow deposit.

0.6

115.1 Rosemont junction on left. This road passes the Helvetia-Rosemont porphyry copper deposit which is on the east side of the northern Santa Rita Mountains at 8:00. The road also connects with Helvetia west of the main ridge. Mineral deposits of the Helvetia-Rosemont area are thought to be closely affiliated with 53.3 to 57.6 m.y. (Drewes, 1976b) quartz latite porphyry dikes which are abundant throughout the northern Santa Rita Mountains.

Reserves as of 1973 for the Rosemont deposit were estimated at 320 million tons of 0.64% sulfide copper and 20 million tons of 0.55% oxide copper. Production data for the Rosemont-Helvetia district (1908 to 1975) is 34,860,000 pounds of copper, 521,000 pounds of lead, 1,360,000 pounds of zinc, 346,900 ounces of silver and 158 ounces of gold. Gold placers in the Greaterville area at 7:00 are popular with weekend gold seekers from the Tucson area.

For more discussion of the geology of the northern Santa Rita Mountains see Drewes (1971a, b, c, 1972, 1976b) and **Supplemental Road Log No. 1.**

0.1

115.2 Roadside table on left. Here a thin veneer of terrace alluvium rests unconformably on northwest-striking, moderately southeast-dipping Pantano Formation. Road ahead crosses Davidson Canyon where a major fault separates Pantano Formation from the exotic block member of Salero Formation.

0.8

116.0 Bridge across Davidson Canyon. Roadcuts for next several miles are in exotic block member of Salero Formation, which is the lower member of this Upper Cretaceous formation. Note altered and poorly indurated character and poor outcrop expression of these rocks. These characteristics are typical of volcanics of this age throughout southeastern Arizona **(see Hayes and Drewes, this guidebook).**

The name Salero comes from the Salero mine, which is reputed to be one of the oldest in southern Arizona. It is said to have been worked by Jesuits in the 17th century, although no documentary evidence has been found to substantiate this. However, it is known that it was worked from about 1828 to 1830 by Mexicans. Hinton related a legend that the padres at San Jose de Tumacacori were expecting a bishop for dinner who had

Figure 114.4. Angular unconformity between valley fill (V) and underlying Pantano Formatio (Tp) exposed in roadcut on right of highway (R. Mortimer photo).

complained about a lack of salt for his dinner. The priests fashioned a salt cellar from a piece of ore taken from the Salero mine (Barnes, 1960).

Historically, the Salero mine is an example of the extreme hardships imposed by Apaches in the late 1850's and early 1860's. In 1857 John and William Wrightson became owners of the old mine, forming the company in 1858 with H. C. Grosvenor as engineer, Raphael Pumpelly as geologist and Gilbert W. Hopkins as mineralogist with headquarters at Tubac. Only Pumpelly escaped death at the hands of Indians, and he had plenty of hair-raising escapes as told by his journals (Pumpelly, 1918).

0.5

116.5 Southeast-dipping Horquilla Limestone is on the main crest of the Empire Mountains at 12:00. East of the main ridge the entire Naco Group is exposed with only minor structural complications. This section is accessible by a dirt road on the right 1.1 mi ahead. Roadcuts continue in exotic block member of Salero Formation.

1.0

117.5 Milepost 49. Roadcuts in quartz latite porphyry dike. This dike is part of the widespread dike swarms which crop out throughout the northern Santa Rita Mountains, thought to be closely associated with porphyry copper mineralization. Such rocks are popularly known among exploration geologists as "mill rocks" because when you stand on one of these rocks you are usually within view of a mine, smelter or mill. The westerly trending ridges at 8:00 are quartzite beds in the Bisbee Group, which forms a west-northwest trending isoclinal syncline that is overturned to the south.

0.1

117.6 Road on right is main access to Empire Mountains (2:00 to 4:00) and the upper Paleozoic and Bisbee Group sections. Ahead terrace alluvium rests unconformably on exotic block member of Salero Formation.

0.9

118.5 Milepost 50. Near here several dikes of quartz latite porphyry intrude exotic block member of Salero Formation. Well-developed, but now dissected, depositional stream terraces are on the east side of Davidson Canyon ahead on right. Hills southwest of road are capped by Pantano Formation, which unconformably overlies exotic block member of Salero Formation.

0.7

119.2 Quartz latite porphyry dike intrudes Willow Canyon Formation in the ridge from 1:00 to 2:00.

0.3

119.5 Milepost 51. Roadcuts are in contact-altered Bisbee Group at the west edge of the Sycamore stock. A quartz latite porphyry dike cuts this assemblage at north end of roadcut on left; beyond, roadcuts are in the Sycamore stock. Road ahead crosses the west edge of this stock which has an area of about 4 mi^2. The stock is well exposed in the central Empire Mountains where it intrudes a southeast-dipping Paleozoic section. Mineralization in contact-altered zones and veins in these Paleozoic rocks may be related to this stock. Recorded production through 1972 for the Empire mining district is 344,000 pounds of copper, 16,671,000 pounds of lead, 515,000 pounds of zinc, 206,400 ounces of silver and 744 ounces of gold.

0.5

120.0 Low hills to west and roadcut ahead on left are in Bisbee Group that is tightly folded about east-trending fold axes.

0.5

120.5 Limestone ledges at 2:00 are Rain Valley(?) or Concha(?) limestone overlain by exotic block member of the Salero Formation (Finnell, 1970a, 1971). For about 1.5 mi highway parallels north-striking Empire thrust. Glance Conglomerate, Triassic Gardner Canyon equivalent(?) volcanics and red beds, and Rain Valley and Concha limestones are in upper plate; Bisbee Group strata are in lower plate.

0.4

120.9 Old Sonoita highway sign. Drewes and Fin-

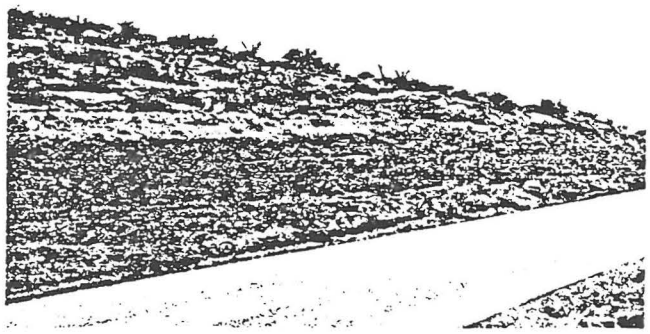

Figure 120.9. "Controversial" roadcut on left of highway. Any comment? (R. Mortimer photo).

nell (1968) described rocks in these roadcuts as Bisbee "Formation" and conglomeratic mudstones of Triassic(?) age with the Empire thrust fault intervening between them. On the Finnell (1971) geologic map the thrust is shown to cut the exotic block member of the Salero Formation; on the Drewes and Finnell (1968) generalized geologic map the thrust is shown to place upper Paleozoic rocks over Bisbee Group with no Salero Formation shown.

Another interpretation is possible. The upper greenish and fragmental-bearing, "punky" rock in the upper part of the left roadcut is probably the exotic block member of Salero Formation. The underlying, steeply upturned, generally east-striking beds in the lower part of the roadcut are probably clastic sedimentary rocks in either the Shellenberger Canyon or Apache Canyon formations. Close inspection of the contact between these two rock units suggests a surface of relief and channelling phenomena which would indicate an unconformable relationship between the two units. A number of flat faults or flat shear surfaces cut the overlying Salero Formation and locally parallel and offset the low-relief, flat-lying erosional contact. Observed displacement on several of these fault strands where they cut the underlying Bisbee Group or offset the unconformable contact is no more than a few feet.

The strong angular discordance between the underlying Bisbee strata and the overlying lower Salero Formation indicates a major Late Cretaceous tectonic event which post-dates Lower to mid-Cretaceous Bisbee Group (as young as 94 m.y.) and predates Salero Formation (possibly as old as 80 m.y.). This angular truncation of Bisbee Group by lower Salero Formation is noted by Drewes and Finnell (1968) at a number of other localities in the northern Santa Rita Mountains, although not noted by them at this particular spot. The relations in this roadcut suggest that much of the tectonism in the northern Empire Mountains occurred after Bisbee deposition and before Salero with minor tectonism after deposition of the lower Salero.

The strongly upturned, east-striking Bisbee Group is part of the major belt of Late Cretaceous east-west folds and reverse faults. This belt extends from the northern Santa Rita Mountains through the Empire Mountains to the northern Whetstone Mountains and would correspond to the first north-south compressive orogeny of Gilluly (1956) in the Tombstone Hills.

0.3

121.2 Ledge at top of hill at 2:00 (on skyline) is Glance Conglomerate, which unconformably rests on maroon redbeds and siltstones mapped by Finnell (1971) as an equivalent of the Triassic Gardner Canyon Formation. Rhyolite tuff intercalated within the red beds in this area yielded a lead-alpha age on zircon of 170 ± 35 m.y. (Marvin and others, 1973).

East of Total Wreck Ridge at 3:30 (which is capped by Concha Limestone) is a large, southward-thinning, fanglomerate wedge of Glance Conglomerate which contains clasts of Pinal Schist and Precambrian granite derived from an upthrown block north of the east-striking Empire thrust. North of the Empire fault Glance Conglomerate is thin or absent, as are the Willow Canyon and Shellenberger Canyon formations. The Empire thrust is apparently another fault which has experienced repeated reactivations in Mesozoic and Cenozoic time (see Bilodeau, this guidebook).

0.1

121.3 Hill at 12:30 is capped by Rain Valley Formation with Concha Limestone in lower slopes. Low divide between that hill and hill topped by Glance Conglomerate at 2:00 is capped by presumed Triassic Gardner Canyon equivalent.

0.2

121.5 Milepost 53. Roadcuts on right are Permian Concha Limestone; hill on right is capped by Rain Valley Formation. At north end of roadcuts quartz latite porphyry is in fault contact with contact-altered Concha Limestone.

Observe extensive dissected pediment that was developed in the northern Santa Rita Mountains.

0.4

121.9 Roadcuts in Shellenberger Canyon Formation. These strata are intruded by a quartz latite porphyry dike, which is part of an extensive west- to west-northwest dike swarm in the northwestern Santa Rita Mountains. Copper mineralization in the Cuprite mine area may be associated with these dikes.

1.1

123.0 Roadcut on right in upturned Shellenberger Canyon Formation angularly overlain by terrace alluvium which fills channels in an erosion surface.

0.4

123.4 Roadcuts on left are in upturned Bisbee

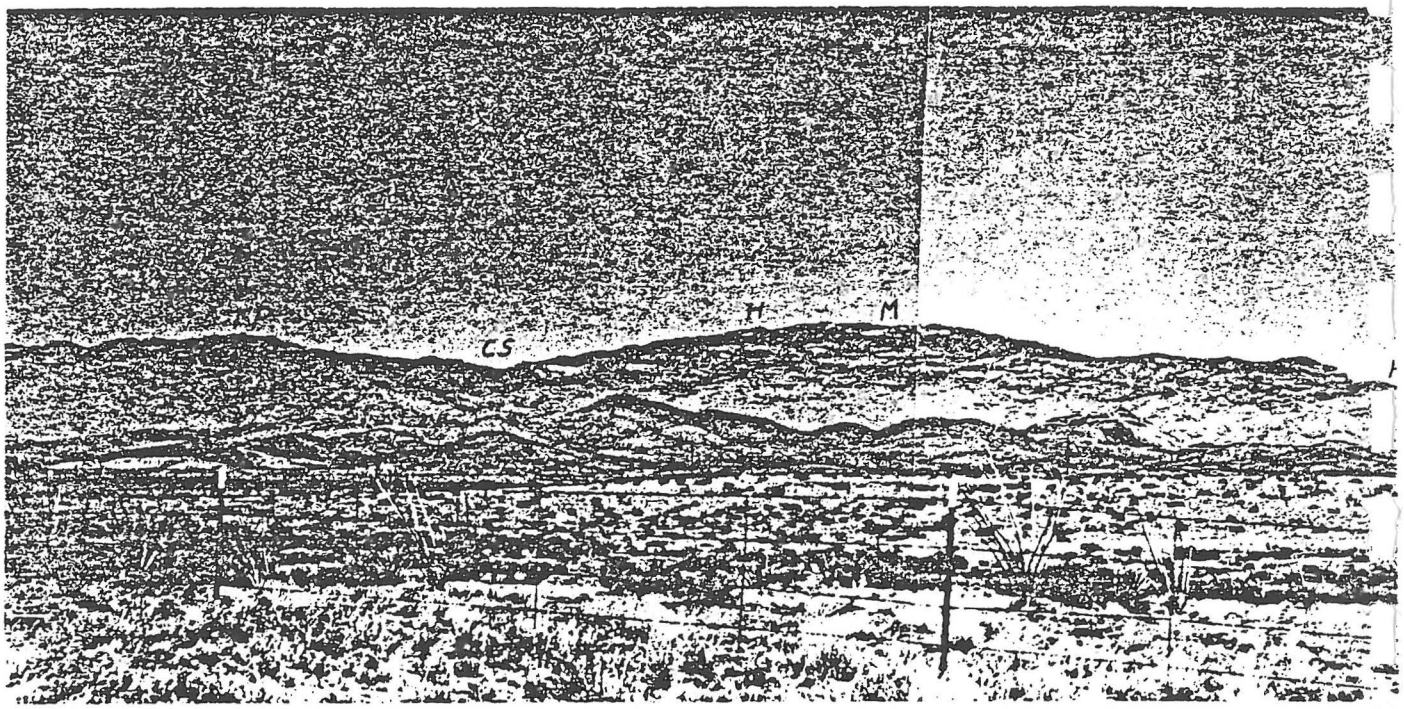

Figure 126.6. View north of Rincon Hills. Tanque Verde Peak (TP) on crest of Tanque Verde Ridge, Cowhead Saddle (CS), Pistol Hill (P), Helen's Dome (H), Mica

Group intruded by quartz latite porphyry dikes.

0.2

123.6 Milepost 55. Low ridge to right contains Precambrian granite depositionally overlain by Shellenberger Canyon Formation and various members of Salero Formation. Uplift and erosion of the entire Paleozoic section probably is coincident with deposition of the thick Glance Conglomerate fanglomerate wedge shed onto Permian rocks south of this block. Road traverses veneer of terrace gravels resting on an extensive pediment.

0.4

124.0 Sahuarita road on left.

0.6

124.6 Milepost 56. Roadcuts ahead in alluvium unconformably resting on an intrusive rock mapped as Paleocene quartz latite porphyry by Finnell (1971) at north end of roadcut on left.

0.4

125.0 Roadcut on left and outcrop on right are quartz latite porphyry. These are the last bedrock outcrops on this log. Ahead road passes onto alluvium and valley fill in Tucson basin. The size of the pediment in the northern Santa Rita Mountains emphasizes the structural size of the horst blocks as compared to the graben blocks in the valley. The fault is now concealed by valley fill. Following Basin and Range faulting, which terminated in this area approximately 5 m.y. ago, extensive pediments developed as mountain fronts retreated as much as several miles.

1.6

126.6 Broad domal physiography of the Rincon, Catalina and Tortolita mountains dominates the skyline from 11:30 to 3:00. At 11:15 are Picacho Mountains with Picacho Peak at 11:00, about 50 mi distant (if visibility permits). Rugged peaks of Tucson Mountains on skyline from 10:00 to 11:00. Del Bac Hills south of Tucson Mountains at 9:45. In far distance at 9:15 loom the Coyote and Quinlan Mountains with Kitt Peak Astronomical Observatory at 9:10. The Sierrita Mountains form a broad, very flat cone at 9:00. Tortolita Mountains form a low ridge at 11:30 behind jagged peaks of Pusch Ridge (11:30 to 12:30) in the western Catalinas.

The large rounded peak at 1:00 in the Rincon Mountains is Mica Mountain (8,666 ft). The conspicuous ridge trending west-southwest from Mica Mountain is Tanque Verde Ridge or the Tanque Verde Mountains. Cow Head Saddle separates Tanque Verde Ridge from Mica Mountain. The top of Tanque Verde Ridge gently plunges southwestward and generally marks the culmination of a

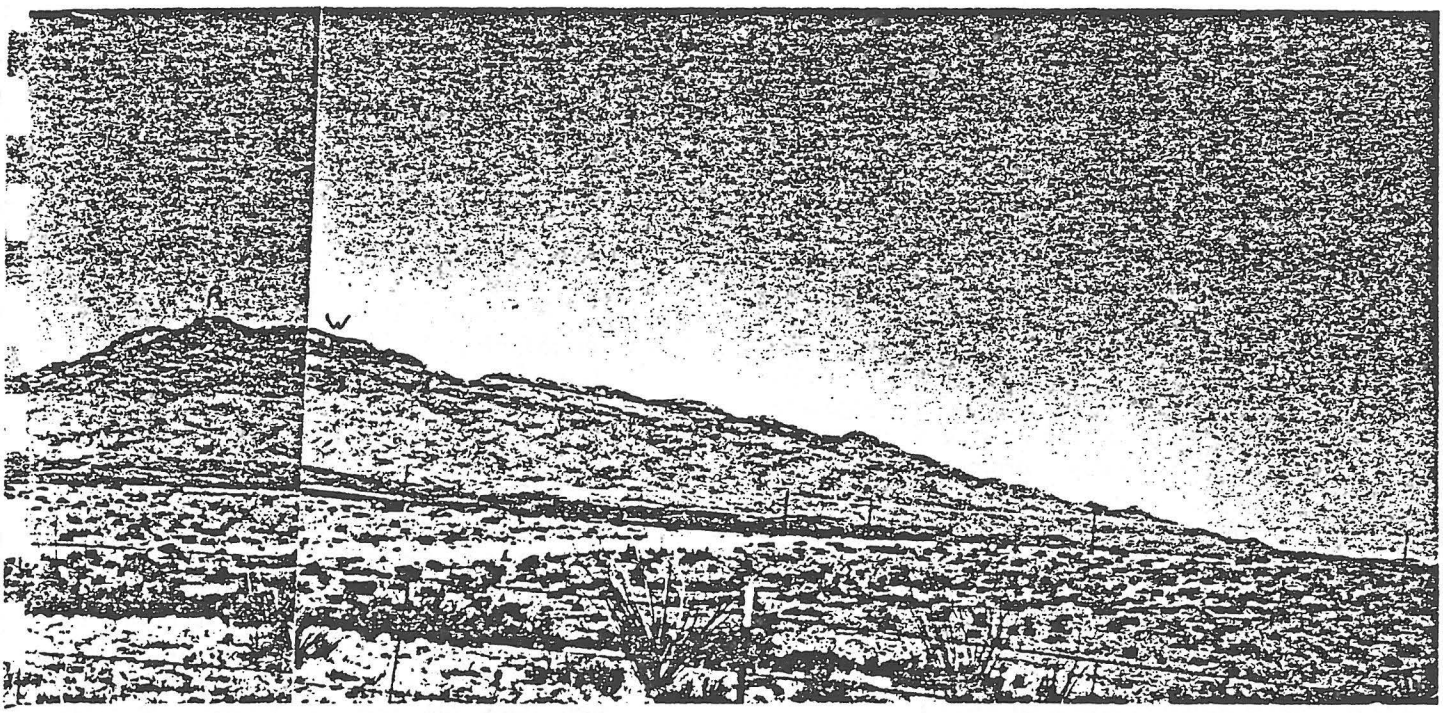

Mountain (M), Colossal Cave (C), Happy Valley Saddle (HV), Rincon Peak (R), Agua Verde Hill (A) and Wrong Mountain (W) (R. Mortimer photo).

large, antiformal foliation arch in mylonitic gneisses. Mica Mountain is separated from Rincon Peak (8,482 ft at 2:00) by Happy Valley Saddle. The small peak north of the cuesta-like peak and south of Rincon Peak is Wrong Mountain which is the type locality of the two mica-garnet-bearing Wrong Mountain Quartz Monzonite which crops out extensively throughout the Rincon Mountains.

Wrong Mountain Quartz Monzonite is mineralogically similar to the Wilderness Granite in the Santa Catalina Mountains and is extensively interlayered with a darker gneiss, which Drewes (1977) considers to be deformed Rincon Valley and Continental Granodiorites. Age dates on undeformed Rincon Valley Granodiorite outside of the metamorphic area yield K-Ar ages of 1380 to 1560 m.y. on various minerals (Marvin and others, 1973; Drewes, 1977). A specimen of Rincon Valley Granodiorite from Saguaro National Monument northwest of Tanque Verde Ridge gave a 1440 m.y. Rb-Sr age. Drewes (1977) also assigns a Precambrian age to Wrong Mountain Quartz Monzonite based on a hybrid Rb-Sr age of 295 m.y. and by analogy with 1650 m.y. zircons extracted from deformed Wilderness Granite at Windy Point (Catanzaro and Kulp, 1964) **(see Silver, this guidebook).**

Layers of mylonite schist commonly separate layers of Wrong Mountain Quartz Monzonite from the darker layers of deformed Continental Granodiorite. These schistose lenses have been correlated with Pinal Schist by Drewes (1977).

Low foothills from 12:30 to 2:00 in middle distance are underlain by Paleozoic rocks. Colossal Cave, a local tourist attraction, is in the foothill at 1:30. Paleozoic rocks in the Agua Verde-Colossal Cave area are part of a series of deformed Phanerozoic rocks that also occur at Martinez ranch at the base of the Rincon Mountains at 2:30, in the Loma Alta area (12:30) at the southern base of Tanque Verde Ridge, and in the Saguaro National Monument area just northeast of the nose of Tanque Verde ridge at 12:00. A large pediment in Rincon Valley between Loma Alta and Colossal Cave is cut on Precambrian Rincon Valley Granodiorite.

The Precambrian and Paleozoics are in the upper plate of the major, low-angle, Santa Catalina fault, which is located at the break in slope between the main Rincon massif and the foothill block. The Santa Catalina fault separates the unmetamorphosed, but highly deformed, upper plate rocks from lineated mylonites of the metamorphic core in the main Rincon Mountain mass. Inevitably these

complicated geometric relationships have several interpretations. Davis (1975) analyzed fold geometries in Paleozoic and Mesozoic rocks of the upper plate and concluded that they represented a period of major gravitational sliding of the cover down the Santa Catalina fault surface in mid-Tertiary time. Drewes (1977) recognized this mid-Tertiary gravity-induced movement, but also suggested that the low-angle fault was older and represented former thrusts which were emplaced about 73 m.y. ago via regional northeast-southwest compression of Laramide age. These faults were reactivated in Oligocene time (25 m.y.) during arching of the mylonite rocks of the metamorphic core.

0.3

126.9 Old Sonoita highway on right rejoins Arizona 83.

0.3

127.2 Overpass; Junction with Interstate 10. **Intersection with Supplemental Road Log No. 3.**

0.4

127.6 Merge with westbound lane of I-10.

0.3

127.9 I-10 traverses aggradational surface on Plio-Pleistocene valley fill. Red soil horizon formerly on this surface has generally been removed throughout Tucson basin.

1.4

129.3 Exit 279; Colossal Cave and Vail road. Colossal Cave to northeast is a small, dry cave in Escabrosa Limestone, which is in the allochthonous Paleozoic section above the Catalina fault.

1.5

130.8 Catalina Mountains are from 1:00 to 2:30 with the high summit of Mount Lemmon (9,157 ft) at 2:30. The five major peaks which comprise Pusch Ridge (1:00 to 3:00) from left to right are Pusch Peak, Table Mountain, Mount Kimball, Finger Rock and Cathedral Peak. Pusch Ridge is composed of gently dipping, light and dark layers of banded gneiss which contain mylonite-capped cataclastic rocks. Pusch Ridge is separated from the main mass of the Catalinas by Romero Pass. A low ridge, called the Forerange, extending east from Cathedral Peak, is also composed of layered cataclastic gneisses.

In the background, the crest of main range is capped by metamorphosed younger Precambrian Apache Group and lower Paleozoic rocks. Below the crest these rocks are intruded by a large, sill-like pluton named the Wilderness Granite by Shakel and others (1977), who reported a minimum uranium-lead monazite age of 45 m.y. from this rock. Below the summit of Mount Lemmon and above the Wilderness of Rocks (the type area for the Wilderness Granite) are some prominent, white "teeth"-like cliffs. These mark the position of an extensive alasko-pegmatite border phase of Wilderness Granite which extensively intrudes the overlying younger Precambrian and Paleozoic strata at the crest of the range and the Leatherwood Quartz Diorite just north of the crest. According to the mapping of Banks (1976), sill-like appendages from this pluton occur between dark layers of the banded gneiss in the Forerange. Zircons extracted by Shakel and others (1977) from those dark layers strongly suggest a correlation with once undeformed 1400-1450 m.y. old Precambrian granite. The Wilderness pluton is part of an extensive Oligocene composite batholith which pervades the entire Catalina Mountains according to Creasey and others (1977). They cite numerous mid-Tertiary age dates by K-Ar and fission track methods to support the mid-Tertiary age assignment. Large muscovite books extracted from the alasko-pegmatitic complex near Summerhaven on Mount Lemmon have yielded 47.9 m.y. K-Ar ages, which Damon and others (1968) interpreted as an intermediate age inherited from some unknown older age. Rincon Mountains are at 2:00 to 4:00 with Mica Mountain now at 3:15.

2.4

133.2 Exit 275; Houghton road to Saguaro National Monument and east Tucson on right and to Pima County Fairgrounds on left.

2.3

135.5 Exit 273; Rita road.

2.1

137.6 Wilmot road sign on right. At 9:30 a water tower presides over a collection of shacks known as Galeyville.

Exxon drilled a deep stratigraphic test into the Tucson basin 2 mi south of here. The upper 7,277 ft is sand, gravel and clay, filling Basin and Range grabens formed after 12 m.y. From 7,277 to 9,000 ft the hole penetrated a volcanic section of tuff, andesite and rhyolite. Selected cuttings from a tuff at 7,940 to 7,960 ft yielded a K-Ar age of 23.4 m.y. Below the volcanic section from 9,000 to 9,500 ft reddish brown conglomerates were encountered. At 9,500 to 10,000 ft another volcanic unit was found which yielded K-Ar ages of 16.1 and 18.0 m.y. This was interpreted to be an intrusive dike or sill.

From 10,000 to 12,000 ft more reddish brown conglomerates, silts and shales were drilled. At 12,000 ft to the total depth of 12,590 ft was a quartz monzonite dated at 61 m.y. by K-Ar and 120 m.y. by Rb-Sr methods. Eberly and Stanley (1978) regard the section from 7,277 to 12,000 ft as deposited after the Eocene and before the Basin and Range faulting about 13 m.y. ago. A seismic profile by Exxon shows the deep part of Tucson basin is surprisingly narrow and shows extensive pediments buried by a basinward thickening sequence of alluvial basin-fill (see Scarborough and Peirce, this guidebook).

4.2

141.8 Benson highway (Tucson airport) exit.

2.0

143.8 Tucson Mountains on skyline from 10:00 to 12:30. From left to right are Beehive Peaks (10:30), Cat Mountain (11:00), Golden Gate Mountain (11:15) and Bren Mountain (11:30). The highest point in the Tucson Mountains is Wasson Peak (4,877 ft) at 11:55. Tumamoc Hill, location of the University of Arizona Palynology and Vertebrate Paleontology laboratories, is at 12:30; Safford Peak at 12:45 marks the northern end of Tucson Mountains.

West of Interstate 10 at the foot of "A" Mountain (Sentinel Peak), where Mission Road crosses the Santa Cruz River, is the site of San Agustin del Tucson. Tucson means "at the foot of the Black Mountain." The downtown governmental center is built over the site of a Spanish colonial presidio (Polzer, oral comm.).

Barnes (1960), briefly describes the early history of Tucson:

The Papago name for Sentinel Mountain (q.v.) *is Chuk Shon, referring to the fact that the base of the mountain has a darker color than the summit. The Papagos customarily name their villages after distinctive landmarks, and an old Indian village was once located at the base of this mountain. Spanish pronunciation was an approximation of the Papago name, Tuqui Son or, in its current form, Tucson. Hodge states that Tu-uk-so-on means "black base." The rancheria at this point has long since disappeared.*

That there was prehistoric civilization where present-day Tucson exists is beyond question. When the Pima County Court House was constructed in Tucson in 1928, workmen excavating for the footings not only uncovered a part of the old presidio wall, but also found evidence of prehistoric civilization. Again in December 1954, workmen excavating for a proposed building found the northern wall for the same presidio and below it a Hohokam pit house dating at least to 900 A.D. The ruins were covered and plans for a new building abandoned.

Records have much to say about Tucson. Its first mention by a Spanish missionary was that made by Fr. Kino in 1697. However, the place to which Kino referred was about three miles north of the present courthouse and hence outside the original town limits by a considerable distance. This was San Augustín de Oiaur. Kino noted that it was on the banks of the Santa Cruz River, which was then running with some force, and that between that point and San Xavier del Bac was the most thickly populated and fertile spot in the whole Santa Cruz Valley. It is to be noted that Kino did not apply the word Tucson to this place. Co-existent with this place was Chuk Son near Sentinel Peak.

Many years passed and with them vanished the supremacy of the Jesuits, who fell out of favor with the Spanish court. The Franciscan order took the place of the Jesuit in Arizona, and in 1751 the Indian settlement of Chuk Son became a visita *of San Xavier del Bac. During the Pima revolt (1751), both the* visita *and the mission were abandoned. A few years later, Fr. Francisco Garcés was sent into southern Arizona. It was he who, to protect the peaceful Indians against the raiding Apaches, caused a small pueblo with a church and a wall to be constructed for defense in 1769. The fact that there was a wall completely around this small community is the origin of the currently used nickname for Tucson, the Old Pueblo. The name San Augustín del Tuquison was transferred to this place to distinguish it from the nearby Chuk Son (or Kuck Son) which was called San Augustín de Pueblito de Tucson. The latter place was reported to have two hundred families in 1772, but by 1774 only eighty families remained. To protect the missions and the peaceful Indians the Spaniards had previously established a detachment of the military at Tubac* (q.v., *Santa Cruz County). In 1776 these soldiers were moved to San Augustín de Tucson.*

In 1822 Tucson was in the newly created Mexico. Tucson was the military outpost of Mexico until the area in which the settlement was located became part of the United States with the Gadsden Purchase in 1853. Apache troubles in the Santa Cruz Valley caused Tuc-

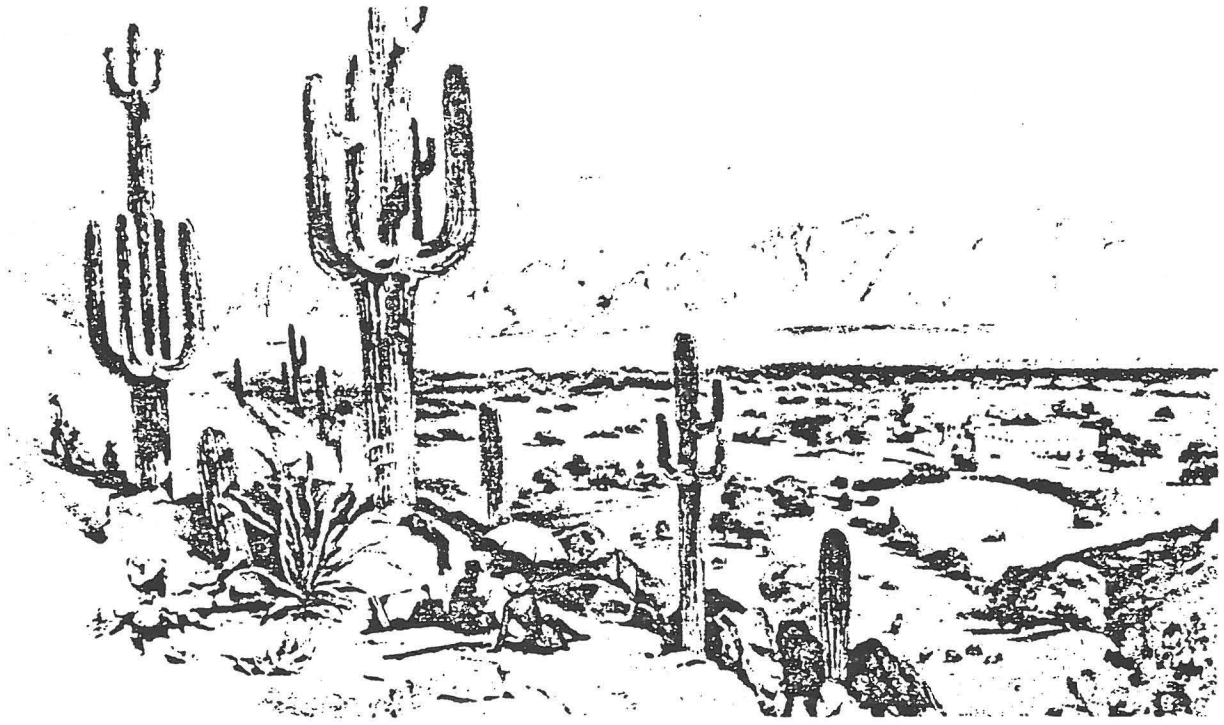

Figure 143.8. Time-comparative scenes of Tucson from similar locations on Sentinel Peak. **Above:** *Watercolor sketch by J. R. Bartlett, 1852.* **Below:** *Present metropolis of Tucson (H. L. James photo).*

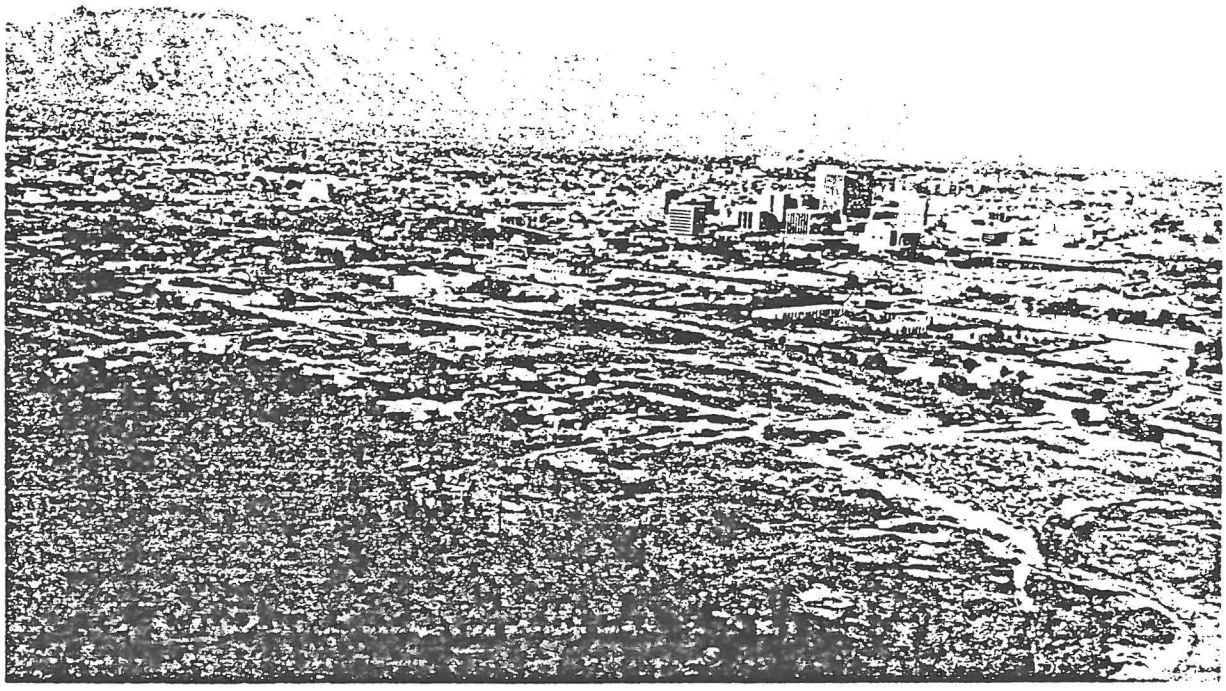

son's population to fluctuate and after 1848 to increase because of refugees from Tubac and Tumacacori seeking safety within its environs. In 1846 the Mormon Battalion passed through under Gen. Philip St. George Cooke. It was at this time that the Mexican presidio moved permanently from the Old Pueblo.

In 1856 the U.S. Government sent four companies of the First Dragoons, who stayed a very brief time at Tucson before being moved to the vicinity of Calabasas in October. It is this fact which has led to some confusion about the date of the establishment of the post office at Tucson (cf. Fort Buchanan, Santa Cruz).

In the summer of 1861, Tucson had a total of sixty-eight American voters. This handful of men assembled in a convention and elected a "territorial delegate" (Granville Oury, cf. Mount Oury) to the Confederate Congress. In February 1862, Confederates from Texas under Capt. Sherod Hunter marched unopposed into the Old Pueblo. Their stay was a brief one, for they retreated on May 20 before the oncoming California Volunteers, who entered the town and raised the flag of the United States. In June, James H. Carleton, Commander of the California Column, reached Tucson, and Arizona, which had since August 1861 been part of the Confederacy, returned to the Union.

Two years later in May 1864, Gov. John N. Goodwin (who had recently taken up his duties as the first actual governor of Arizona Territory) declared Tucson a municipality, which was tantamount to its incorporation. There was much haggling to establish the permanent capital for the territory at various places and Tucson exerted pressure for her own selection. In 1877 the capital was moved back to Prescott.

In 1879 thousands of people flocking to the Tombstone District had their effect on the economy of Tucson, which began to emerge from being a tiny sleepy village into its life as a city. The fact that it was sleepy applied mostly to the daylight hours, for Tucson had a reputation of being wide open, rough, and ready. A favorite story was that concerning the tenderfoot from the East who stepped down from a dusty stage trip at four o'clock in the morning. He made tracks for the nearest bar, which wasn't difficult to locate. The tenderfoot made some comment about it being late for the bar to be open, to which the bartender replied that it was late for the night before last, but "just the shank of the evening for tonight."

P.O. est. July 13, 1865. Mark Aldrich, p.m. Wells Fargo Station, 1879. Incorporated February 7, 1877.

Principal rock types in the Tucson Mountains are Laramide volcanic and plutonic

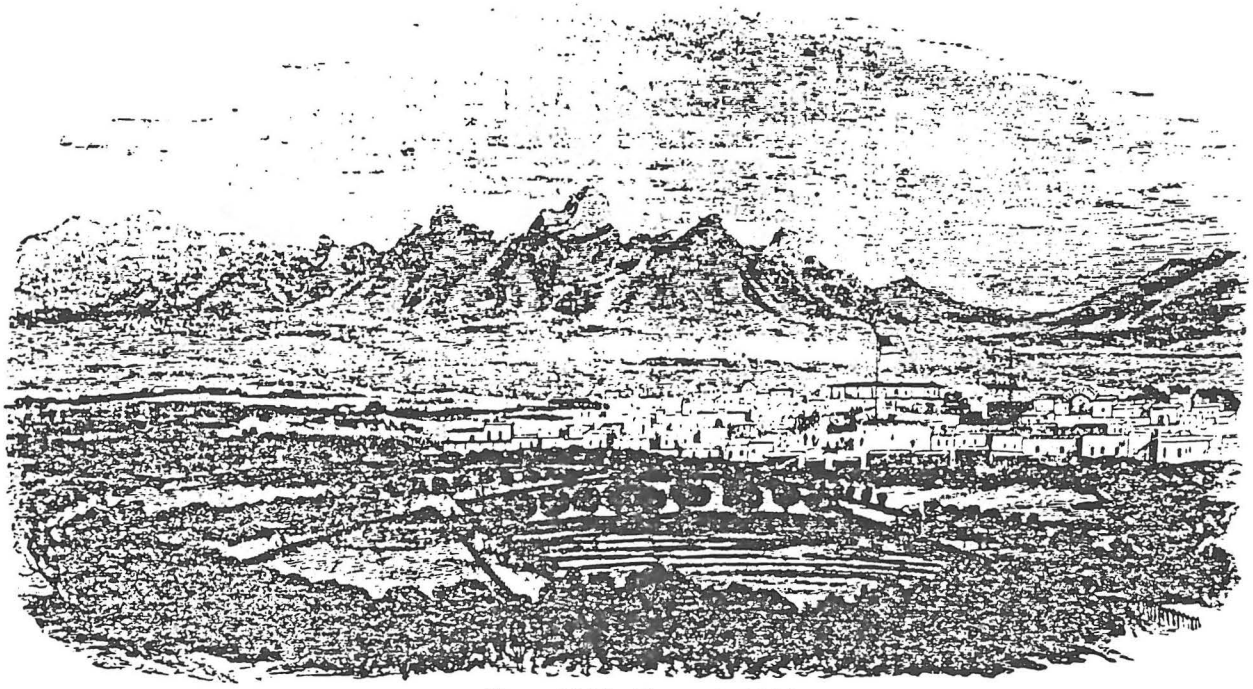

Figure 144.9. Tucson in 1864.

Figure 150.3. Tucson street scene in the 1880s.

rocks (75-56 m.y.). These overlie strongly deformed Amole Arkose, correlated by Hayes (1970b) with the Bisbee Group. Tertiary volcanics and agglomerates (28 to 24 m.y.) unconformably overlie Laramide volcanic rocks. **See Supplemental Road Log No. 1.**

The Tortolita Mountains at 1:00 include an extension of the metamorphic geology in the western Santa Catalina Mountains. Note the contrast between the Tortolita-Catalina-Rincon metamorphic ranges and the Tucson, northern Santa Rita and Empire mountains. Why have these ranges escaped the metamorphism which pervades the Santa Catalina-Rincon-Tortolita complex?

0.3

144.1 Palo Verde road-Irvington road exit.

0.8

144.9 Entering Tucson. **Continue on I-10 to downtown Tucson.**

5.4

150.3 **Take Congress Street exit** (east) to Marriott Hotel, 180 West Broadway. Marriot is site of banquet and tomorrow's assembly area. **End of road log.**

See References, page 139.

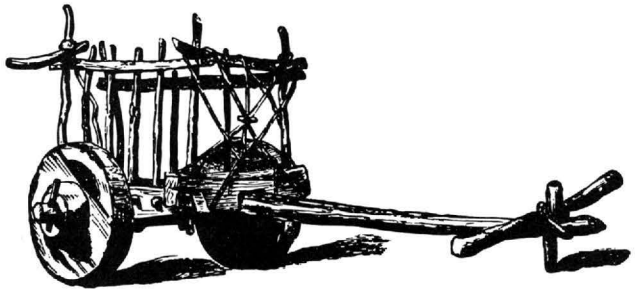

[Section 2]

Laramide Cordilleran Decretion
Southwestern North America

LARAMIDE CORDILLERAN DECRETION IN SOUTHWESTERN NORTH AMERICA

by Stanley B. Keith and Richard F. Livaccari, April, 1983

INTRODUCTION

Within the past ten years concepts about Laramide orogeny in southwestern North America have undergone changes in thinking that are as mobile as the orogeny itself. Past thinking about Laramide orogeny in the type area of the Colorado-Wyoming Rockies has generally treated the phenomenon as a one-event, one-style orogeny. For example, much debate has, and currently is, centered on the style of Laramide orogeny; namely are the Laramide basement uplifts in Colorado, predominantly of a vertical nature (Sterns, 1978) or of a horizontal nature (Berg, 1962; Gries, 1983). Similarly, in southern Arizona arguments about Laramide orogeny have also centered on style. For example, is Laramide orogeny characterized by large-scale thrusting (Drewes, 1981), by forced, compressively-induced, basement-rooted uplifts (Davis, 1979), or by differential vertical uplift and extension (Jones, 1963, 1966; Rehrig & Heidrick, 1972, 1976; Lowell, 1974; Mayo & Davis, 1976; Titley, 1976; Heidrick & Titley, 1982).

An important aspect of Laramide orogeny that is not commonly emphasized is its long time length; for example in southern Arizona most workers regard Laramide orogeny as occurring between 90 m.y. B.P. and 40 m.y. B.P. This represents a considerable amount of time during which Laramide orogeny might progressively evolve through several events, each with a different style. This theme of changing tectonic style has been stressed in several recent papers (Drewes, 1973; Keith, 1975, 1978, 1979, 1981, 1982; Chapin and Cather, 1981; and Livaccari and Engebretson, 1983).

The Keith, Chapin and Cather, and Livaccari and Engebretson papers specifically implicate flattening subduction of the underriding Farallon plate as the underlying plate tectonic cause for evolving tectonic style of the Laramide orogeny. Within this framework, attention is being focused by the above workers on the Eocene time period when subduction reached its lowest angle and Laramide orogeny reached its greatest intensity. Indeed, Eocene aspects of Laramide orogeny in the southern Arizona region have largely gone unnoticed in previous work. However, the recent discovery of large, Paloeocene-Eocene, peraluminous, two-mica, garnet-bearing plutons that intrude the porphyry copper related plutons has added a dramatic new stratigraphic dimension to Laramide orogeny. This new stratigraphic package forces a complete resynthesis of Cretaceous-Cenozoic tectonic phenomena in the southern Arizona region. It is from this resynthesis that the notion of decretion is born.

DECRETION

The concept of Cordilleran decretion refers to the tectonic erosion and imbrication of an overriding continental plate during low-angle subduction of an oceanic plate. In effect, material is tectonically removed (decreted or scraped off) from the base of the overriding plate as it advances over the shallowly subducting oceanic plate. The decreted material is then laterally transferred continentward away from the trench. The decretional process is manifested by several tectonic phenomena.

Magmatically, decretion may be expressed by crustally derived, lithophile-depleted, peraluminous plutonism. These deep level plutons (generally 8 km or deeper) plutons lack the lithophile enrichment that is common to more familiar peraluminous plutons in Europe and elsewhere. Keith and Reynolds (1981) and Reynolds and Keith (1983) have interpreted the depleted nature of peraluminous Cordilleran plutons in the western U. S. to have been derived from depleted, underthrust graywacke materials or from depleted, lower crustal, granulitic material in the base of the overriding plate during low-angle subduction of the Farallon OCEANIC plate during Cordilleran decretion (this paper and Livacarri and Keith, in prep.). In contrast, they interpret the lithophile nature of Hercynian and Caledonide peraluminous plutons in Europe to have resulted from partial melting of lithophile enriched material in the upper part of a shallowly underthrust CONTINENTAL plate during continental collision (Reynolds & Keith, 1983).

Structurally, decretion may be manifested in the upper plate by large-scale, trench-directed thrust faults and nappe-sized recumbent folds. The trench-directed thrust faults and folds may link into regional tectonic zones that dip shallowly continentward and contain extensive areas of mylonitization, especially where these tectonic zones are injected by the above mentioned peraluminous plutons. The lineation of the mylonites commonly contains an S-C fabric that indicates trench-directed simple shear. Lineation in these mylonites thus represents the direction of trenchward shear and forms at a high angle to the trench. Preliminary data assembled by Livaccari and Keith (in prep.) suggests that decretional lineation may reflect the absolute motion of the overriding continental plate during low-angle subduction. The decreted leading edge of the continental plate may be replaced by underthrust oceanic materials, such as graywackes or accreted oceanic basalts in any former melange wedges at the edge of the continent that existed during higher angle subduction.

Radiometrically, decretion may be expressed by large areas of reduced K-Ar and fission track ages from older rocks in the overriding continental plate. These large areas of reset ages could represent isostatic uplift of the overriding continental plate due to lithospheric thickening. This thickening could

occur from the coupling of the continental plate with the underriding oceanic plate or from addition of laterally transferred lower crustal materials from the leading edge of the overriding plate to continental plate further away from a subduction zone. The isostatic uplift is accompanied by the development of extensive peneplanation erosion surfaces that regionally slope towards the continental interior of the overriding plate.

Sedimentologically, decretion is manifested by internally drained sedimentary basins that develop as large, asymmetric, clastic wedges that accumulate immediately trenchward of trenchward-directed fold-thrust uplifts. Hence, in ideal cases coarse clastic material resides on the continentward side of the basin adjacent to the fold-thrust uplifts, whereas finer grained fluvial materials would exist on the trenchward side of the basin. Decretional basins are distinctly asymmetric prisms with their thickest part towards the continent. Because of the regional paleoslope that is inclined toward the continent, the trenchward side of decretional sedimentary basins is fed by low-energy, low-gradient, fluvial systems that drain the paleoslope region trenchward of the main sedimentary basin. Also, extensive lacustrine sedimentation may occur in the basin at the bottom of large lakes in interior basins immediately trenchward of the fold-thrust uplifts.

Metallogenetically, decretion is expressed as orthomagmatic sulfide systems produced during the final crystallization of peraluminous granitoids or as hydrothermal metamorphic systems produced during dehydration of crustal materials during amphibolite-grade metamorphism in decretional tectonic zones. Both orthomagmatic and metamorphic hydrothermal systems are characterized by low sulfur contents (that is low total sulfide content), high CO2-rich fluid inclusions and abundant quartz veins that commonly contain tungsten.

Sulfide systems replaced into areas above decreted continental lithosphere appear to be more oceanic in character; especially where the decreted lower lithosphere has been replaced by depleted melange-wedge materials. These deposits contain elevated gold contents and low silver contents and may yield byproduct copper, followed by lesser amounts of byproduct lead. These deposits are commonly developed in large areas of chlorite-epidote alteration that may reflect extensive iron-magnesium metasomatism of the host rocks during the metallogenic event.

Sulfide systems developed in the non-decreted overriding continental plate are more continental in character, to wit, they contain highly radiogenic lead (the principal produced base metal), and much more silver relative to gold (silver:gold ratios are generally greater than 30:1). Copper is a common byproduct,

followed by zinc. The lead-silver-copper deposits are generally emplaced at some distance laterally from the peraluminous plutons; consequently their orthomagmatic origin is in some doubt. Indeed, these systems could be deposited from metamorphic hydrothermal brines derived from dehydration of continental basment during amphibolite grade metamorphism in decretionary tectonic zones. This observation also applies to gold deposits that lack a spatial association with peraluminous granitoids. However, there does appear to be a more orthomagmatic tungsten-bearing quartz vein association in and immediately adjacent to peraluminous series granitoids. Here the tungsten occurs primarily as huebnerite-wolframite series mineralogy, but scheelite is also not uncommon in many peraluminous granitoid-related mineral districts. It is very important to point out that uranium, beryllium, thorium, tin, and lithium, which are commonly associated with alkaline peraluminous series granitoids in continental collision tectonic settings are conspicuous by their absence in subalkaline series peraluminous granitoids in decretionary tectonic settings.

Specific examples from southwest North America for all of the tectonic manifestations of decretion that are discussed above are shown in Part C of Figure 1.

CORDILLERAN DECRETION IN SOUTHWESTERN NORTH AMERICA

Figure 1 is a plate tectonic model for Sevier-Laramide Cordilleran tectonic development. During the Sevier orogeny the Cordilleran orogen contained three major tectonic elements and was a classic two-sided orogen in the sense of Burchfiel and Davis (1968). To the west of a thermal axis in the magmatic arc was an accretionary assemblage that consisted of the Franciscan melange-wedge and the Great Valley forearc basin between the wedge and the magmatic arc. East of the magmatic arc thermal axis existed a thin-skinned, foreland fold-thrust belt east of which lay a foreland retroarc basin in downbowed continental lithosphere. The thrust belts east and west of the arc were driven by lateral underthrusting of oceanic and continental lithosphere to the west and east, respectively towards the thermally softened region in the arc thermal axis. The above tectonic configuration remained relatively stationary from about 145 m.y. to 85 m.y. when Cordilleran subduction maintained a constant dip of an estimated 50 degrees (Keith, 1982). Eastward migration of the Sevier foreland fold-thrust belt during this time was coordinated with a slow eastward migration of the magmatic arc thermal axis. Eastward migration of the thermal axis may have in part been due to thermal depletion of the mantle below the initial 145-105 m.y. magmatic arc forcing a down dip migration of isotherms and partial melting (that is, constant dip-variable depth subduction in the sense of Keith, 1978).

About 85 m.y. ago global plate reorganization and increased

convergence rates forced variable dip subduction at the Farallon-North American trench (Coney and Reynolds, 1977; Keith, 1978, 1982; Dickinson and Snyder, 1978; Cross and Pilger, 1978). In contrast to Sevier orogeny Laramide tectonic patterns were very mobile and diachronous reflecting variable dip flattening. During the early part of Laramide orogeny before anomalously low angle subduction was achieved about 55 m.y. ago, three major tectonic assemblages were apparent and resembled those of the antecedant Sevier orogeny.

To the west near the trench a decretionary assemblage existed between the arc thermal axis and the trench. Rather than accreting as it had prior to 85 m.y. ago the melange wedge now began to decrete with decreted melange material being transferred laterally beneath the westward advancing North American continental plate. The forearc basin between the magmatic arc and the decreting melange wedge progressively widened, shallowed, and shoaled. Deep level peraluminous magmas now began to be generated by fusion of crustal materials in the decretionary region west of the metaluminous volcanic arc. These magmas intruded the now extinct coastal batholiths of Sevier age and were syntectonic with major southwest-directed shear zones in the overriding North American plate, such as the Peninsular Ranges tectonic zone along the entire eastern edge of the Peninsular Range batholith in southern California.

To the east the eastward edge of the metaluminous magmatic arc began to rapidly migrate eastward (Keith and Reynolds, 1981). The arc itself progressively widened with magmatism becoming increasingly more dispersed with decreasing age because of the increasing width of the arc. East of the arc continent-directed thrust faults also rapidly migrated eastward south of the Colorado Plateau to establish a new orogenic front in the west Texas-Chihuahua tectonic belt about 65 m.y. ago. To the north in the Colorado Plateau region predominantly east-facing uplifts were established throughout the region after 72 m.y. ago and by 70 m.y. ago the east-facing Colorado Front Range uplifts became active in central Colorado (Tweto, 1975; Lawton, 1983).

It is clear from the preceding paragraph that, like the Sevier orogeny, the early Laramide orogeny consisted of three major tectonic packages: 1. a decretionary assemblage near the trench, 2. an axial assemblage represented by the volcanic arc, and 3. the foreland assemblage east of the arc. As the subduction zone progressively flattened, the eastward margin of each of the above assemblages progressively migrated eastward into areas formerly occupied by more easterly assemblages. Consequently, the Laramide-Sevier stratigraphic record in any given area records the progressive, but orderly, overprinting of successively younger assemblages. In effect then, the foreland assemblage which was widest during Sevier orogeny becomes progressively foreshortened during Laramide orogeny and is ultimately replaced

by an extremely wide decretionary zone during late Laramide orogeny.

The ultimate decretionary style of Laramide orogeny fully developed in early to middle Eocene time throughout southwestern North America. It was then that truly large-scale and regionally integrated, spectacular tectonic events occurred. We are only now beginning to appreciate the scale of these phenomena. To the west the melange wedge virtually disappeared from the advancing edge of the North American plate south of San Francisco. By Eocene time the Great Valley forearc basin was extinct as a basin phenomenon. In the former coastal batholith region, the batholith had been uplifted and eroded to expose mesozonal plutons. Fluvial systems depositing Eocene gravels flowed westward across a low relief, peneplanational erosional surface from a continental divide somewhere in western Nevada, the Colorado River region and northwestern Sonora. In north central California these rivers deposited the great Mother Lode placer gold deposits from the eroded 145-105 m.y. Sierra Nevadan arc. In the south the enigmatic Poway Conglomerates accumulated. East of the continental drainage divide a broad, northeast-dipping paleoslope was apparent. Low-energy fluvial systems meandered their way to the northeast and deposited their loads in large internally drained lakes south of the Unita-White River uplift in the Utah-Colorado River region as the Green River and Uinta Formations. North of the Uinta Mountains other deep decretional sedimentary basins developed south and west of the Wind River-Granite Mountain uplifts and the Owl Creek-Casper arch uplift. In effect, the above mentioned uplifts were a response to the attempted underthrusting of the Colorado Plateau beneath the North American craton to the east and north. Right shear along the eastern margin of the Colorado Plateau between Denver, Colorado, and El Paso, Texas, produced structural modification of the former Paleocene, predominantly east-facing, front range uplifts into en echelon fold-uplifts. Echo Park-type basins, as defined by Chapin and Cather (1981), accumulated in the synclinal troughs of the en echelon fold systems.

To the southwest in the southern Arizona California region major ductile deformation and peraluminous magmatism took place at deeper levels within the lithosphere as the crust in this area began to underflow beneath the Colorado Plateau. At this time major ductile, shallowly northeast-dipping, southwest-directed mylonitic zones were formed. These zones were particularly thick where they were injected by peraluminous granitoids. Further to the southwest even more spectacular tectonic developments were taking place in southern California and southwestern Arizona near Yuma. Here major decretion of the North American lithosphere occurred and metagraywackes of probable Franciscan affinity replaced areas formerly occupied by North American plate. These phenomena are presently exposed as the Orocopia-Pelona schist and Chocolate-Vincent thrust fault in uplifted areas adjacent to the

Late Cenozoic transform faults in southern California. Indeed, Franciscan material may have been underthrust much further to the northeast where it now occurs as blue schist, Franciscan-like, eclogite inclusions in the Colorado Plateau diatremes of the Four Corners Region (Helmstaedt and Doig, 1975). The decreted North American lithosphere must also have been transferred laterally beneath the Colorado Plateau region where it may now exist as a deep level, underplated slab as indicated by geophysical evidence. Plate thickening associated with lateral transfer of sialic crustal materials from the west beneath the Colorado Plateau and tectonic fusion of the overriding North American plate with young, hot and therefore buoyant, underthrusting, oceanic Farallon plate produced a major isostatic, epeirogenic uplift response that is manifested by extensive, mid-to late Eocene peneplanational erosion surfaces. All of the above decretional phenomena discussed in the preceding paragraphs are schematically illustrated in Figure 1-C.

Another way to portray the mobilistic nature of Laramide tectonics in the southwestern U. S. is with the aid of time slice paleotectonic maps (Figures 2-7). These maps document in a geographic way the concepts outlined in Figure 1. Perusal of these maps by the interested reader will also reveal that during the flattening process, there appeared to be major changes in plate orientations that produced regional reorientations of structural developments as they migrated eastward. A more detailed synthetic treatment of these maps is in preparation by Keith and Livaccari.

PLATE TECTONIC MODEL

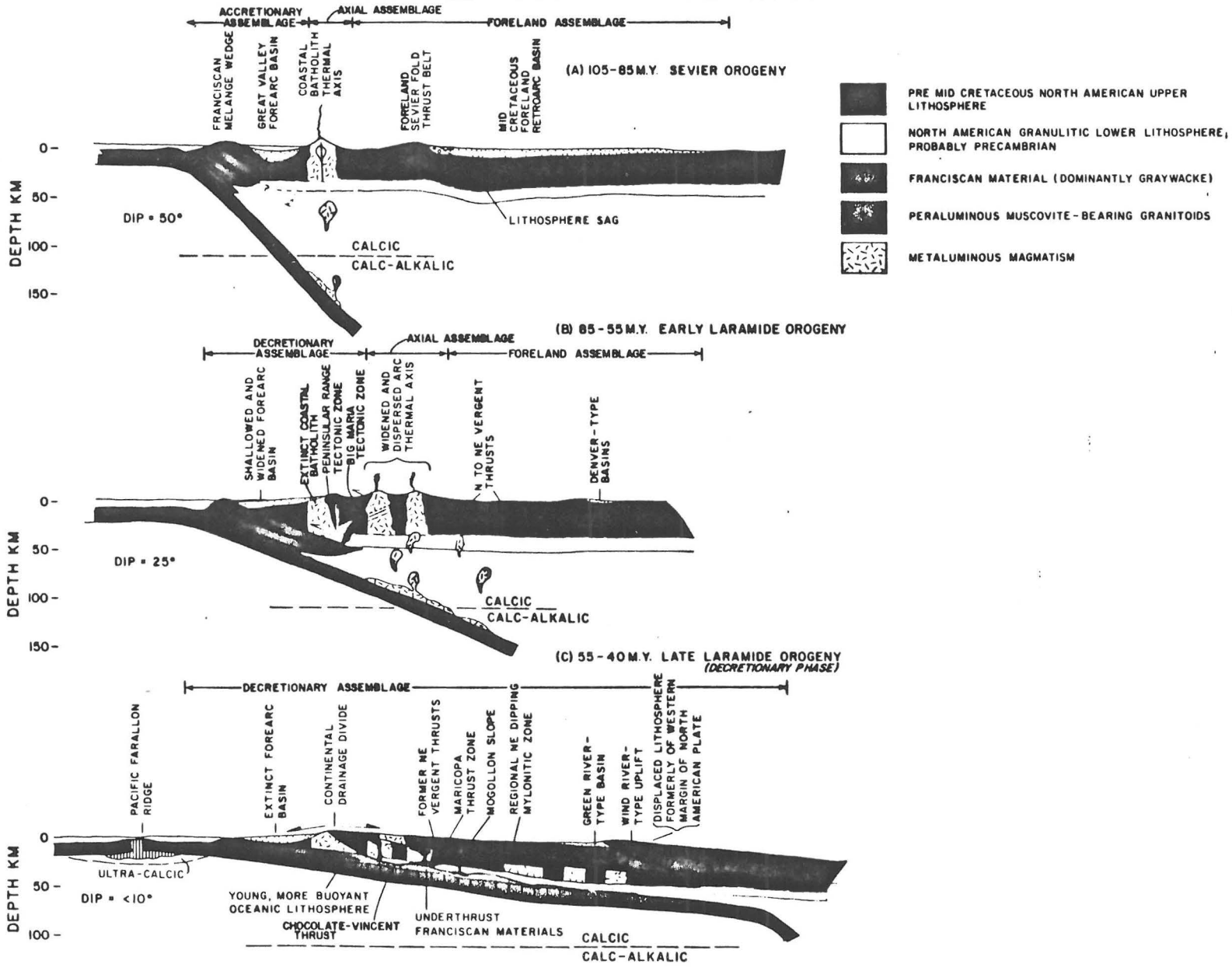

Figure 1

145 - 125 m.y. B.P.

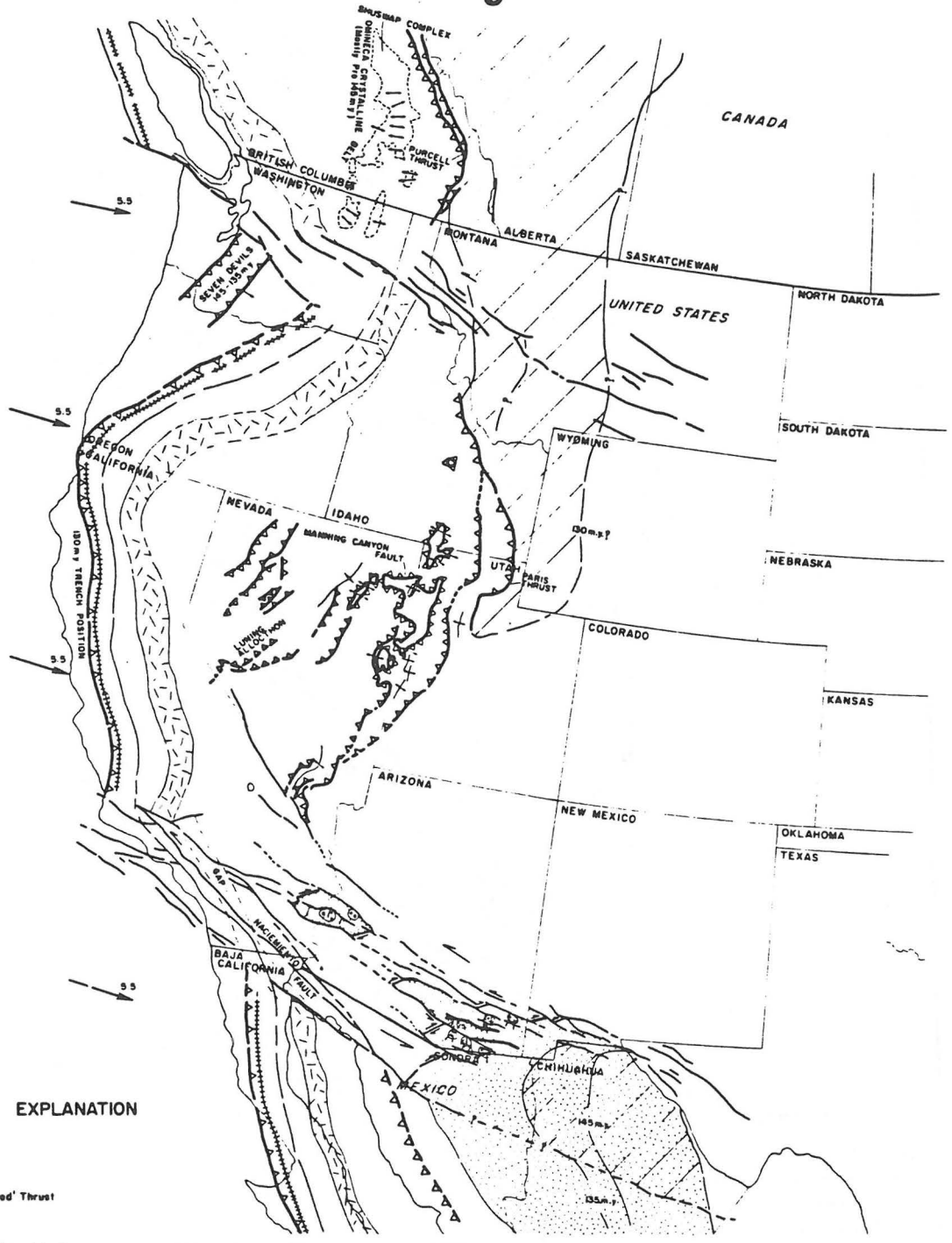

EXPLANATION

STRUCTURE

- 'Thin-skinned' Thrust
- 'Basement-rooted or cored' Thrust
- Decretionary Thrust
- Low-angle normal detachment fault
- High-angle normal fault
- Strike slip fault
- Axis of melange wedge
- Monocline
- Anticline
- Syncline
- Overturned fold

ROCKS

- Retroarc foreland Marine facies
- Regressive lagoonal Delta Plain and coal swamp facies
- Fanglomerate facies
- Fluvial facies; circles indicate conglomeratic facies
- Peraluminous muscovite, garnet-bearing granitoids
- Metaluminous volcanics and plutonics

MISCELLANEOUS

- Area(s) of reduced K-Ar and/or fission track ages
- Dike and/or vein swarm
- Direction of lineation
- Farallon-North America or Kula-North America convergence vectors; Number indicates amount of convergence in cm/yr
- Absolute motion vector for North America plate

N

PALEOTECTONIC MAP for the WESTERN UNITED STATES and VICINITY

Compiled by
Stanley B. Keith and Richard F. Livaccari

APRIL 1983

0 100 200 Miles
0 100 200 Kilometers
SCALE 1:5,000,000

SUE ANGELON

Figure 2

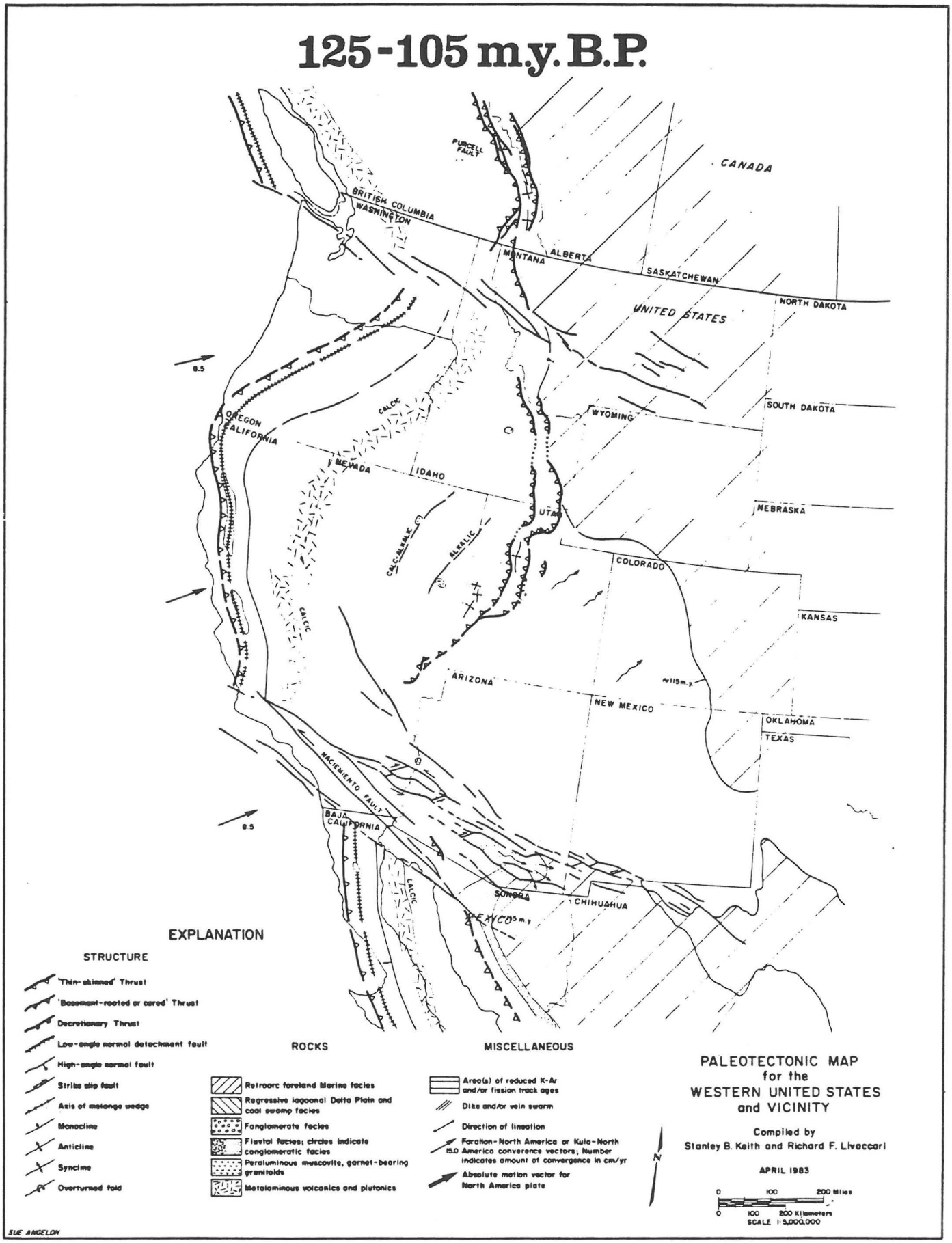
125-105 m.y. B.P.
CANADA
PURCELL FAULT
BRITISH COLUMBIA
WASHINGTON
MONTANA
ALBERTA
SASKATCHEWAN
NORTH DAKOTA
UNITED STATES
SOUTH DAKOTA
WYOMING
OREGON
CALIFORNIA
NEVADA
IDAHO
UTAH
NEBRASKA
COLORADO
KANSAS
ARIZONA
NEW MEXICO
OKLAHOMA
TEXAS
MACIMIENTO FAULT
BAJA CALIFORNIA
SONORA
CHIHUAHUA
CALCIC
CALC-ALKALIC
ALKALIC
EXPLANATION
STRUCTURE
'Thin-skinned' Thrust
'Basement-rooted or cored' Thrust
Decretionary Thrust
Low-angle normal detachment fault
High-angle normal fault
Strike slip fault
Axis of melange wedge
Monocline
Anticline
Syncline
Overturned fold
ROCKS
Retroarc foreland Marine facies
Regressive lagoonal Delta Plain and coal swamp facies
Fanglomerate facies
Fluvial facies; circles indicate conglomeratic facies
Peraluminous muscovite, garnet-bearing granitoids
Metaluminous volcanics and plutonics
MISCELLANEOUS
Area(s) of reduced K-Ar and/or fission track ages
Dike and/or vein swarm
Direction of lineation
Farallon-North America or Kula-North America convergence vectors; Number indicates amount of convergence in cm/yr
Absolute motion vector for North America plate
N
PALEOTECTONIC MAP
for the
WESTERN UNITED STATES
and VICINITY
Compiled by
Stanley B. Keith and Richard F. Livaccari
APRIL 1983
0 100 200 Miles
0 100 200 Kilometers
SCALE 1:5,000,000
SUE ANGELON

Figure 3

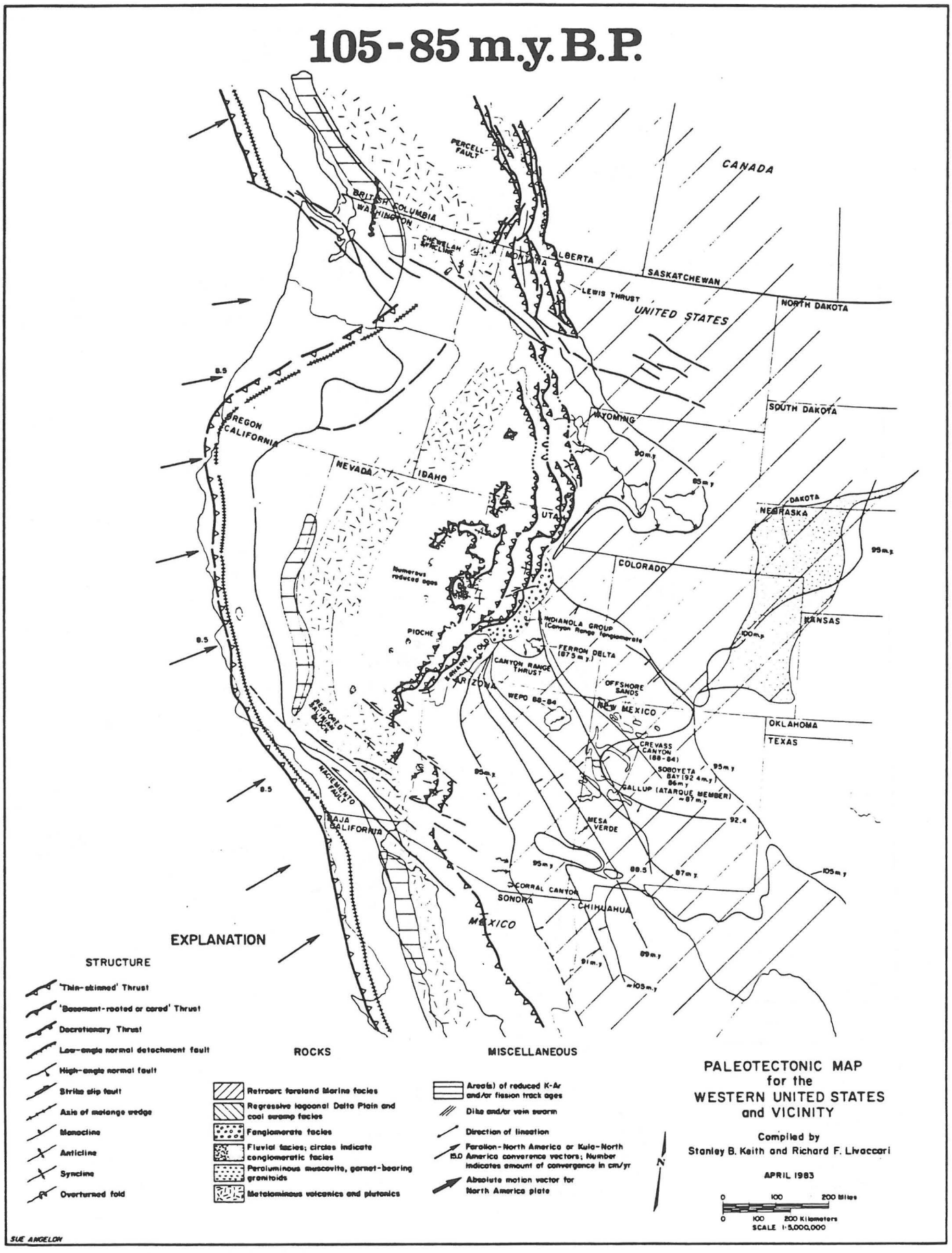
105-85 m.y. B.P.
CANADA
PERCELL FAULT
BRITISH COLUMBIA
WASHINGTON
CHEWELAH SYNCLINE
ALBERTA
SASKATCHEWAN
LEWIS THRUST
UNITED STATES
NORTH DAKOTA
SOUTH DAKOTA
WYOMING
OREGON
CALIFORNIA
NEVADA
IDAHO
UTAH
COLORADO
NEBRASKA
DAKOTA
KANSAS
OKLAHOMA
TEXAS
NEW MEXICO
ARIZONA
Numerous reduced ages
PIOCHE
INDIANOLA GROUP (Canyon Range conglomerate)
FERRON DELTA (87.5 m.y.)
CANYON RANGE THRUST
KINGMAN FOLD
OFFSHORE SANDS
WEPO 88-84
CREVASS CANYON (88-84)
SOBOYETA BAY (92.4 m.y.)
GALLUP (ATARQUE MEMBER) ~87 m.y.
MESA VERDE
CORRAL CANYON
SONORA
CHIHUAHUA
MEXICO
RESTORED SAN ANDREAS BLOCK
NACIMIENTO FAULT
BAJA CALIFORNIA
EXPLANATION
STRUCTURE
'Thin-skinned' Thrust
'Basement-rooted or cored' Thrust
Decretionary Thrust
Low-angle normal detachment fault
High-angle normal fault
Strike slip fault
Axis of melange wedge
Monocline
Anticline
Syncline
Overturned fold
ROCKS
Retroarc foreland Marine facies
Regressive lagoonal Delta Plain and coal swamp facies
Fanglomerate facies
Fluvial facies; circles indicate conglomeratic facies
Peraluminous muscovite, garnet-bearing granitoids
Metaluminous volcanics and plutonics
MISCELLANEOUS
Area(s) of reduced K-Ar and/or fission track ages
Dike and/or vein swarm
Direction of lineation
Farallon-North America or Kula-North America convergence vectors; Number indicates amount of convergence in cm/yr
Absolute motion vector for North America plate
N
PALEOTECTONIC MAP for the WESTERN UNITED STATES and VICINITY
Compiled by
Stanley B. Keith and Richard F. Livaccari
APRIL 1983
0 100 200 Miles
0 100 200 Kilometers
SCALE 1:5,000,000
SUE ANGELON

Figure 4

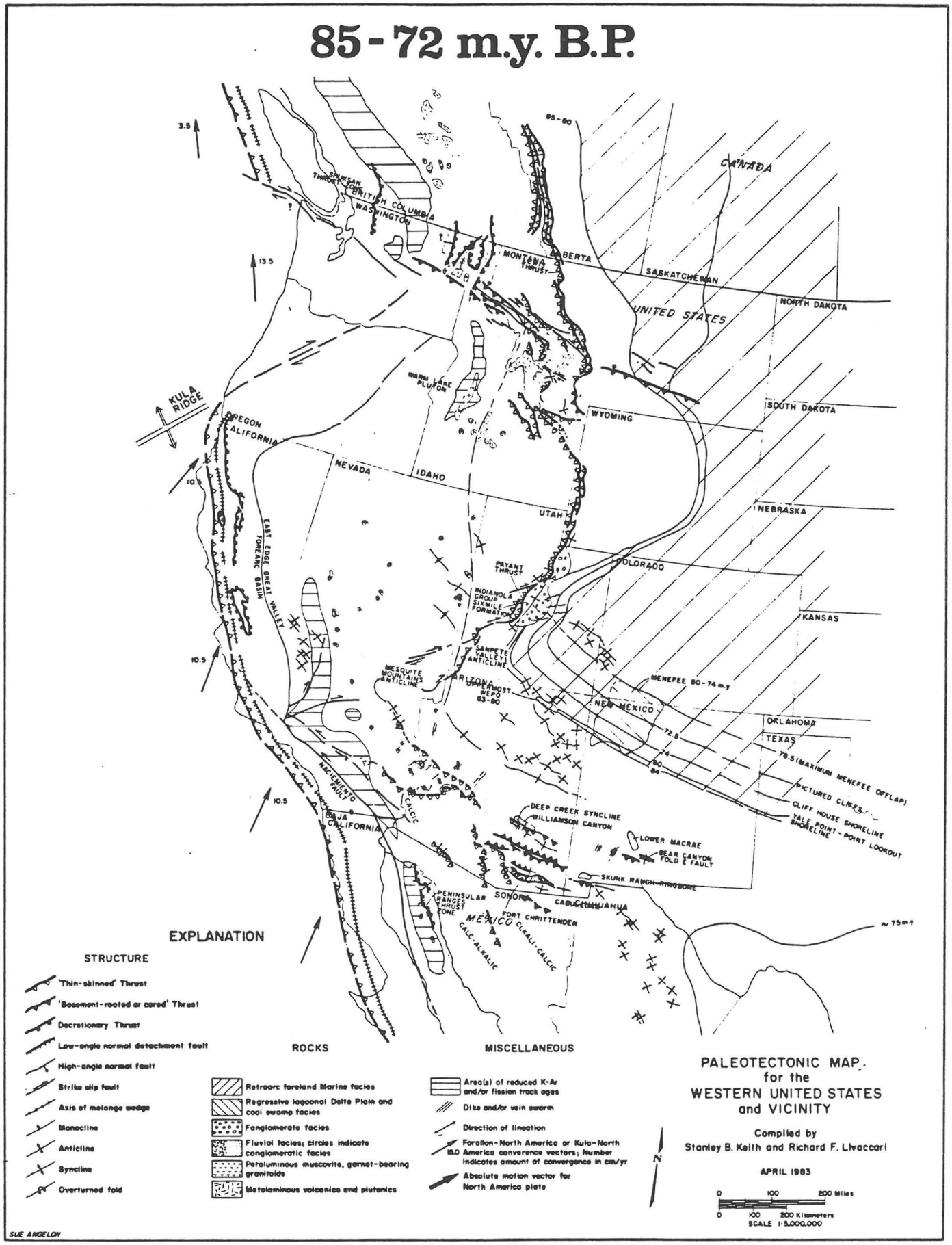
85-72 m.y. B.P.
CANADA
BRITISH COLUMBIA
WASHINGTON
MONTANA
ALBERTA
SASKATCHEWAN
NORTH DAKOTA
UNITED STATES
SOUTH DAKOTA
WYOMING
NEBRASKA
COLORADO
KANSAS
OKLAHOMA
TEXAS
NEW MEXICO
ARIZONA
NEVADA
IDAHO
UTAH
OREGON
CALIFORNIA
BAJA CALIFORNIA
SONORA
CHIHUAHUA
MEXICO
KULA RIDGE
MONTANA THRUST
SANPETE VALLEY ANTICLINE
MESQUITE MOUNTAINS ANTICLINE
MACIMIENTO FAULT
DEEP CREEK SYNCLINE
WILLIAMSON CANYON
LOWER MACRAE
BEAR CANYON FOLD & FAULT
SKUNK RANCH-RINGBONE
FORT CRITTENDEN
PENINSULAR RANGES THRUST ZONE
CALC-ALKALIC
ALKALI-CALCIC
MENEFEE 80-74 m.y.
78.5 (MAXIMUM MENEFEE OFFLAP)
PICTURED CLIFFS
CLIFF HOUSE SHORELINE
YALE POINT - POINT LOOKOUT SHORELINE
EXPLANATION
STRUCTURE
'Thin-skinned' Thrust
'Basement-rooted or cored' Thrust
Decretionary Thrust
Low-angle normal detachment fault
High-angle normal fault
Strike slip fault
Axis of melange wedge
Monocline
Anticline
Syncline
Overturned fold
ROCKS
Retroarc foreland Marine facies
Regressive lagoonal Delta Plain and coal swamp facies
Fanglomerate facies
Fluvial facies; circles indicate conglomeratic facies
Peraluminous muscovite, garnet-bearing granitoids
Metaluminous volcanics and plutonics
MISCELLANEOUS
Area(s) of reduced K-Ar and/or fission track ages
Dike and/or vein swarm
Direction of lineation
Farallon-North America or Kula-North America convergence vectors; Number indicates amount of convergence in cm/yr
Absolute motion vector for North America plate
PALEOTECTONIC MAP for the WESTERN UNITED STATES and VICINITY
Compiled by
Stanley B. Keith and Richard F. Livaccari
APRIL 1983
0 100 200 Miles
0 100 200 Kilometers
SCALE 1:5,000,000
SUE ANGELON

Figure 5

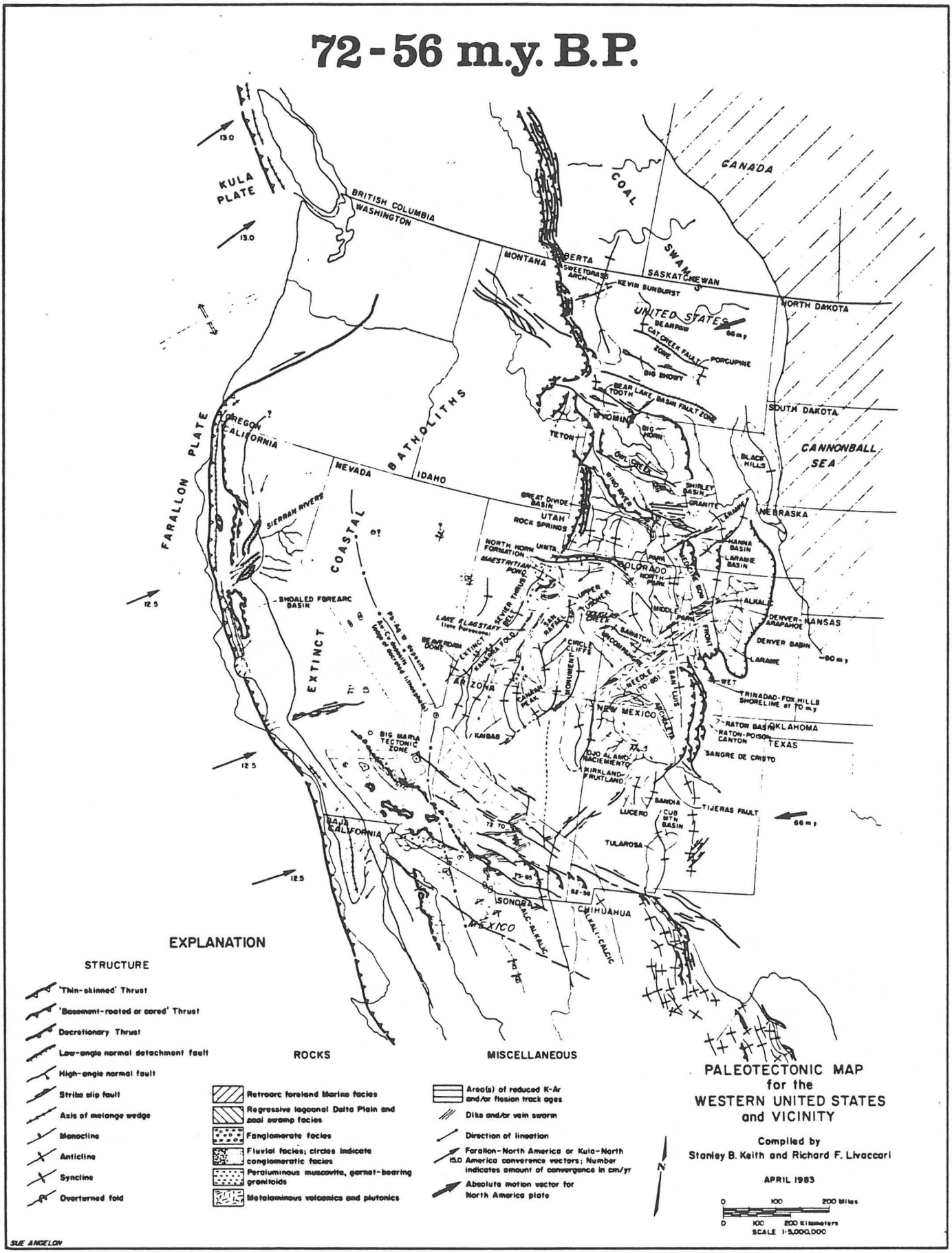
72 - 56 m.y. B.P.
KULA PLATE
FARALLON PLATE
BRITISH COLUMBIA
WASHINGTON
OREGON
CALIFORNIA
NEVADA
IDAHO
MONTANA
ALBERTA
SASKATCHEWAN
CANADA
COAL SWAMP
NORTH DAKOTA
SOUTH DAKOTA
NEBRASKA
UNITED STATES
CANNONBALL SEA
BATHOLITHS
COASTAL
EXTINCT
SMOALED FOREARC BASIN
SIERRAN RIVERS
SWEETGRASS ARCH
KEVIN SUNBURST
BEARPAW
CAT CREEK FAULT ZONE
PORCUPINE
BIG SNOWY
BEAR LAKE BASIN FAULT ZONE
WYOMING
TETON
BIG HORN
CHEYENNE
BLACK HILLS
SHIRLEY BASIN
GRANITE
LARAMIE
GREAT DIVIDE BASIN
WIND RIVER
UTAH
ROCK SPRINGS
NORTH HORN FORMATION
UINTA
MAESTRICHTIAN POND
COLORADO
NORTH PARK
PARK
FRONT
HANNA BASIN
LARAMIE BASIN
ALKALI
DENVER-ARAPAHOE
DENVER BASIN
LARAMIE
WET
TRINIDAD-FOX HILLS SHORELINE at 70 m.y.
LAKE FLAGSTAFF (lime Paleocene)
BEAVERHEAD DOME
EXTINCT
RANKIN FOLD
DENVER THRUST BELT
SAN RAFAEL
UPPER
LOWER
DOUGLAS CREEK
WASATCH
MIDDLE
CIRCLE CLIFFS
MONUMENT
ARIZONA
CHAIN PEAK
KAIBAB
NEW MEXICO
NACIMIENTO
SAN LUIS
NEEDLE (TO 80)
RATON BASIN
OKLAHOMA
RATON-POISON CANYON
TEXAS
SANGRE DE CRISTO
DUO ALAMO
MIRKLAND-FRUITLAND
LUCERO
SANDIA
CUB MTN BASIN
TIJERAS FAULT
TULAROSA
BIG MARIA TECTONIC ZONE
BAJA CALIFORNIA
SONORA
MEXICO
CHIHUAHUA
CALI-ALKALI-CALCIC
ALKALI-CALCIC
13.0
12.5
60 m.y.
66 m.y.
EXPLANATION
STRUCTURE
'Thin-skinned' Thrust
'Basement-rooted or cored' Thrust
Decretionary Thrust
Low-angle normal detachment fault
High-angle normal fault
Strike slip fault
Axis of melange wedge
Monocline
Anticline
Syncline
Overturned fold
ROCKS
Retroarc foreland Marine facies
Regressive lagoonal Delta Plain and coal swamp facies
Fanglomerate facies
Fluvial facies; circles indicate conglomeratic facies
Peraluminous muscovite, garnet-bearing granitoids
Metaluminous volcanics and plutonics
MISCELLANEOUS
Area(s) of reduced K-Ar and/or fission track ages
Dike and/or vein swarm
Direction of lineation
Farallon-North America or Kula-North America convergence vectors; Number indicates amount of convergence in cm/yr
Absolute motion vector for North America plate
N
PALEOTECTONIC MAP
for the
WESTERN UNITED STATES
and VICINITY
Compiled by
Stanley B. Keith and Richard F. Livaccari
APRIL 1983
0 100 200 Miles
0 100 200 Kilometers
SCALE 1:5,000,000
SUE ANGELON

Figure 6

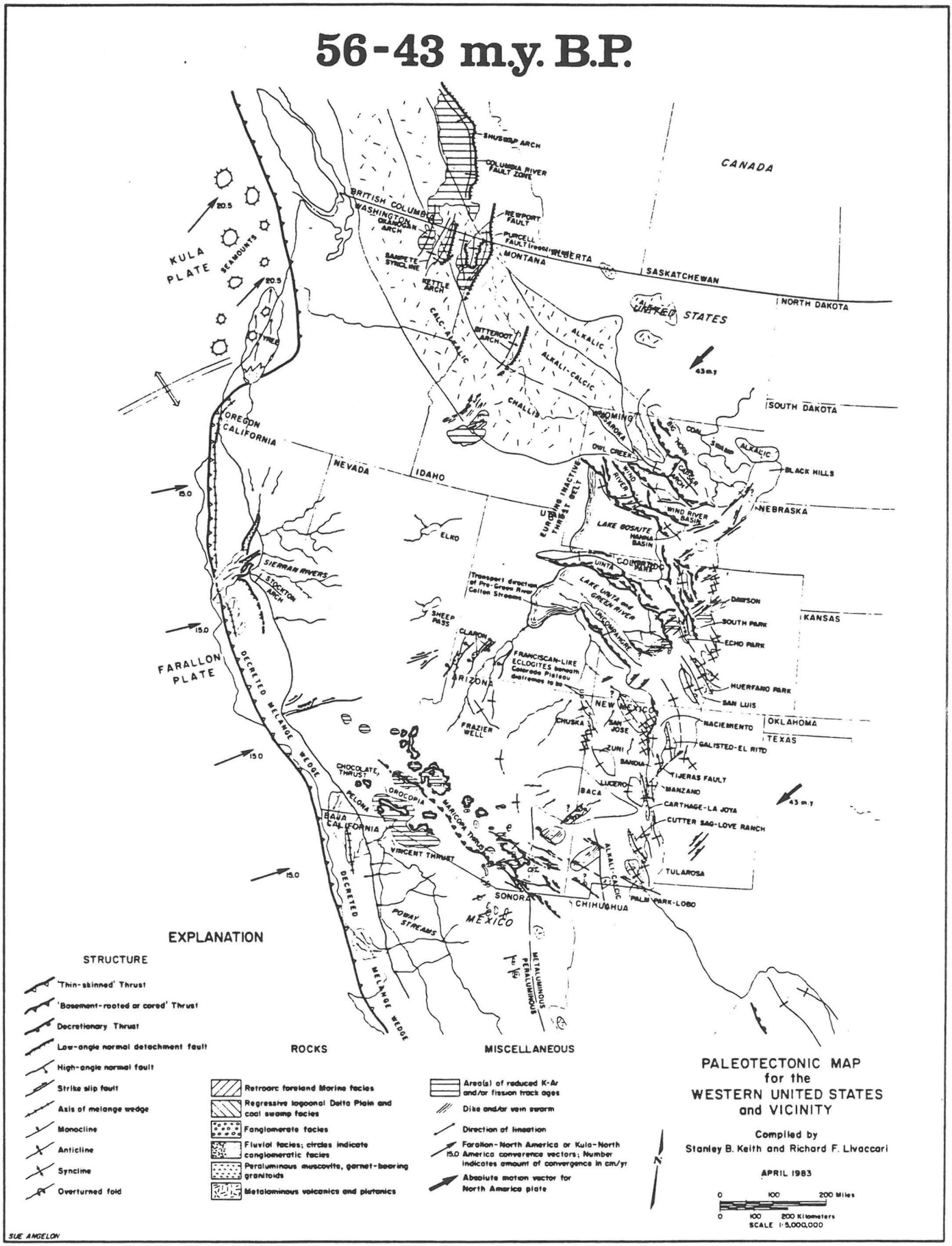
56-43 m.y. B.P.
CANADA
SHUSWAP ARCH
COLUMBIA RIVER FAULT ZONE
BRITISH COLUMBIA
WASHINGTON
OKANOGAN ARCH
NEWPORT FAULT
PURCELL FAULT
ALBERTA
MONTANA
SASKATCHEWAN
NORTH DAKOTA
SANPETE SYNCLINE
KETTLE ARCH
CALC-ALKALIC
BITTEROOT ARCH
ALKALIC
ALKALI-CALCIC
UNITED STATES
KULA PLATE
SEAMOUNTS
20.5
THRB
43 m.y.
CHALLIS
WYOMING
SOUTH DAKOTA
OREGON
CALIFORNIA
NEVADA
IDAHO
OWL CREEK
WIND RIVER
CASPER ARCH
ALKALIC
BLACK HILLS
EUREKA-SEVIER INACTIVE THRUST BELT
NEBRASKA
WIND RIVER BASIN
LAKE GOSAUTE
HANNA BASIN
ELKO
UINTA
COLORADO PLATEAU
SIERRAN RIVERS
STOCKTON ARCH
Transport direction of Pre-Green River Colton Streams
LAKE UINTA and GREEN RIVER
UNCOMPAHGRE
DAWSON
SOUTH PARK
ECHO PARK
KANSAS
SHEEP PASS
CLARON
FARALLON PLATE
15.0
FRANCISCAN-LIKE ECLOGITES beneath Colorado Plateau
ARIZONA
HUERFANO PARK
SAN LUIS
NEW MEXICO
OKLAHOMA
TEXAS
RACIMENTO
GALISTEO-EL RITO
DECRETED MELANGE WEDGE
FRAZIER WELL
CHUSKA
SAN JOSE
ZUNI
BANDA
TIJERAS FAULT
MANZANO
CHOCOLATE THRUST
PELONA
OROCOPIA
MARICOPA THRUST
LUCERO
BACA
CARTHAGE-LA JOYA
CUTTER SAG-LOVE RANCH
BAJA CALIFORNIA
VINCENT THRUST
TULAROSA
ALKALI-CALCIC
PALM PARK-LOBO
SONORA
CHIHUAHUA
MEXICO
POWAY STREAMS
METALUMINOUS
PERALUMINOUS
EXPLANATION
STRUCTURE
'Thin-skinned' Thrust
'Basement-rooted or cored' Thrust
Decretionary Thrust
Low-angle normal detachment fault
High-angle normal fault
Strike slip fault
Axis of melange wedge
Monocline
Anticline
Syncline
Overturned fold
ROCKS
Retroarc foreland Marine facies
Regressive lagoonal Delta Plain and coal swamp facies
Fanglomerate facies
Fluvial facies; circles indicate conglomeratic facies
Peraluminous muscovite, garnet-bearing granitoids
Metaluminous volcanics and plutonics
MISCELLANEOUS
Area(s) of reduced K-Ar and/or fission track ages
Dike and/or vein swarm
Direction of intrusion
Farallon-North America or Kula-North America convergence vectors; Number indicates amount of convergence in cm/yr
Absolute motion vector for North America plate
N
PALEOTECTONIC MAP for the WESTERN UNITED STATES and VICINITY
Compiled by
Stanley B. Keith and Richard F. Livaccari
APRIL 1983
0 100 200 Miles
0 100 200 Kilometers
SCALE 1:5,000,000
SUE ANGELON

Figure 7

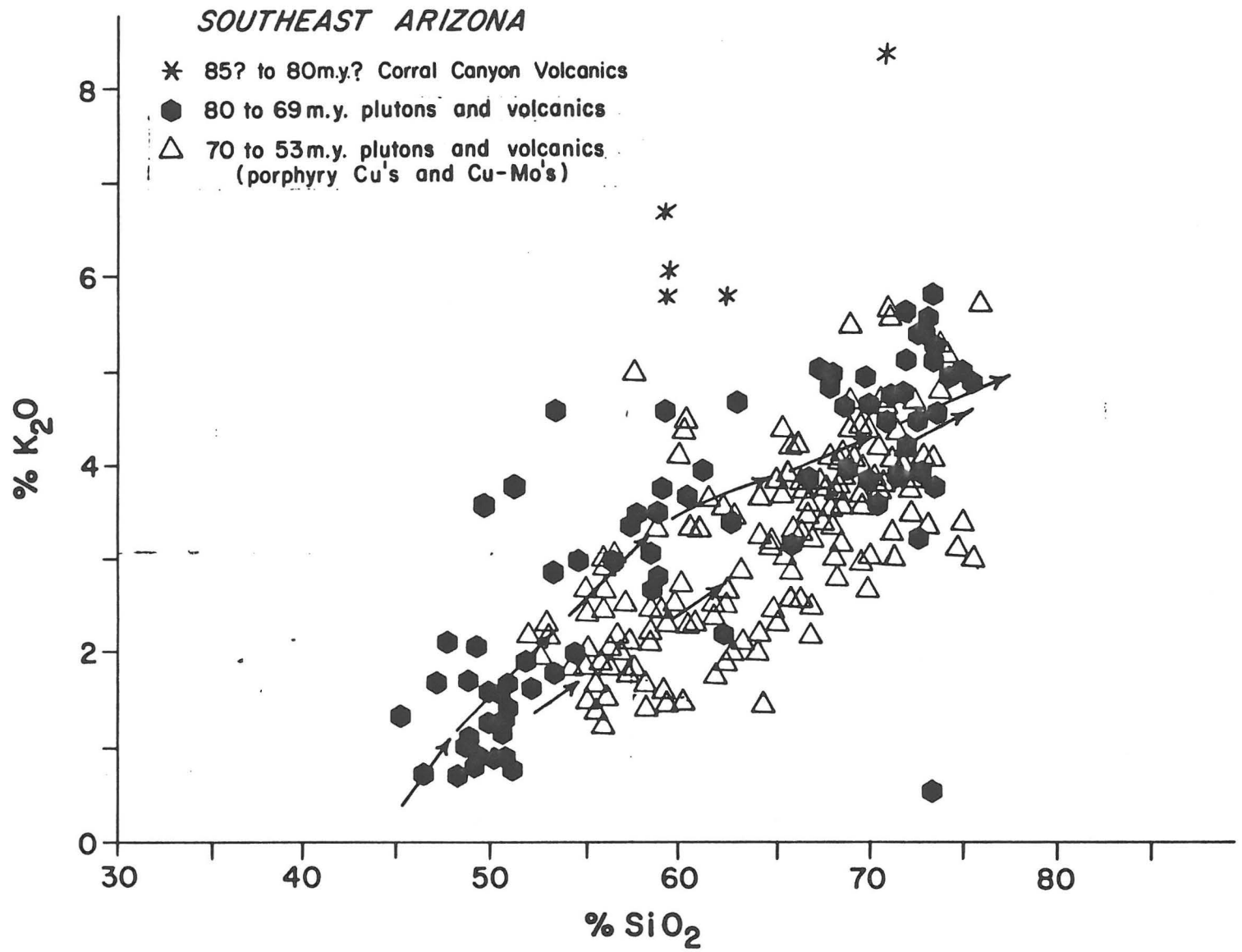
SOUTHEAST ARIZONA
85? to 80m.y.? Corral Canyon Volcanics
80 to 69 m.y. plutons and volcanics
70 to 53m.y. plutons and volcanics (porphyry Cu's and Cu-Mo's)
% K2O
% SiO2
0
2
4
6
8
30
40
50
60
70
80

Figure 8.

[Section 3]

Drewes and Finnel
Box Canyon Road Log

Drewes & Finnell, 1968, Box Canyon section of road log:
Ariz. Geol. Soc. Guidebook III.

MESOZOIC STRATIGRAPHY AND LARAMIDE TECTONICS OF PART OF THE SANTA RITA AND EMPIRE MOUNTAINS SOUTHEAST OF TUCSON, ARIZONA

FIELD TRIP II

By

Harald Drewes and Tommy L. Finnell
U.S. Geological Survey, Denver, Colorado

INTRODUCTION

The Santa Rita and Empire Mountains are the nearest ranges southeast of Tucson; their northermost ends lie only 20 miles away. Much of the geology in this area is typical of a larger region lying roughly between Tucson, Nogales, Benson, and Bisbee, in which the U. S. Geological Survey has almost completed a series of detailed maps and related stratigraphic and structural studies during the last 8 years. J. R. Cooper, S.C. Creasey, P.T. Hayes, R.B. Raup, Jr., F. S. Simons, and the present authors have been, or are still, engaged in this work.

This field trip is planned to illustrate two of the more important geologic features, whose recognitions are results of this work: (1) a relatively complete Mesozoic stratigraphy, and (2) a complex 3-phased deformation during the Laramide orogeny. Although not all areas investigated include a fully developed Mesozoic sequence or evidence of the entire Laramide history, most areas contain some parts of the sequence or some aspects of this history. In a few areas that will not be visited on this field trip because of the greater distance from Tucson, certain rocks or structural relations are even more clearly illustrated than they are in the northern Santa Rita and Empire Mountains.

Geology

In brief, the geologic record of the region begins with Precambrian Pinal Schist into which coarsely porphyritic granitic rocks were intruded. During Paleozoic time about 5,000 feet of marine sediments were deposited discontinuously. The largest disconformities in this sequence occur between Cambrian and Devonian strata, between Devonian and Mississippian strata, and between Mississippian and Pennsylvanian strata. By the middle of the Permian the seas had left the area.

During the Triassic and possibly also parts of the Permian and Jurassic a thick pile of rhyolitic and dacitic volcanics were deposited in a subaerial environment. The volcanics contain intercalated conglomerate and eolian sandstone, and are associated with red beds. More rhyolitic tuff overlies the red beds. The age of these rocks is obtained from radiometric determinations and is supported by geologic relations to other dated rocks. During Late (?) Triassic time a monzonite pluton was emplaced and during Middle Jurassic time several major granite plutons were also emplaced. The earliest hints of post-Paleozoic faulting go back to this interval.

During latest Jurassic or earliest Cretaceous time the region was strongly uplifted. Rhyolitic to dacitic volcanic rocks were deposited in several ranges and, on them, sedimentary rocks many thousands of feet thick were deposited in much of the region during the late Early Cretaceous; most widespread and best dated of these deposits is the Bisbee Formation (Bisbee Group to the southeast).

During early Late Cretaceous we find the earliest signs of the first phase of the Laramide orogeny in the form of a major unconformity in the sedimentary record, and of northeast-southwest-directed compression and, locally at least, thrust faults in the tectonic record. During the late Late Cretaceous many more thousands of feet of sedimentary rocks were deposited, apparently in local basins. These rocks are also folded by northeast-southwest compression, providing the latest signs of the first phase of the orogeny. Toward the end of the Late Cretaceous dacitic breccia and rhyodacitic welded tuff were spread, apparently from several centers, as forerunners of the major magmatic activity that followed. All the present ranges received some plutonic intrusions of granitic rocks during the next phase (or phases) of the Laramide and in some ranges there are numerous stocks and many rock types represented. In most ranges, too, thrusting, normal faulting and tear faulting occurred during the end of the Cretaceous and the beginning of the Tertiary.

In the northern Santa Rita Mountains the geologic record also permits a distinction between a second and a third phase of the Laramide orogeny, both involving northwest-directed tear and thrust faulting. Quartz monzonite plutons were injected between these phases and quartz latite porphyry were intruded after the third phase, so that these phases are datable by radiometric means.

During the field trip we will stop at outcrops representative of the major groups of Mesozoic volcanics and sedimentary rocks: The Triassic volcanics, the red beds associated with them, the Bisbee Formation, the Upper Cretaceous sedimentary rocks, and the uppermost Cretaceous volcanics. We will also stop to see evidence of northeast-directed deformation and the evidence to separate the second from the third phase involving northwest-directed tear and thrust faults. The map pattern of folds in the Lower Cretaceous rocks truncated by unconformably overlying uppermost Cretaceous rocks and the change in the stress picture between phase 1 and 2 must suffice to demonstrate their temporal separation, for outcrops demonstrating the early Late Cretaceous unconformity are not accessible by bus.

ROAD LOG

Leave Tucson, driving east on Interstate Highway 10. Road log begins at junction of Highway 10 with State Highway 83. Figure 1 shows route of field trip and general geology.

Segmental mileage	Cumulative mileage	
0.0	0.0	Junction. TURN RIGHT (S) on State Highway 83, toward Sonoita. Empire Mountains on the left (E) are made up of Paleozoic and Mesozoic sedimentary rocks in a complexly faulted anticline. The core of the anticline is composed of a quartz monzonite stock of Laramide(?) age, which cuts across the Empire thrust fault along the western flank of the mountains. Mt. Fagan, at the north end of the Santa Rita Mountains, on the right (W) consists of Upper Cretaceous dacitic and rhyodacitic volcanic rocks that rest with angular discordance upon folded sedimentary rocks of the Bisbee Formation. In the valley between the Santa Rita and Empire Mountains the Upper Cretaceous volcanic rocks lap across the Empire thrust fault.
1.6	1.6	Roadcuts on right (W) in quartz monzonite of probable early Tertiary age, overlapped to the south by gravel of Tertiary or Quaternary age.
0.5	2.1	Bluffs to left (E) across wash are sedimentary rocks of the Bisbee Formation. In Davidson Canyon, about a mile to the east, these sediments rest unconformably upon diorite gneiss of Precambrian(?) age.
1.4	3.5	Roadcuts in south-dipping rocks of the Bisbee Formation. Hill at 1:00 is part of a west-northwest-trending syncline in quartzites of the Bisbee Formation. Low hill at 11:30 is Permian Concha Limestone and Rainvalley Formation in upper plate of the Empire thrust fault.
0.9	4.4	Enter area shown on figure 1.
1.6	5.1	Empire thrust fault is here concealed. Permian limestone in upper plate strikes north and dips 20° E. Bisbee sedimentary rocks in lower plate strike west and dip steeply north.
0.6	5.7	SLOW for sharp turn to left off highway.
0.1	5.8	Turn left (E) onto old highway and proceed 0.5 mile to STOP 1.
		Hills on right (E) side of road are capped by Glance(?) equivalent that is cut by a dike of quartz latite porphyry.

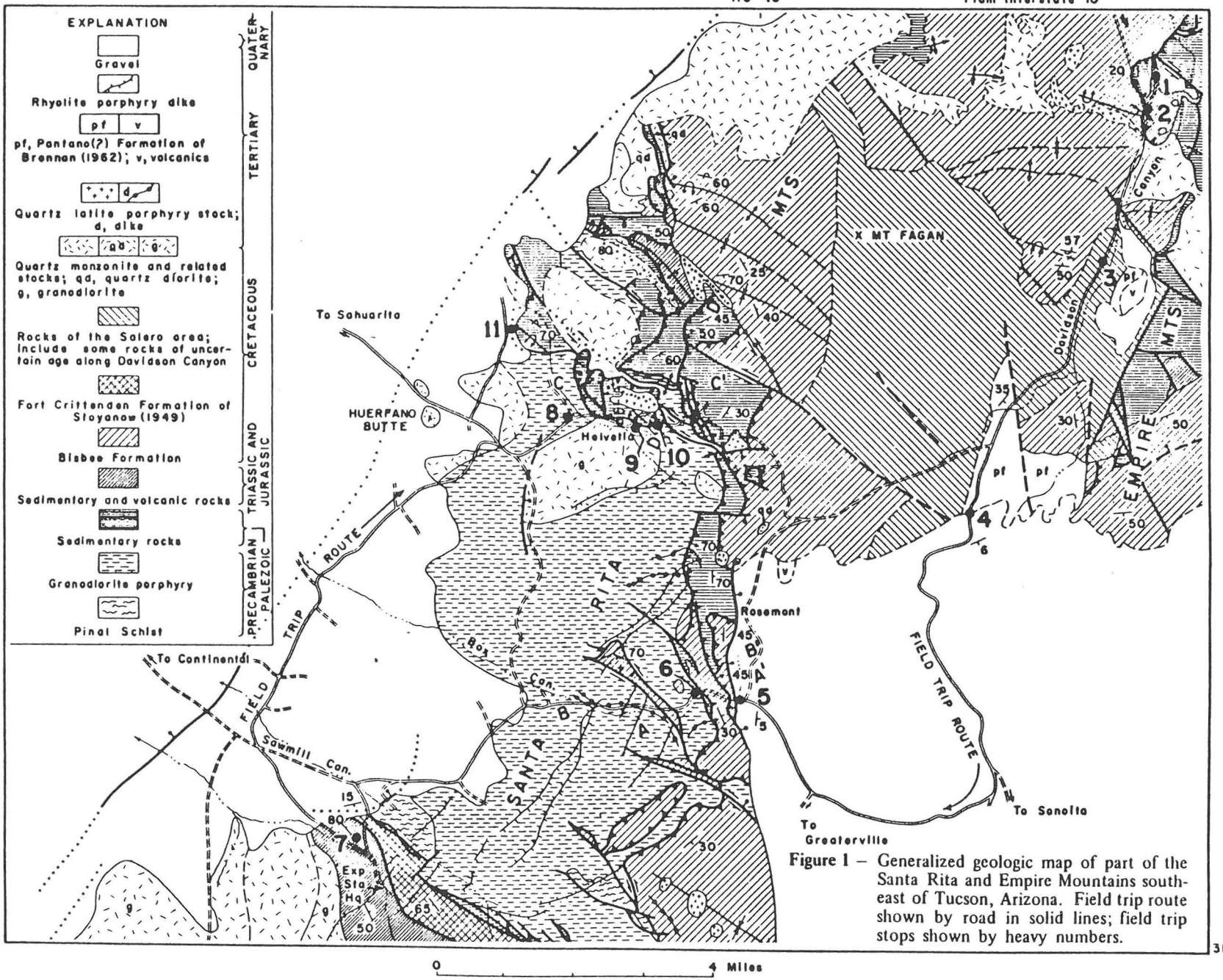

Figure 1 – Generalized geologic map of part of the Santa Rita and Empire Mountains southeast of Tucson, Arizona. Field trip route shown by road in solid lines; field trip stops shown by heavy numbers.

STOP 1. Sedimentary rocks of probable Triassic age are exposed in roadcuts and in the slopes leading down to the arroyo to the west. They rest on the Rainvalley Formation (Permian) that forms the dip slope of the hill west of the arroyo, and they are overlain by limestone pebble conglomerate that is probably correlative to the Glance Conglomerate. Uplift, faulting, and erosion preceded deposition of the Glance(?) in the area so that only about 250 feet of the Triassic(?) sedimentary rocks remain. About a mile east-northeast, a thicker section is exposed that includes some latitic tuff in the upper part.

If the bus cannot turn around at this stop, it may proceed 0.4 mile to borrow pit on left, turn around, and return to pick up party at STOP 1. Return to Highway 83 and STOP 2. (Road log mileage does not include detour for STOP 1.)

STOP 2. Roadcuts in shaly rocks of the Bisbee Formation and conglomeratic mudstone of Triassic(?) age. The Empire thrust fault zone between them dips 5-10° E. Rhyolitic dikes with conspicuous flow banding seem to cut the fault zone.

0.2	6.0	Pediment gravel to left (E) across Davidson Canyon rests on eroded surface of quartz monzonite. Foothills of Empire Mountains are synclinal roof pendants of Paleozoic and Mesozoic sedimentary rocks. Hill at 12:00, west of road, is Scherrer Formation (Permian) in the west limb of the syncline. Mesozoic sediments form ridge east of road.
1.1	7.1	Quartz monzonite beneath gravel in roadcut appears to underlie the Scherrer Formation at 1:00.
		For the next 3 miles, the bedrock near the road is of sedimentary and volcanic breccias of intermediate composition of Late Cretaceous age. Some rhyolitic dikes of Tertiary age cut them.
1.4	9.0	STOP 3 (Optional). Park on left (E) at entrance to ranch road. Cuts expose volcanic conglomerate of Late Cretaceous age. Clasts in the conglomerate include sandstone and siltstone derived from the Bisbee Formation.
1.5	10.5	Pantano(?) Formation of mid-Tertiary age of Brennan, (1962) on west side of road, faulted against the Upper Cretaceous volcanic rocks.
0.3	7.4	Prospect pit at 2:30 is in carbonates of the middle member of the Scherrer Formation. The contact with quartz monzonite is a few feet below the prospect. Roadcuts ahead are in a complex of quartz monzonite, quartz latite porphyry, and rhyolite. They contain some inclusions of hornfelsed sedimentary rocks of uncertain age.
0.2	7.6	Dike of quartz latite strikes northwest, and dips 70° SW. The westerly trending ridges at 2:00 are of quartzite beds in the Bisbee Formation, which form an isoclinal syncline overturned to the south. The axial plane of the syncline dips about 55° N.
		Exposures from here to STOP 4 are of the Pantano(?) Formation.
1.0	11.5	Road to Rosemont on right. Dumps of the Rosemont mining district at 2:30 near crest of ridge.
0.2	11.7	Mid-Tertiary conglomerate along road to STOP 4.

0.6	12.3	STOP 4. Unconformable contact of Pliocene and Pleistocene gravel on conglomerate of the mid-Tertiary Pantano(?) Formation. Panorama of the south end of the Empire Mountains to the east across Davidson Canyon. Sediments of the lower part of the Bisbee Formation dip as much as 60° southeast and south in the allochthonous block of the Empire Thrust fault. Between the vantage point and Davidson Canyon sedimentary rocks of the upper part of the Bisbee Formation dip as much as 50° E. in the autochthonous block. Upper Cretaceous volcanic breccia laps across the Empire thrust fault and rests unconformably on the upturned and eroded Bisbee Formation of both blocks, indicating that the Late Cretaceous volcanism occurred after the displacement of the Empire thrust fault. Escarpment to south is eroded in Pliocene and Pleistocene gravels that are well-exposed along the road for the next 2 miles. The beds dip as much as 10° SE.
4.7	16.8	Turn right (SW) onto Greaterville and Box Canyon road.
.4	17.2	Turn right (W) at junction, keeping on main road.
1.6	18.8	Slow for Thurber Ranch.
1.3	20.1	Turn right (NW) at Greaterville junction, keeping on Box Canyon road.
1.4	21.5	Outcrops to left (SW) are of Pliocene and Pleistocene gravel, slightly tilted eastward past their initial dip.
.4	21.9	STOP 5. Bisbee Formation. Glance(?) equivalent in a limestone pebble facies, crops out south of the wash. Maroon siltstone and arkosic sandstone of the Morita(?) equivalent (Willow Canyon Formation of the Bisbee Group of Tyrrell 1964) dip eastward in roadcuts to the west. Instead of underlying the Morita (?) as is normal, the Glance(?) equivalent is thrust over that formation, where it dips westward. Small slivers of Devonian Martin Formation (not shown on generalized geologic map) are caught along the thrust fault. One such sliver is exposed low on the slope north of the road. Half a mile to the north, Mississippian Escabrosa Limestone lies along the thrust fault. The normal fault between the probable Glance and the Pliocene and Pleistocene gravel to the east is exposed in a small prospect north of the road. See sections A-A′ and B-B′ of figure 2.
.7	22.6	STOP 6. Bisbee Formation and Precambrian granodiorite. Series of roadcuts from east to west shows, respectively: (a) Morita(?) equivalent (Willow Canyon Formation of Tyrrell 1964) red siltstone and light-gray arkosic grit and sandstone, grading downward into (b) arkose, arkosic conglomerate, and arkosic sedimentary breccia facies of the Glance(?) equivalent and (c) granodiorite source rock of the arkose. Faulting near the base of the Glance is minor and the slice of Cambrian Bolsa Quartzite between the granodiorite and the arkosic conglomerate exposed south of the canyon is probably nearly in place as an erosional remnant beneath the pre-Bisbee unconformity. A half mile north of the road there is a large body of Bolsa Quartzite and the overlying Cambrian Abrigo Formation in a similar position between granodiorite and Glance(?). The rapid change in facies of the Glance(?) between STOPS 1 and 2 may be partly due to tectonic telescoping, but it may also be due to rapid initial changes that reflect local deposition around hills of pre-Bisbee age of various provenance. The age of the granodiorite has been interpreted from field evidence either as Jurassic or as Precambrian. Geologic relations used to infer a Jurassic (specifically

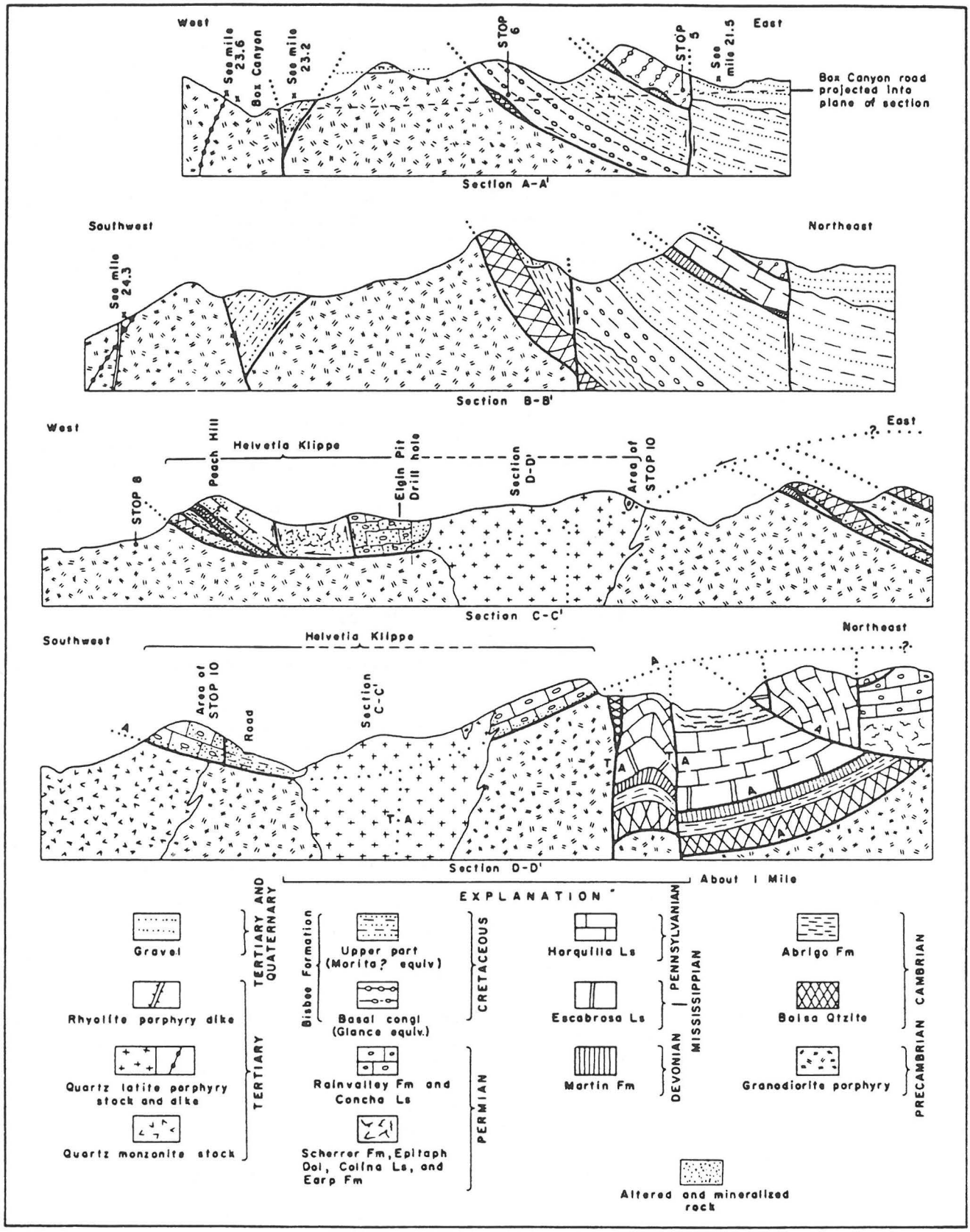

Figure 2 – Diagrammatic structure sections in area shown on figure 1. A-A′ and B-B′ along Box Canyon, C-C′ and D-D′ at Helvetia show approximate endpoints of sections (fig. 1)

a post-Paleozoic–pre-Early Cretaceous) age occur 2 1/2 miles north of Box Canyon, where there is a peculiar mixture of granodiorite and Bolsa Quartzite, a mixture suggestive of flowage of the granodiorite into the quartzite, but presently interpreted as a flowage of remobilized quartzite into the granodiorite. In most places, moreover, the basal part of the Bolsa, a 25-foot thick conglomerate, is present and is parallel to the basal contact. The shearing that does occur along that contact is probably minor south of the complexly deformed area around Helvetia and need only reflect local adjustment as the rocks were tilted and minor thrusting where the overlying Bisbee is folded. About 1 1/4 miles north of STOP 6 some of this shearing may even have predated the deposition of the Bisbee Formation.

Radiometric dates of the granodiorite include:

Pb-alpha	(zircon)	1450 ± 160 m.y.
Sr-Rb	(whole rock)	800 ± 80 m.y.
K-Ar	(biotite)	55.5 ± 1.7 m.y.

These dates are interpreted to mean that the rock was initially crystallized during the Precambrian but that reheating of some rock during the Laramide recrystallized the biotite. Recrystallization of biotite is verified under the microscope.

.6	23.2	Red beds of the Bisbee Formation appear along the road in a graben in the granodiorite. A component of tear faulting is suspected along the bounding faults but can not be unequivocally determined.
.4	23.6	Precambrian granodiorite 200 feet southeast of dry(?) waterfall was sampled for Pb-alpha and Sr-Rb radiometric dates. A thick northeast-trending rhyolite porphyry dike lies north of the road a few hundred yards west of the fall, and a thin quartz latite porphyry dike an additional few hundred yards west of the rhyolite dike.
.7	24.3	Two dikes of rhyolite porphyry (Pb-alpha, 40 ± 10 m.y.; K-Ar, 26.1 ± 0.8 m.y.) are part of a swarm of dikes that fill post-Laramide tension fractures. In the southern part of the Santa Rita Mountains a mineralized quartz vein swarm fills this fracture system. The rhyolite porphyry dikes cut a quartz latite porphyry dike exposed near the switchback 0.1 mile farther west and is again exposed downhill (W) of the switchback. .These dikes form part of an older group, some of which are shoots of the late Laramide quartz latite porphyry plutons.
1.0	25.3	Precambrian granodiorite a few hundred yards below the switchback provides datable biotite (K-Ar, 55.5 ± 1.7 m.y., probably a recrystallization age).
.2	25.5	Turn left (SW) toward Madera Canyon and Continental.
2.4	27.9	Spur to left (SE) is underlain by Pinal Schist intruded by the Precambrian granodiorite. Small white cut on far side of wash about 1/4 mile south of the road exposes a gouge consisting of schist to the east and of the oldest local gravel (Pliocene and Pleistocene) to the west. Nearby, this gravel dips as much as 15° into the range. Similar young range-front faults appear along northeast-trending segments of the Santa Rita and Patagonia Mountains.
.8	28.7	Sharp turn to left (SE) just past the wash of Sawmill Canyon.
.7	29.4	STOP 7. Low roadcuts expose reddish-gray sandstone, conglomerate, and siltstone of the Upper Cretaceous sedimentary rocks. These lie along the Sawmill Canyon

fault zone, which trends southeastward across the range and contains numerous slices of Paleozoic rocks. The nearest small slice of Paleozoic rock lies on the low hill half a mile to the southeast; farther southeast the Paleozoic slices become more numerous and larger, and the stratigraphic sequence of individual fault slices is more complete. The fault zone has had a long and complex history, possibly beginning during Triassic time, and certainly involving movement during early Late Cretaceous and early Tertiary, but ending before the close of the Oligocene. Much movement need only have been vertical but some early thrust faulting occurred, and lateral displacement may also be significant, but has not been conclusively demonstrated.

Walk west to low hill. Bus continues, empty, to the sharp junction, turning right (W). It may be necessary for the bus to turn at the entrance to the corral another .4 mile up the road and then to return to the junction, now turning left (W) toward Continental.

.5	29.9	Road log mileage measurements continue to the sharp junction, and beyond the junction to pickup area but do not include the distance to corral and back.
.5	30.4	STOP 7 (continued). Bus waits at foot of hill for walkers. Outcrops on hill are of rhyodacite welded tuff and a few intercalated thin beds of quartzitic sandstone of the middle member of the formation of Mt. Wrightson (Triassic). Highest ridge to south is an extension of this unit; ridge to south-southeast is capped by andesitic and rhyolite volcanics, thick eolian sandstone, and some pillow lavas, all of the upper member of that formation; spur to west-southwest is underlain by a leucocratic quartz monzonite of Laramide age; and the saddle west of the spur is underlain by a Laramide granodiorite.
.4	30.8	Junction. Keep on main road to right (NW).
1.3	32.1	Junction. CAUTION. Turn right (NE) through cattle guard and then immediately to the left (N) onto Helvetia road.
.6	32.7	Junction. Keep straight ahead (NE) on main road.
.5	33.2	Crossroad. Keep straight ahead (NE).
1.1	34.3	Junction. Keep straight (NE) ahead on main road.
0.4	34.7	Junction. Turn right (NE) on main road crossing Box Canyon wash.
1.7	36.4	Junctions. Keep straight ahead (NE) on main road.
.6	37.0	Precambrian granodiorite east of road contains abundant pods and dikes of aplite. Huerfano Butte and pediment to northwest are underlain by Laramide quartz monzonite. At the butte there also is altered aplite.
1.5	38.5	Junction. Keep straight ahead (E) on Sahuarita-Helvetia road.
.1	38.6	Junction. Turn left (NE) on main road, to Helvetia.
.3	38.9	Cemetery on left (NW) side of road.
.9	39.8	STOP 8. Park at junction. Review geology of west side of Helvetia district. Peach Hill to northeast is underlain, in rising succession, by Precambrian granodiorite, a brown rib of tectonically thinned Cambrian Bolsa Quartzite, slivers of

metamorphosed Cambrian Abrigo Formation and Devonian Martin Formation, and a cap of Pennsylvanian Horquilla Limestone. A major thrust fault underlies the quartzite and minor ones overlie it and overlie the Martin. East of Peach Hill the rocks above this major thrust fault also include Permian and Cretaceous rocks. Together they are here called rocks of the Helvetia klippe.

The Helvetia klippe is 1 1/2 miles long and 3/4 mile wide; its well-exposed basal thrust fault dips inward to form a saucer-shaped surface. Abundant drill holes, as reported by A. M. Heyman and by F. A. Michel in their unpublished MS theses (Univ. of Arizona), provide more detail on the position and configureation of this thrust fault, and show that, where penetrated by drilling, the klippe lies on granitic rock. Present work indicates that the klippe rests on the edges of two stocks of Laramide quartz monzonite (K-Ar 52.2 ± 1.6 m.y.) and probably on a septum of Precambrian granodiorite separating the stocks. The center and eastern end of the klippe is cut by (or contains?) a small quartz latite porphyry stock of late Laramide (56.3 ± 1.7 m.y.) age. Evaluating these ages presents an additional problem, which need not involve a discrepancy with the geologic relations.

Resume trip, keeping to main road (E).

0.5	40.3	Junction. Keep to main road, straight ahead (E) and past the ghost town of Helvetia. Production has been largely of Cu, Pb, and Ag, valued at about $4 million between 1908 and 1950.
.2	40.5	Junction. Keep to main road, straight ahead (E).
.2	40.7	STOP 9. Roadcut exposes thrust fault at the base of the Helvetia klippe, here consisting of the Permian Scherrer Formation. The klippe overlies Laramide quartz monzonite (K-Ar 52.2 ± 1.6 m.y.) that underlies the entire basin to the south. Therefore the fault is part of phase 3 of Laramide deformation. Hill to east is capped by the Permian Concha Limestone, a slice of which the road crosses just to the north. Farther along the road to the northeast the Concha is separated from altered rocks of the Bisbee by a northwest-trending vertical fault zone, along which there has been considerable mineralization.
0.4	41.1	STOP 10. Walk up road on hill to the southwest for a review of the geology of the east side of Helvetia district. Range crest to the southeast is underlain by the Precambrian granodiorite, capped by steeply eastward-dipping Bolsa Quartzite. The hill on the range crest to the east, between the roads, is underlain by a small stock of quartz latite porphyry that is suggested by Michel and Heyman to be the root area of the quartz latite porphyry body involved in the Helvetia klippe. The ridge north of this hill is capped by Permian Concha Limestone and Rainvalley Formation. The low hills half a mile to the northeast of STOP 10 contain imbricate thrust slices of lower Paleozoic rocks and of Precambrian granodiorite. These thrust plates truncate several northwest-trending tear faults, a pattern repeated at other places in the district (see fig. 1). Note on the map that other tear faults merge with thrust faults, to show their contemporaneity. Several of the quartz monzonite stocks cut thrust faults and locally are injected along tear faults, thereby concealing portions of the tear. These stocks, then, serve to separate phase 2 from phase 3 of the Laramide orogeny; the one phase of deformation predates the stocks, the other phase of deformation postdates the stocks directly, or postdates the structures that controlled the emplacement of the stocks.

A problem arises here concerning the geologic relations between the quartz latite porphyry stock associated with the Helvetia klippe and the thrust fault beneath the Helvetia klippe. Does the stock cut the thrust fault, or has it been transported in, perhaps from the stock along the range crest to the east? Neither the evidence obtained from a drill hole through the edge of the small outlier of the stock directly north of Helvetia townsite, as cited by Michel and Heyman, nor the relations around the east edge of the stock provide conclusive evidence of the relations. Although the solution of this problem is immaterial to the 3-phase Laramide thesis, it may be important to the explanation of the timing and of the controls of mineral emplacement.

Walking tour of area of tear faults,east edge of Helvetia kilippe, and stock follows.

Resume trip, returning past Helvetia townsite and STOP 8.

2.5	43.6	Junction. Keep right (W) on main road toward Sahuarita.
.1	43.7	Junction. Keep right (NW) on main road toward Sahuarita.
.8	44.5	Crossroad. Turn right (NE).
1.4	45.9	STOP 11. (optional). Park at junction immediately past the cattle guard. Bus turns while group walks north along road about 100 yards to see the overturned fold of Mississippian Escabrosa Limestone and Pennsylvanian Horquilla Limestone. Dark-gray conglomeratic phyllite lies at or near the base of the Horquilla where it is as severely metamorphosed as it is here; elsewhere there are two thin clastic beds 50 to 120 feet above the base. Note that the fold axis strikes parallel to the tear faults of phases 2 and 3, to suggest the fold was formed before the northwest-trending tear faults and their associated thrust faults. The early deformation (deformations?) is geologically dated in 3 situations: (1) In several places in the Santa Rita and Empire Mountains undeformed uppermost Cretaceous volcanics lie unconformably on folded Lower Cretaceous rocks; (2) An unconformity in the northern Huachuca Mountains. 30 miles southeast of Helvetia, places Upper Cretaceous rocks across a tear fault which bounds thrust faults in Lower Cretaceous rocks; (3) Some rocks of Late Cretaceous age in the southern Santa Rita and Huachuca Mountains are folded in a system parallel to the folds in nearby Lower Cretaceous rocks. Phase 1, then, occurred during early Late Cretaceous or slightly later Late Cretaceous time, and it may not be fully synchronous throughout the region.

Return to Sahuarita-Helvetia road.

1.4	47.3	Crossroad. Turn right (NW) on main road.
10.5	57.8	Follow main road to the fields along the Santa Cruz River Valley. Turn left (W).
.7	58.5	Sahuarita. End of field trip. Turn right (N) on Highway 89 for Tucson.

REFERENCES

Brennan, D.J., 1962, Tertiary sedimentary rocks and structures of the Cienega Gap area, Pima County, Arizona: Arizona Geol. Soc. Digest, v. 5, p. 45-58.

Heyman, A.M., 1958, Geology of the Peach-Elgin copper deposit, Helvetia district, Arizona: unpublished MS thesis, Univ. of Arizona.

Michel, F.A., 1959, Geology of the King Mine area, Helvetia, Arizona: unpublished MS thesis, Univ. of Arizona.

Stoyanow, A.A., 1949, Lower Cretaceous stratigraphy in southeast Arizona: Geol. Soc. America Mem. 38, 169 p.

Tyrrell, W.W., 1964, Geology of the Whetstone Mountain area, Cochise and Pima Counties, Arizona [abs.]: Dissert. Abs., v. 25, no. 6, p. 3516.

[Section 4]

Drewes
Helvetia Road Log

Drewes, 1982, Helvetia section of road log: Rocky Mountain Assoc. of Geologists Guidebook.

118.2 Hill at 10:00 marks the west end of the Helvetia klippe. Bear right in next wash, keeping to main road.

118.6 **STOP 8,** Lunch at Helvetia ghost town — Busses may have to remain here (to be determined by drivers at this stop). Very likely after lunch the participants will continue on foot up the road (fig. 24). Beverage vehicle and other cars, possibly carrying the slow walkers, will proceed up the road. Empty busses may proceed 0.7 mi up the road to the turn-around at the saddle, h, to be reboarded after completion of walking tour. See Drewes (1972, pl. 4) for 1:12,000 map of area, and Drewes (1971b) for map coverage at 1:48,000 of the northern end of the Santa Rita Mountains. The Helvetia district was mainly a producer of copper, with also some lead, zinc, silver, and gold.

Road cuts and mine areas along road are in metamorphosed Permian Scherrer Formation (quartzite), Permian Concha Limestone, and Lower Cretaceous Bisbee Group (shale). Slopes across the canyon to the north are underlain by Paleocene quartz latite porphyry and the high hill beyond the porphyry is underlain by more Concha. The sedimentary rocks on that hill (fig. 25) and along the road are in the Helvetia klippe and are thrust faulted upon Precambrian and Paleocene granitic rocks and then intruded by the porphyry.

120.1 All cars park in flat below large Leader Mine dump at 9:00 (where road crosses thrust fault *D* on pl. 4) and all walkers collect. Further walking along route of sketch map of figure 24. The local stratigraphic column is given on figure 26.

a. — Drill site at lower member of the Permian Epitaph Formation, mainly a marlstone and dolomitic siltstone, and some interbedded argillite and limestone. Note the gypsum in tectonic pods. Slope to east is underlain by the Permian Scherrer Formation, mainly a fine-grained very light pinkish gray quartzite or sandstone, and by the overlying Concha Limestone and Rainvalley Formation.

b. — Hill underlain by upended and metamorphosed Horquilla Limestone provides an overview of Paleozoic formations, and of thrust faults and tear faults of Paleocene age (Helvetian, or late phase of the Cordilleran orogeny of this region), shown by the panorama of figure 27.

c. — Thrust-faulted slivers of the Upper Devonian Martin Formation (brown dolomite, limestone, and some sandstone), here much altered to calc-silicate minerals, Middle and Upper Cambrian Abrigo Formation (thin-bedded shale, siltstone, and some limestone), also altered to calc-silicates, and Middle Cambrian Bolsa Quartzite (a coarse-grained, light-gray, brownish- to purplish-gray, slightly arkosic rock). To the west is the northeast corner of the Helvetia klippe again (fig. 28).

d. — Continental Granodiorite thrust slice. Rock is coarse grained and very coarsely porphyritic. It is dated at 1,450 m.y., but may be as old as 1,600-1,700 m.y. Locally, however, its K-Ar age is reset to 55 m.y., the age of the late Cordilleran stocks (Drewes, 1976, p. 9-17).

e. — Second thrust plate of lower Paleozoic formations.

f. — Another slice of the Continental.

g. — Recrystallized Bolsa Quartzite along the Gunsight Notch fault zone, a tear fault bounding the southwest side of some of the thrust plates.

Return to road and walk down to east end of the Helvetia klippe. Car drivers return to vehicles and follow down the road to saddle at east end of Helvetia klippe.

h. — The Paleocene granodiorite stock of the flats south of Helvetia is cut by the thrust fault beneath the klippe, and a quartz latite porphyry stock cuts the klippe, thereby closely dating this phase of faulting at 54-56 m.y. Board busses, or walk back to lunch site if busses do not come up to saddle. Cars may ferry slow walkers.

i. — Road cut of thrust fault beneath klippe located 0.1 mi down road from sharp curve. Lower quartzite member of the Scherrer Formation lies thrust faulted upon Paleocene granodiorite-quartz monzonite. (Resume mileage from mine dump.)

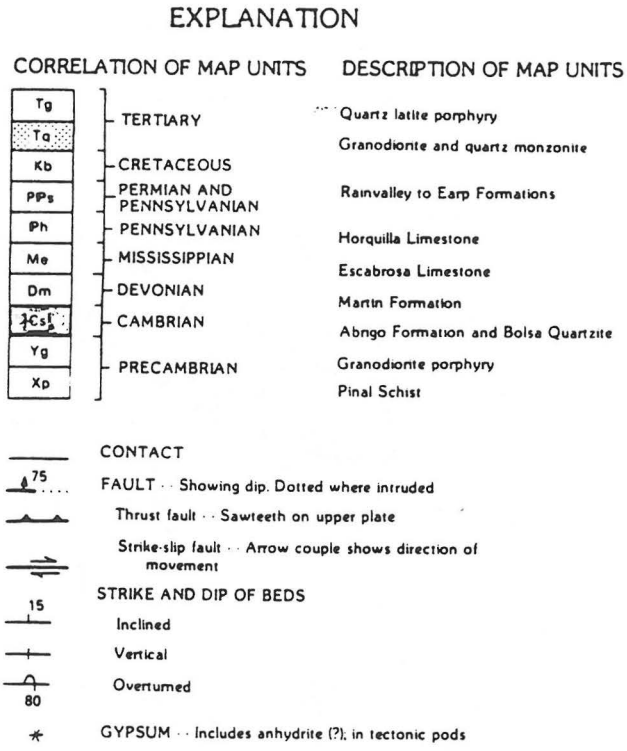

121.6 Pass lunch stop site.

122.3 **STOP 9** (optional) — Southwest side of wash. View of west side of klippe. Brown ledge is the Bolsa Quartzite. Overlying gentle slope contains the Abrigo and Martin Formations and the cap of hill is Horquilla Limestone. The thrust fault beneath the klippe is well exposed on all sides, and has been penetrated by drill holes, showing it to be saucer-shaped. Copper mineralization is related to the quartz latite porphyry (ore porphyry) and has spread along faults and replaced particularly the Abrigo and Martin Formations.

Knoll to the northwest, less than 1 mi (about 1 km) distant is underlain by Mississippian Escabrosa and Pennsylvanian Horquilla Limestones, which are folded about a northwest-trending axis and southwest-inclined axial plane, formed during the main phase (75 m.y.) deformation. The Escabrosa northeast of this knoll has been quarried for smelter flux (fig. 29).

123.9 Bear right at junction.

123.95 Bear right again, returning to paved road.

135.7 Turn left (W) on Sahuarita road, driving through pecan groves and crossing the Santa Cruz River and the railroad.

136.35 Cross U.S. Highway 89 at Sahuarita and continue straight ahead, westward. Between 10:30 and 1:30 tailings and dumps from several major open-pit copper mines, including, from left to right, Sierrita and Esperanza, Twin Buttes, and Pima and Mission, all on the flank of the Sierrita Mountains. These mountains are underlain by a mixed terrane of plutonic, volcanic, and sedimentary rocks of Precambrian through Tertiary ages. The record of thrust,

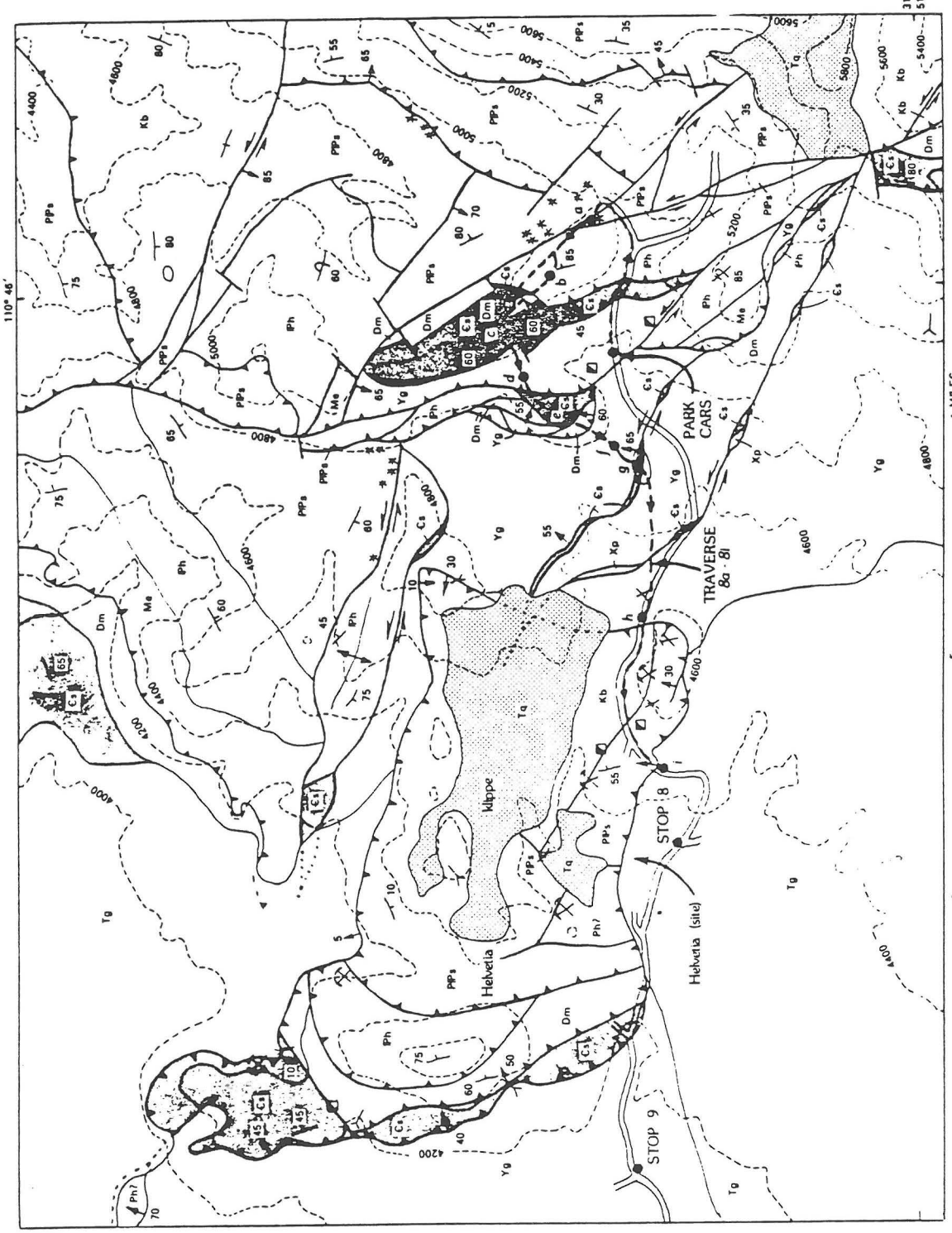

Figure 24. Geology of the central part of the Helvetia area showing route of walking tour of STOP 8 (Drewes, 1972, pl. 4).

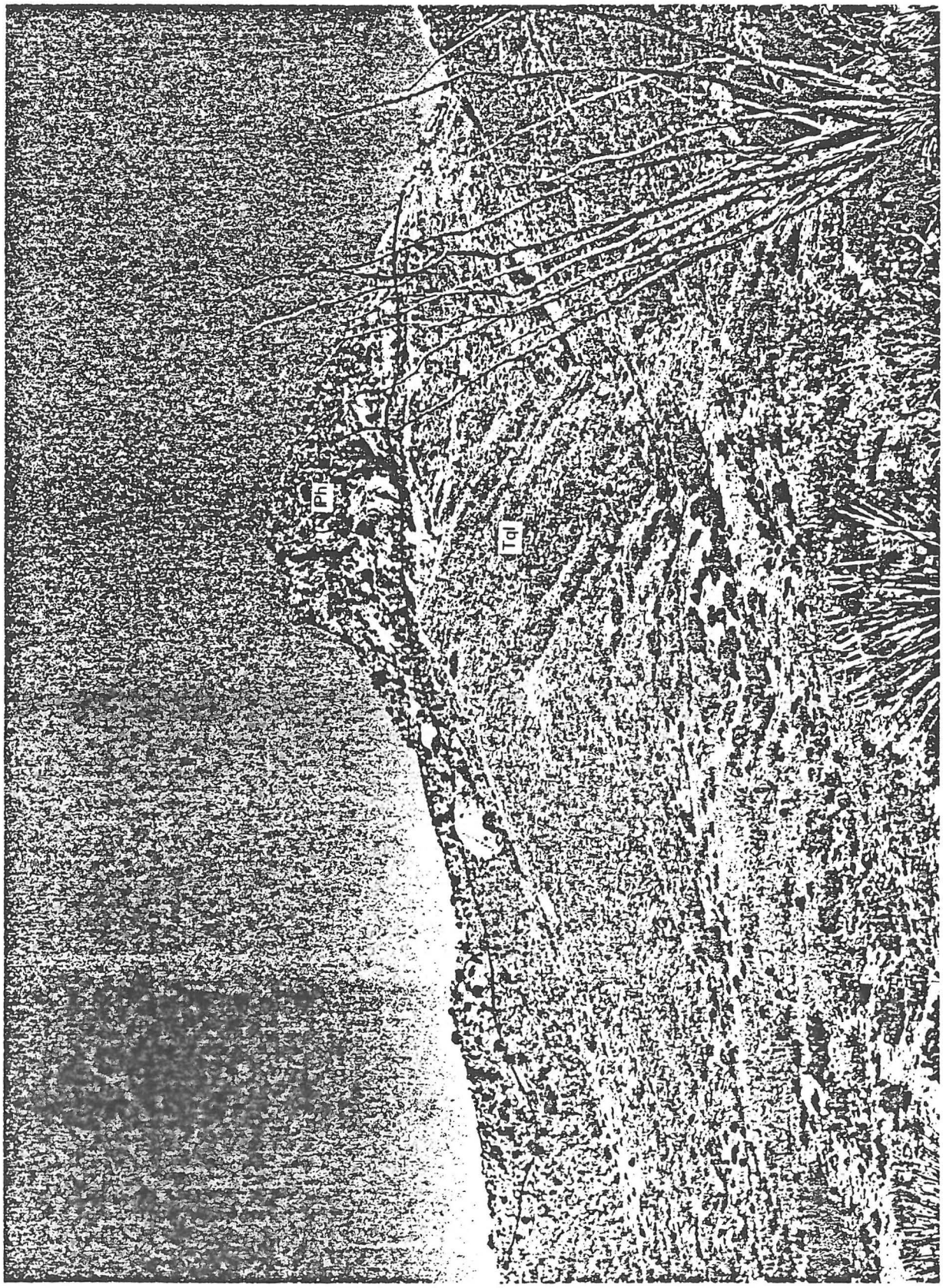

Figure 25. Hill marking northeast corner of the Helvetia klippe, underlain by Permian Concha Limestone. Slopes beneath the limestone are underlain by Paleocene quartz latite porphyry that intrudes the klippe. Photo by Jack Rathbone.

AGE		FORMATION	DESCRIPTION	THICKNESS (m)
QUATERNARY	Holocene Pleistocene		Gravel and sand	
TERTIARY	Pliocene			
	Miocene			
	Oligocene	unnamed	Rhyolite dikes	
	Paleocene	unnamed	Quartz latite dikes and plugs of the Greaterville intrusives and Quartz monzonite of the Helvetia stocks	
CRETACEOUS	Late Cretaceous	Elephant Head Quartz Monzonite Madera Canyon Granodiorite	Stocks	
		Salero Formation	Rhyolite, andesite, and sedimentary rocks	2000 ±
		Fort Crittenden Formation	Conglomerate, sandstone, and shale; tuff in upper part	3000 ±
	Early Cretaceous	Bisbee Group	Arkose, sandstone, shale, and siltstone	2700 ±
JURASSIC				
TRIASSIC		Canelo Hills Volcanics	Arkose, conglomerate, shale, and tuff	180 +
		Gardner Canyon Formation	Red mudstone, dacite, and conglomerate	600 +
		Mount Wrightson Formation	Rhyolite, andesite, and sandstone	2600 ±
PERMIAN	Early Permian	Rainvalley Formation	Limestone, dolomite, and sandstone	0-90
		Concha Limestone	Cherty limestone	120-175
		Scherrer Formation	Quartzite, dolomite, and sandstone	220 ±
		Epitaph Dolomite	Limestone and dolomite	300 ±
		Colina Limestone	Limestone	110 ±
PENNSYLVANIAN	Late Pennsylvanian	Earp Formation	Siltstone and marlstone	250 ±
	Late to Early Pennsylvanian	Horquilla Limestone	Fine-grained limestone	300 ±
MISSISSIPPIAN		Escabrosa Limestone	Coarse-grained limestone	170 ±
DEVONIAN		Martin Formation	Dolomite, limestone, and siltstone	120 ±
SILURIAN				
ORDOVICIAN				
CAMBRIAN	Late Cambrian	Abrigo Formation	Shale, sandstone, and limestone	225-275
	Middle Cambrian	Bolsa Quartzite	Quartzite	140 ±
	Early Cambrian			
PRECAMBRIAN		Continental Granodiorite	Granodiorite porphyry	
		Pinal Schist	Gneiss and schist	

Figure 26. Stratigraphic section of the Helvetia area and the Sahuarita quadrangle (Drewes, 1971).

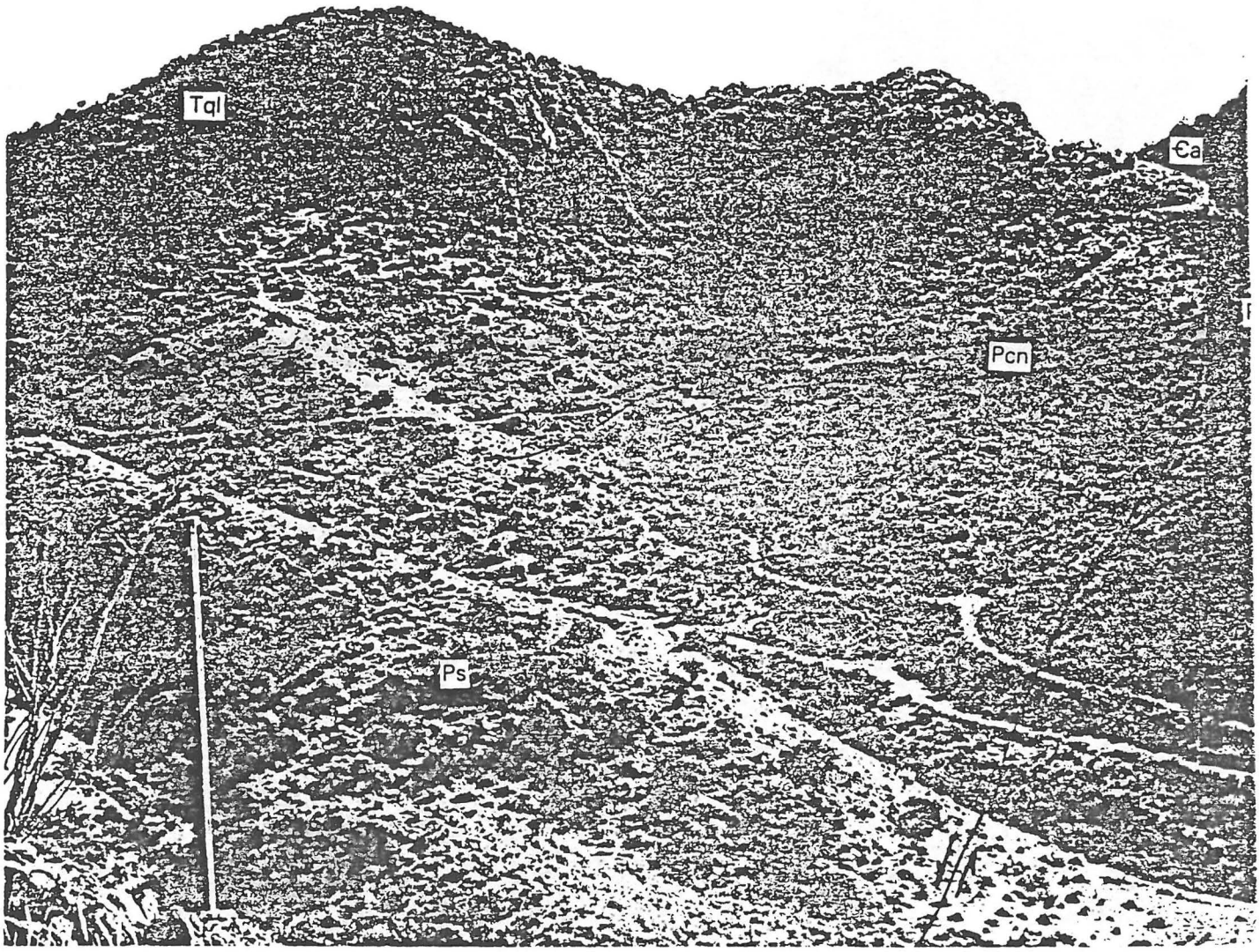

Figure 27. Panorama to east and southeast from STOP 8b. Slope to east is underlain mainly by the Permian Scherrer Formation and Permian Concha Limestone, which are separated by a bedding-plane thrust fault. The low spur to the southeast is mostly of Pensylvanian Horquilla Limestone, and high hill beyond and left of the spur has a plug of quartz latite porphyry. Gunsight Notch lies between the plug and the bold knob of Middle Cambrian Bolsa Quartzite and Precambrian Continental Granodiorite. The thrust faults we shall cross in the next part of the traverse (d-f) merge with strands of a left-lateral strike-slip fault that crosses the range at the notch. Photos by Jack Rathbone.

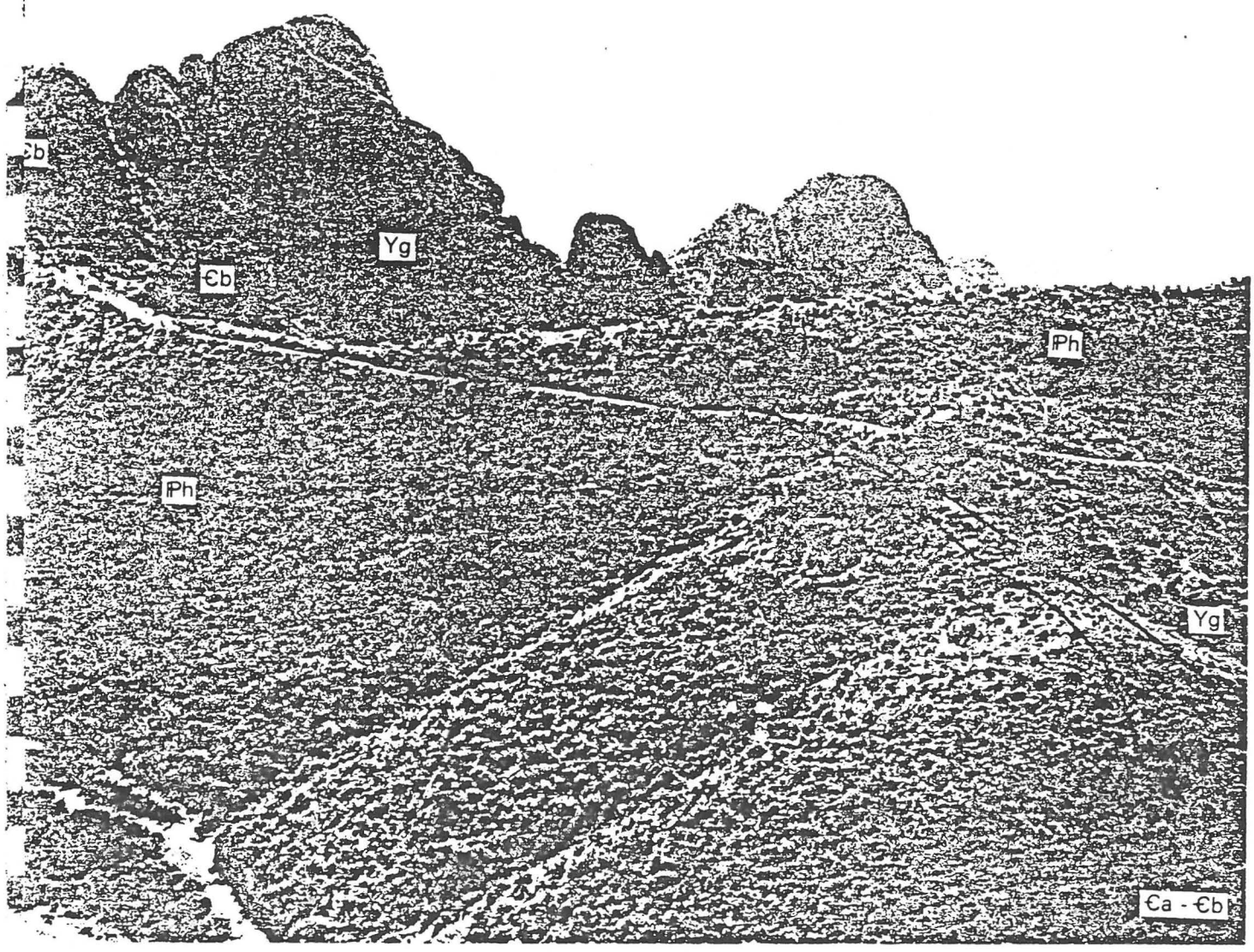
Cb
Yg
Cb
Ph
Ph
Yg
Ca - Cb

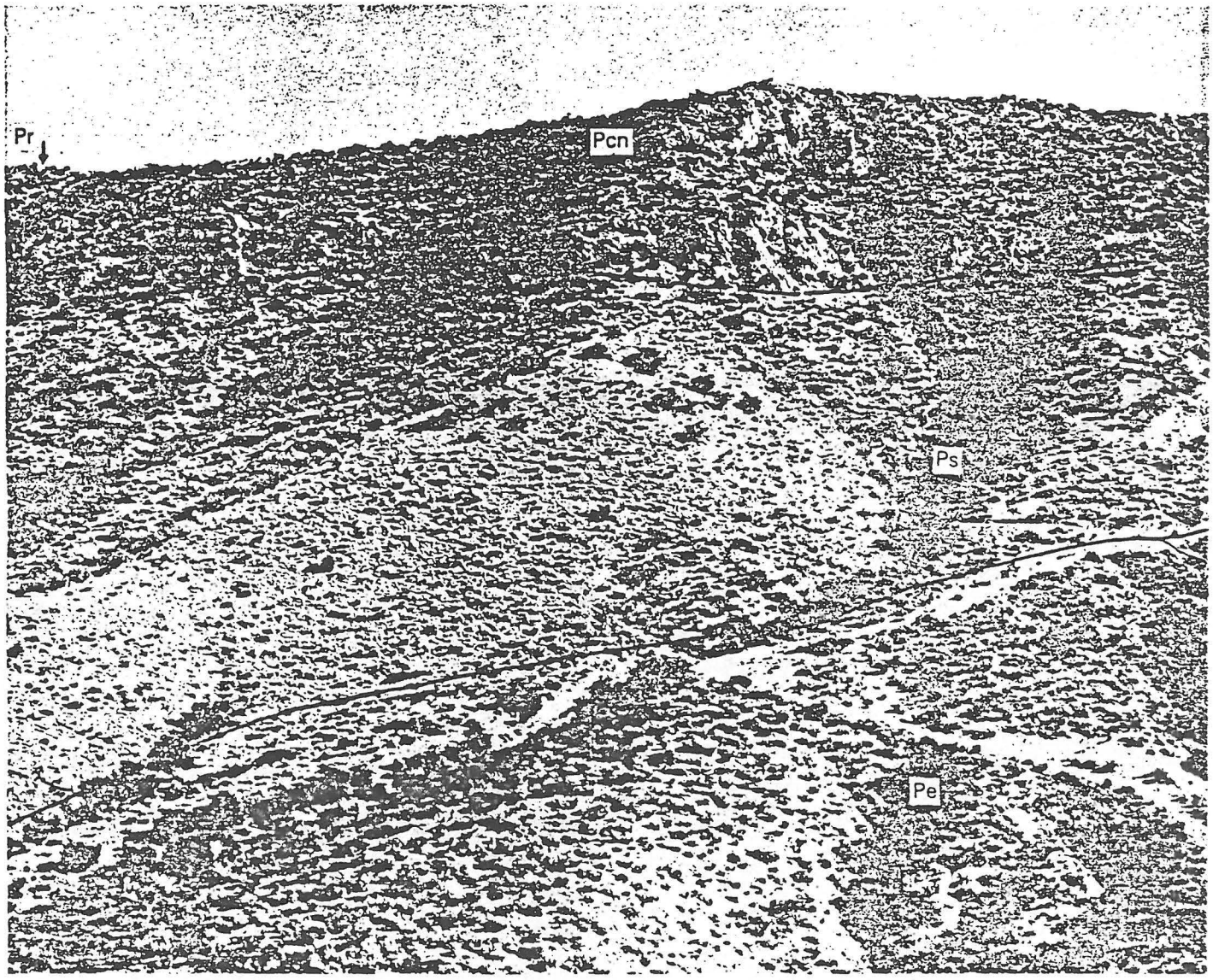
Pr
Pcn
Ps
Pe

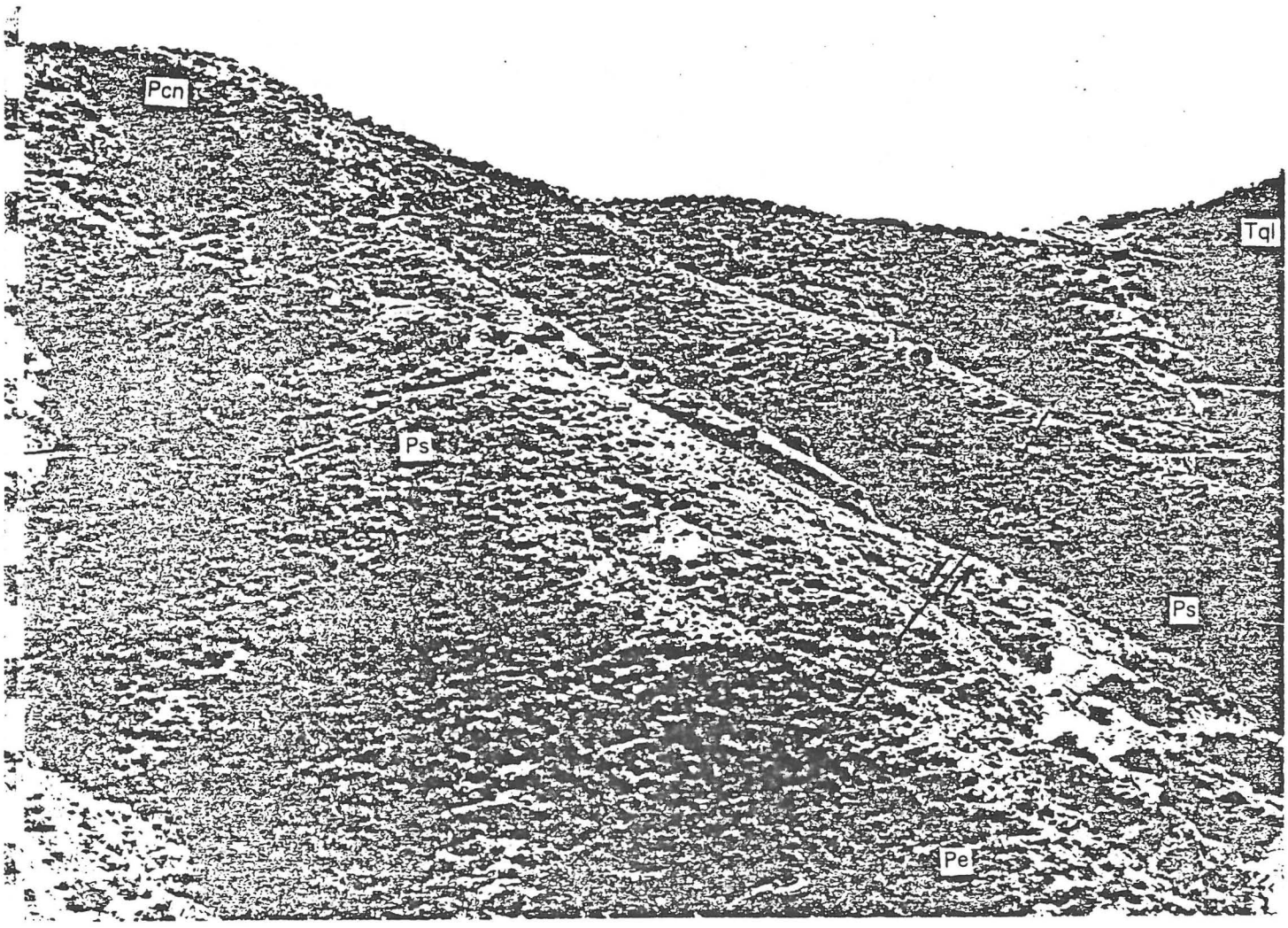
Pcn
Tql
Ps
Ps
Pe

Figure 28. View west of the Helvetia klippe and of a northwest-trending left-lateral tear fault between Precambrian granodiorite to left and Horquilla Limestone to right. This fault is truncated by the thrust plates we will cross at STOP 8e. Across the Santa Cruz Valley are mine dumps of a string of porphyry copper pits. Photo by Jack Rathbone.

Figure 29. Quarry in the Mississippian Escabrosa Limestone, thrust faulted upon Cambrian and Devonian formations and upon another northwest-trending tear fault, against which the Bolsa Quartzite and Precambrian granodiorite are truncated left of the bold hill in the foreground. Photo by Jack Rathbone.

tear, and glide faulting is fragmentary and partly concealed by the intrusion of large stocks, by reactivated movement on structures, and by widespread pediment gravels (Cooper, 1973; Cooper and Drewes, 1973).

141.8 Eastern knolls of the Del Bac Hills, with one road cut, at 3:00, showing tilted and faulted conglomerate. The nearby hills are capped by 24- to 27-m.y.-old andesite, mapped by Percious (1968). San Xavier Mission is nestled among the low hills about 1 km west of highway.

At about 11:00 are the Tucson Mountains. Many of the sharp hills are underlain by Upper Cretaceous rhyolitic ash-flow tuff, and some by a slightly younger granitic stock or by mid-Tertiary volcanic rocks. The ash-flow tuff typically overlies an andesitic breccia sheet which resembles the Hidalgo Volcanics in some ways but contains abundant exotic blocks of Mesozoic, Paleozoic, and other rock that are otherwise unexposed or only sparsely exposed in the mountains. The older rocks show evidence of compressive deformation of the kind and age attributable to the Cordilleran orogeny (Drewes, 1981b, p. 80-86; pl. 9), but ascribed to other causes in some studies (Brown, 1939; Mayo and Davis, 1976).

At 12:00-1:00 are the Santa Catalina Mountains behind Tucson, another gneiss-cored dome like the Rincon Mountains, to be described tomorrow.

147.2 Junction I-10 and I-19. End of logged traverse. Continue on I-10, westbound, to quarters, probably the Ramada Inn at the St. Mary Street exit.

Evening symposium session, to be arranged.

END OF DAY 2

[Section 5]

Miscellaneous Notes
Helvetia-Rosemont Ore Deposit Geology
by Michael Rauschkolb

Miscellaneous Notes on

HELVTIA-ROSEMONT

Ore Deposit Geology

compiled by

Michael Rauschkolb

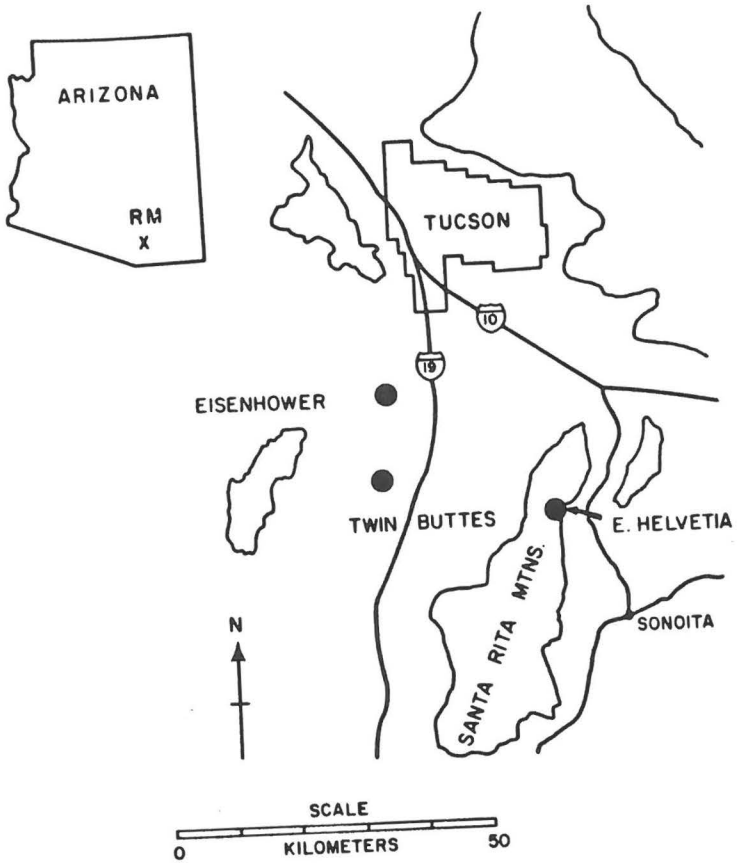

Figure 1. Location map for the Rosemont mining district.

(McNew, 1981)

The Rosemont mining district is located on the northeastern side of the Santa Rita Mountains, approximately 48 km southeast of Tucson, Arizona (Figure 1). A body of bulk low-grade copper mineralization, predominantly in tactite, has been delineated by the Anamax Mining Company in the southern half of the district. Announced reserves for this deposit are 337.3 million tons of ore with an average grade of 0.54 percent sulfide copper and 0.012 percent molybdenum.

The tactite alteration in the southern half of the Rosemont district occurs predominantly in a sequence of north-south striking, eastward dipping, Paleozoic sedimentary rocks. Although no major igneous intrusive body has been observed in association with this alteration, several nearly horizontal dikes of quartz latite porphyry and porphyritic quartz latite, apparently related to the alteration, occur near the center of the district. A thrust place composed chiefly of Cretaceous sedimentary and volcanic rocks overlies the altered Paleozoic strata in the northern and eastern portions of the southern half of the district. The rocks in this thrust plate have also been considerably altered, although the thrust faulting appears to have occurred after the alteration event.

Tactite alteration is most intense near the center of the district and gradually decreases to the south. This alteration was studied over a 2.1 km interval along the strike of the Paleozoic strata. The accompanying mineralization exhibits a zonal pattern from north to south consisting of:

1) low grade sulfides and iron oxides both disseminated and in veinlets;
2) higher grade copper sulfides and lesser pyrite, sphalerite and minor molybdenite, disseminated and in veinlets;
3) copper and zinc sulfides restricted to major faults or fractures;
4) zinc and lead sulfides in major faults or fractures near the edge of tactite alteration;

Rosemont - Economic Geology

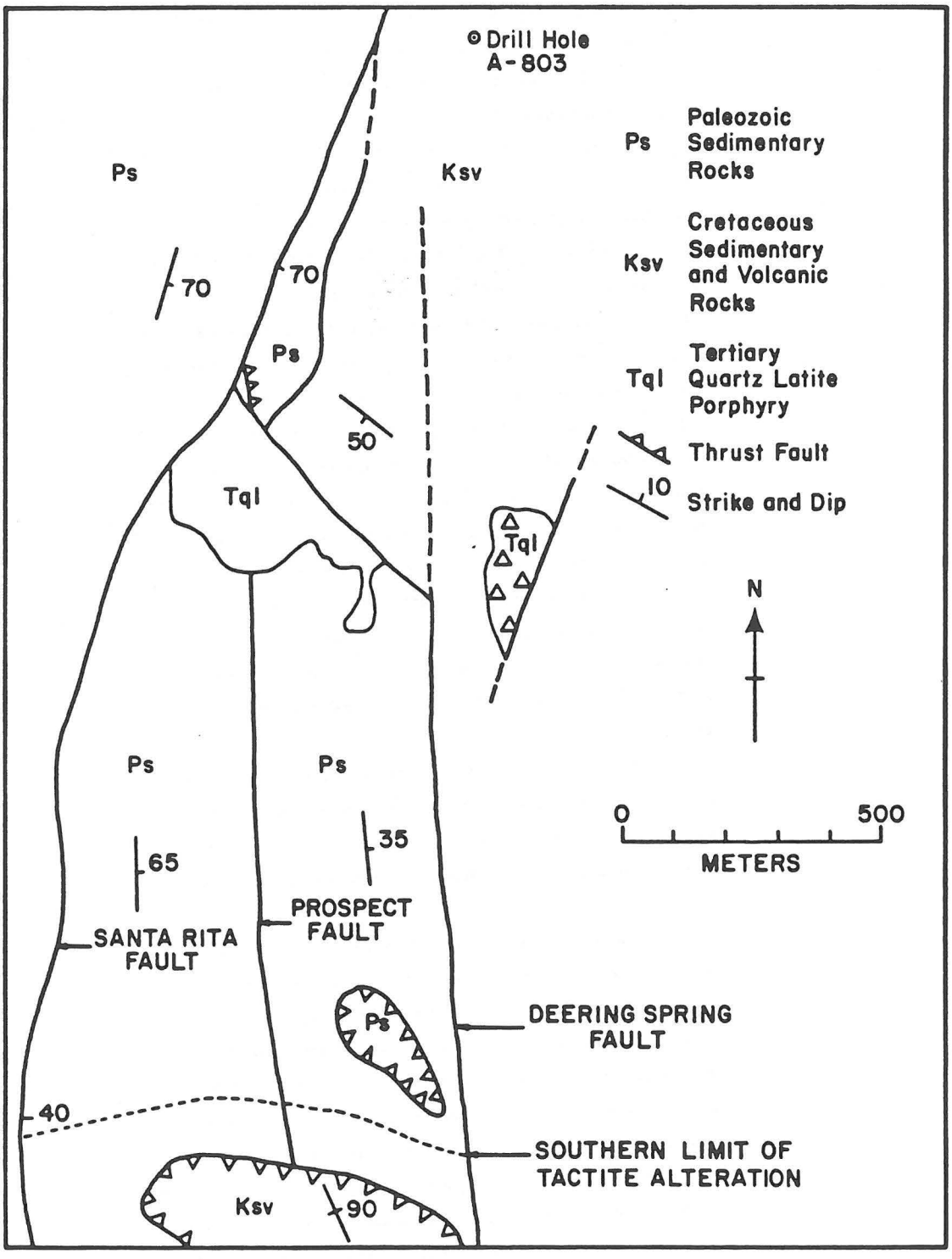

Figure 4. Generalized geologic map of the southern half of the Rosemont mining district.

McNew, Gregory E. (1991) Tactite alteration and its late stage replacement in the southern half of the Rosemont mining district, Arizona: Unpublished M.S. thesis, University of Arizona, 80 p.

ROSEMONT (McNew, 1981)

Structural Geology

Although the structural history of the Rosemont mining district is complicated, it has fortunately not obscured a relatively simple pattern of north-south-striking Paleozoic strata. Several north-south-trending faults and one or more low-angle thrust faults (Figure 4) offset the stratigraphic sequence, but not the continuity of the strata along strike.

The most important of the north-south-trending faults, the Santa Rita fault, occurs in the western portion of the study area. This fault forms the western border of the presently-outlined copper ore body, and is also the major mineralized structure associated with the lead-zinc and gold-silver deposits at the southern end of the district (Haury, 1946, Heatwole, 1966). The Santa Rita fault is a fairly complex structure with numerous fault strands and evidence for more than one period of movement. Drill hole information indicates that this fault dips to the east approximately 40° near the southern end of the study area (Haury, 1946), but steepens to approximately 70° in the northern portion. The thrust plate overlying the Paleozoic strata in the northern third of the study area is terminated by this fault along most of its western border.

The Prospect fault is located about 350 meters east of the Santa Rita fault and is parallel to it. This fault generally is observed to dip steeply to the east. Local concentrations of copper sulfide mineralization can be seen in several prospect workings along this fault.

The Deering Spring fault forms the eastern limit of the exposure of Paleozoic strata in the southern half of the study area. This fault dips steeply to the west. Unlike the Santa Rita and Prospect faults, this fault appears to postdate alteration and mineralization.

A largely unexposed low-angle eastward dipping thrust fault is known, from drill hole evidence, to overlie the Paleozoic strata in the northern and eastern portions of the study area, and is seen in two exposures near the southern end of the area (Figure 4). The upper plate of this fault is made up principally of Cretaceous rocks, with a relatively thin zone of carbonates and quartzite from the upper part of the Paleozoic section occurring locally at the base. Thrust faulting postdates, at least in part, the period of igneous intrusion and tactite alteration, although the rocks in the upper plate were also intruded and extensively altered. This relationship, along with the local occurrence of upper Paleozoic rocks at the base of the thrust plate, suggest that thrust displacement was no more than a few kilometers and was directed to the west.

ROSEMONT - HYDROTHERMAL ALTERATION (McNew, 1981)

SUMMARY AND CONCLUSIONS

Tactite alteration in the southern half of the Rosemont mining district shows a zonal variation over a 2.1 km interval from the center of the district to the south. Igneous intrusive rocks believed to be related to this alteration consist of quartz latite porphyry and porphyritic (?)quartz latite occurring in several dike-like bodies in the northern half of this interval. The relatively small volume of these dike-like bodies compared to the extent of tactite alteration, along with the poor correlation between their location and the district-wide alteration zoning, suggests that they may represent the upward extension of a larger body of igneous rock at depth which was more directly responsible for the alteration.

Near the center of the district, alteration of the impure, generally thin-bedded Horquilla Limestone consists of pervasive replacement by andradite and minor diopside, which was later veined and partially replaced by quartz and calcite. Nearly pure limestone of the Escabrosa and Colina Limestones is partially replaced in this area by andradite, diopside, and forsterite, associated with locally abundant late replacement by serpentine. Sulfide mineralization is generally not abundant in this section of the studied alteration interval, and is usually associated with a greater volume of hematite and magnetite.

To the south of the center of the district, a transition zone occurs in the Horquilla Limestone between the pervasive replacement near the center and selective replacement further to the south. Diopside, wollastonite, and vesuvianite increase in abundance to the south in this transition zone whereas garnet, quartz, and calcite decrease in abundance in this direction. Garnet has a wide range in composition in this transition zone, but in general becomes more aluminum-rich to the south. Abundant copper sulfide mineralization in this transition zone results from the overlap of an early period of sulfide deposition (associated predominantly with contemporaneous wollastonite) and a later period of sulfide deposition (associated with quartz-calcite veins and replacement of earlier tactite minerals).

To the south of this transition zone (starting at approximately the center of the study area) tactite alteration in the Horquilla Limestone becomes largely restricted to silty limestone beds. Diopside, tremolite, K-feldspar, and epidote increase in abundance to the south in the tactite in the southern half of the study area; whereas, garnet, vesuvianite and wollastonite decrease in abundance in this direction. The amount of residual unreplaced calcite and detrital quartz in the tactite also increases to the south. Alteration of the nearly pure Escabrosa Limestone in the southern half of the study area is largely limited to the destruction of fossil debris, although small amounts of tactite alteration occur along branches of the Santa Rita Fault. Sulfide mineralization in the southern half of the study area is minor and is largely restricted to major faults or fractures. Sphalerite and galena become the dominant sulfide minerals near the southern limit of tactite alteration, and quartz veins with galena, gold, and silver continue for an additional two kilometers to the south past the limit of tactite alteration.

Alteration formed during three stages. An early stage of disseminated diopside and tremolite alteration appears to have been a largely isochemical metamorphism. The following Main Tactite Stage was responsible for the major alteration of calcareous rock to tactite, and the deposition of locally abundant sulfide minerals. Alteration during this stage involved considerable metasomatism in the northern half ot he study area, but graded to increasingly isochemical alteration to the south. The final Tactite Replacement Stage was responsible for widespread sulfide deposition and a large amount of replacement of earlier formed tactite by quartz, calcite, and a variety of other minerals (Table 2). A close association exists between sulfide deposition and part of the tactite replacement occurring during this period, suggesting that the sulfide deposition was in part a response to the acid neutralization, and possibly the release of iron, associated with the replacement.

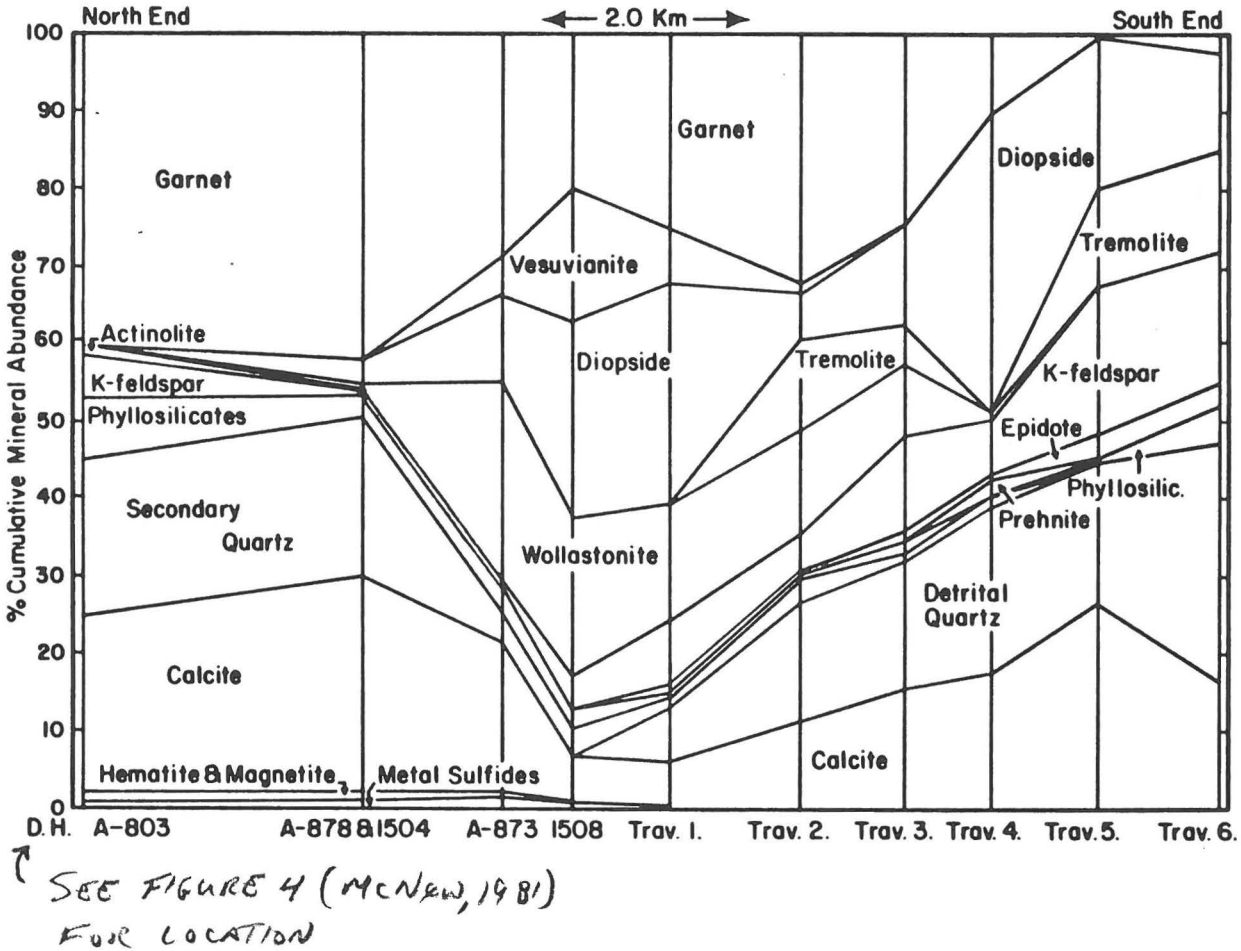

Figure 5. Mineralogy of tactite alteration in the Horquilla Limestone. (McNew, 1981)

ROSEMONT AREA
STREAM SEDIMENT AND MESQUITE ASH SAMPLES

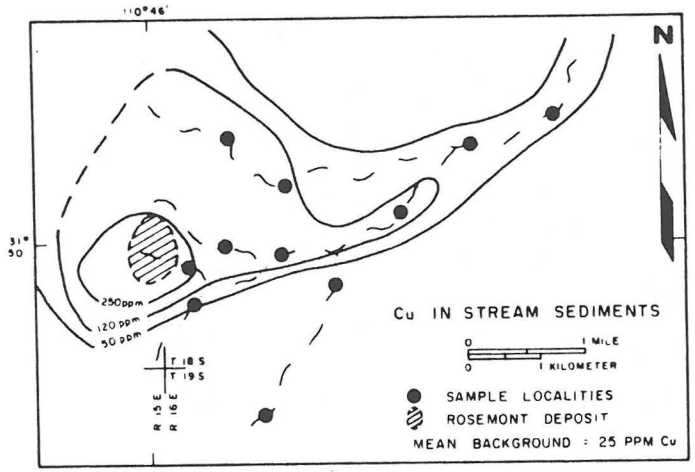

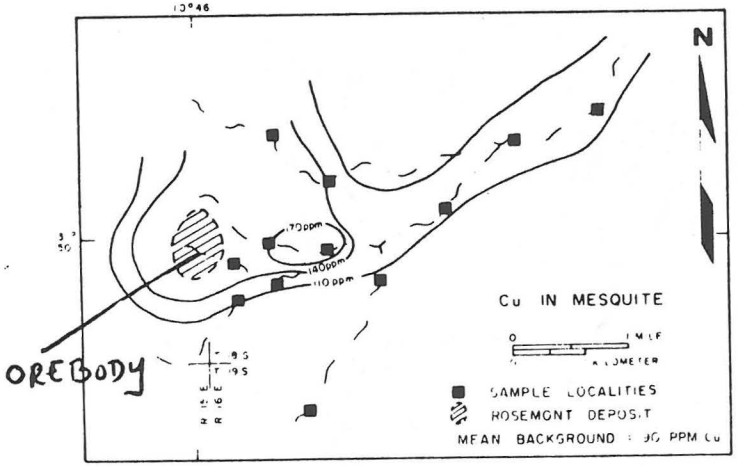

Fig. 52. Geochemical maps of Rosemont area, showing Cu isopleths based on stream-sediment and mesquite samples.

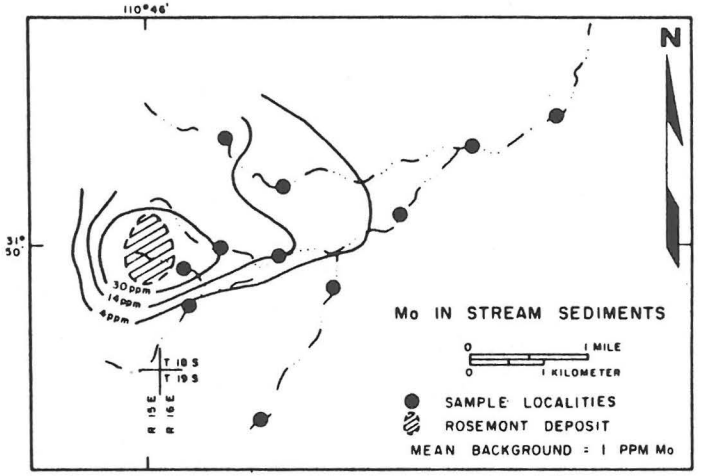

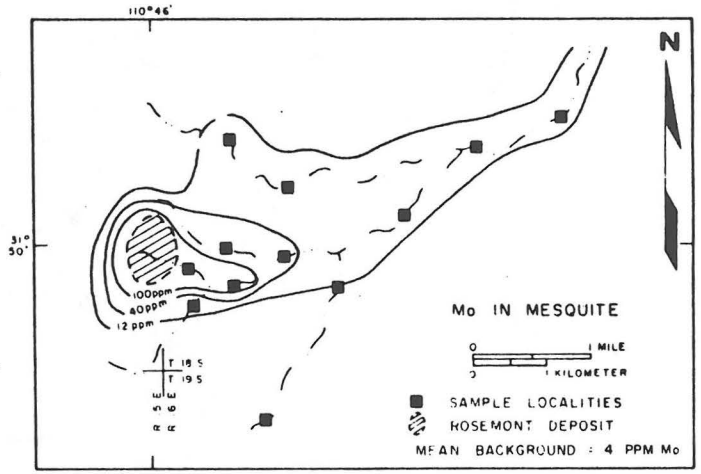

Fig. 53. Geochemical maps of Rosemont area, showing Mo isopleths based on stream-sediment and mesquite samples.

Lovstrom, K.A., 1978, Rosemont deposit, Pima County, Arizona; Jour. Geochemical Exploration, p.232-235.

OVERLAY MAPS OF THE PEACH-ELGIN AREA

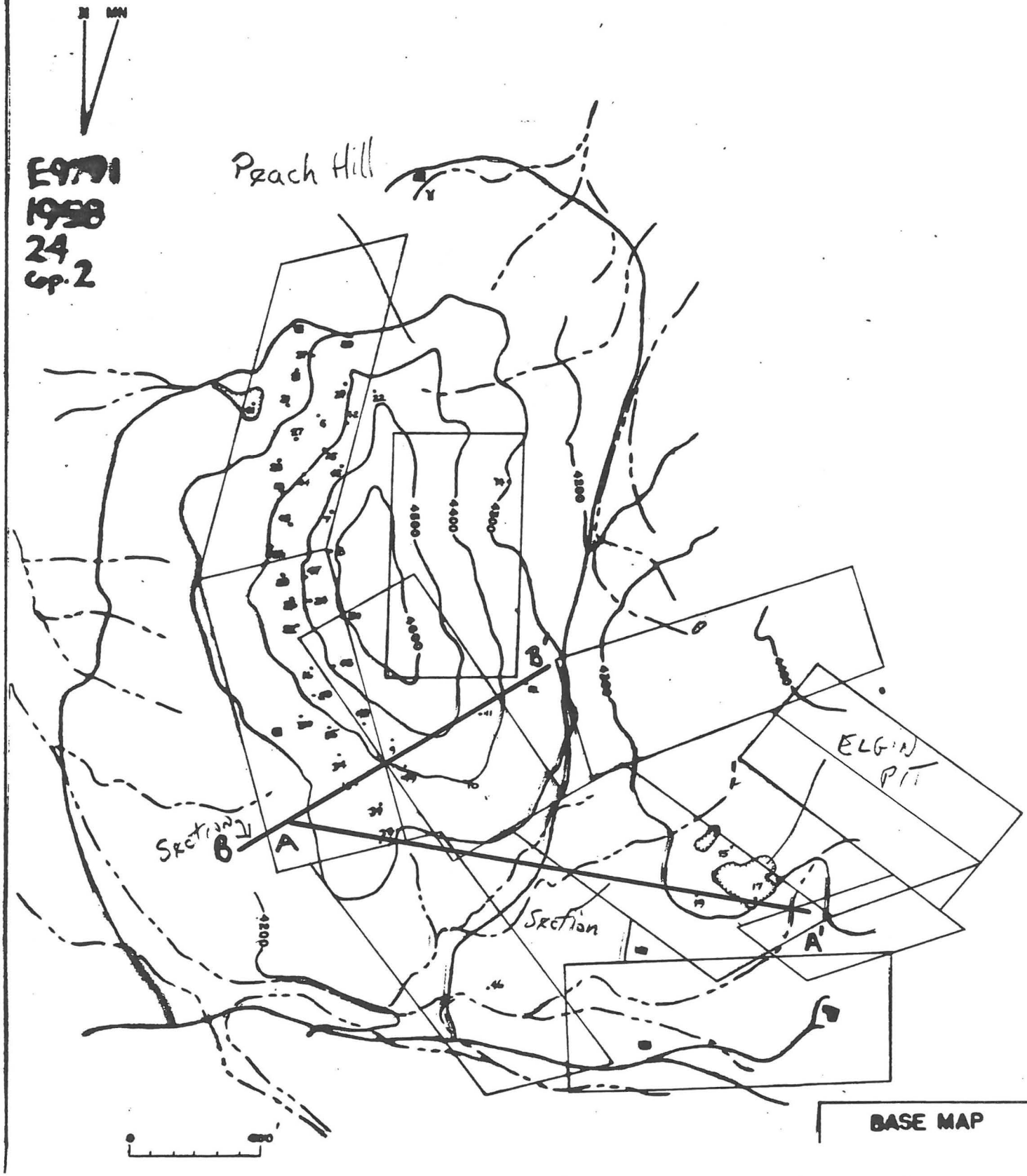

Heyman, A. M., 1958, Geology of the Peach-Elgin copper deposit, Helvetia district, Arizona: Unpublished M.S. Thesis, University of Arizona, Tucson, 66 p.

CROSS SECTIONS THROUGH THE PEACH - ELGIN AREA (See Base Map for location of cross-section

SECTION A - A'

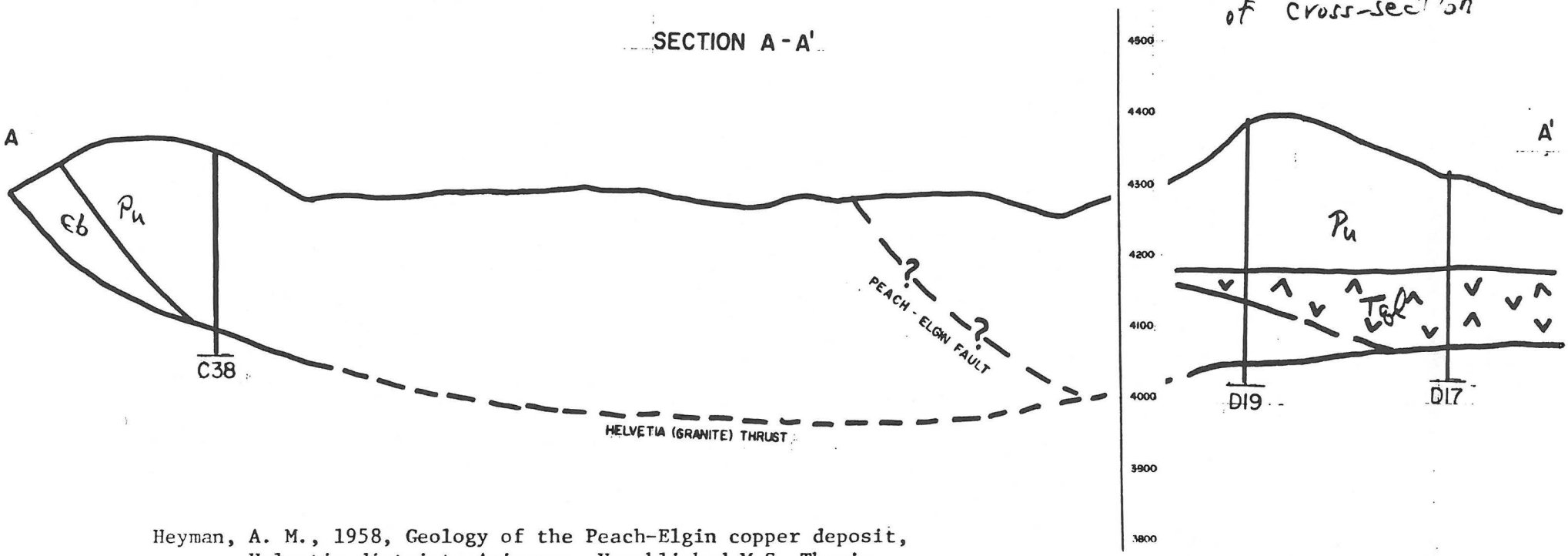

Heyman, A. M., 1958, Geology of the Peach-Elgin copper deposit, Helvetia district, Arizona: Unpublished M.S. Thesis, University of Arizona, Tucson, 66 p.

Heyman, A. M., 1958, Geology of the Peach-Elgin copper deposit, Helvetia district, Arizona: Unpublished M.S. Thesis, University of Arizona, Tucson, 66 p.

STRUCTURAL GEOLOGY

Helvetia thrust.

The major Helvetia thrust underlies the entire Peach-Elgin are area. A structure contour map on the top of the granite indicates the surface dips steeply to the east under the peach hill and gently westerly under the Elgin area (see overlay maps)..... The shear zone averages 10 feet wide, but extremes from 3 inches to 30 feet were observed. Width and intensity of alteration also varies widely. Limestone adjacent to the contact is sometimes bleached and marbleized, sometimes silicated in a narrow band, sometimes completely unmetamorphosed. The granite is chloritized in a zone which varies in width with the intensity of shearing. [Page 30]

In innumerable outcrops and prospect pits on all sides of the Peach - Old Dick - Heavy Weight block, granite can be seen in fault contact with all other rocks. A zone of shearing is present in several exposures of the contact of granite with limestone which is completely free of silication. Shearing is also observed at the granite-quartzite contact on the west side of the Peach Hill. On the east side of the outlier a well exposed west-dipping fault between Concha and granite aligns with the granite-porphyrt contact. No intrusive relations of the porphyry into the older granite can be seen along the relatively straight contact between them, and an aplite dike in the granite stops abruptly at the contact. The contact between granite and porphyry in drill hole D-17 (Elgin area) is thoroughly sheared and is definitely a fault surface lying on the plane of the granite thrust established in other drill holes (section A-A')..... The conclusion that the entire block is the upper plate of a thrust fault can hardly be avoided. [Page 32-33]

The Broad Top porphyry intrudes Concha limestone with conformable relations to the bedding and is in fault contact with Horquilla limestone. The top of the plug with adjacent sedimentaries was sliced off by the Helvetia thrust and moved one and one-half miles west. [Page 8]

The outlier was thrust from the present position of the crest of the range. This conclusion is reached on the basis of the following evidence: (1) The mineral composition and texture of the Broad Top porphyry and the porphyry of the outlier are essentially the same. (2) The porphyry in both areas is intrusive into the Concha limestone and Cretaceous arkose. (3) (3) At no other place in the district is any Cretaceous found so far removed from the large mass on the east side of the range. (4) The formations occuring in both areas are exclusively Horquilla, Concha, and Sherrer, with minor Andrada in the eastern area. North of the outlier and south of Broad Top butte, the entire Paleozoic section has been mapped. (5) The configuration of beds generally striking around the porphyry is pronounced in the outlier and suggestedin the butte. The evidence is not conclusive, but strongly indicative that the outlier was thrust from the area of Broad Top butte.
[pages 33-34]

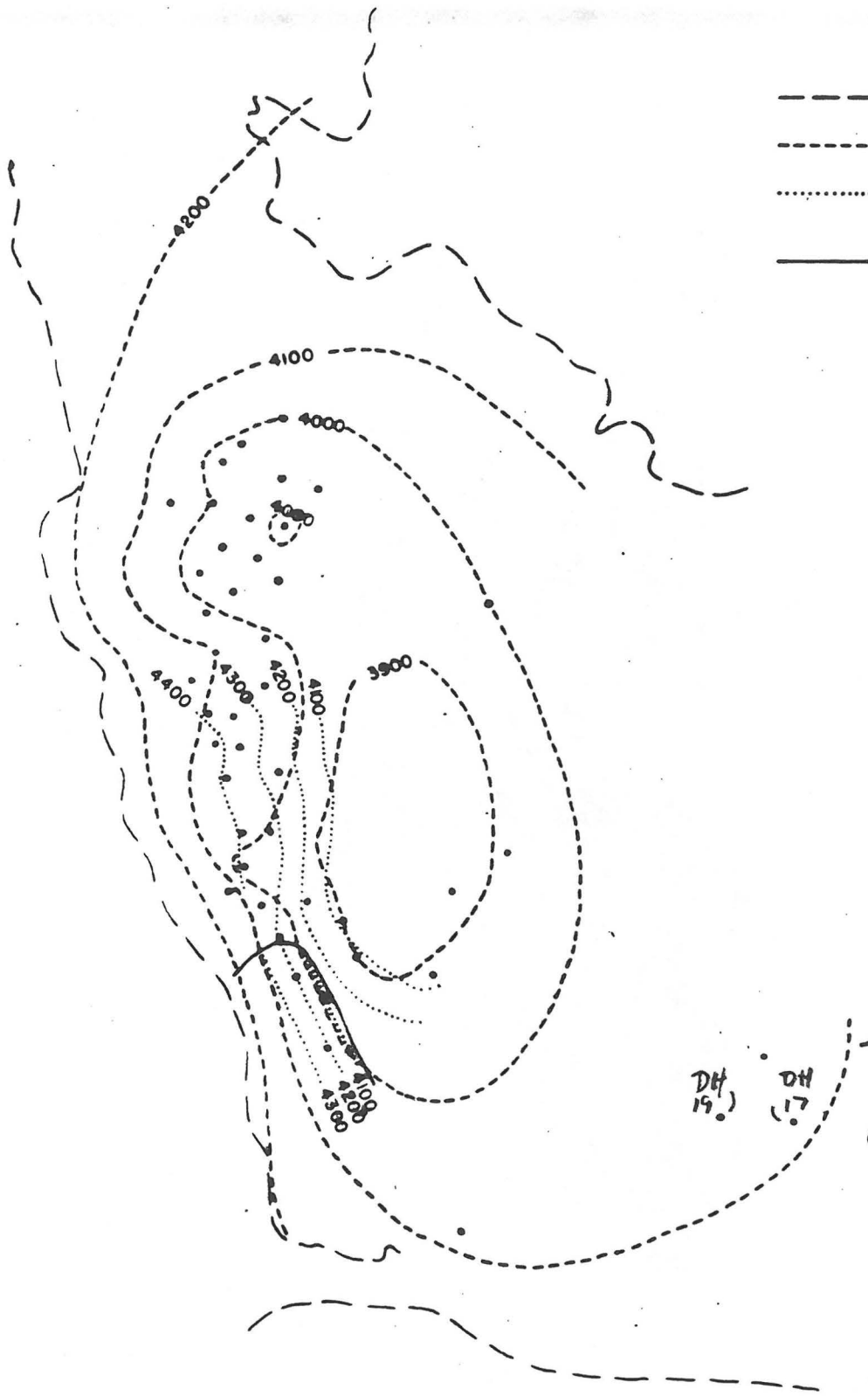

Heyman, A. M., 1958, Geology of the Peach-Elgin copper deposit, Helvetia district, Arizona: Unpublished M.S. Thesis, University of Arizona, Tucson, 66 p.

STRUCTURE MAP

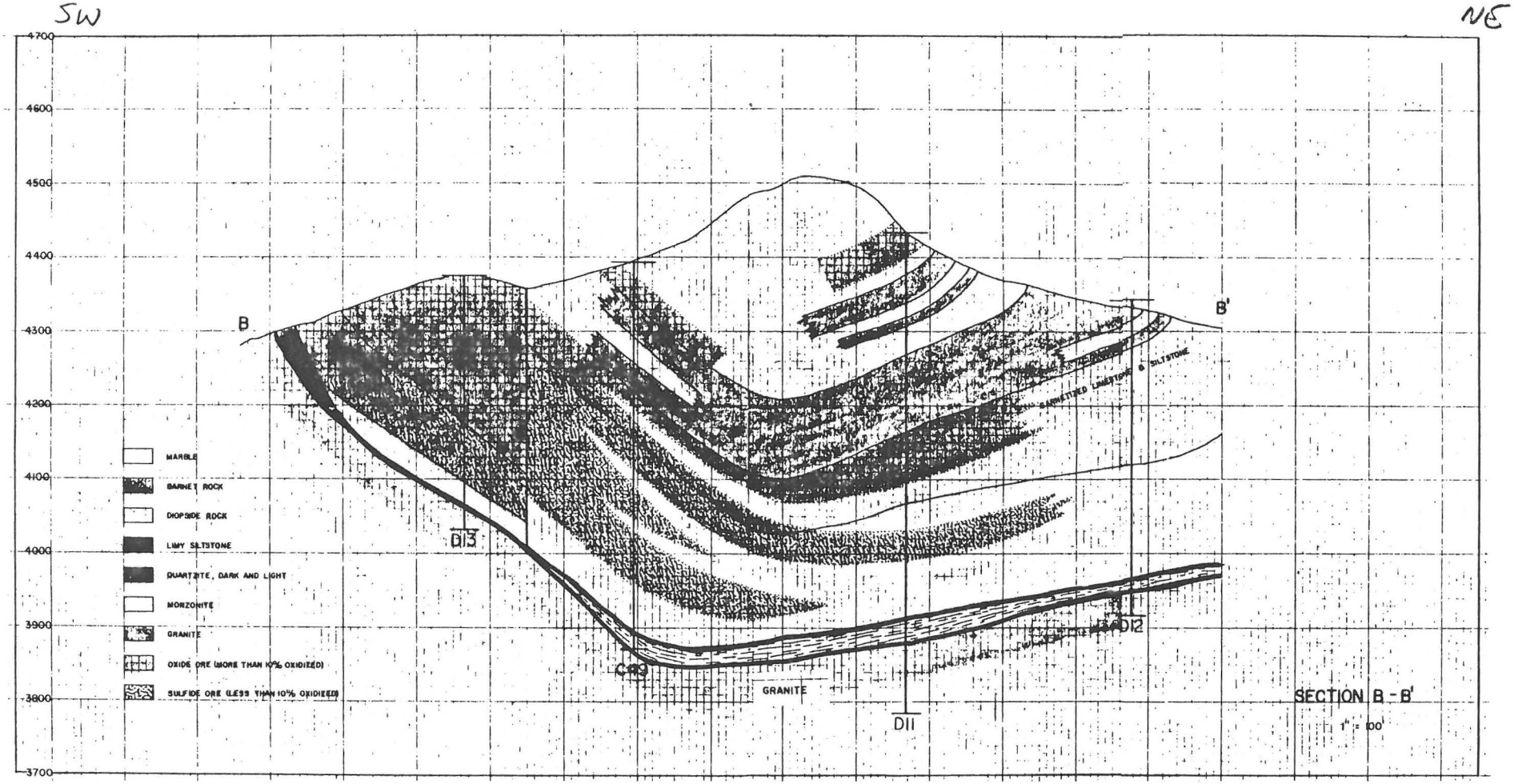

See Heyman's Base Map for location of cross-section

Heyman, A. M., 1958, Geology of the Peach-Elgin copper deposit, Helvetia district, Arizona: Unpublished M.S. Thesis, University of Arizona, Tucson, 66 p.

GENERALIZED GEOLOGIC MAP AND SECTION OF THE AREA ADJACENT TO THE COPPER WORLD AN.
HELVETIA MINING DISTRICT, PIMA COUNTY, ARIZONA from Creasey & Quick (1955)

UNITED STATES DEPARTMENT OF THE INTERIOR
GEOLOGICAL SURVEY

BULLETIN 1027 PLATE 30

200 0 1000 Feet
Contour interval 25 feet
Datum assumed

Contact, dashed where approximately located

65
Fault, showing dip; dashed where approximately located

50
Strike and dip of beds

Vertical shaft

Inclined shaft

Mine workings

Opencut

Dump

Claim corner, approximately located

14°
TRUE NORTH
MAGNETIC NORTH

EXPLANATION

Qal	Alluvium	QUATERNARY
Plm	Lower Manzano equivalent	PERMIAN
Pn	Naco limestone (restricted); interbedded limestone and hornfels	PENNSYLVANIAN
€b	Bolsa quartzite	CAMBRIAN
gr	Monzonite and granite, locally porphyritic	
qz	Granular quartz	

COPPER WORLD
OWASKO
BRUNSWICK
LEADER
TALLY HO
DEFEND
DAVE

BLACK HORSE SHAFT
COPPER WORLD SHAFT 1
COPPER WORLD SHAFT 2
LEADER SHAFT
Portal to Leader Mine
200 FOOT LEVEL

A
A'

SW.
NE.

COPPER WORLD SHAFT 1 (Projected)
COPPER WORLD SHAFT 2
Main drift, Leader mine
4800
4600

Topography by H. H. Sullwold and G. L. Quick, 1943

INTERIOR GEOLOGICAL SURVEY

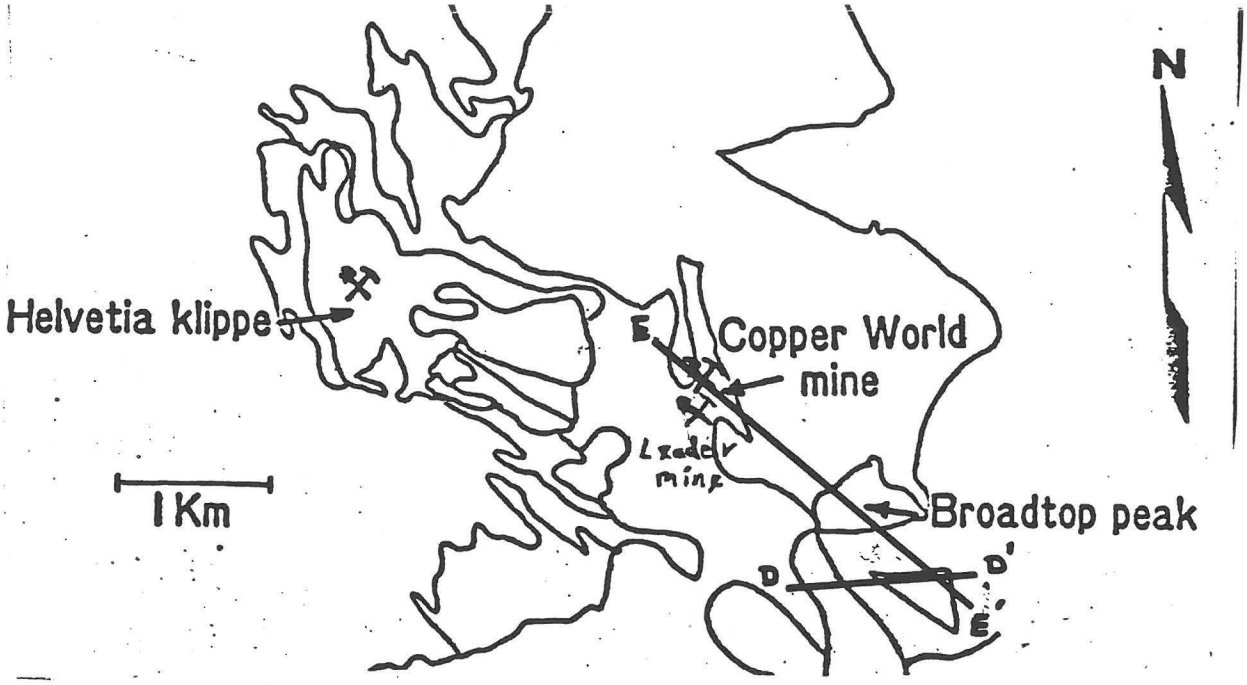

The Helvetia district has been intensely deformed, and complex structures resulted from high-angle normal faults, folds, and thrusts. Apparent thrust faults were active over a considerable period, for the quartz monzonite porphyry is both older and younger than thrust faulting..... Folding in the limestone is widespread throughout the mapped area, but it is not evenly distributed. The limestone in some of the thrust plates is contorted into tight, nearly isoclinal folds, whereas in other plates the folds are open or the beds overturned. [Page 301,311]

Creasy, S. C., Quick, G. L., 1955, Copper deposits of part of the Helvetia mining district, Pima Co., Arizona: U.S. Geol. Survey Bull. 1027-F, p. 301-323.

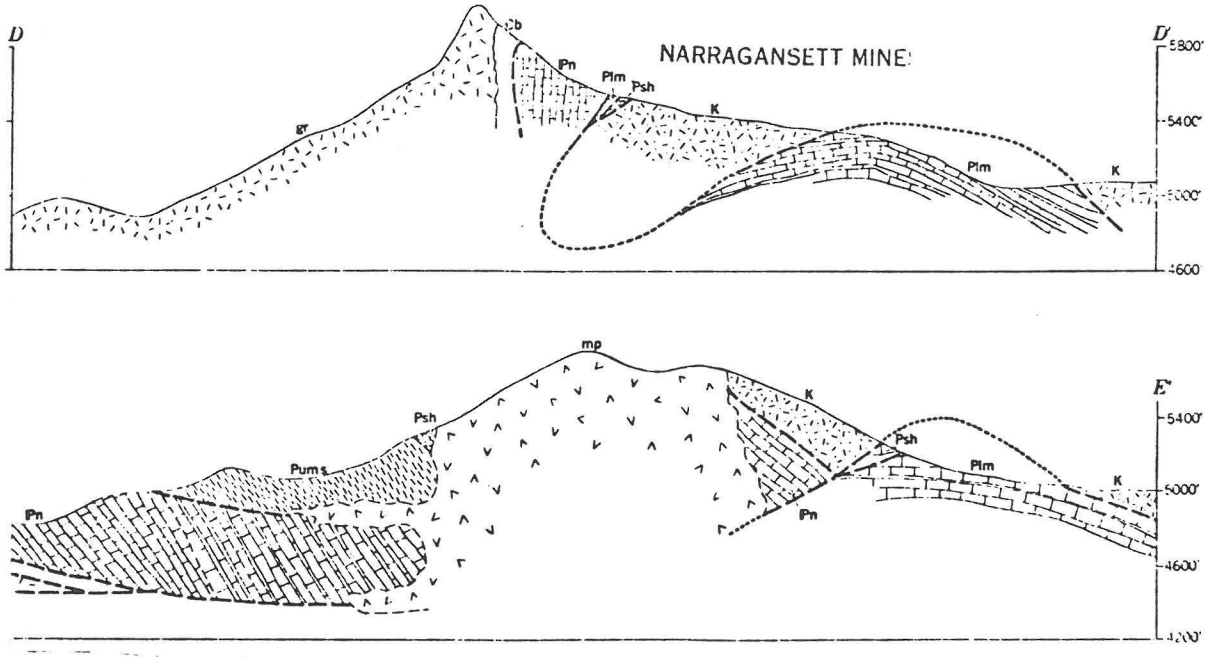

TECTONIC MAP
OF
PART OF THE SAHUARITA QUADRANGLE
(modified from Drewes, 1971, 1972)

by
Stanley B. Keith
April, 1983

scale: 1:48,000

0 1 2 3 KILOMETERS

EXPLANATION

lower Plate

- Tg_1 — Paleocene Helvetia plutons
- Kw_1 — lower Cretaceous Willow Canyon Formation
- Kg_1 — lower Cretaceous Glance granite clast conglomerate
- Pz_1 — Paleozoic sedimentary rocks
- pE_1 — Precambrian Continental Granodiorite

upper Plate

- Tq_2 — Paleocene Quartz latite plugs
- Tm — Late Cretaceous Corona Monzonite
- Kw_2 — lower Cretaceous
- Kv_2 — lower Cretaceous volcanic flows
- Kg_2 — lower Cretaceous Glance limestone clast conglomerate
- Pz_2 — Paleozoic sedimentary rocks
- pE_2 — Precambrian Continental? Granodiorite

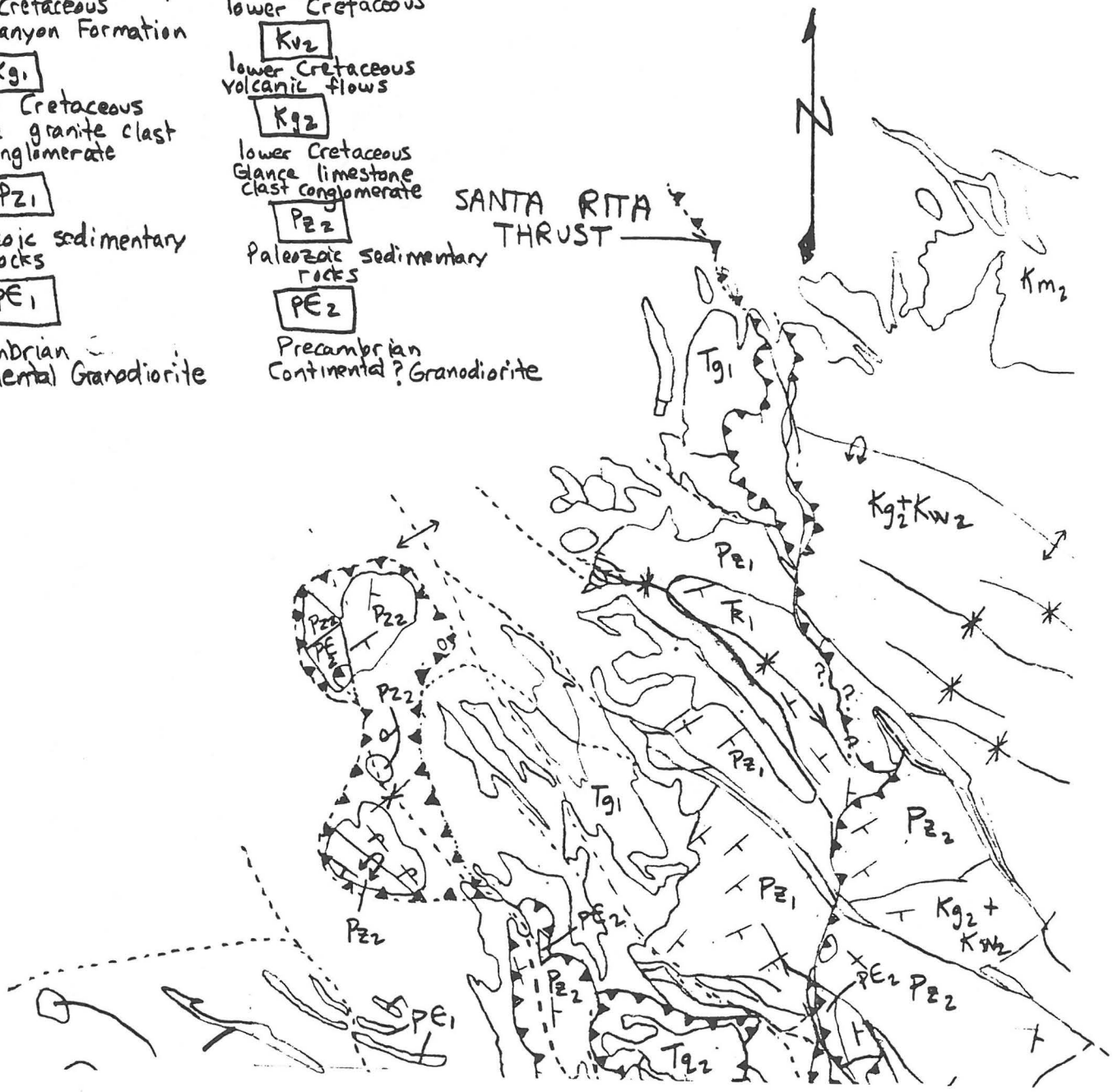

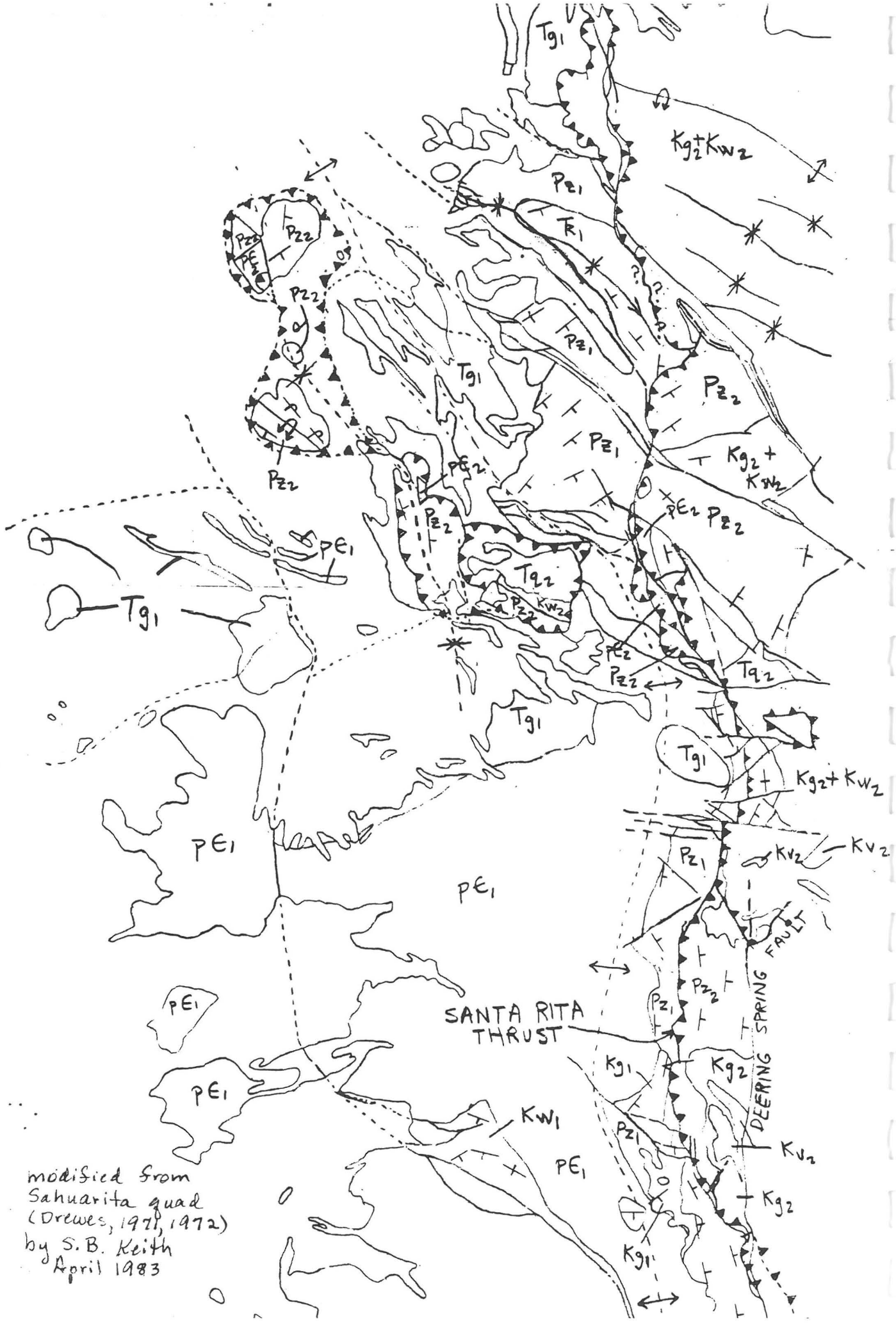

modified from Sahuarita quad (Drewes, 1971, 1972) by S.B. Keith April 1983

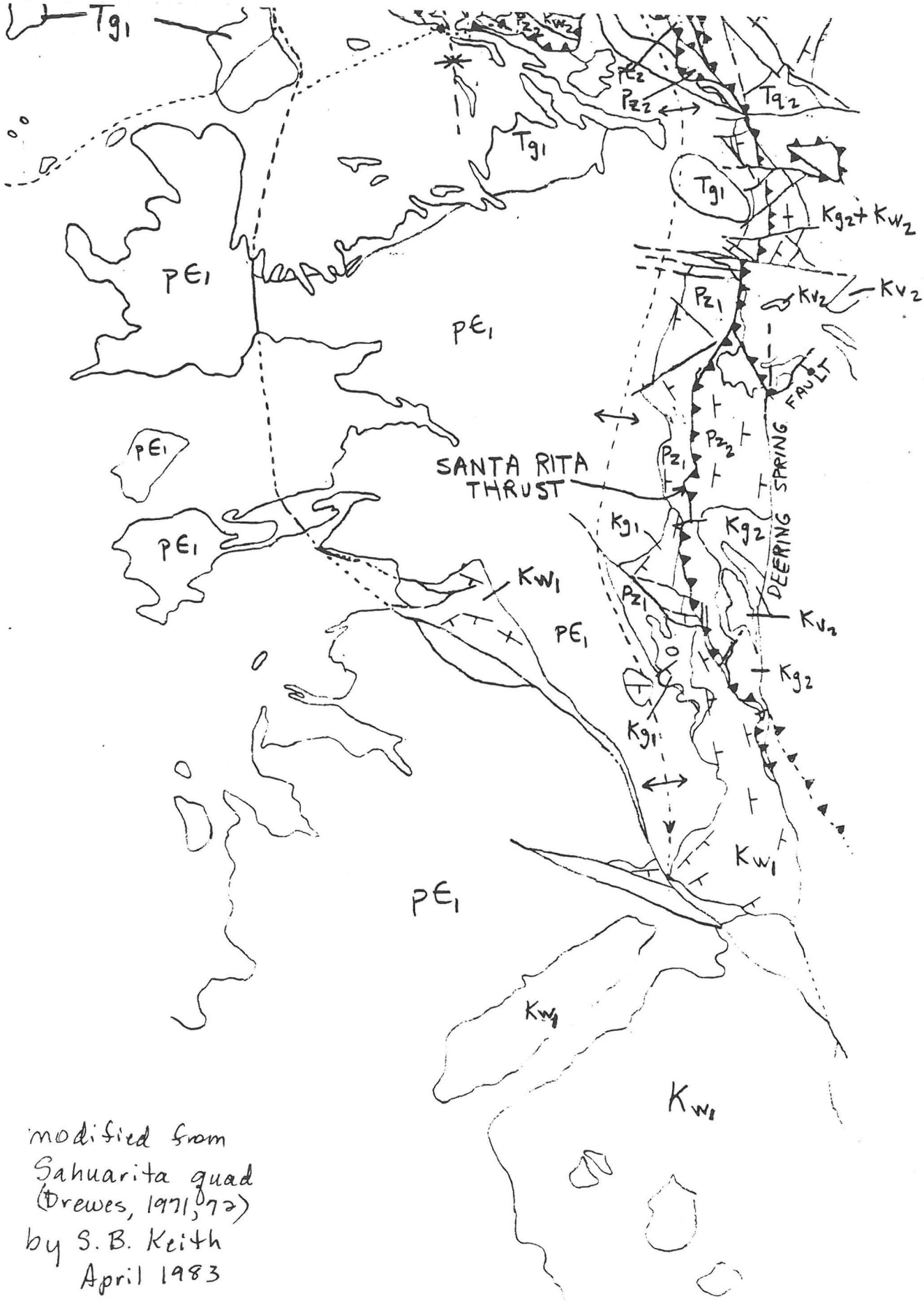

modified from
Sahuarita quad
(Drewes, 1971, 72)
by S. B. Keith
April 1983

[Section 6]

Road Log
Santa Catalina Mountains - Catalina Highway

and

Intrusion and Deformation
Santa Catalina-Rincon-Tortolita Crystalline Complex

SUPPLEMENTAL ROAD LOG 2

SANTA CATALINA MOUNTAINS VIA CATALINA HIGHWAY

DOUGLAS W. SHAKEL

This road log is a self-guided tour to the southern half of the Santa Catalina Mountains, as observed from the Tucson-Mt. Lemmon highway (Catalina highway). Near the crest of the range, several additional sites along the unpaved Oracle-Mt. Lemmon road are also included due to their current geochronological significance. The guide begins at the south end of the Catalina highway.

ROAD AND WEATHER INFORMATION

The Catalina highway provides good, nearly all-weather paved access to the summit of the Santa Catalina Mountains at Mt. Lemmon (9,157 ft) and to the forest recreational community of Summerhaven at about 7,800 ft. Several U.S. Forest Service picnic areas and campgrounds and a number of private organizational camps are also reached from this highway. Campsite and picnic ground availability is sometimes restricted due to snow, fire conditions, excessive use and so forth, so the Catalina District of Coronado National Forest should be contacted for current status of these facilities if your journey is dependent on their use.

The highway is generally open to Summerhaven and to the Mt. Lemmon ski area except for occasional 12-36 hour closures immediately after heavy winter snows. The uppermost mile, between the ski area and the summit, is sometimes closed in winter to all but official vehicles. The rest of the highway is also sometimes restricted to 4-wheel drive vehicles and (or) residents only, due to icy conditions and fire problems.

Near the crest of the range, the Tucson-Mt. Lemmon highway connects with the older, unpaved Oracle-Mt. Lemmon road. This road is not maintained for passenger vehicle use and is nearly always very rough, especially at higher elevations. It is open much of the year, but during most winters parts are impassable from the time of the first heavy snow (November to January) until thaw (usually March or April). However, the lower part of this road, up to the site of the old Control mine and the junction with the road up to Dan's Saddle, is generally graded, clear and passable all year round.

At any time of the year, temperatures in the higher parts of the Santa Catalinas run 20°F colder than those in the desert below. Even in mid-summer, travelers leaving the scorching heat of Tucson may find light sweaters or windbreakers comfortable on top of Mt. Lemmon, especially if a stay after sunset is planned. In winter months, midday highs of less than 32°F are not uncommon. During both the winter and late summer rainy seasons, precipitation is more likely at higher elevations on the mountain than in the adjoining valleys, so rain gear may be useful on the mountain even when the weather in the Tucson basin is only partly cloudy.

Gasoline is presently *not* available anywhere on the mountain; limited groceries and refreshments are obtainable at Summerhaven, and prepared food is seasonally available at the ski hut at the Mt. Lemmon ski area. This is the southernmost ski area in the United States and has notoriously erratic season lengths and snow conditions. Overnight public lodging is not currently available anywhere on the mountain. A Pima County deputy sheriff is based near Summerhaven, and U.S. Forest

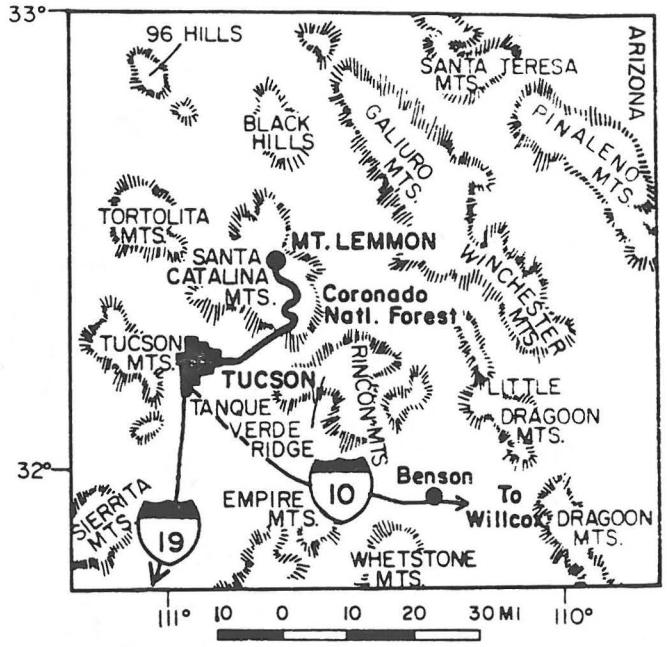

Service personnel can provide emergency communications and some services at the Palisades Ranger Station, near milepost 20.

Travel time from the base of the mountain to the crest of the range by geologists with a desire to make perhaps a half dozen stops in connection with this road guide is about 3 hours. The return drive straight back to Tucson should take about one hour. A full traverse of the range, in good weather and including return to Tucson via Oracle, Oracle Junction and Catalina, will consume the better part of a day. Such a traverse should not be attempted with less than a full tank of gas, by low-clearance vehicles or during inclement weather.

GENERAL GEOLOGIC STATEMENT

The Santa Catalina and Rincon mountains form a single geologic entity which produces a dramatic northern and eastern skyline for the Tucson metropolitan area. In spite of their strikingly sedimentary appearance, the parts of these ranges which lie closest to Tucson consist almost entirely of quartzofeldspathic gneisses (Catalina Gneiss) which have long fascinated geologists, and which continue to be puzzling with respect to their origin and the nature and timing of their deformation(s). In 1977 these rocks were part of the reason for convening a Geological Society of America Penrose Conference on "Cordilleran Metamorphic Core Complexes." Recent attention has focused on: 1) the association of these gneisses with décollement features and gravity-tectonic debris, especially at the southwestern end of the Tanque Verde Ridge turtleback and along the base of the Rincon Mountains (see **Davis, Third Day Road Log**); 2) the debate over the role of these gneisses and associated gravity-tectonic features in large-scale regional thrusting proposed by Drewes (1978), and 3) the enigmatic geochronological relations revealed over the years through studies by Damon and Bikerman (1964), Damon and

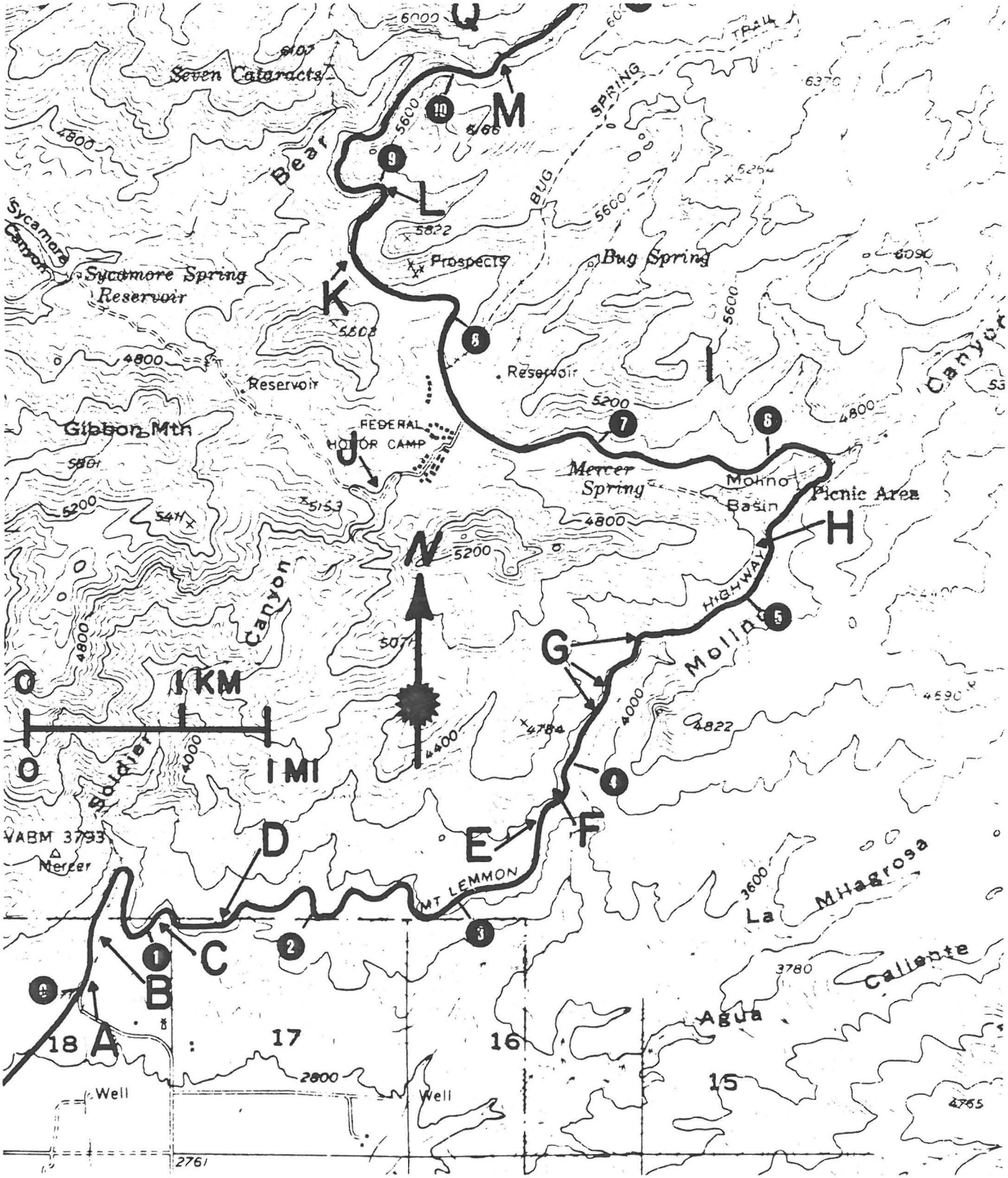

Map 1. Forerange and Bear Canyon traverse. Lowest eight miles of Tucson-Mt. Lemmon highway afford excellent exposures of Forerange gneisses and cross-section of Forerange fold. Vegetation ranges from saguaro, ocotillo and paloverde association of Sonoran Desert lowlands at about 2,800 ft to scrub oak and manzanita chaparral at 5,500 ft. Excellent views of Tucson, the Tucson Mountains to the west, the eastern section of Saguaro National Monument and the Tanque Verde Ridge turtleback structure to the south may be seen between mileposts 1 and 4.

others (1963), Livingston and others (1970), Shakel (1974), Shakel and others (1977), Silver (in prep.) and Creasey and others (1977).

Much simpler geologic relationships, involving unmetamorphosed units of the Precambrian through Cenozoic stratigraphic column of central and southeastern Arizona, are well displayed on the northern and eastern (far) sides of the Santa Catalina and Rincon ranges. The Oracle-Mt. Lemmon road traverses many of these rocks, but they are not treated in detail in this guide. These rocks were, however, described in a road log presented in the 1952 guidebook of the Arizona Geological Society (Butler and others, 1952).

INTRODUCTION

This supplemental road log begins at the southern end of the Catalina highway, at the intersection with the 9000 block of East Tanque Verde road. Mileposts (numbers in black circles on maps) are well maintained along mountain part of highway. Letters on maps refer to roadlog descriptions on page facing map. Black dots are vista points. Base maps are U.S.G.S. *Bellota Ranch* and *Mt. Lemmon* 15′ quadrangles, and a modified composite of these maps published by the Southern Arizona Hiking Club.

A Road traverses trace of Catalina fault, low-angle normal fault which generally separates Catalina Gneiss in footwall from fanglomerates of Oligocene Pantano Formation in hanging wall. Good exposures of fault are lacking along this part of mountain front.

B Boulder levees (remnants of debris flows ?), such as displayed here at mouth of Soldier Canyon, are a distinguishing feature of most drainages along southern base of mountains.

C Sign denoting Coronado National Forest boundary. This is a reasonable place to park and closely examine the variety of lithologies which constitute Forerange phases of Catalina Gneiss. Creasey and Theodore (1975) mapped these rocks as Precambrian Oracle Granite intruded by mid-Tertiary quartz monzonite of Samaniego Ridge. Note the presence of more than two lithologies of gneiss. Cataclasis is pervasive and has produced both foliation and lineation. Parallelism between cataclastic foliation and compositional layering is only approximate. Persistent east-northeast lineation is characteristic of most rocks in the Catalina metamorphic complex. Southward dip of foliation and layering at this locality relates to its position on the south limb of Forerange fold. **Use caution when returning to pavement!**

D Highway crosses axis of east-southeast plunging Forerange fold. This antiformal structure can be traced as far west as Ventana Canyon, but to east it loses definition a few miles south of Bellota Ranch headquarters. This generally N. 80°W.-trending structure appears to post-date all foliation and lineation in the gneissic rocks of the range, as well as the smaller amplitude and shorter wavelength east-northeast trending folds near Sabino Canyon, Agua Caliente Hill, etc., discussed by Pashley (1964).

E, G Downhill travelers can see vertical cliff faces exposing spectacularly intricate contact relationships between dark gneissic host rocks cut by numerous light phases of granitic composition. These cliff faces, which cut rock fabric approximately normal to both lineation and foliation, best display the crosscutting relationships which are generally present throughout the Forerange gneisses. This crosscutting is, however, not usually evident where these rocks are viewed on surfaces cut parallel to lineation. Note also the exposures across the canyon in its east wall.

F Zircon separates from biotite augen gneiss (dark phase of Forerange gneiss exposed in this roadcut) plot on 1440 m.y. old discordia chord previously determined by Silver and reported in Shakel and others (1977) for undeformed Oracle Granite of the type region at far north end of range, thus confirming presence of Precambrian granitic components within Catalina Gneiss as proposed by Creasey and others (1977).

J Molino basin and this basin to the west which once was site of federal correctional facilities are the easternmost manifestations of the more than 12-mi long "Romero Pass zone" of McCullough (1963), which controls the locations of the east and west forks of Sabino Creek, which in turn separate forerange to the south from main mass of Santa Catalina to the north.

I Dark components of gneiss are not nearly as abundant between mileposts 6 and 9 as in forerange farther south. Peterson (1968) and others ascribed this to a gradual northward transition of layered gneisses of forerange into "granitic gneiss-gneissic granite" of the main range. However, a "stratigraphic" transition between more homogeneous phases above and more anisotropic rocks typical of forerange below cannot be ruled out.

H Dark phases of gneiss exposed here are atypical of Forerange gneiss, and are cut by two different kinds of leucocratic pegmatite. This dark material has been regarded by some to be outliers of Leatherwood Quartz Diorite, but it lacks the small vitrous lime-green epidote crystals that distinguish the Leatherwood throughout most of the range.

K Excellent view westward of central parts of forerange, with culmination at Cathedral Peak (7,952 ft). Morning light excellently displays antiformal structure of Forerange fold. Steep dips in north limb of fold flatten out northward but retain a gentle northward dip as cataclastic gneisses pass to the right (north) and under Wilderness granite in the drainage basin of upper Lemmon Creek—the Wilderness of Rocks. Forerange gneisses grade upward into Windy Point-type gneiss and Wilderness granite in uppermost 1,000 ft of Cathedral Peak.

L Deadman's Curve—on close inspection, superficially homogeneous gneiss reveals faint layering with structures resembling cross-bedding. These features are best seen in cliff face just above highway milepost marker.

M Highest exposures of Forerange-type interlayered dark and light gneiss exposed along highway traverse. Spectacular exposures of intricately folded leucocratic phases are well displayed in both sides of deep roadcut immediately south of crossing of upper Bear Creek. Nearest safe parking is approximately 150 ft downhill, or 250 ft uphill. Folds are best seen at eye level, and in full shade.

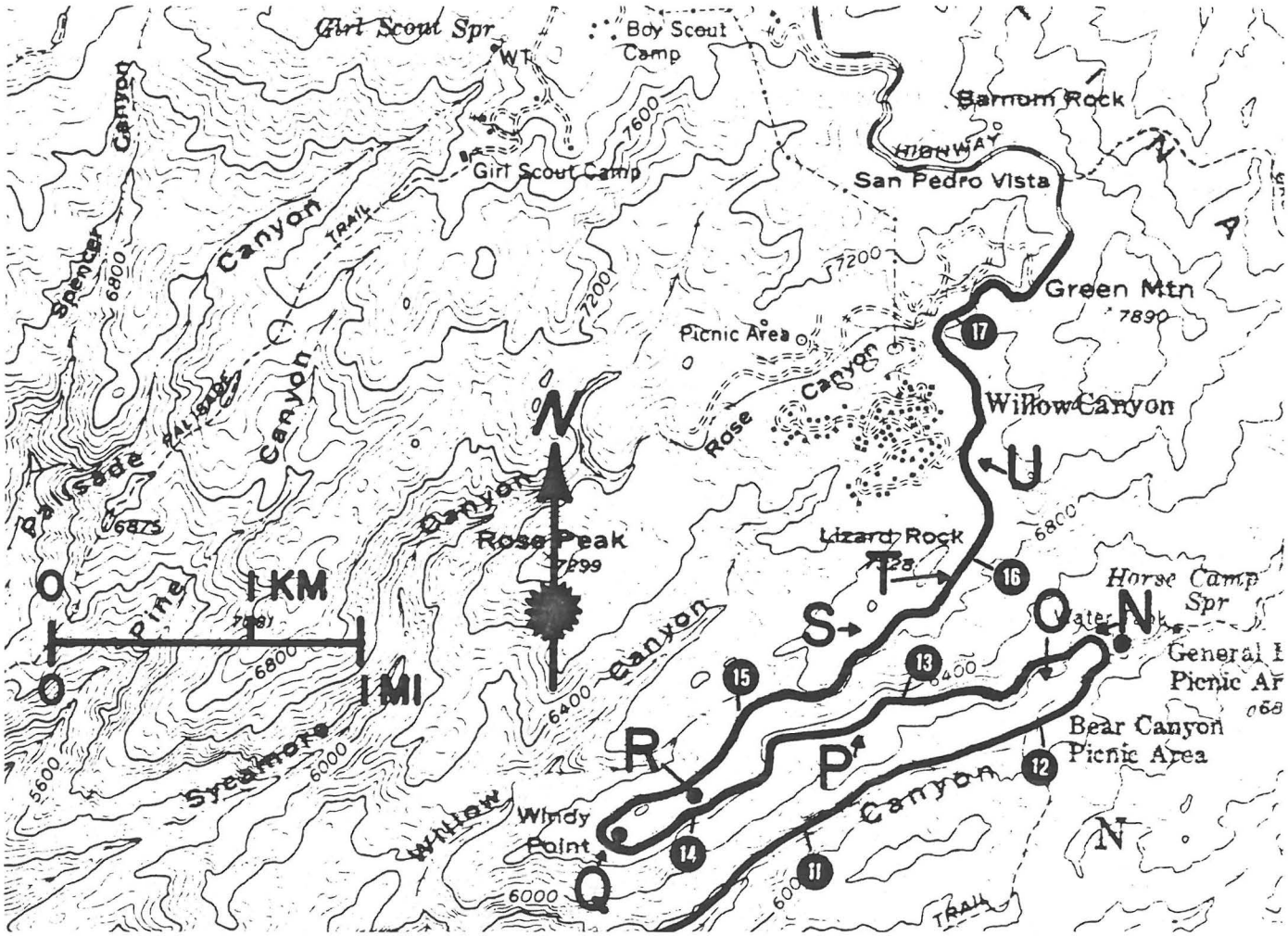

Map 2. Upper Bear Canyon, Windy Point and Geology Vista; transition between layered gneisses and granitoid rocks. This segment of highway takes the traveler from the pinon-juniper zone to ponderosa forests at 7,000 ft. The rocks are generally transitional between the northernmost layered Forerange gneiss and Wilderness granite and its cataclastic affiliates. The transition between Windy Point gneiss and Wilderness granite is particularly enigmatic, but well displayed since the highway crosses the contact zone three times in the course of negotiating the Upper Bear Canyon switchbacks.

N Roadcut just northwest of turnoff into Hitchcock picnic area contains freshest outcrops of Wilderness Granite exposed along highway.

HITCHCOCK PICNIC AREA. Main outcrop area and type locality of Wilderness granite is in Wilderness of Rocks, the basin of Lemmon Creek immediately south of Mt. Lemmon. Wilderness granite is typically white, garnet-rich, muscovite-biotite granite, with muscovite often as distinctive thin, 6-12 mm diameter, hexagonal plates, but in this roadcut, garnet is a bit more sparse and the muscovite is less euhedral than usual. Wilderness granite grades into cataclastic Windy Point gneiss downward and southward, and grades into garnet-free biotite-muscovite granite or Lemmon Rock leucogranite complex northward and upward. Contacts between Wilderness granite and other rock units have not been reported. Monazite separated from Wilderness granite at this locality gives U-Th-Pb ages of 44-47 m.y. (Shakel and others, 1977). This establishes a younger age limit for any metamorphic event in these rocks at or more severe than high greenschist facies, and is also in agreement with monazite ages obtained for cataclastically deformed granitoid gneiss from the westernmost end of the forerange. These ages,

do not, however, contravene the 25-27 m.y. K-Ar refrigeration ages determined by Damon and others (1963) or the fission-track confirmation of the K-Ar date reported by Creasey and others (1977). Creasey and others mapped this lithology as part of their "quartz monzonite of Samaniego Ridge."

O Natural arch visible in fin at southwest end of hill on southeast side of highway, approximately ½ mi above lower switchback. (Uphill travelers look left; downhill travelers look right; drivers continue to look forward and skip view!)

P Section of road between switchbacks traverses steep northwest side of upper Bear Canyon through closely spaced N.50°E.-trending fracture set that controls location and straightness of this segment of Bear Canyon drainage.

Q Windy Point and Hitchcock Monument—plaque set in gneiss about 25 ft above pavement on north side of highway is dedicated to General F. H. Hitchcock, longtime resident of Tucson who was principal figure in urging Federal support and completion of Tucson-Mt. Lemmon highway subsequent to World War II. Prior to 1950's, the only vehicular access to the crest of Santa Catalinas was via Oracle and Control road, on north side of range. Excellent views of south-central Arizona and metropolitan Tucson area are possible from here on clear days.

WINDY POINT. U.S. Forest Service exhibits describe vegetation and scenic attributes visible from here. In middle distance to south and southeast, west-northwest and east-southeast trending east and west forks of Sabino Creek form major drainage elements and separate forerange from main range along "Romero Pass zone" of McCullough (1963). Rock here is highly cataclastic quartzofeldspathic gneiss, with abundant muscovite and lesser amounts of biotite and garnet. Foliation is very gentle towards the northeast and is nearly horizontal, while lineation trends N.40°E. Garnetiferous quartz-feldspar pegmatite and alaskite form dramatic sills and subhorizontal dikes which cut the gneiss at low angles. Zircons separated from this gneiss and analyzed by Catanzaro and Kulp (1964) yielded very discordant U-Pb ages which plot close to but below the 1650 m.y. discordia chord determined by Silver and Deutsch (1963) for Johnny Lyon Granodiorite, a major plutonic component of the regional basement terrain some 30 mi east-southeast of here (Damon and others, 1963).

R Geology Vista provides view generally similar to that visible from Windy Point, but with better parking and safer access. U.S. Forest Service exhibit (when not vandalized) incorporates specimens of Catalina Granite, Barnes Conglomerate and dark augen gneiss, probably from somewhere in the forerange.

GEOLOGY VISTA. Catalina Granite forms a 30 km^2 pluton exposed on west flank of range, east of the community of Catalina, but is nowhere accessible by easily traversible roads. Banks (1976) included Catalina Granite as part of his mid-Tertiary "quartz monzonite of Samaniego Ridge." The pluton is nearly devoid of cataclastic textures and has sharply cross-cutting relationships with all other rocks where contacts are observable. Superficially similar megascopic appearances led early workers to correlate this rock with Precambrian Oracle Granite, and several recent compilations, including the current (1969) Geologic Map of Arizona, continue this error. Catalina Granite is a hornblende biotite quartz monzonite with abundant, large (up to 8 mm diameter) honey brown sphene crystals. Oracle Granite is a generally more thoroughly weathered and darker, biotite quartz monzonite. Both rocks tend to be porphyritic, with K-spar phenocrysts up to 4 cm long, but the Catalina Granite is more consistently so. Contacts are extremely difficult to locate where Catalina Granite has intruded Oracle granite. U-Th-Pb analyses of zircons from Catalina Granite collected at Golder Dam spillway give an emplacement age of 28 m.y. (Shakel and others, 1977) confirming the K-Ar age of 25 m.y. reported by Damon and others (1963) and the fission track age of 28 m.y. reported by Creasey and others (1977). The 90 m.y. Rb-Sr isochron reported by Shakel and others (1972) appears to be spurious and remains unexplained.

Barnes Conglomerate is now considered to be the basal member of the Dripping Spring Quartzite, a unit of the younger Precambrian Apache Group, and is a major marker unit of well rounded, ovoid quartzite cobbles and pebbles set in an arkosic quartzite matrix. Apache Group rocks are widely distributed in east-central Arizona, especially in Gila County, 75-100 mi north of here. There Apache Group and overlying Paleozoic strata are generally flat-lying and well preserved, but southward they are more commonly tilted and cut by faults. These conditions persist southward to the northern parts of the Santa Catalina Mountains, from whence this specimen probably comes. In the high crestal regions of the Santa Catalinas, especially south of Summerhaven, moderate metamorphism and severe deformation have affected the younger Precambrian and Paleozoic section so as to render these rocks almost unrecognizable. However, metaconglomerates in the area south of Summerhaven, particularly in the vicinity of the Marshall Gulch picnic area, were recognized by Peirce (1958) as meta-Barnes and meta-Scanlan conglomerates, and thus permitted him to make correlations with the Apache Group exposed farther north in the range. Apache Group rocks are unknown south of the Santa Catalina and Little Dragoon mountains.

S Natural arch with span of about 20 ft is visible in thin fin of gneiss parallel and above highway on northwest side. This arch is difficult to spot from moving vehicles, and is best seen by uphill travelers just prior to entry into curve immediately south of arch, although from there it has vegetation visible through it rather than sky.

T Two to five-inch thick zones of true mylonite are developed here and elsewhere in rock transitional between foliated Wilderness granite and Windy Point gneiss. Mylonite zones dip northwest at moderate angles. Flaser structure and wholly aphanitic textures characteristic of true mylonite are well developed. These features are not generally visible from moving vehicles, and parking in this vicinity is poor—use caution!

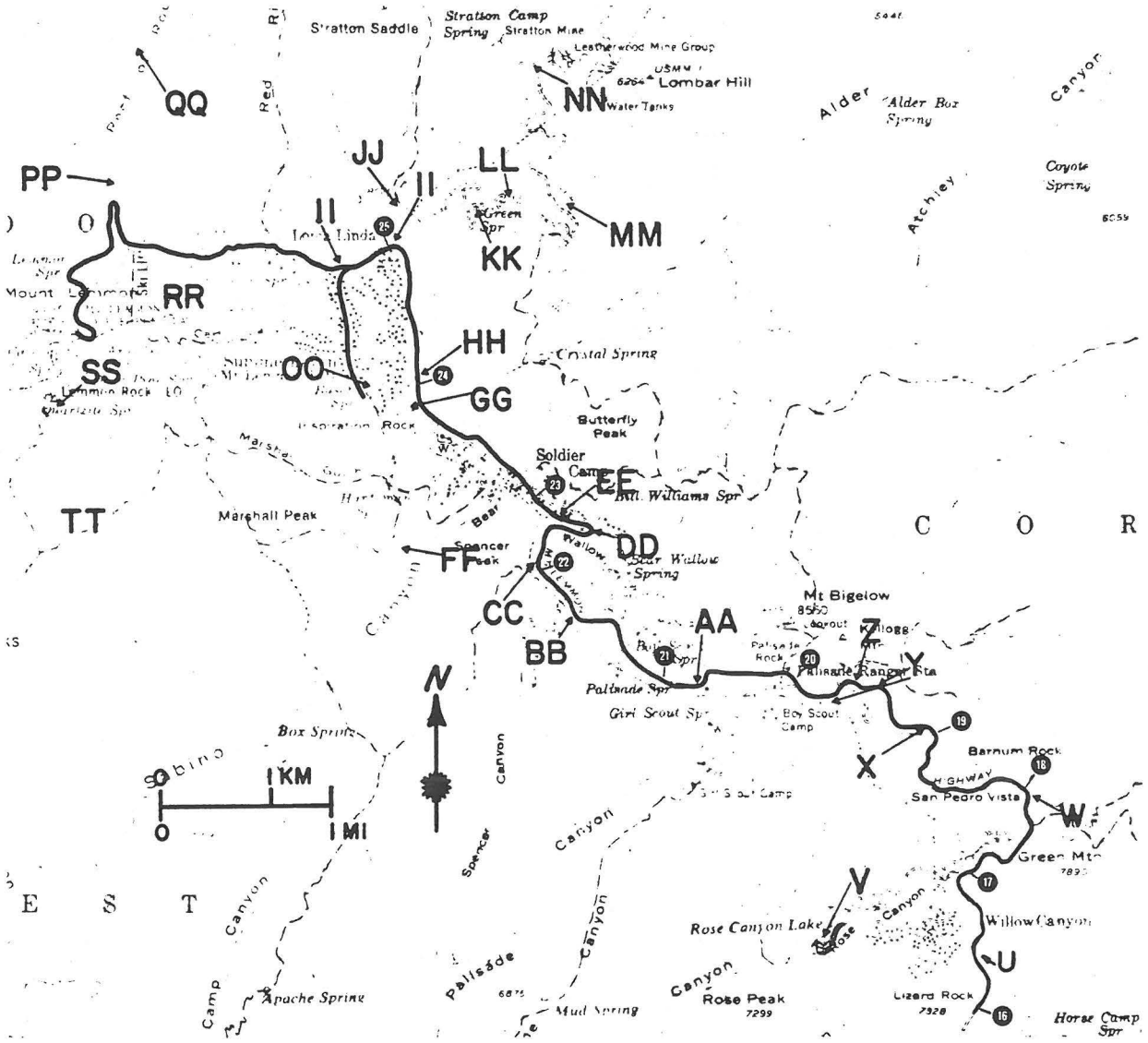

Map 3. Catalina high country. Between mileposts 16 and 23 the highway traverses the heavily developed recreational portion of the range, almost entirely in ponderosa pine forest. Rocks are mainly foliated granitoids of the Wilderness/Windy Point/Lemmon Rock association. Only a few dark schistose masses visible from the highway belie the presence of the granite-metasediment boundary which generally controls the location of the range crest several hundred feet above the highway to the north between mileposts 18 and 22.

Mount Lemmon and Summerhaven areas. These highest parts of the range include spruce-fir plant associations, with groves of aspen indicating old burn sites. Metasediments are extensively intruded by dark grey Leatherwood Quartz Diorite, which is in turn intruded by aplites, alaskites and pegmatites of the Lemmon Rock leucogranite complex. Several of the sites noted on the map will require short hikes, so lowlanders should remember that this area is above 7,600 ft.

U Moderately foliated two-mica granitoid rocks such as exposed in these roadcuts are typical of most of the light colored plutonic rocks north of here.

V Excellent exposures around shores of Rose Canyon Lake display typical diffuse and enigmatic contacts between slightly foliated Wilderness granite, pegmatite and alaskite phases of Lemmon Rock leucogranite, and two-mica garnet-free probable border phase of Wilderness pluton.

W View northeastward from San Pedro vista reveals faulted younger Precambrian Apache Group and overlying Paleozoic section typical of southern Arizona dipping moderately north-northeastward and forming northeastern flanks of range. Similar relations obtain along most of the northeastern slopes of entire Santa Catalina-Rincon massif. Prominent cliff-forming units in middle distance are Precambrian Barnes Conglomerate (basal) member of Dripping Spring Quartzite in middle of bold slopes facing vista, capped by white uppermost layers of Cambrian Bolsa Quartzite, followed by Mississippian Escabrosa Limestone at crest of ridge. Younger, less deformed and generally flat-lying volcanic and volcaniclastic rocks of mid-Tertiary age form the bulk of the Galiuro Mountains northeastward beyond valley of San Pedro River. Tailings

and smokestacks at San Manuel smelter and town are visible in north from south end of vista wall. San Manuel mine, presently the largest block-caved copper mine in North America, lies 7 mi north-northwest of the town, but is not visible from here. On clear days, the Pinaleño Mountains and Mt. Graham (10,713 ft) form the farthest northeast skyline, while the Winchester Mountains lie on the horizon to the far right (due east).

X Opposite the access road on downhill side of highway near sign denoting Sollers Point is dike of garnetiferous pegmatite (Lemmon Rock leucogranite) in deformed Wilderness granite(?). Drill holes date from study by Matter (1969) who investigated geochemistry of dike emplacement.

Y Small masses of metasedimentary rock, generally regarded as meta-Apache Group, are exposed in roadcuts. Rocks are mostly quartz-mica schists.

Z Small mass of intensely isoclinally folded metamorphic rocks exposed 35 ft above highway on north side. Best observed by uphill travelers. Rocks include calc-silicate, mica schist and amphibolite.

AA Mass of crinkle-folded metasediments which have been synkinematically intruded by biotite-rich two-mica granite. Granite is devoid of garnets and is thought to be border phase of Wilderness pluton.

BB Biotite-rich two-mica granite exposed along highway and throughout most of Spencer recreation area is possible garnet-free border phase of Wilderness pluton.

CC Contact between plutonic rocks of southern Santa Catalinas and metamorphic rocks typical of northern side of range.

DD Parking available on inside (west side) of curve, where one can observe in opposite (east) roadcut multiple fold sets in meta-Dripping Spring Quartzite. Present are several northward dipping but curved (concave down to southeast) axial surfaces of F_2 structures which have folded earlier and more tightly isoclinal F_1 axial planes that now have gentle southward dips. These and other structures were investigated by Waag (1968), who concluded that F_1 folds formed synchronously with metamorphism and that F_2 deformation may have occurred only a short time later, perhaps as waning stages of F_1 event.

EE Parking area on south side of highway provides good vantage point for intravehicular discussion of fold/fault structure in roadcut opposite. Close examination of apparently horizontal strata in east (right) part of structure reveals numerous very tight isoclinal folds, with nearly horizontal axial planes and axes which are nearly parallel with the plane of the roadcut. Waag (1968) mapped these strata as meta-Dripping Spring Quartzite.

FF Metaconglomerates here enabled Peirce (1958) to identify the metasediments at and near the crest of the range as units of the Precambrian Apache Group. Below here, diffuse contacts between deformed Oracle Granite(?) and garnet-poor Wilderness granite(?) illustrate the difficulties in unraveling the geology of this part of the range.

GG Deep red garnets in biotite schist occur below top of hill west of here.

HH Southernmost exposures of Leatherwood Quartz Diorite seen along highway. This pluton is generally sill-like or laccolithic and forms most of the crestal area around Summerhaven and to the north as far as Marble Peak. Fresh exposures are difficult to obtain. The rock is nearly always riddled with dikes of leucogranite.

II Spectacular dike sets of Lemmon Rock leucogranite in Leatherwood Quartz Diorite. Roadcut just west of junction with road to Summerhaven was blasted from fresh rock in early 1970's. Note rapid rate at which Leatherwood deteriorates in this climate.

JJ Only view of Reef of Rock from road area is seen from entrance to sawmill area (look north-northwest).

KK Leatherwood Quartz Diorite from this locality yielded zircons which gave very discordant U-Th-Pb ages, indications a high degree of zircon inheritance, possibly from 1440 m.y. old Precambrian terrain (Shakel and others, 1977).

LL Note green sand in road gutters, derived from sorting of lime-green epidote crystals which readily weather out of Leatherwood Quartz Diorite.

MM Foliated Leatherwood occurs at several locations along road in this area.

NN Colluvial debris of white marble are only chance to examine meta-Paleozoic carbonate rocks probably metamorphosed during Leatherwood plutonism. Prospecting activities have focused on Cu and Au developed as skarn deposits along igneous-metasediment contacts.

OO Spectacular intersection dikes of "line rock" (Jahns, 1954) developed by zones of red garnet in pegmatite phase of Lemmon Rock leucogranite. K-feldspar crystals up to 25 cm also present. Note also inclusions of Leatherwood Quartz Diorite. K-Ar and Rb-Sr ages of this rock (44-45 m.y.) establish younger limit for cataclasis in this part of range (Shakel and others, 1977).

PP Andalusite has been identified in meta-Abrigo Formation(?) from this locality.

QQ Reef of Rock is barren massif formed of dike-like mass of young leucocratic granite intruded between Catalina granite on west and Leatherwood Quartz Diorite on east. Feature was studied by Sueminicht (1977).

RR Metasedimentary rocks between ski area and summit are generally accepted as upper Apache Group and Bolsa Quartzite equivalents. Calc-silicates are probably remnants of Mescal Limestone.

SS Type locality of Lemmon Rock leucogranite. Phase here is feldspar-quartz-muscovite-garnet pegmatite. Precariously perched ranger station affords spectacular view of Wilderness of Rocks basin and Pusch Ridge Wilderness area.

TT Wilderness of Rocks is type locality of Wilderness granite, a distinctive inclusion-free, medium-grained, garnet-bearing two-mica granite, usually white on fresh exposure.

See References, page 139.

Geological Society of America
Memoir 153
1980

Evidence for multiple intrusion and deformation within the Santa Catalina–Rincon–Tortolita crystalline complex, southeastern Arizona

STANLEY B. KEITH *Bureau of Geology and Mineral Technology*
University of Arizona, Tucson, Arizona 85721

STEPHEN J. REYNOLDS *Department of Geosciences*
University of Arizona, Tucson, Arizona 85721

PAUL E. DAMON AND MUHAMMAD SHAFIQULLAH
Laboratory of Isotope Geochemistry, Department of Geosciences
University of Arizona, Tucson, Arizona 85721

DONALD E. LIVINGSTON *Bendix Field Engineering, Geochemical Division*
P.O. Box 1569, Grand Junction, Colorado 81501

PAUL D. PUSHKAR *Department of Geology*
Wright State University, Dayton, Ohio 45431

The central feature of the range, as worked out by Mr. Tolman, is a great post-Carboniferous intrusive mass of siliceous muscovite granite modified to a gneissic rock near its margins, surrounded by an intense contact metamorphism in which rocks of widely different kinds have been conspicuously affected. The oldest rock cut by this granite is a coarse biotite granite which apparently as a result of the later granitic intrusion, grades into augen gneiss, and locally this rock in turn has been transformed into a thinly fissile schist.

Interpretation by C. F. Tolman of the geology of the Santa Catalina Mountains as told by Ransome, 1916, p. 144

ABSTRACT

Recent field work and accumulated Rb-Sr studies, when combined with previous U-Th-Pb and K-Ar investigations, allow a new synthesis of the crystalline terrane within the Santa Catalina–Rincon–Tortolita crystalline complex. When all the available data are integrated, it is apparent that the crystalline core is mainly a composite batholith that has been deformed by variable amounts of cataclasis. The batholith was formed by three episodes of geologically, mineralogically, geochemically, and geochronologically distinct plutons. The first episode (75 to 60 m.y. B.P.) consisted of at least two

(and probably three) calc-alkalic, epidote-bearing biotite granodiorite plutons (Leatherwood suite). The Leatherwood suite is intruded by distinctive leucocratic muscovite-bearing peraluminous granitic plutons (Wilderness suite), which are 44 to 50 m.y. old. At least three Wilderness suite plutons are known, and their origin has been much debated. Leatherwood and Wilderness plutons are intruded by a third suite of four biotite quartz monzonite to granite plutons (Catalina suite) that mark the final consolidation of the batholith 29 to 25 m.y. ago.

Much of the mylonitic (cataclastic) deformation of the plutonic rocks and recrystallization of the enclosing host rocks may be related to intrusion of the various plutons. At least three episodes of mylonitization (cataclasis) may be delineated by observing relations between mylonitic and nonmylonitic crosscutting plutons. The southern part of the Leatherwood pluton bears a moderate to strong mylonitic foliation that is cut by undeformed leucogranites and pegmatite phases of the Wilderness pluton.

Elsewhere in the Santa Catalina–Rincon–Tortolita crystalline core, Wilderness suite plutons contain penetrative mylonitic foliation. Foliated Wilderness suite plutons are intruded by an undeformed portion of a Catalina suite pluton. In the Tortolita Mountains, however, intrusions of the Catalina suite themselves contain evidence for at least two events of mylonitic deformation. The most significant of these events is clearly constrained to the Catalina intrusive episode because it formed during or after the emplacement of Tortolita quartz monzonite (about 27 m.y. B.P.) but before the intrusion of postfoliation dikes (about 24 m.y. B.P.). All three episodes of mylonitization contain the distinctive and much discussed east-northeast–trending lineations. All events of mylonitization are constrained to a 50-m.y. interval of time from 70 to 20 m.y. ago. Although continuous mylonitization from 70 to 20 m.y. ago cannot be unequivocally disproved, the strong association of mylonitization with the three plutonic episodes suggests that deformation in the Santa Catalina–Rincon–Tortolita crystalline core, like intrusion, was episodic.

INTRODUCTION

The Santa Catalina–Rincon–Tortolita crystalline complex is located (Fig. 1) at the southeast end of a zone of crystalline complexes that trends northwest through southern Arizona (Rehrig and Reynolds, this volume; Banks, this volume; Davis and others, this volume; Davis, this volume). Crystalline complexes in this zone are in part characterized by chiefly mylonitic varieties of cataclastic rocks whose gently dipping foliation defines broad arches or domes (Davis, this volume; Coney, 1979 and this volume; Rehrig and Reynolds, this volume; Reynolds and Rehrig, this volume). Evidence of post-Paleozoic plutonism, metamorphism, mylonitization, and cataclasis abound in all of the complexes. Latest cooling ages in the Arizona crystalline complexes are generally middle Tertiary (Damon and others, 1963; Mauger and others, 1968; Creasey and others, 1977; Banks and others, 1978; Banks, this volume; Rehrig and Reynolds, this volume). On some gently dipping sides of the domes, the upper levels of the mylonitic gneisses are jointed, brecciated, chloritic, and hematitic. The mylonitic gneisses are overlain by a low-angle dislocation surface (for definition of this term, see Rehrig and Reynolds, this volume). Above the dislocation surface lie highly faulted and locally folded (Davis, 1975) rocks that are generally unmetamorphosed and lack the mylonitic textures that characterize the basement below the dislocation surface.

The Santa Catalina–Rincon–Tortolita crystalline complex is within the Basin and Range province, an area characterized by late Tertiary fault-block mountain ranges and valleys. The oldest rocks exposed in the ranges (Fig. 2) consist of middle Proterozoic metasedimentary and metaigneous rocks that underwent a major metamorphic-deformational-plutonic event about 1.65 b.y. ago and a later episode of granitic intrusion 1.45 b.y. ago (Silver, 1978). These rocks were beveled by erosion and

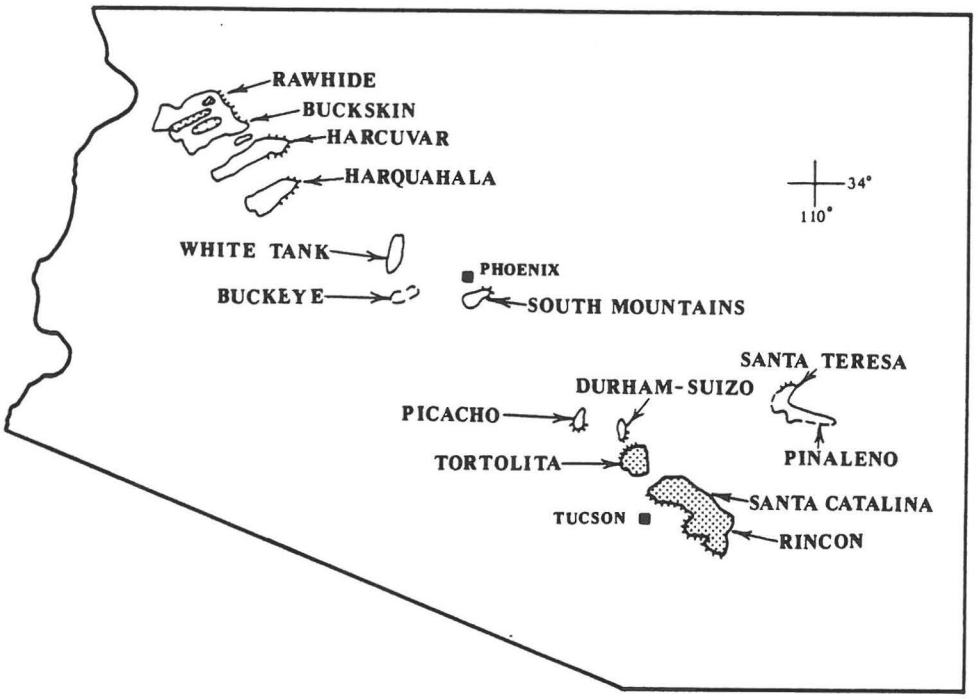

Figure 1. Map of southern Arizona showing location of Santa Catalina–Rincon–Tortolita crystalline complex (dot pattern). Similar complexes are outlined, and dislocation surfaces are depicted by hachures (from Rehrig and Reynolds, this volume).

overlain by 1.4- to 1.1-b.y.-old sedimentary rocks of the Apache Group and associated diabase (Shride, 1967). Apache Group rocks are overlain by a cratonic sequence of Paleozoic carbonate and fine-grained clastic rocks (Bryant, 1968; Peirce, 1976). Mesozoic rocks of the region represent a period of volcanism, plutonism, and tectonic instability (Hayes, 1970; Hayes and Drewes, 1968, 1978; Titley, 1976). The Late Cretaceous–early Tertiary Laramide orogeny was also a time of deformation (Drewes, 1976a; Davis, 1979) and alkali-calcic to calc-alkalic magmatism (Keith, 1978). After a period of *relative* quiescence, high potassium–calc-alkalic magmatism and deformation were renewed in middle Tertiary time (Damon and Mauger, 1966; Shafiqullah and others, 1978; Keith, 1978). These events were followed after 15 m.y. B.P. by block faulting and basaltic volcanism (Shafiqullah and others, 1976; Eberly and Stanley, 1978; Scarborough and Peirce, 1978).

Within this regional geologic framework, the Santa Catalina–Rincon–Tortolita crystalline complex has been an enigma since research started on it in the early 1900s. The purpose of this paper is to summarize published and unpublished geologic and geochronologic studies and to integrate these into a discussion concerning ages and correlations of major rock units within the complex. Particular attention will be given to post-Paleozoic intrusions that together constitute a composite batholith which dominates the geology of the complex.

Igneous rock nomenclature in this paper follows traditional usage of rock names within the Santa Catalina–Rincon–Tortolita crystalline complex except where noted in the text. Rocks described by the term "mylonitic" possess a foliation (fluxion structure of Higgins, 1971) and in thin section show comminuted and brittlely deformed feldspars (from 60% to 80% of rock) and recrystallized, sutured aggregates of quartz (as much as 40% of rock). The mylonitic rocks are similar to photographs of hand

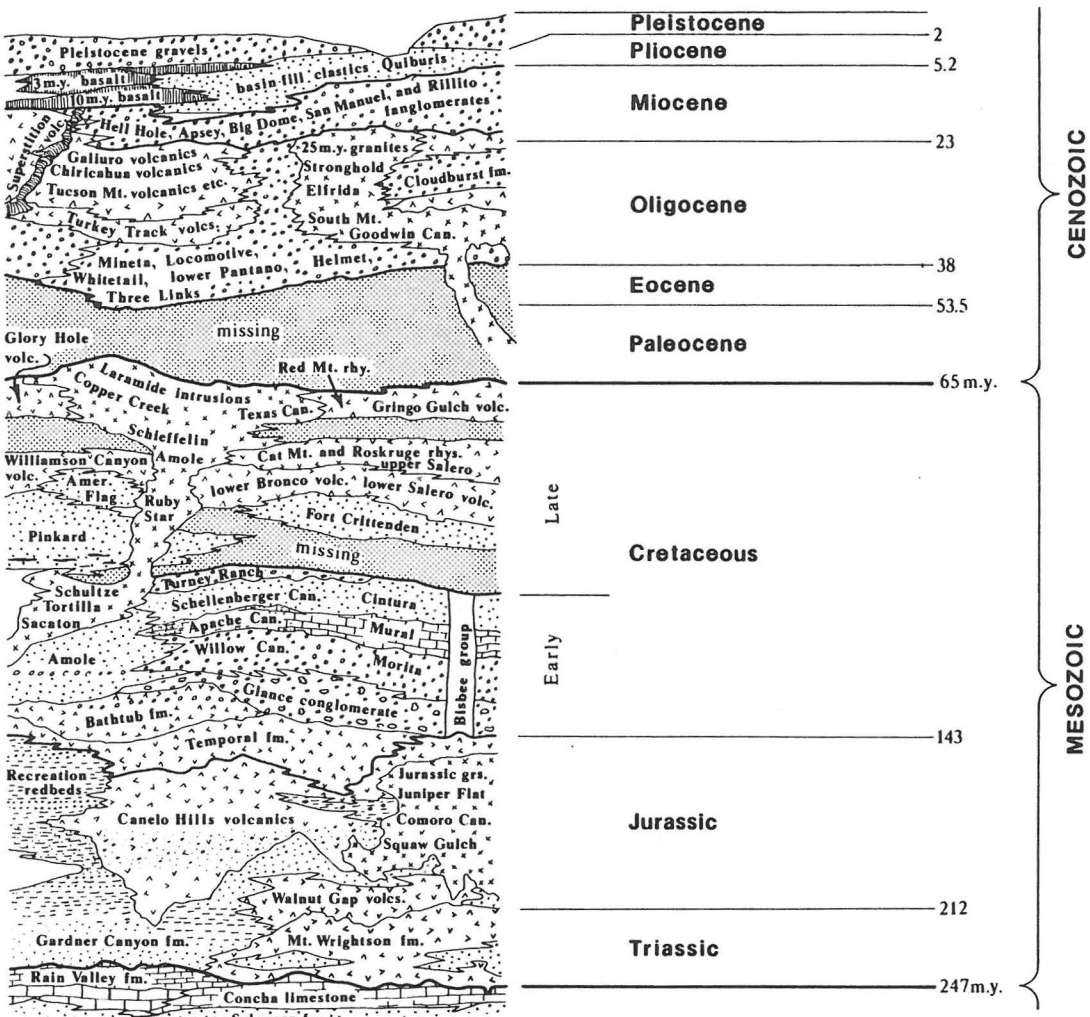
Pleistocene gravels
3 m.y. basalt
10 m.y. basalt
basin fill clastics
Quiburis
San Manuel, and Rillito
conglomerates
Hell Hole, Apsey, Big Dome,
Superstition volc.
25 m.y. granites
Galiuro volcanics
Chiricahua volcanics
Stronghold
Cloudburst fm.
Tucson Mt. volcanics etc.
Elfrida
South Mt.
Turkey Track volcs.
Goodwin Can.
Mineta, Locomotive,
Whitetail, lower Pantano,
Helmet,
Three Links
missing
Glory Hole volc.
Red Mt. rhy.
Laramide intrusions
Copper Creek
Texas Can.
Gringo Gulch volc.
Schieffelin
Williamson Canyon volc.
Amole
Cat Mt. and Roskruge rhys.
upper Salero
Amer. Flag
Ruby Star
lower Bronco volc.
lower Salero volc.
Fort Crittenden
Pinkard
missing
Turney Ranch
Schultze
Tortilla
Sacaton
Schellenberger Can.
Cintura
Apache Can.
Mural
Willow Can.
Morita
Amole
Glance conglomerate
Bisbee group
Bathtub fm.
Temporal fm.
Recreation redbeds
Jurassic grs.
Juniper Flat
Canelo Hills volcanics
Comoro Can.
Squaw Gulch
Walnut Gap volcs.
Gardner Canyon fm.
Mt. Wrightson fm.
Rain Valley fm.
Concha limestone
Scherrer fm.
Pleistocene
2
Pliocene
5.2
Miocene
23
Oligocene
38
Eocene
53.5
Paleocene
65 m.y.
Late
Early
Cretaceous
143
Jurassic
212
Triassic
247 m.y.
CENOZOIC
MESOZOIC

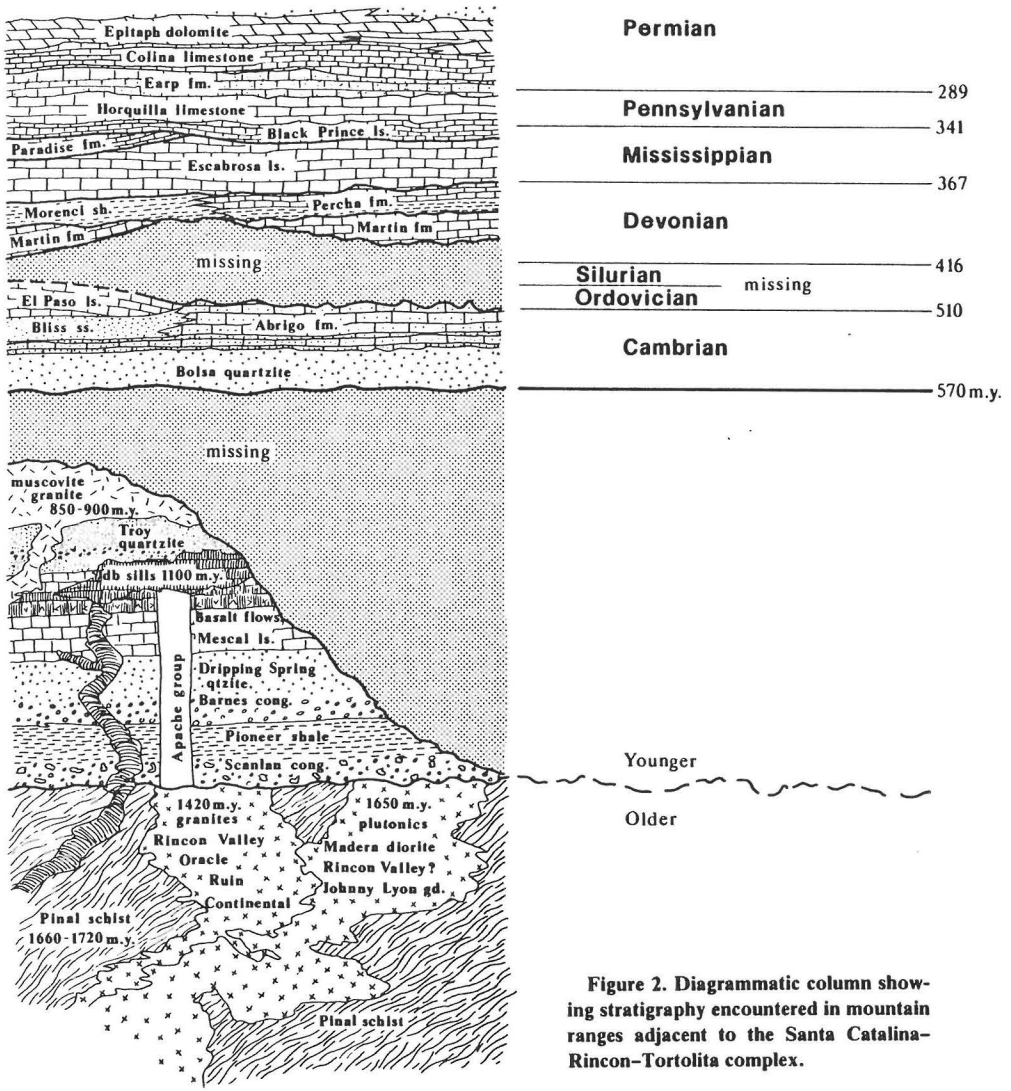

Figure 2. Diagrammatic column showing stratigraphy encountered in mountain ranges adjacent to the Santa Catalina–Rincon–Tortolita complex.

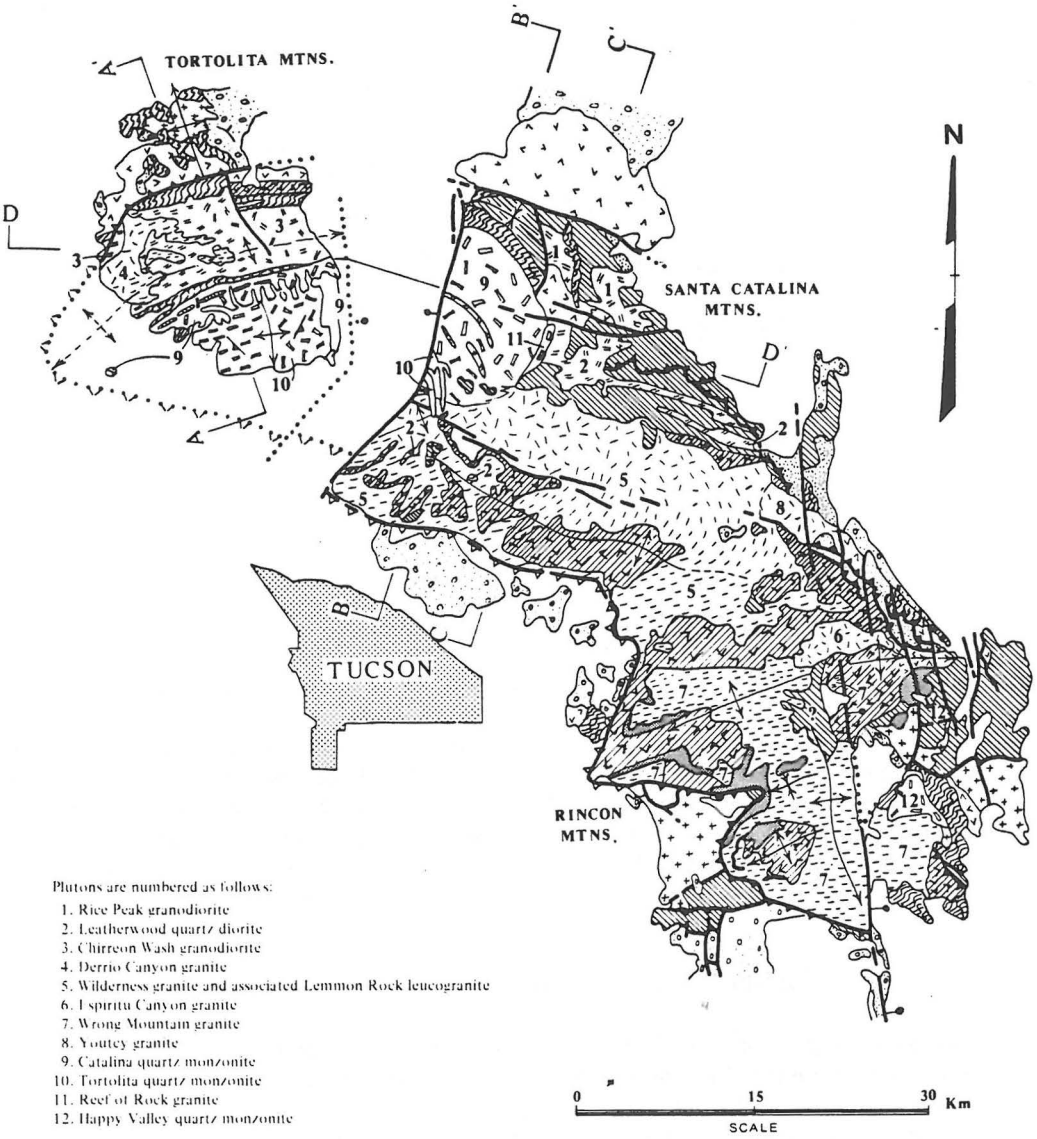

Figure 3. Generalized geologic map of Santa Catalina–Rincon–Tortolita crystalline complex showing locations of cross sections and plutons discussed in text. Sources of map data are as follows: for Tortolita Mountains—Budden (1975), Banks and others (1977), and Keith (unpub. mapping); for Santa Catalina Mountains—Tolman (1914, unpub. mapping as presented in Wilson and others, 1969), Creasey (1967), Shakel (1974), Creasey and Theodore (1975), Banks (1976), Hoelle (1976), Suemnicht (1977), Wilson (1977), and Keith (unpub. mapping); for Rincon Mountains—Drewes (1974, 1977) and Thorman and Drewes (1978). Aligned patterns in Late Cretaceous through Oligocene intrusions show deformed areas of mylonitic gneiss, and random patterns show undeformed areas. East-northeast–trending ruled lines show areas of mylonitically deformed porphyritic mesocratic gneiss believed to have been previously undeformed 1,400- to 1,450-m.y.-old biotite granitic rocks (shown by random pattern). Barbed heavy lines are low-angle faults with barbs in upper plate. Heavy lines are high-angle normal faults with bar and ball on downthrown side.

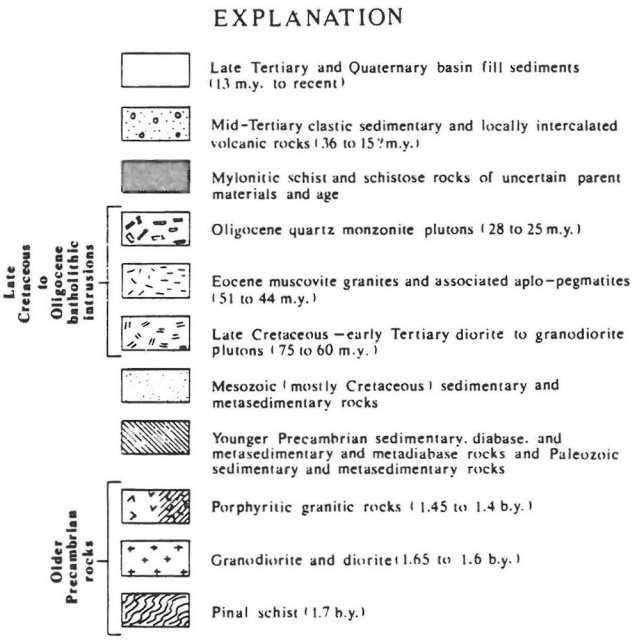

specimens and photomicrographs of protomylonite, mylonite, and mylonite gneiss as presented in the classification of cataclastic rocks proposed by Higgins (1971). Some areas of mylonitic gneiss contain very coarse-grained pegmatites concordantly interlayered with the mylonitic augen gneisses. The interiors of these pegmatites are commonly highly broken or brecciated, possess no foliation, and are more properly referred to as cataclasites in the classification scheme of Higgins (1971). Areas we call "mylonitic" may contain variable fractions (usually minor) of pegmatite cataclasites.

GENERAL GEOLOGY OF THE CRYSTALLINE COMPLEX

General geology of the Santa Catalina–Rincon–Tortolita crystalline complex is presented in simplified map form in Figure 3 and depicted diagrammatically in four cross sections (Figs. 4, 5, 6, and 7). Frequently mentioned localities are shown geographically in Figure 8. Readers are directed to discussions and references cited in Creasey and others (1977), Budden (1975), Shakel (1974, 1978), Davis (1975, 1977a, 1977b, 1978, and this volume), Drewes (1977), Drewes and Thorman (1978), Thorman (1977), Davis and Coney (1979), and Banks (this volume) for other recent perspectives.

In a general way, the Santa Catalina–Rincon–Tortolita complex is composed of a crystalline core that is dominated by Phanerozoic plutonic rocks (~75% of outcrop). The remainder of the crystalline core consists of middle Proterozoic plutonic rocks (~20% of outcrop) and subordinate amounts of middle Proterozoic and Phanerozoic metasedimentary rocks. The crystalline core is mostly fault-bounded, except for segments of its north and northeast margins which are intrusive in nature.

The Phanerozoic plutonic rocks form a large composite batholith within which at least 10 and possibly 12 or more individual plutons (Fig. 3) have been delineated (see App. 1 for discussion of nomenclature of these bodies). Individual plutons are generally compositionally zoned and commonly

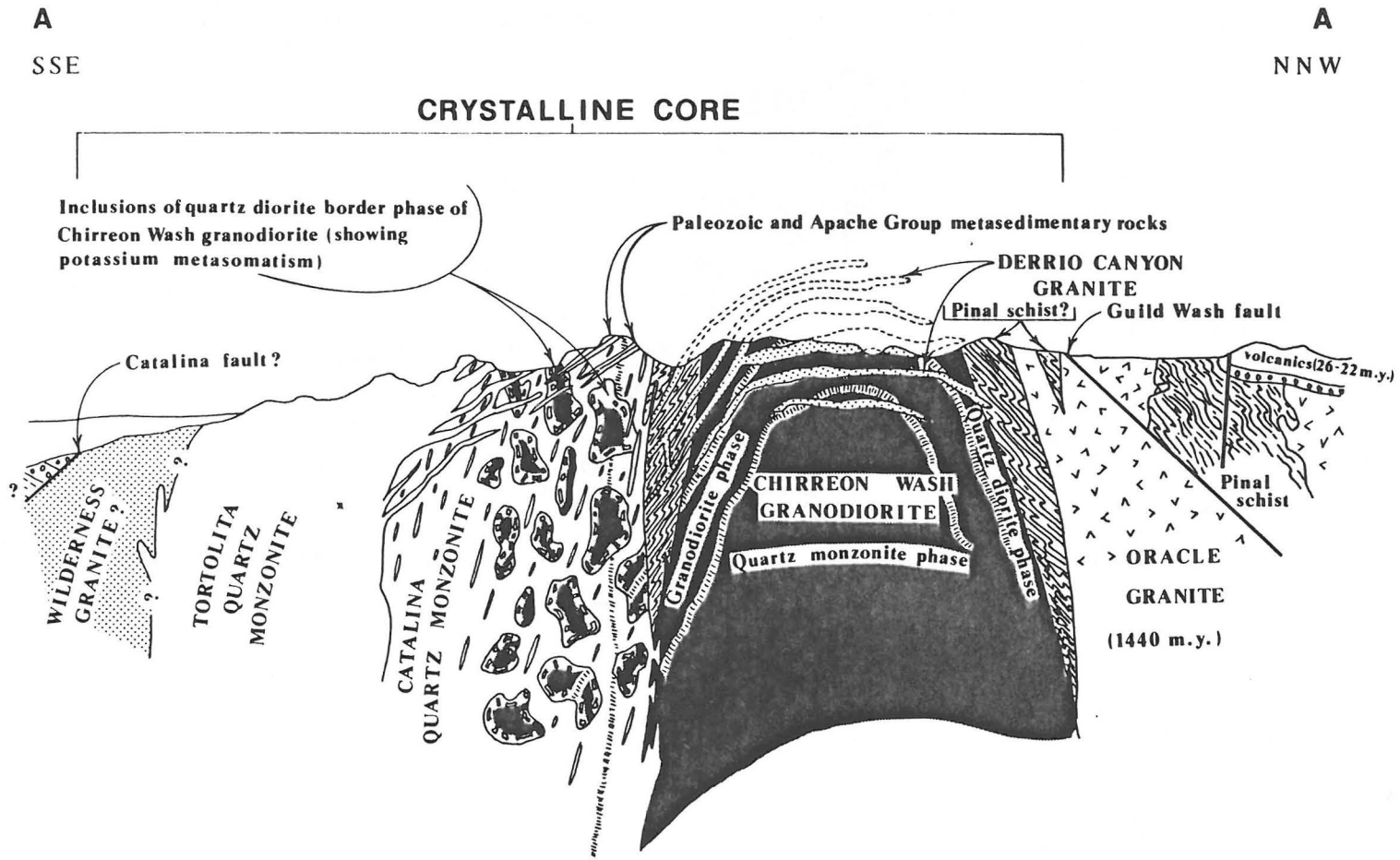

Figure 4. Diagrammatic cross section A–A′ through Tortolita Mountains. Location of section shown in Figure 3.

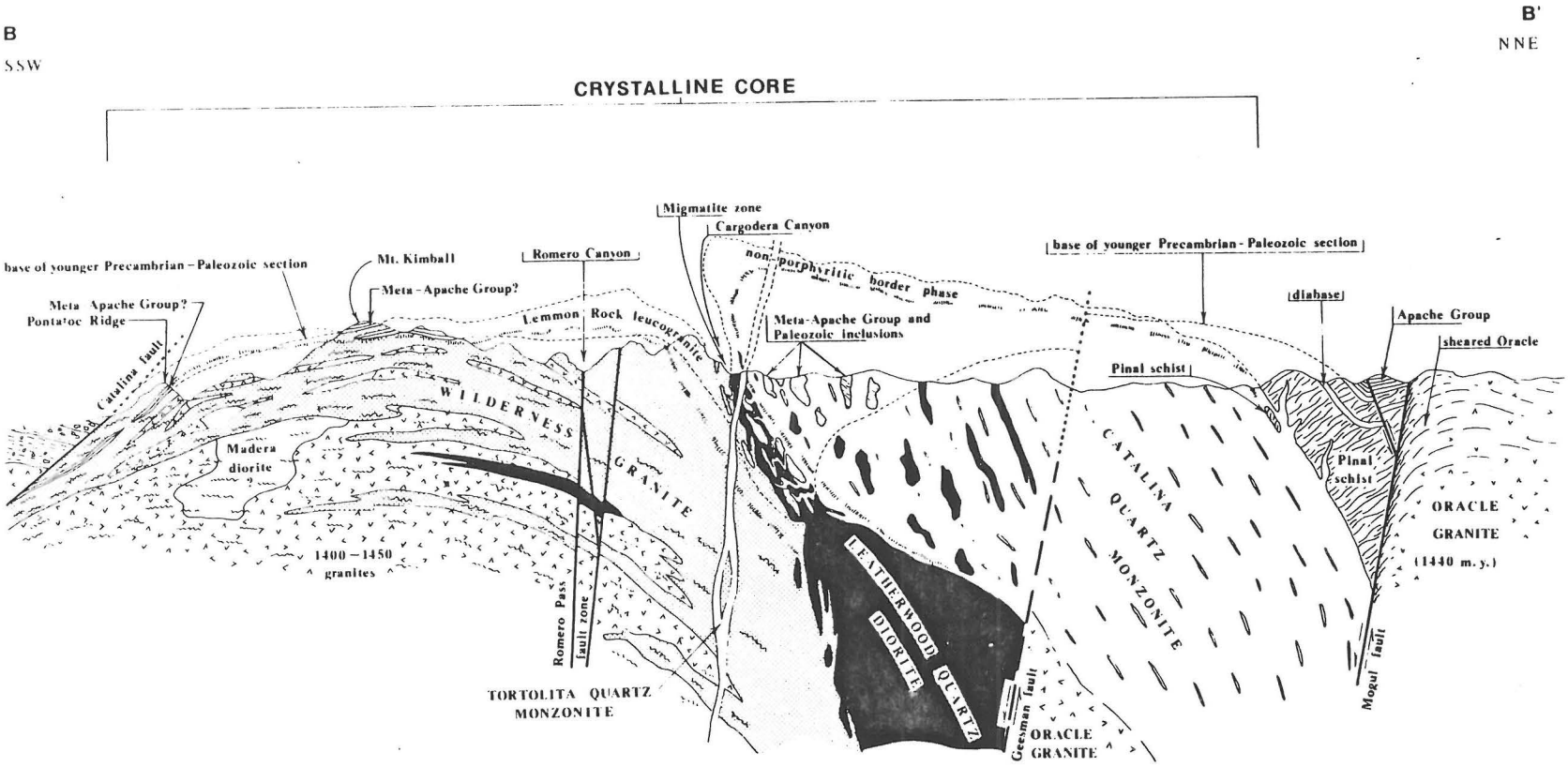

Figure 5. Diagrammatic cross section B–B′ through western Santa Catalina Mountains. Location of section shown in Figure 3. Mylonitic rocks shown by wavy lines.

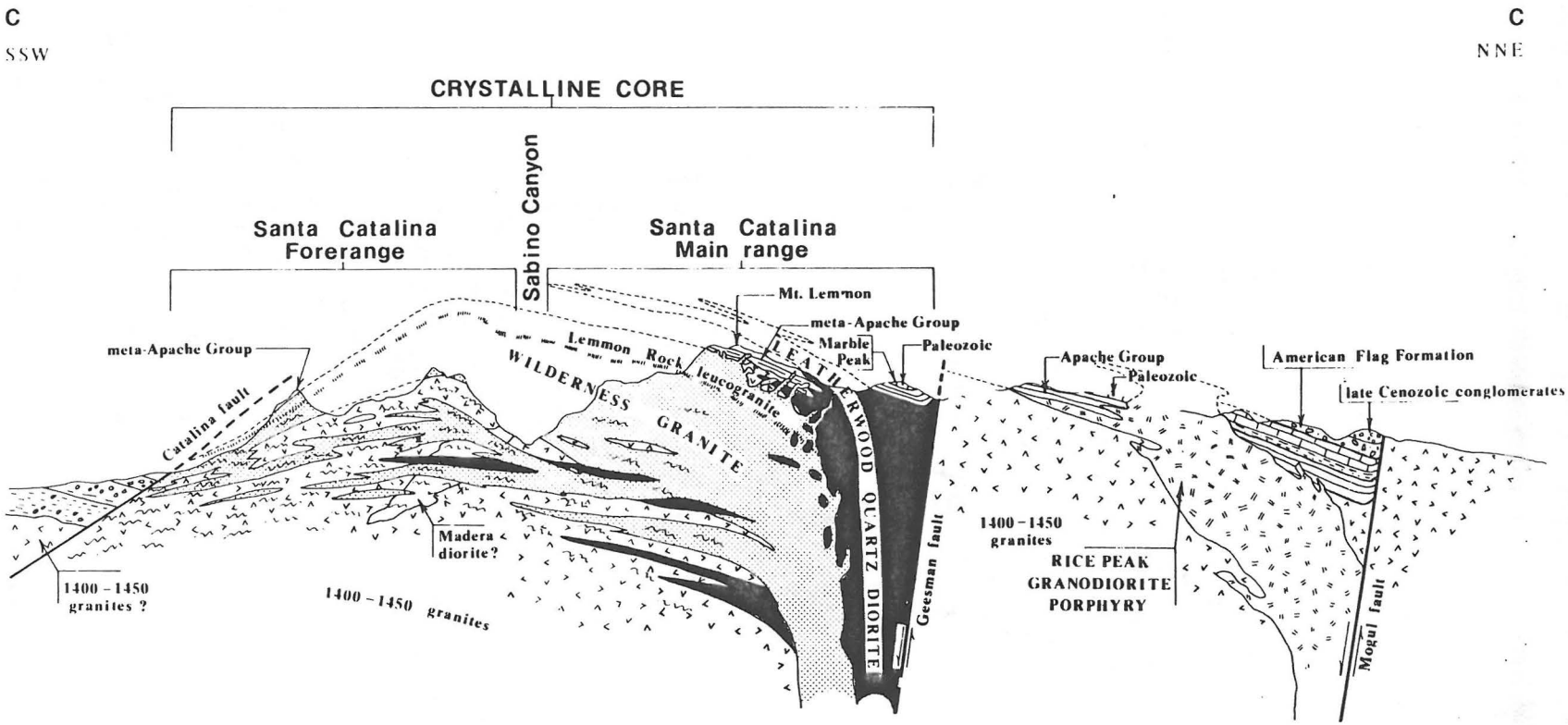

Figure 6. Diagrammatic cross section C–C′ through central Santa Catalina Mountains. Location of section shown in Figure 3. Mylonitic rocks shown by wavy lines.

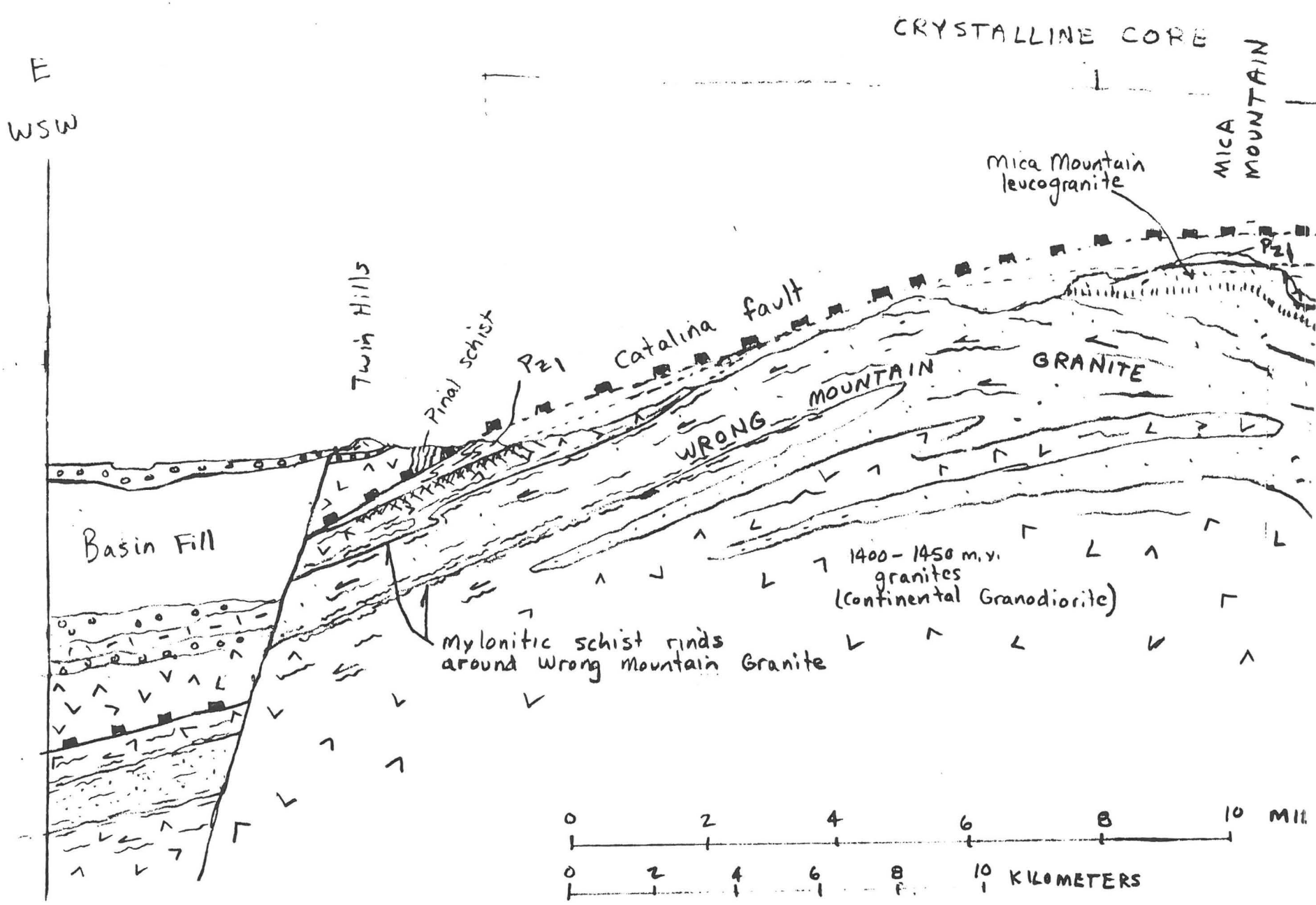

Diagrammatic cross section E-E' through northern of simple shear as determined from 'S' and 'C' planes in older mylonites.

Keith 1983

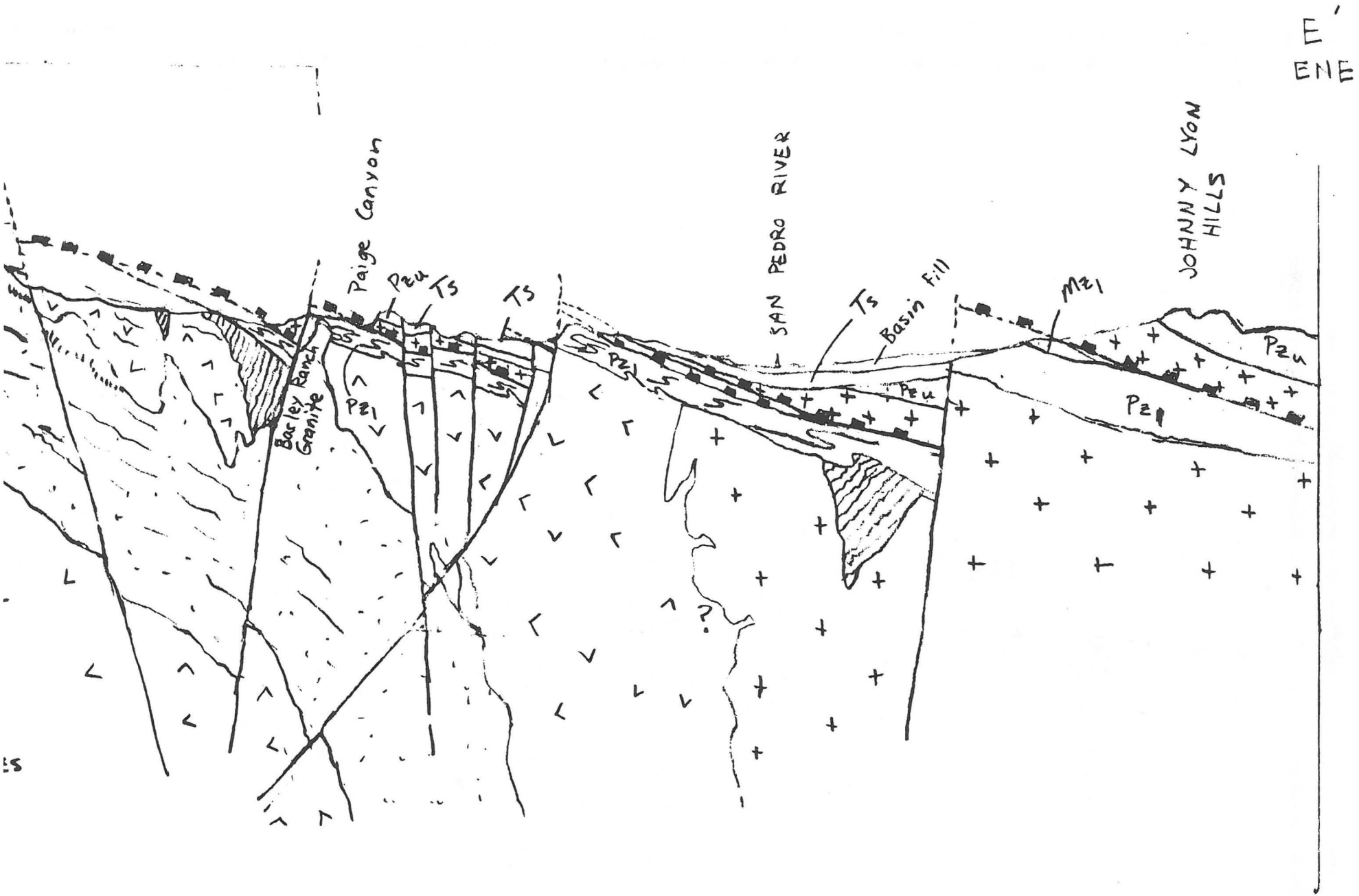

Rincon Mountains. mylonitic rocks shown by wavy lines (arrows show direction
nd imbricated micas). Hashured area east of Twin Hills shows chloritic brecciation

Keith 1983

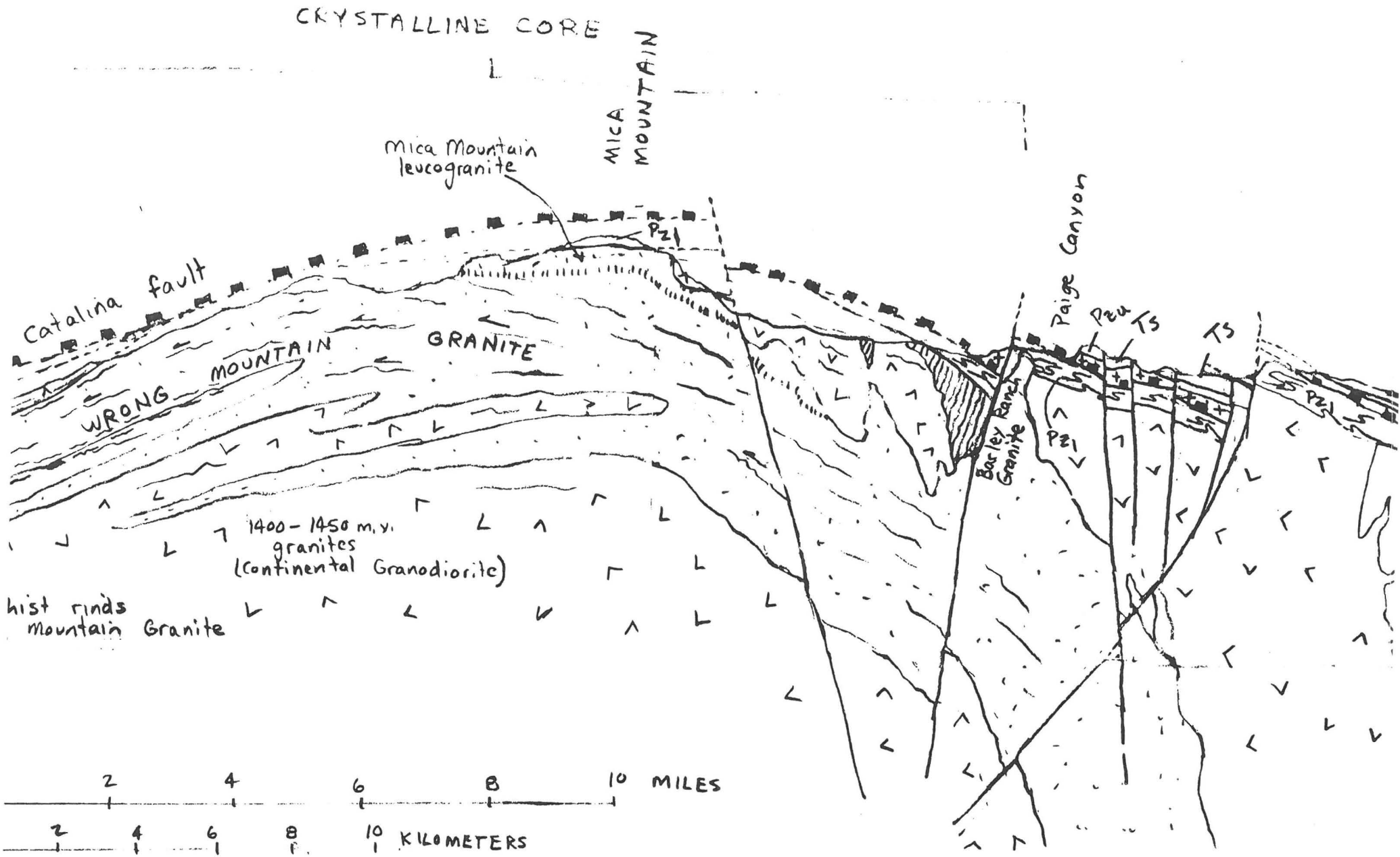

matic cross section E-E' through
le shear as determined from 'S' and 'C' northern Rincon Mountains. mylonitic rocks shown by wavy li
r mylonites. planes and imbricated micas). Hashured area east of Twin

Keith 1983

have asymmetric laccolithic shapes. The tops of many of the laccolithic bodies and sills occur just below or at the Precambrian Apache Group unconformity with older Precambrian rocks or within the Apache Group (Figs. 2, 5, 6). The asymmetric laccolithic geometry is spectacularly displayed in the western end of the Santa Catalina Mountains (Fig. 9) where a batholithic sill of Wilderness granite extends southward into the Catalina forerange from its root zone in Cargodera Canyon. The asymmetric, flat-lying parts of the various intrusions occupy large areas throughout the complex and, together with their host rocks, have been affected by a conspicuous mylonitization which has imposed on the rocks a penetrative, gently inclined mylonitic foliation. Although all three ranges of the complex have these general attributes in common, enough differences exist to merit brief discussions of the geology of each range.

Santa Catalina Mountains

The Santa Catalina part of the complex (Figs. 3, 5, 6, 7) has received the most intense study (see discussions and references in Shakel, 1974, 1978; Budden, 1975; Davis, 1975, 1978, and this volume; Creasey and others, 1977; Drewes, 1977; Banks, 1977 and this volume). The southern part of the range (Santa Catalina forerange in Fig. 8) is predominantly composed of interlayered dark and light gneissic bands of variable thickness. In order of decreasing abundance, the dark layers are composed of mylonitic biotite quartz monzonite gneiss, epidote-bearing and non–epidote-bearing mylonitic diorite gneiss, mylonite schist, and amphibolite. Layers and lenses of probable metasedimentary rocks are locally present. The above rocks are interlayered with, contained within, or injected by abundant light-colored layers and dikes of garnet- and biotite-bearing muscovite granite and pegmatites. Most of the rocks in the forerange are deformed by a pervasive low-angle mylonitic foliation which contains conspicuous lineation trending west-southwest. Gently dipping patterns of mylonitic foliation in gneisses of the forerange define a broad arch whose axis trends west-northwest. Mylonitic gneisses deep in the forerange arch are structurally the lowest of the rocks exposed in the complex. Up structural section to the south, the gneisses become jointed, brecciated, and chloritic. Ultimately, the highly broken mylonitic gneisses are overlain by the Catalina fault named by Pashley (1966), a dislocation surface that dips gently to the south. Up structural section to the north of the forerange, the proportion of dark-colored mylonitic quartz monzonite and diorite gneiss gradually decreases until the rock is entirely a light-colored mylonitic two-mica granite. Farther up section, mylonitization of the granite in a general way becomes less intense, and in many places the rock is essentially an undeformed biotite-muscovite-garnet–bearing granite (Wilderness granite of Shakel, 1978). To the north, the upper parts of the granite commonly grade into alaskite and pegmatite (Lemmon Rock leucogranite of Shakel, 1978). The entire sill sequence from its lowest exposed levels in the forerange on the south to the crest of the main range on the north is thicker than 4.5 km. In the Mount Lemmon area, pegmatite and alaskite associated with the leucogranite pervasively intrude the Leatherwood quartz diorite (Peirce, 1958; Hanson, 1966) and adjacent metamorphosed and locally highly deformed Apache Group rocks (Pilkington, 1962; Waag, 1968). Farther east, the granitic main phase of the Wilderness pluton directly intrudes the Leatherwood quartz diorite (Pilkington, 1962; Wilson, 1977). Many parts of the Leatherwood pluton have been deformed into mylonitic schist and gneiss, especially where the Leatherwood has concordantly intruded metamorphosed rocks of the Apache Group. Deformed Leatherwood quartz diorite is commonly intruded by undeformed Lemmon Rock leucogranite or Wilderness granite (Pilkington, 1962; Hanson, 1966; Wilson, 1977). The Leatherwood and its intruded cover of Apache Group and Paleozoic strata are terminated to the north by the Geesman fault and a low-angle normal fault mapped by Creasey and Theodore (1975). North of these faults, exposed rocks are more typical of southern Arizona geology—that is, ~1.7-b.y.-old Pinal Schist, 1.44-b.y.-old Oracle Granite (Shakel and others, 1977), and less-metamorphosed Apache Group and Paleozoic and

D

WNW

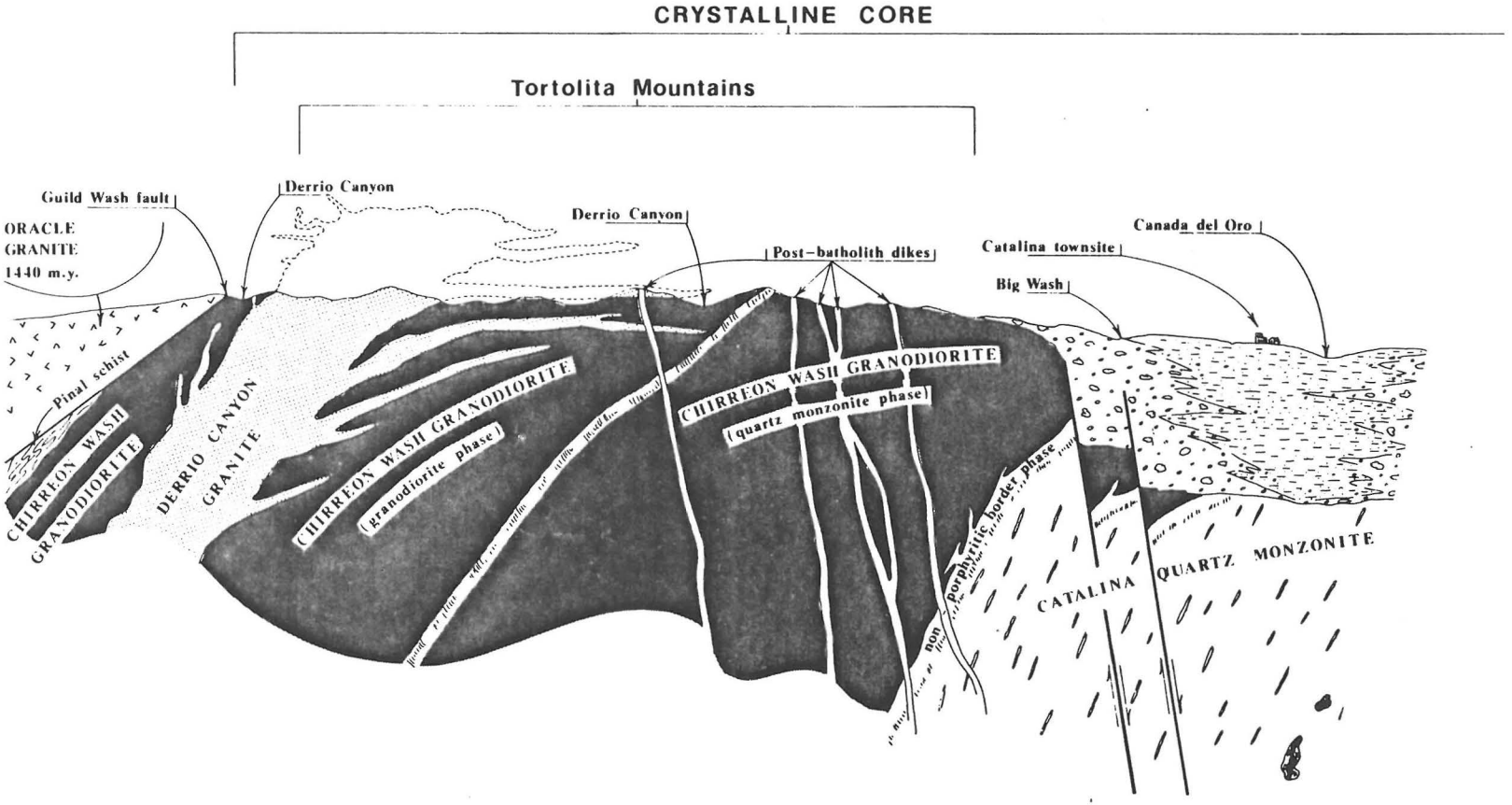
CRYSTALLINE CORE
Tortolita Mountains
Guild Wash fault
ORACLE GRANITE 1440 m.y.
Derrio Canyon
Derrio Canyon
Post-batholith dikes
Canada del Oro
Catalina townsite
Big Wash
Pinal schist
CHIRREON WASH GRANODIORITE
DERRIO CANYON GRANITE
CHIRREON WASH GRANODIORITE (granodiorite phase)
CHIRREON WASH GRANODIORITE (quartz monzonite phase)
porphyritic border phase
CATALINA QUARTZ MONZONITE

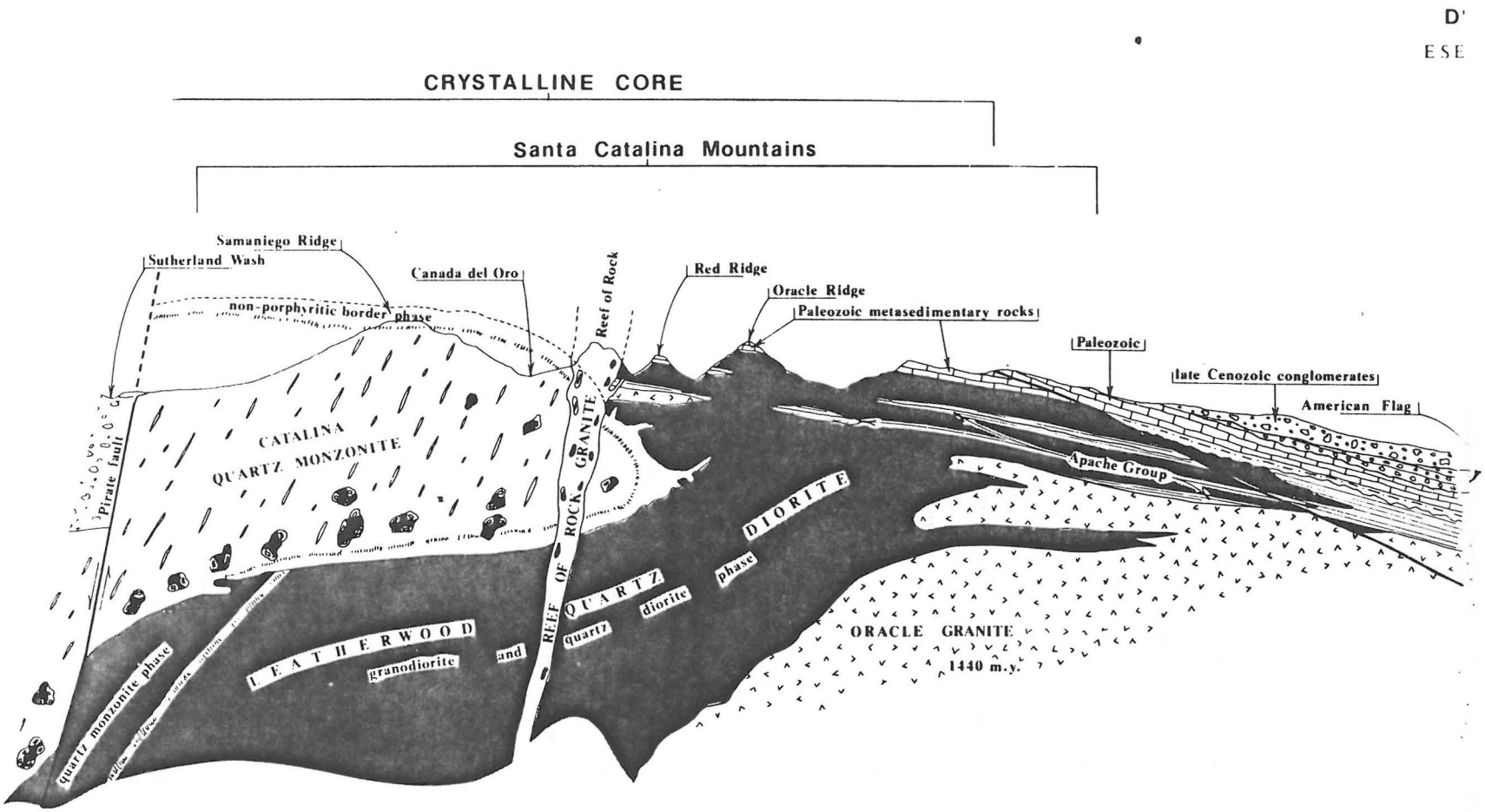

Figure 7 (facing pages). Diagrammatic cross section D–D′ through central Tortolita Mountains and northern Santa Catalina Mountains.

Mesozoic strata—all intruded by the Rice Peak granodiorite porphyry of presumed Laramide age and middle Tertiary porphyritic sphene-bearing hornblende-biotite Catalina quartz monzonite (Hoelle, 1976; Suemnicht, 1977; Shakel, 1978). At the far north end of the range, the Mogul fault juxtaposes these rocks against Oracle Granite in the upthrown northern block. In the western part of the Santa Catalina Mountains, undeformed Catalina quartz monzonite intrudes foliated Wilderness granite in Cargodera Canyon. Catalina quartz monzonite also intrudes and contains inclusions of Leatherwood quartz diorite (Suemnicht, 1977).

Tortolita Mountains

The western termination of the Santa Catalina Mountains is along the Pirate fault, a north-northeast–trending fault of late Tertiary age. Except for the alluvium-covered interval west of the Pirate fault, much of the Santa Catalina Mountains geology continues (Fig. 7) westward into the Tortolita Mountains (Budden, 1975; Banks and others, 1977; Davis, this volume). In this range, arches in mylonitic foliation are difficult to place precisely, but probably exist. The northern part of the crystalline core in the Tortolita Mountains consists of the Chirreon Wash granodiorite, an east-northeast–to due-east–trending composite pluton with quartz diorite, granodiorite, and quartz monzonite phases (Fig. 7). Intruding the granodiorite in its western exposures are abundant tabular bodies of granite, pegmatites, and alaskite herein referred to as Derrio Canyon granite. These plutons are locally mylonitic and bordered by east-trending schistose bands on both the north and south. To the

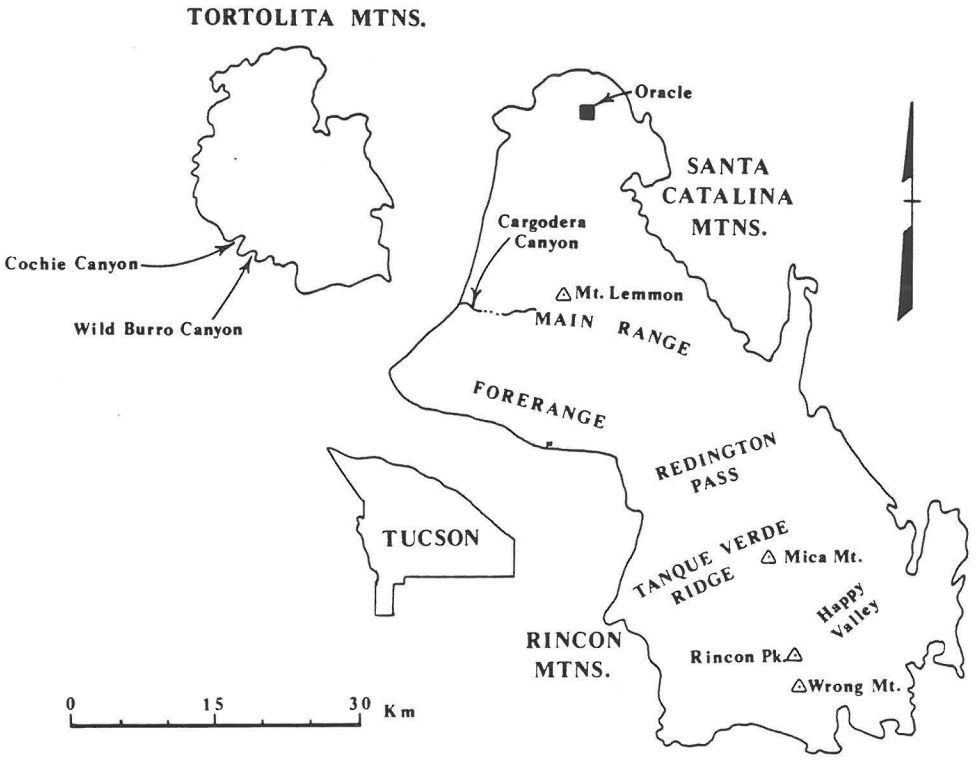

Figure 8. Outline map of the Tortolita, Santa Catalina, and Rincon Mountains showing localities frequently mentioned in text and Appendix 1.

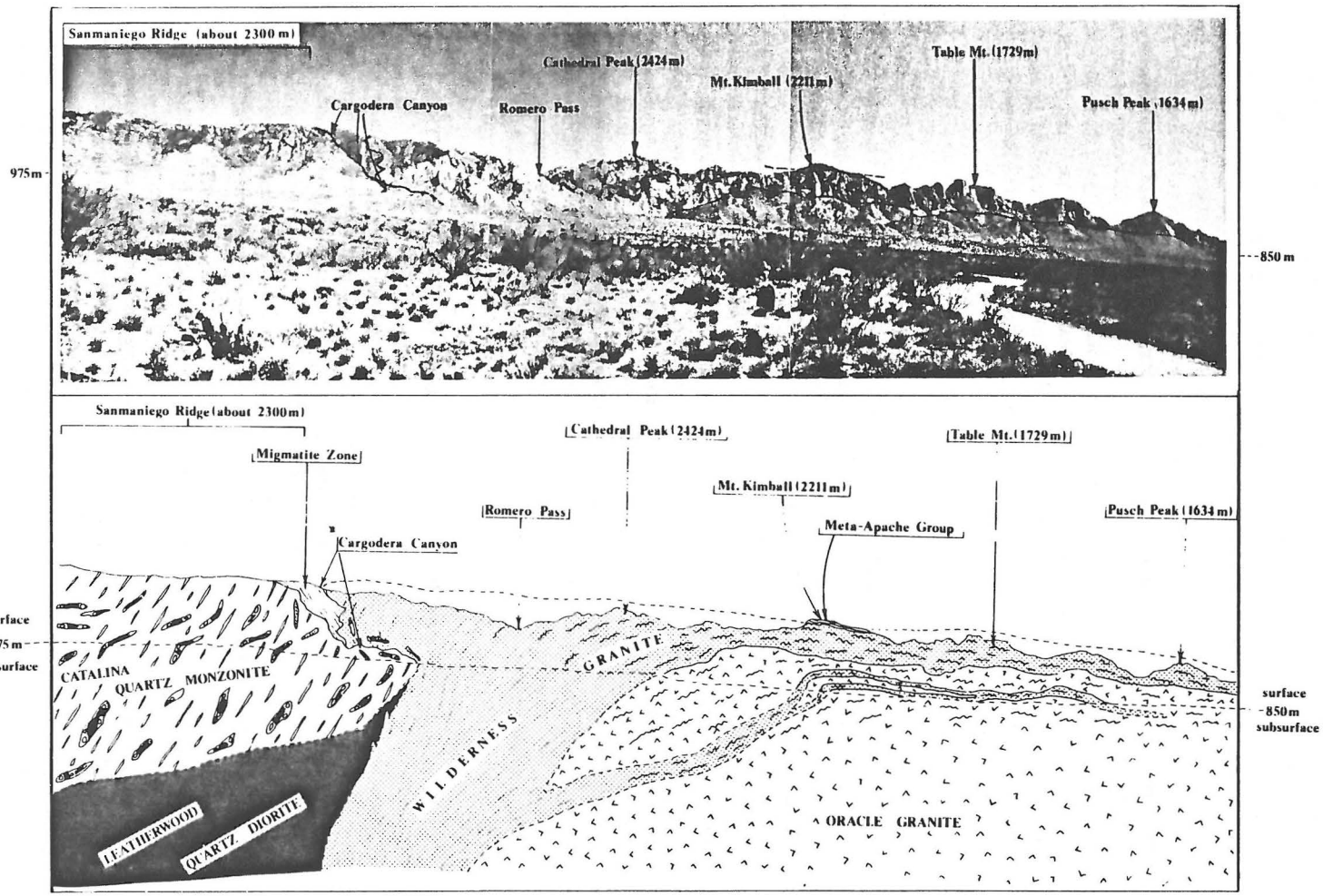

Figure 9. Panorama of the western Santa Catalina Mountains looking southeast. Photo and interpretative diagram show the asymmetric laccolithic geometry of the Wilderness granite batholith and, with less certainty, the inferred laccolithic geometry of the Catalina quartz monzonite intrusion. Mylonitic rocks are shown by wavy lines. Field of view is 25 km wide.

north, the schistose rocks are in contact with mylonitized Oracle Granite. Farther to the northwest, both Oracle Granite and the schistose rocks are chloritized, brecciated, and overlain by a dislocation surface (Guild Wash fault). The schistose band that borders the Chirreon Wash pluton on the south is intruded on its south side by an east-northeast–trending mass of quartz monzonite which is lithologically similar to and correlated by us with the Catalina quartz monzonite of the northwest Santa Catalina Mountains. The Catalina quartz monzonite locally contains large quartz diorite inclusions of presumed Chirreon Wash granodiorite and truncates pegmatite apophyses of Derrio Canyon granite in the east-central Tortolita Mountains. In turn, the Catalina quartz monzonite is intruded by numerous apophyses of the Tortolita quartz monzonite pluton that crops out to the south-southeast. Both the Catalina and Tortolita intrusions locally contain a low-angle mylonitic foliation. The mylonitic foliation in all plutons is crosscut by northwest-striking, high-angle normal faults and shears that in many places are intruded by northwest-striking, undeformed to locally foliated granodiorite, quartz monzonite, and quartz latite dikes.

Rincon Mountains

The Rincon Mountains are geologically more similar to the Santa Catalina Mountains than they are to the Tortolita Mountains. Much of the Rincon Mountains is composed of muscovite-garnet–bearing granite (Wrong Mountain Quartz Monzonite of Drewes, 1977). The granite commonly envelops a dark biotitic augen gneiss (Continental Granodiorite of Drewes, 1977). Some parts of the granite have abundant pegmatite and alaskite. Both the granite and the dark augen gneiss exhibit the distinctive low-angle mylonitic foliation. This mylonitic gneiss complex is overlain to the northeast by metamorphosed and locally highly deformed younger Precambrian and Paleozoic rocks which become lower grade and less deformed up section (Drewes, 1974; Frost, 1977; Davis, this volume). The western and southern boundaries of the mylonitic complex are—like those of the southern Santa Catalina forerange—highly jointed, brecciated, chloritized, and overlain by the Catalina fault, a dislocation surface which dips gently off the flanks of the range (Pashley, 1966; Davis, 1975; Davis and Frost, 1976; Drewes, 1977). The low-angle mylonitic fabric has been deformed into several broad west-southwest–plunging arches and one north-northwest–trending arch and is intruded by several north-northwest–striking undeformed dikes (Thorman and Drewes, 1978).

CORRELATION AND GEOCHRONOLOGY OF ROCK UNITS

We have correlated rock units throughout the Santa Catalina–Rincon–Tortolita crystalline complex by considering rock types and field relationships in conjunction with trace-element and isotope geochemistry. Where possible, we have suggested correlation of rocks exposed within the complex to those exposed outside it. Correlation of rock units within the complex has been hampered by problems in nomenclature, presence of a pervasive mylonitic overprint, intense metamorphism of sedimentary protoliths adjacent to plutons, and, for all rock types, ubiquitous 20- to 30-m.y. K-Ar and fission-track cooling ages that present difficulties in determining original emplacement ages.

Perhaps the most serious problem is nomenclature because genetic bias is inherent in most of the terminology (see App. 1 for detailed discussion). Terms that contain the term "gneiss" in the Santa Catalina–Rincon–Tortolita complex commonly carry a metamorphic connotation of in situ anatexis, partial melting, hydrothermal metamorphism, or alkali-silica metasomatism (see, for example, Hernon, 1932; DuBois, 1959a, 1959b; Mayo, 1964; Peterson, 1968; Shakel, 1974; Sherwonit, 1974; Drewes, 1977; Banks, this volume). Terms that carry a plutonic name (such as quartz monzonite) in the complex traditionally have the genetic connotation of being fundamentally intrusive in origin (see for

example, Tolman, as reported in Ransome, 1916; Creasey and others, 1977).

Another serious obstacle for correlation has resulted from one or more pervasive events of mylonitization. Large areas of the complex have been affected by an event (or by events) of mylonitization that largely obliterated original rock textures. Recognition of the importance of mylonitization (Creasey and Theodore, 1975; Davis and others, 1975; Banks, 1976) represents a fundamental change from earlier workers who regarded the mylonitic fabric as a "minor" event that was secondary to processes of metamorphism, anatexis, and alkali-silica metasomatism (Hernon, 1932; DuBois, 1959a, 1959b; Pilkington, 1962; Mayo, 1964; Peterson, 1968; Sherwonit, 1974; Shakel, 1974). These earlier workers believed that original protolith compositions were greatly obscured by drastic chemical changes which accompanied a "metamorphic transformation." In contrast, implicit in a "mylonitic model" is that a rock's present-day fabric is only a *textural* modification of an earlier protolith and that the bulk-rock chemistry need not have been significantly affected. In other words, "metamorphism" (mylonitization) could have been largely isochemical. The "mylonitic model" is strongly supported by our data because we can match Rb-Sr geochemistry of mylonitically deformed rocks within the Santa Catalina–Rincon–Tortolita crystalline complex to nondeformed counterparts in or adjacent to it (see succeeding sections).

The mylonitic model provides an additional caveat to the interpretation of various schistose tracts within the Santa Catalina–Rincon–Tortolita crystalline complex. It was or is widely believed that many of the gneissic rocks were derived from possible Precambrian Pinal Schist (Blake, 1908a, 1908b; DuBois, 1959a, 1959b; Pilkington, 1962; Mayo, 1964; Peterson, 1968; Sherwonit, 1974; Drewes, 1974, 1977). As a result, many of the schistose exposures in the gneisses have been mapped as Pinal Schist (for example, Drewes, 1974, 1977). However, the distinct probability now exists that many of these schistose bodies are mylonite schists derived during mylonitization at contacts between igneous protoliths of different compositions (for example, Davis, 1978, this volume). Conversely, it is equally possible, as we shall attempt to show in the Tortolita Mountains, to mistake real Pinal Schist for mylonitic schist. It is also possible to mistake recrystallized clastic rocks of the Apache Group for Pinal Schist or vice versa.

Most K-Ar and fission-track dates fall within the range of 20 to 30 m.y. B.P. (Damon and others, 1963; Mauger and others, 1968; Marvin and others, 1973, 1978; Creasey and others, 1977; Banks and others, 1978; this paper). These dates, which represent the termination of a thermal event, cannot alone be used to distinguish and correlate intrusive events within the complex. However, they do provide a cooling history for the most recent thermal events which suggests that the structurally lowest part of the complex cooled from about 400 °C 28 m.y. ago to 100 °C about 21 m.y. ago (Damon, 1968; Creasey and others, 1977) under a steep geothermal gradient (Mauger and others, 1968).

In order to document events that occurred before the late cooling history, Rb-Sr whole-rock studies were instituted in 1962. Little has been reported (Shakel, 1972, 1974; Shakel and others, 1972; Hoelle, 1976) until now because the results obtained were difficult to interpret. Reported U-Th-Pb studies (Shakel and others, 1977), the rediscovery of Tolman's deformed laccolith model by Creasey and others (1977), and recent field observations by us have provided a new perspective from which to evaluate the Rb-Sr data. Consequently, this is the first discussion that has as its data base the recently reported U-Pb studies (Shakel and others, 1977; Shakel, 1978), the recently summarized K-Ar and fission-track data (Creasey and others, 1977; Marvin and others, 1978; Damon and others, 1980), and numerous, previously unpublished Rb-Sr analyses determined by workers of the Laboratory of Isotope Geochemistry, University of Arizona, during the past 18 yr. When data from all these methods are considered together, an internally consistent evolutionary picture of the complex emerges. We will discuss rocks of the complex from oldest to youngest, beginning with Pinal Schist. The reader is referred to Damon and others (1980) for location, rock type, Rb-Sr analytical data, and geologic significance of each data point and to Table 1 for a summary of all available isotopic dates. Selected

TABLE 1. SUMMARY OF ISOTOPIC DATA FOR PLUTONS IN AND ADJACENT TO THE SANTA CATALINA–RINCON–TORTOLITA CRYSTALLINE COMPLEX

Rock name and comments	Reference* and sample no.	Age (m.y.)	Method	Area
MIDDLE PROTEROZOIC GRANITIC ROCKS				
Madera Diorite				
Emplacement age is probably around 1,670 m.y. Younger ages are variously reduced by younger metamorphisms or intrusive events	11: DEL-9 - 13-65	1,695 ± 30	Rb-Sr whole-rock isochron	Pinal Mts.
	6: PED-2-59	1,665 ± 40	K-Ar biotite	Pinal Mts.
	1: 24H	1,645 ± 60	K-Ar hornblende	Ray mine area
	1: 24B	100 ± 2	K-Ar biotite	Ray mine area
	11: DEL-12 & 16-65	1,540 ± 50	Rb-Sr mineral isochron	Pinal Mts.
	2: TMN-93	1,440 ± 10	K-Ar biotite	Tortolita Mts.
Johnny Lyon Granodiorite				
1,625 m.y. is probably emplacement age. 1,545-m.y. age is reduced age on Rincon Valley Granodiorite mapped by Drewes (1974). Correlated with Johnny Lyon Granodiorite by Silver (1978)	21: L-312, L-609	1,625 ± 10	U-Pb zircon	Johnny Lyon Hills
	14: 69D64	1,545 ± 60	K-Ar biotite	E. Rincon Mts.
Rincon Valley Granodiorite				
Rock petrographically resembles Johnny Lyon Granodiorite. K-Ar ages probably reduced (Silver, 1978)	14: 69D61	1,455 ± 50	K-Ar biotite	Rincon Valley
	14: 69D61	1,560 ± 100	K-Ar hornblende	Rincon Valley
Oracle Granite				
Emplacement age is about 1,440 m.y. Cenozoic ages reflect resetting by Late Cretaceous-Tertiary thermal events	6: PED-3-58	1,425 ± 40	K-Ar muscovite	near Oracle
	12: PED-2-58	1,410 ± 40	Rb-Sr biotite	near Oracle
	6: PED-2-58	1,430 ± 40	K-Ar biotite	near Oracle
	12: DEL-13-62	1,380 ± 39	K-Ar biotite	near Oracle
	12: DEL-13-62	1,425 ± 40	K-Ar plagioclase	near Oracle
	19: Unknown	1,440	U-Pb zircon	near Oracle
	11: Several	1,380	Rb-Sr whole-rock isochron	Oracle-Sierra Ancha regions
	7: PED-27-57	39.4 ± 1.2	K-Ar biotite	Oracle
Ruin Granite				
Emplacement age is about 1,425 m.y.	12: PED-32-61	1,470 ± 40	K-Ar biotite	Sierra Ancha
	12: DEL-3-62	1,415 ± 40	K-Ar biotite	Hess Canyon, Gila Mts.
	12: DEL-3-62	1,435 ± 40	K-Ar plagioclase	Hess Canyon, Gila Mts.
	12: DEL-3-62	1,455 ± 40	K-Ar biotite	Hess Canyon, Gila Mts.
	12: DEL-3-62	1,385	Rb-Sr biotite	Hess Canyon, Gila Mts.
Continental Granodiorite				
Most exposures are coarsely porphyritic and petrographically resemble other members of the 1,400- to 1,450-m.y. granitic suite. Silver (1978) showed that outcrops in type area in northern Santa Rita Mountains contain rocks of Johnny Lyon and and Oracle ages. Most of the Precambrian ages of various exposures suggest most outcrops of Continental Granodiorite are 1,400 m.y. old. We have restricted the term "Continental Granodiorite" to exposures of coarsely porphyritic 1,400-m.y.-old rocks and their mylonitic equivalents within the Rincon Mountain part of the crystalline core of the complex. Younger ages reflect subsequent thermal events	14: 66D46	1,360 ± 200	Pb-α zircon	N. Santa Rita Mts.
	14: 66D46	56.8 ± 2.5	K-Ar biotite	N. Santa Rita Mts.
	14: 65D914	1,450 ± 160	Pb-α zircon	N. Santa Rita Mts.
	14: 65D914	825 ± 80	Rb-Sr whole rock	N. Santa Rita Mts.
	13: 74D62	1,340 ± 60	K-Ar biotite	Tanque Verde Mts.
	13: 74D62	1,415 ± 50	K-Ar muscovite	Tanque Verde Mts.
	13: 74D62	1,410 ± 50	Rb-Sr whole rock	Tanque Verde Mts.
	13: 74D62	26.1 ± 3.5	Fission-track apatite	Tanque Verde Mts.
	13: 74D57	1,395 ± 50	K-Ar biotite	Tanque Verde Mts.
	13: 74D57	1,390 ± 50	K-Ar muscovite	Tanque Verde Mts.
	13: 74D57	~800	Fission-track zircon	Tanque Verde Mts.
	13: 74D57	55.0 ± 4.2	Fission-track apatite	Tanque Verde Mts.
	20: Unknown	1,430	U-Pb zircon	N. Santa Rita Mts.
	20: Unknown	1,600+	U-Pb zircon	N. Santa Rita Mts.
	20: Unknown	1,420	U-Pb zircon	Little Rincon Mts.
	9: PED-14-59	1,375 ± 40	K-Ar muscovite	N. Empire Mts.
POST-PALEOZOIC BATHOLITHIC ROCKS				
Quartz diorite-granodiorite (Leatherwood) suite				
Chirreon Wash Granodiorite	2: UAKA-75-86	25.1 ± 0.5	K-Ar biotite	N.-central Tortolita Mts.
Leatherwood quartz diorite				
Emplacement age is probably 75 to 65 m.y. Younger ages are interpreted as reduced ages (see text). 73-m.y. Rb-Sr whole-rock isochron is a composite of Leatherwood plus Chirreon Wash plutons. 70-m.y. Rb-Sr whole-rock isochron is Leatherwood only. 38-m.y. K-Ar sericite age is from quartz vein that cuts Leatherwood quartz diorite	5: BR 2	27.1 ± 0.5	K-Ar biotite	N. Santa Catalina Mts.
	5: BR 2	64.4 ± 1.0	K-Ar hornblende	N. Santa Catalina Mts.
	5: Unknown	27.1 ± 0.5	K-Ar biotite	N. Santa Catalina Mts.
	5: Unknown	38.4 ± 0.6	K-Ar hornblende	N. Santa Catalina Mts.
	4: ML-60†	23.5 ± 0.7	K-Ar biotite	N. Santa Catalina Mts.
	4: ML-60†	36.8 ± 1.0	K-Ar hornblende	N. Santa Catalina Mts.
	4: ML-60†	21.2 ± 0.7	Fission-track apatite	N. Santa Catalina Mts.
	4: ML-60†	28.6 ± 3.7	Fission-track sphene	N. Santa Catalina Mts.
	22: 24	24.9 ± 1.0	K-Ar whole rock	N. Santa Catalina Mts.
	22: 51	29.6 ± 1.1	K-Ar biotite	N. Santa Catalina Mts.
	22: 30	36.7 ± 2.0	K-Ar hornblende	N. Santa Catalina Mts.
	22: 45	32.2 ± 1.2	K-Ar biotite	N. Santa Catalina Mts.
	22: 52	28.9 ± 1.1	K-Ar biotite	N. Santa Catalina Mts.
	22: 69	28.5 ± 1.1	K-Ar biotite	N. Santa Catalina Mts.
	8: PED-1-68	30.2 ± 0.8	K-Ar biotite	N. Santa Catalina Mts.
	9: PED-1-68	25.7 ± 7.1	Rb-Sr mineral isochron	N. Santa Catalina Mts.
	9: UAKA-76-116	31.7 ± 0.7	K-Ar biotite	N. Santa Catalina Mts.
	9: Several	73	Rb-Sr w.-r. ref. isochron	N. Santa Catalina Mts.
	9: Several	70	Rb-Sr w.-r. ref. isochron	N. Santa Catalina Mts.
	9: UAKA-78-66	37.7 ± 0.8	K-Ar sericite	N. Santa Catalina Mts.
	12: PED-18-62D§	28.3 ± 0.9	K-Ar biotite	Santa Catalina forerange
Muscovite granite (Wilderness) suite				
Wilderness granite				
Emplacement age is probably 44 to 50 m.y. Younger ages are interpreted as variably reduced (see text)	7: PED-4-58	26.5 ± 1.0	K-Ar muscovite	Santa Catalina forerange
	7: PED-4a-58	25.4 ± 1.0	K-Ar biotite	
	7: PED-4a-58	30.2 ± 0.9	K-Ar muscovite	
	7: PED-4a-58	23.3 ± 1.4	Rb-Sr biotite	
	12: PED-4a-58	36.9 ± 1.0	Rb-Sr muscovite	
	3: 100	33 ± 3	K-Ar muscovite	
	3: 100	1,340 ± 30	$^{206}Pb/^{207}Pb$-zircon	Windy Point, Santa Catalina main range
	3: 100	50	U-Pb zircon	
	4: GGN-S1	23.3 ± 0.7	K-Ar biotite	
	4: GGN-S1	24.8 ± 0.7	K-Ar muscovite	
	4: GGN-S1	19.3 ± 2.7	Fission-track apatite	
	12: PED-18-62L§	25.6 ± 1.0	K-Ar biotite	Santa Catalina forerange
	12: PED-18-62L§	26.1 ± 1.0	K-Ar muscovite	Santa Catalina forerange

TABLE 1. *(Continued)*

Rock name and comments	Reference* and sample no.	Age (m.y.)	Method	Area
		Muscovite granite (Wilderness suite *(continued)*		
Wilderness granite *(continued)*				
	12: PED-18-62L§	27.5 ± 0.8	K-Ar orthoclase	Santa Catalina forerange
	12: PED-18-62L§	30.0 ± 1.0	K-Ar plagioclase	Santa Catalina forerange
	16: RM-1-66§	32.0 ± 0.3	K-Ar muscovite	Santa Catalina forerange
	16: PED-56-66§	31.9 ± 0.9	K-Ar muscovite	Santa Catalina forerange
	9: UAKA-71-11§	23.1 ± 0.5	K-Ar muscovite	Santa Catalina forerange
	9: UAKA-72-76§	24.0 ± 0.6	K-Ar K-feldspar	Santa Catalina forerange
	7: PED-15-59	47.9 ± 2.1	K-Ar muscovite	Santa Catalina main range
	15: 77-D-68	21.9 ± 0.8	K-Ar biotite	Redington Pass
	15: 77-D-68	35.1 ± 1.2	K-Ar muscovite	Redington Pass
	19: Unknown	44-47	U-Th-Pb monazite	Santa Catalina main range
	19: Unknown	44-47	U-Th-Pb monazite	W. Santa Catalina forerange
	9: Numerous	47	Rb-Sr w.-r. ref. isochron	Santa Catalina main range
	9: UAKA-71-21	46.5 ± 10.4	K-Ar garnet	Santa Catalina forerange
Youtcy granite				
Possibly an extension of Wilderness pluton; date may reflect age of emplacement	15: 77D81	45.8 ± 1.6	K-Ar muscovite	Redington Pass
Espiritu Canyon granite				
Ages are probably reduced	13: 71D194	27.6 ± 0.9	K-Ar biotite	Mica Mtn.
	13: 71D194	28.5 ± 0.6	K-Ar muscovite	Mica Mtn.
Wrong Mountain granite				
K-Ar ages are probably reduced. Rb-Sr sample plots on 47-m.y. Wilderness Granite isochron. Former older age reported by Drewes (1977) was a model age which assumed a 0.703 initial ratio for $^{87}Sr/^{86}Sr$	14: 71D17	24.1 ± 0.9	K-Ar biotite	E. Rincon Mts.
	14: 71D17	25.4 ± 0.9	K-Ar muscovite	E. Rincon Mts.
	13: 71D17	23.3 ± 5.8	Fission-track apatite	E. Rincon Mts.
	13: 71D17	24.6 ± 4.0	Fission-track zircon	E. Rincon Mts.
	13: 73D52	25.0 ± 0.8	K-Ar biotite	Central Rincon Mts.
	13: 73D52	25.3 ± 2.9	Fission-track apatite	Central Rincon Mts.
	13: 73D52	20-30	Fission-track zircon	Central Rincon Mts.
	9: 73D52	47	Rb-Sr w.-r. ref. isochron	Central Rincon Mts.
	7: PED-30-60	33.5 ± 1.1	K-Ar muscovite	Mica Mtn.
	9: UAKA-74-80	25.4 ± 0.5	K-Ar biotite	E. Rincon Mts.
		Quartz monzonite (Catalina) suite		
Catalina quartz monzonite				
Large degree of concordance implies emplacement age of about 28 to 25 m.y. 90-m.y. isochron included samples of xenoliths (probably Leatherwood), contaminated border phase, and a radiogenically enriched aplite. 90-m.y. age is too old	7: PED-16-59	25.6 ± 0.8	K-Ar biotite	NW. Santa Catalina Mts.
	4: BR 21	23.9 ± 1.2	K-Ar biotite	NW. Santa Catalina Mts.
	4: BR 21	23.7 ± 0.7	K-Ar hornblende	NW. Santa Catalina Mts.
	4: BR 21	30.0 ± 3.0	Fission-track sphene	NW. Santa Catalina Mts.
	4: BR 21	28.9 ± 3.3	Fission-track zircon	NW. Santa Catalina Mts.
	4: BR 21	23.5 ± 2.8	Fission-track apatite	NW. Santa Catalina Mts.
	4: ML 61	22.9 ± 0.7	K-Ar hornblende	NW. Santa Catalina Mts.
	4: ML 61	24.7 ± 0.7	K-Ar biotite	NW. Santa Catalina Mts.
	4: ML 61	28.3 ± 3.1	Fission-track sphene	NW. Santa Catalina Mts.
	4: ML 61	27 1 ± 3.4	Fission-track zircon	NW. Santa Catalina Mts.
	4: ML 61	20.8 ± 2.1	Fission-track apatite	NW. Santa Catalina Mts.
	4: BR 16	23.8 ± 0.7	K-Ar biotite	NW. Santa Catalina Mts.
	4: BR 16	28.0 ± 3.0	Fission-track sphene	NW. Santa Catalina Mts.
	4: BR 16	25.9 ± 2.5	Fission-track zircon	NW. Santa Catalina Mts.
	4: BR 16	21.7 ± 2.1	Fission-track apatite	NW. Santa Catalina Mts.
	16: PED-20-62	28.0 ± 0.9	K-Ar biotite	SW. Tortolita Mts.
	4: RC 3	21.6 ± 0.6	K-Ar hornblende	SW. Tortolita Mts.
	4: RC 3	21.1 ± 0.6	K-Ar biotite	SW. Tortolita Mts.
	19: Unknown	27	U-Pb zircon	NW. Santa Catalina Mts.
	9: Numerous	26	Rb-Sr w.-r. ref. isochron	NW. Santa Catalina Mts.
	18, 10: Numerous	90	Rb-Sr whole-rock isochron	NW. Santa Catalina Mts.
Tortolita quartz monzonite				
Age of emplacement is about 25 m.y.	7: PED-17-59	24.5 ± 0.5	K-Ar biotite	Cargodera Canyon, Santa Catalina Mts.
	4: RC 25	22.7 ± 0.7	K-Ar biotite	Tortolita Mts.
	4: RC 25	18.5 ± 2.4	Fission-track apatite	
	4: ML 105	17.0 ± 2.1	Fission-track apatite	
	9: Numerous	26	Rb-Sr w.-r. ref. isochron	
Happy Valley quartz monzonite				
28 and 38 m.y. K-Ar dates on northern mass may be reduced if pluton is a member of the Wilderness suite	14: 69D93	28.0 ± 1.1	K-Ar biotite	Happy Valley
	14: 69D95	37.7 ± 1.6	K-Ar muscovite	Happy Valley
	14: 71D122	26.9 ± 0.9	K-Ar biotite	Happy Valley
		MISCELLANEOUS ROCKS		
Postbatholith dikes				
Probable emplacement ages	9: UAKA-74-83	24.3 ± 0.5	K-Ar whole rocks	Rincon Mts.
	9, 17: UAKA-72-21	21.0 ± 0.3	K-Ar whole rock	Santa Catalina forerange
	2: UAKA-75-87	24.0 ± 0.5	K-Ar biotite	North-Central Tortolita Mts.
Schistose rocks				
Ages are probably reduced	7: PED-29-60	27.7 ± 1.0	K-Ar muscovite	Mica Mtn.
	14: 69D92	29.1 ± 1.1	K-Ar muscovite	Happy Valley
	14: 70D143	34.6 ± 1.2	K-Ar biotite	Happy Valley
	14: 70D143	29.6 ± 0.9	K-Ar muscovite	Happy Valley

Note: Constants used are $\lambda_\beta = 4.963 \times 10^{-10}yr^{-1}$; $\lambda_e = 0.581 \times 10^{-10}yr^{-1}$, $\lambda = 5.544 \times 10^{-10}yr^{-1}$; $^{40}K/K = 1.167 \times 10^{-4}$ atom/atom; $\lambda_{Rb} = 1.42 \times 10^{-11}yr^{-1}$. Fission-track dates reported by Creasey and others (1977) are recalculated 2.6% older to conform with new K-Ar constants. Rb-Sr w.-r. ref. isochron = Rb-Sr whole-rock reference isochron.

*References as follows: 1, Banks and others (1972); 2, Banks and others (1978); 3, Catanzaro and Kulp (1964); 4, Creasey and others (1977); 5, Creasey (1979, written commun.); 6, Damon and others (1962); 7, Damon and others (1963); 8, Damon and others (1969); 9, Damon and others (1980); 10, Hoelle (1976); 11, Livingston (1969); 12, Livingston and others (1967); 13, Marvin and Cole (1978); 14, Marvin and others (1973); 15, Marvin and others (1978); 16, Mauger and others (1968); 17, Shakel (1974); 18, Shakel and others (1972); 19, Shakel and others (1977); 20, Silver (1978); 21, Silver and Deutsch (1963); 22, Soderman (1979, written commun.).

†Mafic inclusion in Catalina quartz monzonite of unassigned protolith by Creasey and others (1977). Creasey (1979, written commun.) assigned this inclusion to the Leatherwood quartz diorite.

§These samples are found within the forerange mylonitic gneiss complex and are correlated with presumed nonmylonitic counterparts pending further work.

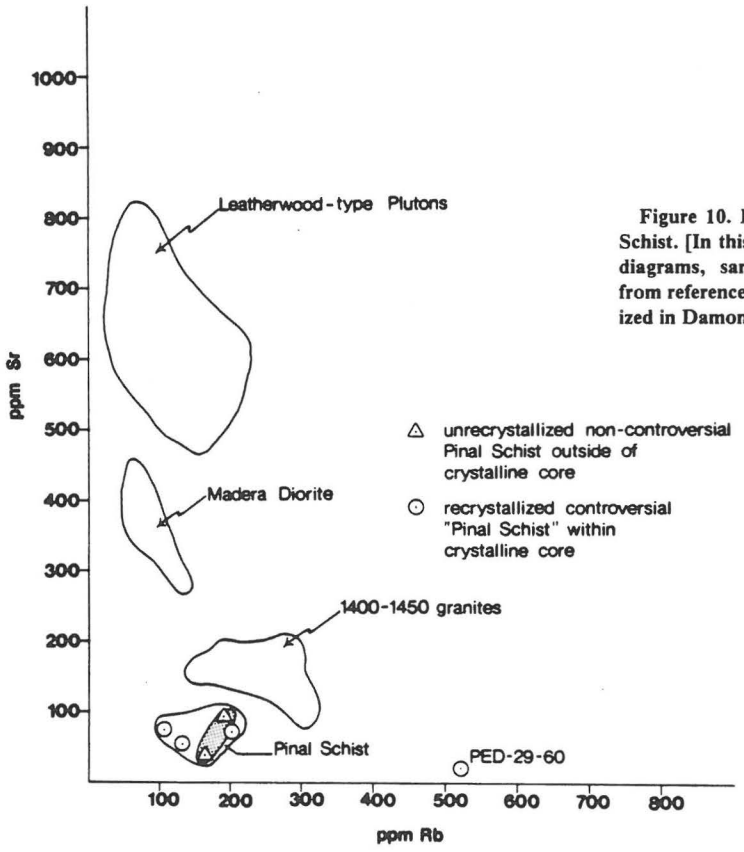

Figure 10. Rb-Sr abundances in Pinal Schist. [In this and all subsequent Rb-Sr diagrams, sample numbers shown are from references cited and will be summarized in Damon and others (1980).]

data points of particular interest are identified in the figures and are discussed in Damon and others (1980).

Pinal Schist

The oldest rocks within the complex are exposures of probable 1.7-b.y.-old Pinal Schist (Fig. 3). Different interpretations currently exist in published maps [see, for example, discussion in map text of Banks and others (1977) in the Tortolita Mountains and Davis (this volume) versus Drewes (1977) in the Tanque Verde Ridge area] regarding which exposures in the complex are indeed Pinal Schist and which are mylonitic schists derived from probable igneous protoliths. Exposures of unequivocal Pinal Schist in the complex are few and probably largely restricted to the northwestern Santa Catalina Mountains and the central Tortolita Mountains. As further support for these contentions, the Rb-Sr abundances and Sr-isotope ratios (Damon and others, 1980) from the schistose bands north and south of Chirreon Wash granodiorite in the Tortolita Mountains are similar to those for unequivocal Pinal Schist outside the complex (Fig. 10). The data do not support the proposal of Banks (this volume) that the schistose bands are mylonite schist derived entirely from the Chirreon Wash pluton and Oracle Granite (in the case of the northern band). Rb-Sr abundances in all of the other samples we have collected are unlike those of Pinal Schist.

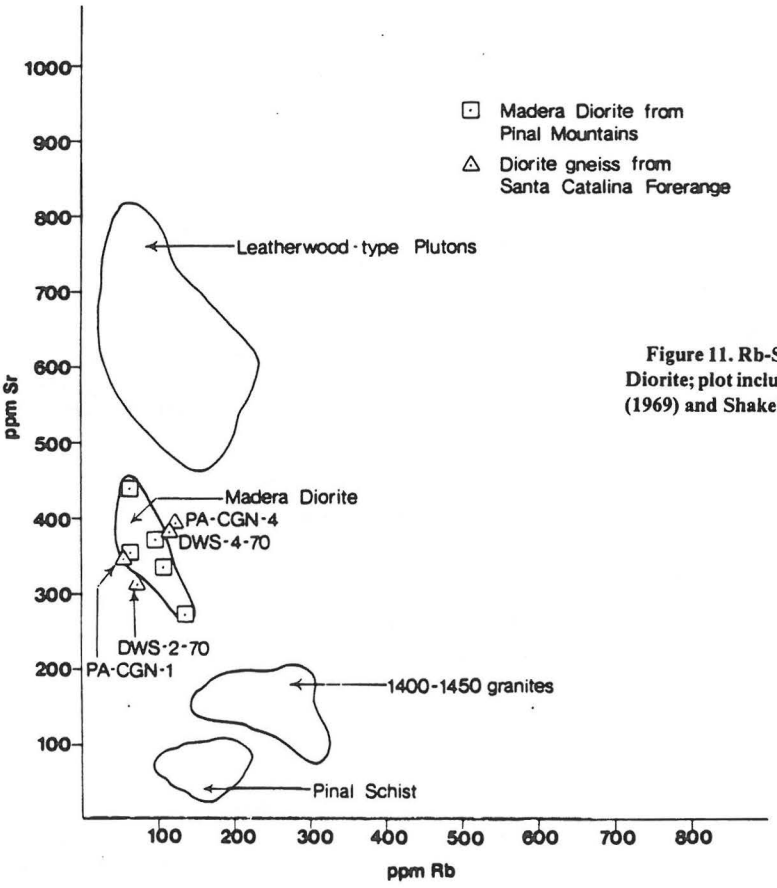

Figure 11. Rb-Sr abundances in Madera Diorite; plot includes data from Livingston (1969) and Shakel (1974).

Precambrian Diorite

Some exposures of foliated diorite (Fig. 3) *may* represent the next oldest rocks in the complex. These diorites lack the abundant epidote and Rb-Sr abundances (Fig. 11) characteristic of the Leatherwood quartz diorite of Late Cretaceous–early Tertiary age. Instead, the Rb-Sr data suggest similarities to 1.65-b.y.-old Madera Diorite of the Pinal Mountains (Ransome, 1903; Livingston and Damon, 1968; Livingston, 1969). This similarity is supported by isotopic data (Fig. 12) for the diorite that plots near a 1.65-b.y. reference isochron through Madera Diorite (Livingston, 1969) at the type locality in the Pinal Mountains. Although the data are somewhat equivocal, the possibility that a Maderalike protolith may constitute part of the dark, mylonitic augen gneisses should not be ignored.

Oracle Granite and Equivalent Granitic Rocks

Creasey and others (1977) suggested that dark augen gneisses of the Catalina forerange are mylonitic equivalents of 1.44-b.y.-old Oracle Granite, a contention which was confirmed by U-Pb systematics in zircons reported by Shakel and others (1977). Rb-Sr abundances (Fig. 13) strongly support this and further indicate that porphyritic varieties of Rincon Valley and Continental Granodiorites (Drewes, 1974, 1977) in the Rincon Mountains and rocks mapped as Oracle Granite in the Tortolita Mountains

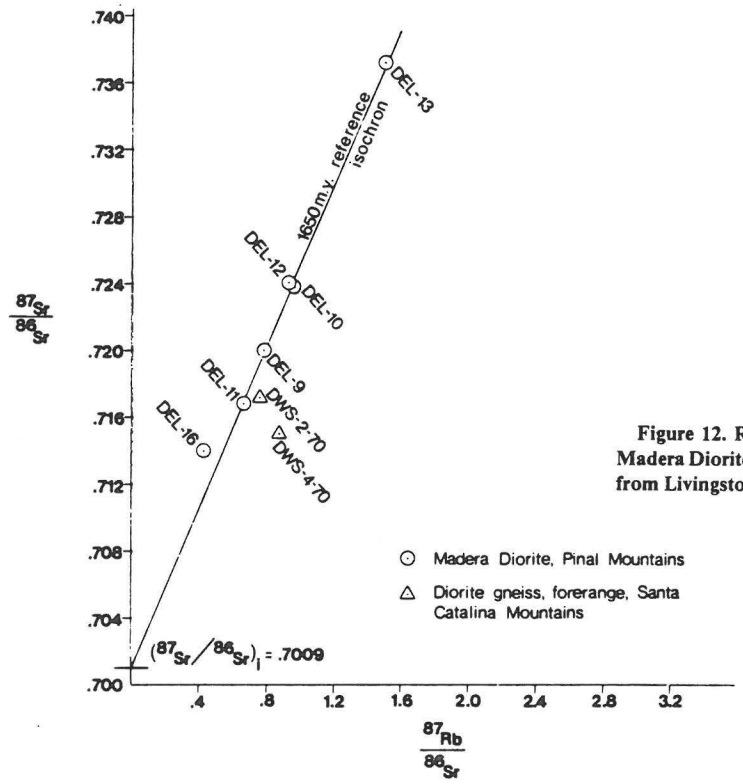

Figure 12. Rb-Sr isochron diagram for Madera Diorite samples; plot includes data from Livingston (1969) and Shakel (1974).

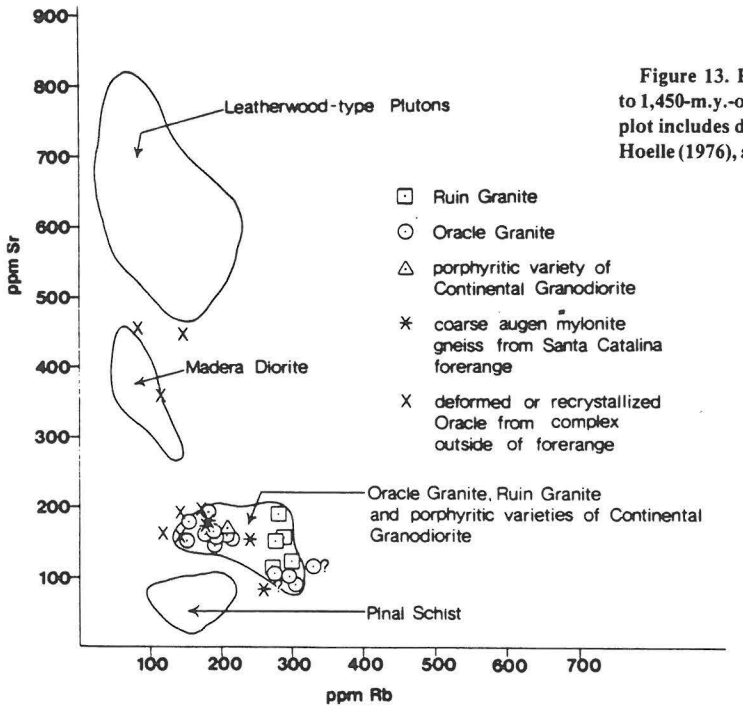

Figure 13. Rb-Sr abundances in 1,400- to 1,450-m.y.-old porphyritic granitic rocks; plot includes data from Livingston (1969), Hoelle (1976), and Marvin and Cole (1978).

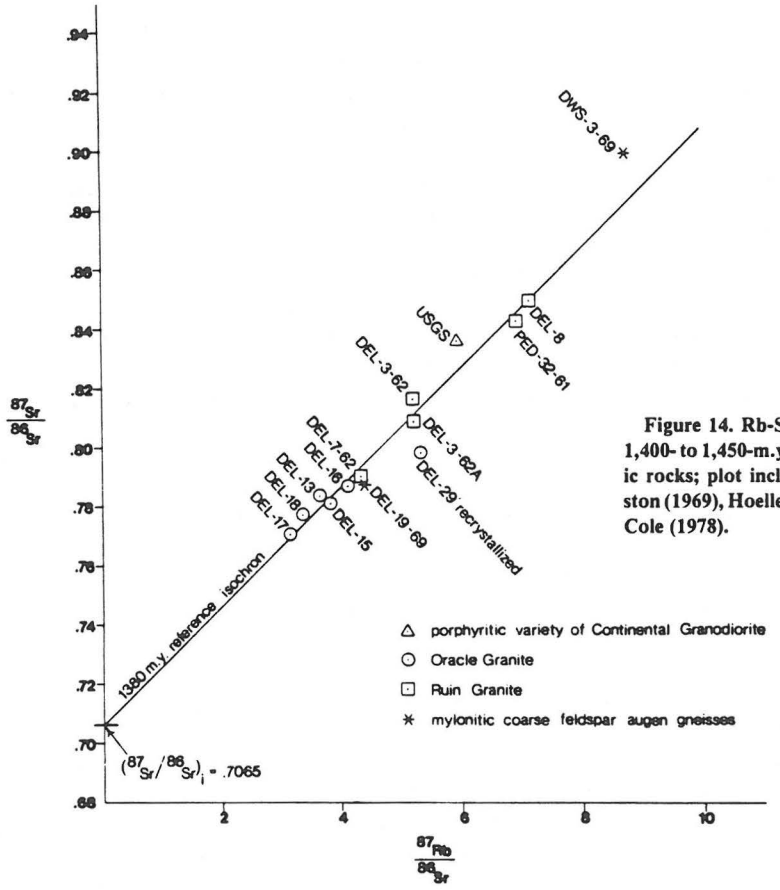

Figure 14. Rb-Sr isochron diagram for 1,400- to 1,450-m.y.-old porphyritic granitic rocks; plot includes data from Livingston (1969), Hoelle (1976), and Marvin and Cole (1978).

(Banks and others, 1977) are members of the 1.4- to 1.45-b.y.-old generation of porphyritic granitic plutons (Damon and Giletti, 1961; Giletti and Damon, 1961; Livingston and Damon, 1968; Silver, 1968, 1978). Isotopic data (Fig. 14) for these rocks, when compared to data for undeformed 1.4-b.y.-old Oracle and Ruin Granites (Livingston, 1969), strengthen the correlation. All available data, therefore, indicate that a *majority* of dark augen gneisses in the complex are deformed 1.4- to 1.45-b.y.old plutons (see App. 1 for further discussion).

Younger Precambrian Apache Group, Diabase, and Paleozoic Rocks

Younger Precambrian Apache Group, diabase, and Paleozoic strata (Fig. 3) occur within the complex and are variably metamorphosed and deformed (Waag, 1968; Budden, 1975; Frost, 1977). Although we have no Rb-Sr data on these rocks, we concur with most of the recent mapping in the Tortolita (Banks and others, 1977) and Santa Catalina Mountains (Creasey and Theodore, 1975; Banks, 1976) about the map position of Apache Group, diabase, and Paleozoic strata. Also, on lithologic grounds, we would add that parts of the southern Santa Catalina forerange rocks (Shakel, 1974, 1978) between Pontatoc and Ventana Canyons (Fig. 5) may equate to metadiabase (amphibolite lenses) or metamorphosed Apache Group strata (quartzite and schist lenses).

Post-Paleozoic Batholithic Rocks

The post-Paleozoic intrusive bodies in the Santa Catalina–Rincon–Tortolita complex can be divided into three suites with plutons of each suite possessing distinctive rock types, field relationships, trace-element and isotopic compositions, and age. The suites are as follows: (1) Late Cretaceous–early Tertiary quartz diorite–granodiorite (Leatherwood suite); (2) Eocene muscovite granite–pegmatite–alaskite with high $^{87}Sr/^{86}Sr$ initial ratios (Wilderness suite); and (3) middle Tertiary quartz monzonite (Catalina suite). The history of nomenclature for each pluton is discussed in Appendix 1, and a summary of the various published radiometric determinations on each pluton is presented in Table 1. Representative modes for plutons of each suite are given in Tables 2 through 5. Analytical data and sample descriptions for new Rb-Sr and K-Ar data will appear in Damon and others (1980).

Late Cretaceous–Early Tertiary (Laramide) Quartz Diorite–Granodiorite (Leatherwood) Suite. Three plutons of quartz dioritic to granodioritic compositions are currently assigned to the Leatherwood suite: the Chirreon Wash granodiorite, an east-elongated, ~40-km² pluton in the east-central Tortolita Mountains; the Rice Peak granodiorite, two probably interconnected stock and sill-like masses, about 12 km², in the northern Santa Catalina Mountains; and the Leatherwood quartz diorite, a 40-km² body in the northeast part of the Santa Catalina Mountains.

Leatherwood suite plutons are characterized by abundant biotite (15% to 25%) in more mafic phases and are mainly quartz dioritic to granodioritic in composition. Epidote is a characteristic accessory mineral of all Leatherwood suite plutons and occurs as several textural varieties (Hanson, 1966; Creasey, 1967; Banks and others, 1978). Representative modes of Leatherwood suite plutons are given in Table 2.

Crosscutting relationships with adjacent plutons indicate that plutons of the Leatherwood suite are the oldest post-Paleozoic intrusions in the complex. Leatherwood quartz diorite and Chirreon Wash granodiorite are both clearly cut by muscovite granite and related aplite, alaskite, and pegmatite apophyses of the Eocene Wilderness suite. In the Tortolita Mountains, Chirreon Wash granodiorite is cut by hundreds of pegmatite dikes and sheets that extend eastward from and grade into or cut the Derrio Canyon muscovite-garnet granite. The Derrio Canyon granite cuts across the Chirreon Wash granodiorite as a north-northeast–trending dikelike mass. The Chirreon Wash granodiorite is older than the middle Tertiary Catalina quartz monzonite, as shown by indirect relationships. The Catalina quartz monzonite occurs in a 2- to 3-km-wide east-northeast– to due-east–trending arcuate belt parallel to and south of the southern contact of the Chirreon Wash granodiorite (Fig. 3). The Chirreon Wash granodiorite is generally separated from the Catalina quartz monzonite by a narrow, arcuate, east-northeast–trending screen of schist tentatively correlated here with the Pinal Schist (see previous

TABLE 2. MODAL MINERALOGY OF LEATHERWOOD SUITE PLUTONS

	1	2	3	4	5	6
Quartz	22	21.0	28	16	19	2-20
K-feldspar	5	7.5	8	6	12	tr.-20
Plagioclase	42 (An_{30-45})	47.0 (An_{38})	31	41	51	36-65 (An_{35-45})
Biotite	19	20.0	18	9	9	10-26
Hornblende	1	3.5	5	..	..	6-18
Epidote	1	..	4	9	4	1-2
Sphene	<1	tr.	..	1	1	1-4
Other	10	..	6	18	3	..
Opaque grains	..	2.0	..	tr.	1	1-4
Apatite	..	tr.	..	tr.	tr.	tr.

Note: Columns as follows: (1) average of 26 thin sections reported by Hanson (1966); (2) sample BR2 from Banks (this volume); (3) sample 5-2-1 from Suemnicht (1977); (4) sample AZ-LWQ-3 from Tom Heidrick (1979, written commun.); (5) sample AZ-LWD-1 from Tom Heidrick (1979, written commun.); (6) range in composition of Chirreon Wash pluton reported by Banks and others (1977). Trace = tr.

TABLE 3. CHEMICAL DATA FOR LEATHERWOOD QUARTZ DIORITE

	BR-2	AZ-LWD-1	AZ-LWD-3
SiO_2	62.7	64.8	62.1
Al_2O_3	16.1	16.3	16.6
Fe_2O_3	2.1	4.3*	4.9*
FeO	2.1	..	..
MgO	2.9	n.d.	n.d.
CaO	4.7	2.38	3.08
Na_2O	3.7	3.94	3.48
K_2O	2.8	2.40	2.28
P_2O_5	0.22	0.13	0.28
TiO_2	0.60	0.61	0.72
L.O.I.	..	0.52	1.0

Note: Samples AZ-LWD-1 and AZ-LWD-3 from Tom Heidrick (1979, written commun.). Sample BR 2 from Banks (this volume). Analysis of AZ samples by Rocky Mountain Geochemical Corp., Midvale, Utah. Loss on ignition (L.O.I.) determined gravimetrically. Other data determined by atomic absorption, except TiO_2 and P_2O_5, which were determined colorimetrically. Not determined = n.d.
*Total Fe expressed as Fe_2O_3.

discussion). Numerous pegmatites related to the Derrio Canyon granite of the Wilderness suite extend eastward across the Chirreon Wash granodiorite, intrude the schistose screen, and are truncated by the Catalina quartz monzonite. Also, large, partially metasomatized inclusions of epidote-bearing biotite quartz diorite are common within the Catalina quartz monzonite. Many of these inclusions bear a strong resemblance to an epidote-bearing biotite quartz diorite phase locally present along the northwest border of the Chirreon Wash granodiorite. If the quartz diorite inclusions correlate with the border phase, the Chirreon Wash granodiorite is older than the Catalina quartz monzonite.

Within the north-central Santa Catalina Mountains, the Leatherwood quartz diorite intrudes upper Paleozoic rocks (Creasey and Theodore, 1975; Banks, 1976) and is, thus, at least a young as Mesozoic. The Leatherwood quartz diorite sill sequence in the Apache Group is abruptly truncated for some 20

TABLE 4. MODAL MINERALOGY OF WILDERNESS GRANITE

	Quartz	Plagioclase	K-Feldspar*	Biotite	Muscovite	Opaque grains	Garnet	Others	Reference
Marshall Gulch pegmatite (part of Lemmon Rock leucogranite)	25	35 (An_{7-12})	37 (m)	Minor	Minor	Minor	Minor	Minor	Matter (1969)
Control Road pegmatite (part of Lemmon Rock leucogranite)	35	31 (An_{7-12})	29 (m)	Minor	More than above	Minor	Minor	Minor	Matter (1969)
Caseco pegmatite—about 30 m below upper contact between Wilderness Granite and metamorphosed Apache Groups	20	42 (An_{7-13})	27	Trace	6	..	4	..	Matter (1969)
Aplite—same location as above	19	32 (An_{7-13})	43	Minor	4	..	1	..	Matter (1969)
Wilderness Granite—various locations within upper half of main sill; average of 10 analyses	28	29 (An_{20-25})	27 (m)	4	7	1 (magnetite)	1-2†	..	Pilkington (1962)
East Fork gneiss#—layer just below base of main Wilderness Granite sill; average of 7 analyses	31.3	26.6 (An_{20-25})§	29.7 (o)	7.4	4.5	0.2	..	0.4	Sherwonit (1974)
Thimble Peak gneiss#—average of 16 analyses	32.9	33.6 (An_{20-25})§	26.6	4.1	2.4	0.2	..	0.2	Sherwonit (1974)
Sabino Narrows gneiss#—light bands; average of 8 analyses	31.6	36.8 (An_{20-25})§	28.2	1.7	1.6	0.1	..	..	Sherwonit (1974)
Gibbons Mountain gneiss#—average of 7 analyses	29.9	35.5 (An_{20-25})§	26.0	7.7	0.3	0.4	..	0.2	Sherwonit (1974)
Soldier Canyon gneiss#—light bands; average of 15 analyses	30.4	37.8 (An_{25-30})§	25.7	4.2	0.6	0.3	..	0.2	Sherwonit (1974)
Seven Falls gneiss#—average of 7 analyses	29.1	41.3 (An_{25-30})§	21.8	7.2	0.1	0.3	..	0.3	Sherwonit (1974)

*Microcline = m; orthoclase = o.
†Included under "others" by Pilkington (1962).
§These An values are from Peterson (1968).
#Terminology for gneiss units in Santa Catalina forerange is from Peterson (1968). These units are interpreted by us as injection sheets on lower levels of the Wilderness sill complex.

TABLE 5. AVERAGE MODAL ANALYSES OF CATALINA SUITE PLUTONS AND ORACLE GRANITE

	1	2	3	4	5	6
Quartz	33	26.8	35.0	39.2	42.2	29.5
K-feldspar	28	34.3	40.2	31.2	41.0	29.8
Plagioclase	28	26.7 (An_{26-35})	16.2 (An_{24})	26.4 (An_{22})	10.4 (An_{25})	35.6 (An_{33-35})
Biotite	9	7.5	7.4	3.2	3.2	0.6
Hornblende	..	0.8	0.2	..	..	..
Opaque grains	..	1.3	2.0	Trace	..	1.0
Sphene	..	0.6	0.6	..	..	..
Apatite	..	0.4	0.1	..	..	Trace
Muscovite	..	..	..	..	..	3.2

Note: Columns as follows:
1. Oracle granite (Banerjee, 1957), average of 38 samples reported under sample 50 by Hoelle (1976, Table 1).
2. Catalina quartz monzonite, main porphyritic phase; average of 11 samples as follows: one sample (48) from Erickson (1962), two samples (BR-21 and ML-61) from Creasey and others (1977), five samples (nos. 6, 9, 10, 11, and 12) from Hoelle (1976), 3 samples (5-3-2, 5-4-2, 5-4-3) from Suemnicht (1977).
3. Catalina quartz monzonite, border phase; average of one sample (BR-16) from Creasey and others (1977) and one sample from Suemnicht (1977).
4. Tortolita quartz monzonite; one sample (ML-105) from Creasey and others (1977).
5. Reef of Rock granite; average of four samples as follows: one sample (53) from Peirce (1958); three samples (5-6-3, 5-6-4, 5-6-5) from Suemnicht (1977).
6. Northern body of Happy Valley quartz monzonite; average of eight samples (A through G) from Miles (1965); the body is questionably assigned to Catalina suite.

km along its west-northwest–trending southern margin by Eocene Wilderness granite and related Lemmon Rock leucogranite. Aplites and pegmatites of the Lemmon Rock leucogranite abundantly intrude Leatherwood quartz diorite in the Mount Lemmon area as originally pointed out by Peirce (1958) and Hanson (1966). Similarly, pegmatite apophyses of presumed Wilderness granite intrude Leatherwood in the Korn Kob mine area 20 km east-southeast of Mount Lemmon (Wilson, 1977; Ted Theodore, 1979, oral commun.).

From the work of Banks (1976) and Suemnicht (1977), Leatherwood quartz diorite is intruded by middle Tertiary Catalina quartz monzonite 5 km north of Mount Lemmon. Here, numerous finer-grained apophyses and the coarse-grained main phase of Catalina quartz monzonite intrude Leatherwood, and large inclusions of Leatherwood are contained in Catalina quartz monzonite (Suemnicht, 1977). Also, the Leatherwood quartz diorite is intruded along its western contact by a large north-northeast–trending dikelike mass of the Catalina suite named Reef of Rock granite (Suemnicht, 1977). Numerous xenoliths of Leatherwood occur in Reef of Rock granite, according to Suemnicht (1977).

In summary, geologic relationships suggest that plutons of the Leatherwood suite are post-Paleozoic but predate granites of the Wilderness suite, which will be shown in the next section to be of Eocene age (44 to 50 m.y. old). The Leatherwood suite is therefore restricted to Mesozoic or earliest Tertiary.

We have Rb-Sr geochemistry for Leatherwood quartz diorite and Chirreon Wash granodiorite. High Sr abundances for both plutons are unique in the Santa Catalina–Rincon–Tortolita crystalline complex (Fig. 15). Poor spread in $^{87}Sr/^{86}Sr$ ratios prohibits a conclusive isochron for either pluton (Fig. 16). However, if the plutons are *assumed* to be comagmatic—a permissible assumption considering their impressively similar rock types, position in the intrusive sequence, and Rb-Sr geochemistry—the data for both plutons approximately conform to a Late Cretaceous (73 m.y. B.P.) reference

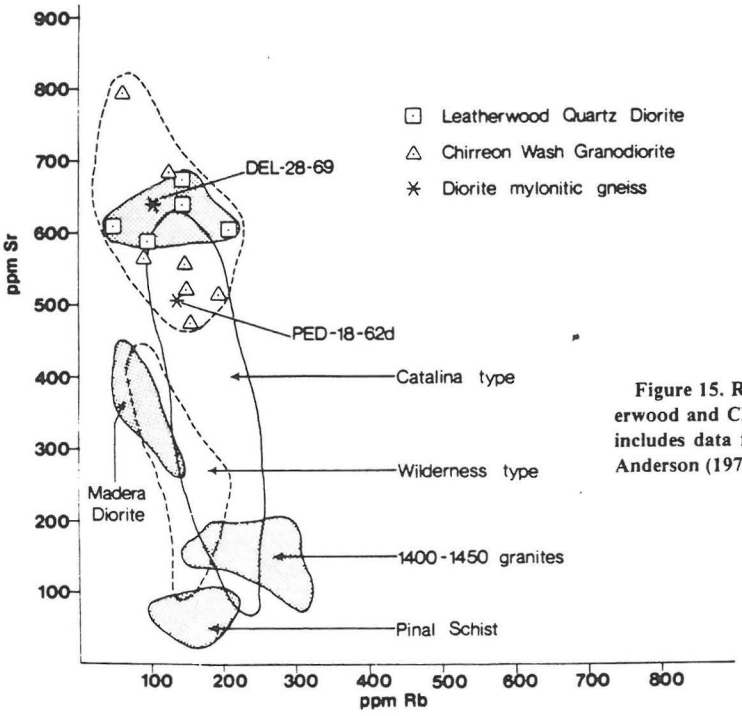

Figure 15. Rb-Sr abundances in Leatherwood and Chirreon Wash plutons; plot includes data from Matter (1969) and P. Anderson (1978, oral commun.).

isochron. The reference isochron, although not rigorously defensible, does not violate any independent geologic age constraints for either or both plutons.

Additional isotopic support for the Laramide age of the Leatherwood quartz diorite was generously provided to us by S. C. Creasey (1979, written commun.) of the U.S. Geological Survey, who has determined K-Ar isotopic ages of two hornblende-biotite mineral pairs. One sample of hornblende-biotite quartz monzonite (Leatherwood) came from Red Ridge about 5 km north of Mount Lemmon and about 150 m (500 ft) east of the contact with the Catalina quartz monzonite. The K-Ar isotopic ages are 38.4 ± 0.7 m.y. on hornblende and 26.1 ± 0.6 m.y. on biotite. These ages agree reasonably well with the K-Ar ages of hornblende (36.8 ± 1.0 m.y.) and biotite (23.5 ± 0.7 m.y.) from an inclusion of Leatherwood in the Catalina quartz monzonite near Cargodera Canyon (location IV in Fig. 2 of Creasey and others, 1977).

The second sample of hornblende-biotite quartz diorite came from near Lombar Hill about 10 km northeast of Mount Lemmon and about 3,960 m (13,000 ft) from the nearest known outcrop of Catalina quartz monzonite. K-Ar isotopic ages are 64.4 ± 1.0 m.y. on hornblende and 27.1 ± 0.5 m.y. on biotite. Creasey (1979, written commun.) indicated that the discordant ages of the mineral pairs are due to the differential Ar loss of the hornblende and biotite from reheating by the Catalina quartz monzonite and that the 64.4-m.y. age of the hornblende from the sample near Lombar Hill approximates the intrusion age of the Leatherwood. He concurred with our interpretation that the age of the Leatherwood is Laramide.

Creasey's K-Ar biotite data are similar to other K-Ar biotite ages of 30.2 (Damon and others, 1969) and 31.7 m.y. (this paper). These ages are complemented by 29.6, 32.2, 28.9, and 28.5 m.y. K-Ar biotite ages for probable Leatherwood sills in the Control mine area about 10 km northeast of Mount Lemmon (S. M. Soderman, 1979, written commun.). A whole-rock determination on one of these sills is 24.9 m.y., a hornblende concentrate yielded a discordant 36.7-m.y. K-Ar apparent age (S. M. Soderman, 1979, written commun.). Additionally, a Rb-Sr whole-rock–mineral isochron on

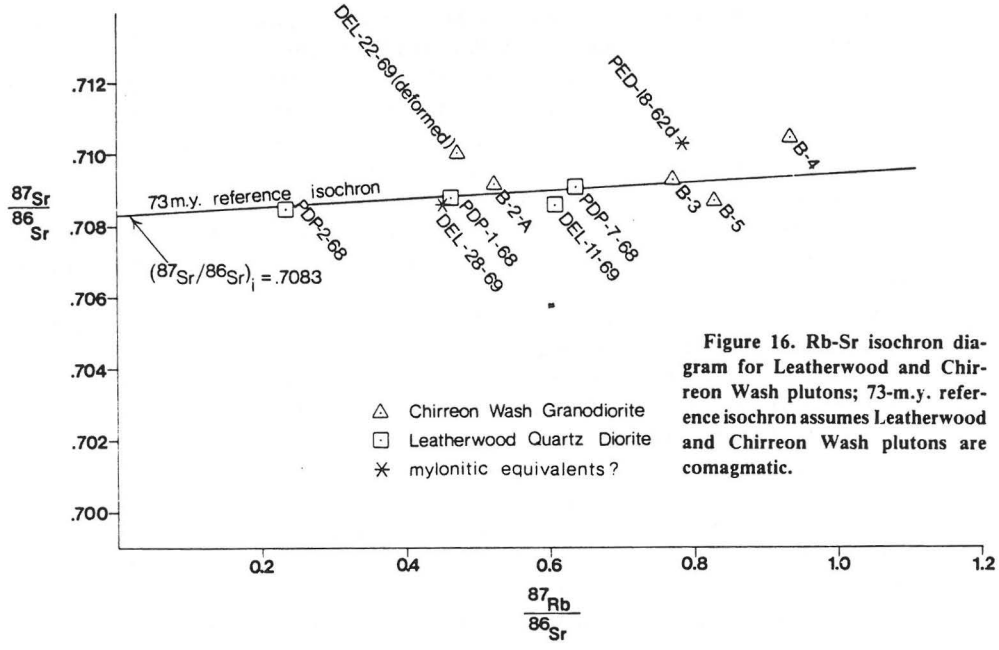

Figure 16. Rb-Sr isochron diagram for Leatherwood and Chirreon Wash plutons; 73-m.y. reference isochron assumes Leatherwood and Chirreon Wash plutons are comagmatic.

biotite, K-feldspar, plagioclase, epidote, and whole-rock from a single sample is 25.7 ± 7.1 m.y. (Damon and others, 1980). We interpret the 32- to 26-m.y. K-Ar biotite ages and Rb-Sr whole-rock–mineral isochron as reduced ages that reflect thermal resetting by Catalina suite plutons or uplift cooling of the complex between 30 and 20 m.y. B.P. The older hornblende ages are less reset because of their higher retentivity. With the exception of the 64-m.y. hornblende age, all K-Ar ages and the Rb-Sr whole-rock–mineral isochron age are reduced because they are all younger than 44 to 51 m.y., the age of Wilderness plutons that clearly intrude the Leatherwood (see next section). The 25-m.y. K-Ar biotite age reported by Banks and others (1978) for the Chirreon Wash pluton is similarly a reduced age.

Attempts to date the Leatherwood quartz diorite by U-Th-Pb techniques on zircons were unsuccessful and gave very discordant U-Th-Pb ages (Shakel, 1978). According to Shakel (1978), the discordant zircons indicated a "high degree of zircon inheritance," possibly from 1,440-m.y.-old Precambrian terrane.

Several additional indirect geologic relationships support the Laramide (75 to 50 m.y. B.P.) age for the Leatherwood suite. The Rice Peak granodiorite has been correlated on petrographic grounds with the Leatherwood quartz diorite by Waag (1968) and Creasey and Theodore (1975). If this correlation is valid, several intriguing implications arise for the age of the Leatherwood suite. The Rice Peak granodiorite clearly intrudes the lower part of the American Flag Formation from which Bromfield (1950) reported the freshwater pelecypod *Unio* (Triassic to Holocene) and the gastropod *Viviparus* (probably Cretaceous to Holocene). The rock type of the lower American Flag Formation is very suggestive of a correlation with the Cretaceous Fort Crittenden Formation (Hayes, 1970). Fort Crittenden equivalents are older than 75 to 72 m.y. on the basis of numerous radiometric ages for widespread overlying volcanic rocks, but are no older than 85 m.y. on the basis of the fossil assemblages contained within those equivalents (see Hayes and Drewes, 1978). *Assuming that all the correlations are valid,* Rice Peak granodiorite (and Leatherwood suite in general) is younger than ~72 m.y., the presumed minimum age of the lower American Flag Formation. Also of interest is the fact that Rice Peak granodiorite has been correlated with a petrographic analogue at San Manuel by Creasey (1967). Two samples of hydrothermal biotite from the granodiorite porphyry at San Manuel gave ages of 65 and 69 m.y. (Creasey, 1965; Rose and Cook, 1965).

Leatherwood quartz diorite is associated with significant porphyry copper–type skarn mineralization at Marble Peak (Braun, 1969) and possibly the Korn Kob mine farther southeast (Wilson, 1977). The time of most porphyry copper–type mineralization in southeast Arizona is essentially coeval with dates from various igneous minerals in spatially and temporally associated intrusions (Creasey and Kistler, 1962; Creasey, 1965; Rose and Cook, 1965; Livingston and others, 1967; Johnson, 1972). With the exception of Bisbee, Arizona, all porphyry copper mineralization is 70 to 50 m.y. old. A K-Ar age of 37.7 ± 0.8 m.y. (Damon and others, 1980) on sericite from a quartz vein that cuts Leatherwood indicates that Leatherwood is at least 38 m .y. old.

Another correlative device is chemical in nature. Three sets of major-element chemical analyses are now available for the Leatherwood quartz diorite (Table 3); K_2O/SiO_2 ratios indicate that the Leatherwood is calc-alkalic in the sense of Keith (1978). Data in the form of hundreds of chemical analyses suggest that true calc-alkalic plutons were emplaced in southeast Arizona only between 70 and 50 m.y. B.P. All other Arizona Phanerozoic plutonic rocks are more alkalic, according to the classification in Keith (1978).

A minimum age of about 50 m.y. for Leatherwood suite plutons is provided by the radiometric age of the Wilderness suite (next section), which clearly intrudes the Leatherwood suite in the Tortolita and Santa Catalina Mountains. Although no technique alone conclusively dates the Leatherwood suite, consideration of all available data converges on a 75- to 64-m.y. age for it.

Eocene Muscovite Granite (Wilderness) Suite. About 65% of the area of the Santa Catalina–Rincon–Tortolita complex is underlain by large sheetlike and laccolith-shaped muscovite granite

plutons. Five asymmetric, laccolithic granitic intrusions are currently assigned to the Wilderness suite. They include the Derrio Canyon granite, a group of irregularly stacked sills in the northwestern Tortolita Mountains (Fig. 4); the Wilderness granite (and associated Lemmon Rock leucogranite), a west-northwest–trending batholith-sized laccolith in the main range of the central Santa Catalina Mountains, and several sills or injection sheets in the Santa Catalina forerange (Figs. 5 and 6); the Youtcy granite, an irregular stocklike mass that may be the east end of the Wilderness pluton in the Redington Pass area, between the Santa Catalina and Rincon Mountains; the Espiritu Canyon granite, an east-northeast–elongated pluton having diffuse contacts with the Wrong Mountain granite 2 km northeast of Mica Mountain in the Tanque Verde Mountains; and the Wrong Mountain granite, a batholith-sized laccolithic mass widespread throughout the Rincon and Tanque Verde Mountains. Previous nomenclature is summarized in Appendix 1. The Wilderness-Youtcy plutons are coextensive with Tolman's original batholith (Moore and others, 1949).

Wilderness-type plutons occupy a distinct mineralogic nitch in the Arizona Phanerozoic magmatic framework. For this reason, we affix the term "granite" to plutons of this suite to emphasize their unique mineralogy, even though some phases are technically quartz monzonites (Peterson, 1961) or monzogranites (Streckeisen, 1976). All Wilderness suite plutons contain muscovite with biotite and garnet as common accessories. Average modes for the Wilderness granite, the best-documented pluton of the suite, are listed in Table 4. The data are listed in ascending structural order so that pegmatites at the top of the mountain represent the top of the ~4.5-km-thick section of granitic rocks, much of which contains low-angle mylonitic deformation. The data seem to suggest several mineralogic changes within the Wilderness pluton. Structurally low sills are characterized by more biotite relative to muscovite and less K-feldspar relative to plagioclase feldspar than structurally higher phases. Garnet is locally present throughout the pluton but is evidently more abundant in upper structural levels, particularly in the Lemmon Rock leucogranite. A biotite-rich phase of the Wilderness granite is present south of Mount Bigelow 8 km east-southeast of Mount Lemmon.

Crosscutting relationships indicate that Wilderness suite granites occupy an intermediate stage in evolution of the Late Cretaceous–middle Tertiary batholith. Contact relationships were previously discussed between plutons of the Leatherwood suite and Wilderness suite. These indicate overwhelmingly that Wilderness suite granites intrude and are younger than Laramide Leatherwood suite plutons.

Contact relationships between different muscovite granite phases are commonly gradational (Shakel, 1978; Thorman and Drewes, 1978). Undeformed phases of two-mica Wilderness granite pass gradationally upward into Lemmon Rock leucogranite 2 km south of Mount Lemmon (Shakel, 1978). The Lemmon Rock leucogranite is composed of a complex of alaskites, pegmatites, and aplites. Several generations of dikes may be present in a single outcrop. In the northwest Tortolita Mountains, pegmatite phases of the Derrio Canyon granite extend some 10 km eastward from the main mass in the northwestern Tortolita Mountains. Many pegmatites become more granitic in texture and imperceptibly grade into the main Derro Canyon mass to the west. A few pegmatites cut this mass, but most exhibit a gradational relationship.

Wilderness suite plutons are clearly older than middle Tertiary quartz monzonites (Catalina suite). In the central Tortolita Mountains, pegmatite apophyses of the Derrio Canyon granite are truncated by Catalina quartz monzonite. In Cargodera Canyon in the western Santa Catalina Mountains, the foliated Lemmon Rock leucogranite phase of the Wilderness granite is intruded by and occurs as inclusions in the border phase of the Catalina quartz monzonite (see subsequent discussion in Catalina suite section). In the eastern Rincon Mountains, apophyses from the southern mass of Happy Valley quartz monzonite intrude Wrong Mountain granite, according to the mapping of Drewes (1975).

In summary, field relationships suggest approximate contemporaneity between various muscovite granite phases. Contact relationships clearly indicate that the muscovite granite suite intrudes and is

younger than the Laramide Leatherwood suite but is intruded by and is therefore older than the middle Tertiary quartz monzonites (Catalina suite).

Most of our Rb-Sr geochemistry (Fig. 17) is on the Wilderness granite and related Lemmon Rock leucogranite and the Derrio Canyon granite. H. Drewes and R. F. Marvin of the U.S. Geological Survey have provided us with one analysis from the Wrong Mountain granite in the Rincon Mountains (1978, written commun.). The Rb and Sr abundances (Fig. 17) define a field for the Wilderness suite granites and their mylonitic equivalents that is offset from all other igneous rock types, a relationship consistent with the suite's unique mineralogy. Pegmatites with low Sr abundances form a distinct field separate from main phases of the Wilderness suite. We interpret these pegmatites to represent a low Sr residuum formed late in the differentiation history of the Wilderness sequence.

Isotopic data for Wilderness suite rocks (Fig. 18) show much scatter that we interpret as being mainly due to large variation in $^{87}Sr/^{86}Sr$ initial ratios and contamination by nearby highly radiogenic host rocks. Samples whose analyses scatter along the 1.44-b.y. reference isochron (Fig. 18) are generally in geologic settings in which they could have been easily contaminated by highly radiogenic Sr from nearby 1.45-b.y.-old Oracle Granite (see Damon and others, 1980). Some samples of pegmatite from the Santa Catalina forerange are anomalously radiogenic (Damon and others, 1980) and could represent radiogenically disturbed pegmatites of original Precambrian ancestry or small pockets of metamorphically differentiated material "sweated out" from Precambrian protoliths during Wilderness intrusion.

An outstanding example of the contamination phenomenon in Wilderness suite rocks occurs in the Lemmon Rock leucogranite phase of the Wilderness granite intrusion east and southeast of Mount

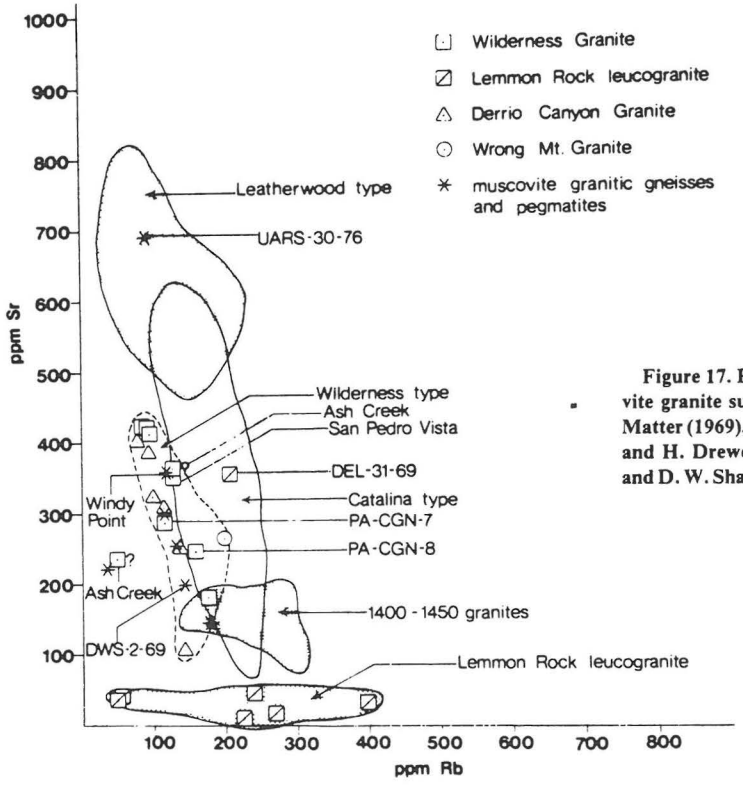

Figure 17. Rb-Sr abundances in muscovite granite suite; plot includes data from Matter (1969), Shakel (1974), R. F. Marvin and H. Drewes (1978, written commun.), and D. W. Shakel (1978, written commun.).

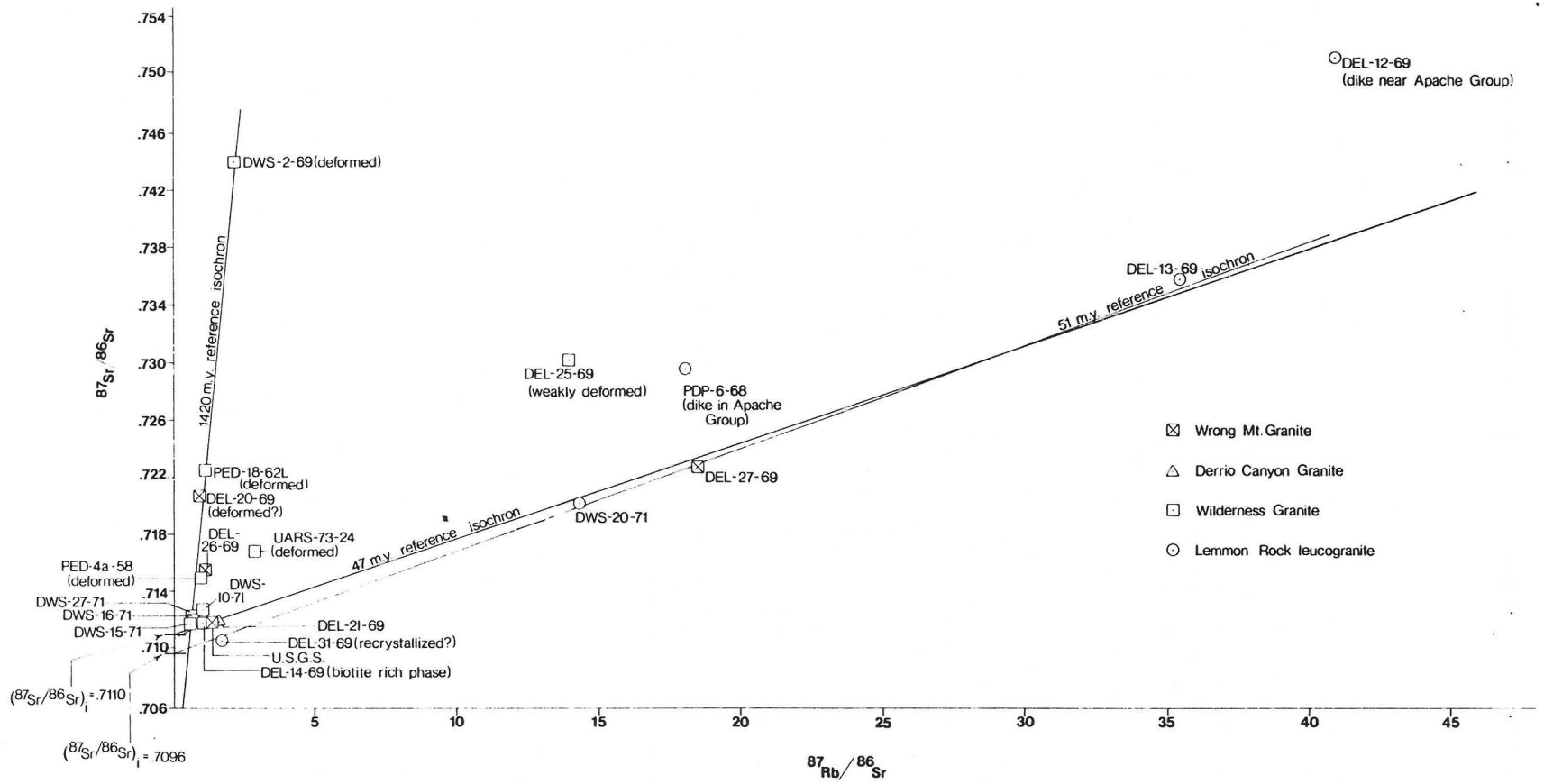

Figure 18. Rb-Sr isochron diagram for muscovite granite suite; plot includes data from Shakel (1974), D. W. Shakel (1978, written commun.), and R. F. Marvin and H. Drewes (1978, written commun.). The 47-m.y. reference isochron is constructed through non-deformed rocks that are sufficient distances from older highly radiogenic host rocks (Damon and others, 1980), and assumes Wilderness granite and Lemmon Rock leucogranite are comagmatic.

Lemmon. A sample of Lemmon Rock leucogranite (DEL-10-69) that contains numerous 1.44-b.y.-old Oracle Granite inclusions about 4 km southeast of Mount Lemmon is anomalously radiogenic ($^{87}Sr/^{86}Sr$ = 0.7772 based on a 49-m.y. assumed age). The Precambrian Oracle Granite host rock in this area (DEL-29-69) is radiogenic enough (0.7936 at 49 m.y. B.P.) to have been a likely source of radiogenic Sr contamination. Also, pegmatite members of Lemmon Rock leucogranite that are near or in Precambrian Apache Group strata (samples PDP-6-68 and DEL-12-69) contain anomalous amounts of radiogenic Sr and plot above the 47-m.y. reference isochron for Wilderness granite. In contrast, samples of Lemmon Rock leucogranite that intrude Leatherwood quartz diorite about 4 km east of Mount Lemmon near Summerhaven (samples DEL-13-69 and DWS-20-71) plot on the 51-m.y. reference isochron (Fig. 18) for the Lemmon Rock leucogranite. Importantly, the Leatherwood quartz diorite is comparatively nonradiogenic (at 49 m.y. measured $^{87}Sr/^{86}Sr$ values for five samples range from 0.7081 to 0.7087). Thus, the only apparent way to explain the large variation in measured ratios from the Lemmon Rock leucogranite in the Mount Lemmon area is by the variable addition of radiogenic Sr to Lemmon Rock leucogranite magma during its intrusion presumably 44 to 50 m.y. ago. Precambrian Oracle Granite and Apache Group hot rocks provided ready sources of radiogenic Sr that was mobilized by hydrothermal metasomatism during emplacement of the water-rich Lemmon Rock leucogranite assemblage of aplites, pegmatites, and alaskites.

Samples of Wilderness suite rocks that were *not* collected near highly radiogenic host rocks and that have only weak or no mylonitic fabric define a 47-m.y. reference isochron which has an initial $^{87}Sr/^{86}Sr$ value of 0.7110. This isochron is based on the assumption that the Wilderness granite and Lemmon Rock leucogranite are comagmatic. The fact that one Derrio Canyon granite analysis and two Wrong Mountain granite analyses fall on the same isochron suggest that these plutons may be comagmatic with Wilderness granite and ~47 m.y. old.

In addition to the Rb-Sr isotope data which indicate a 47-m.y.-age assignment, numerous other radiometric data are concordant with the Rb-Sr data. The first of these data are in the form of K-Ar ages on coarse muscovite (Table 1). Coarse muscovite from the Lemmon Rock leucogranite yielded a 47.9-m.y. K-Ar age. Damon and others (1963) interpreted this age as an incomplete degassing of Ar due to the large dimensions of the mica books. The age in this context was a minimum or inherited age for the pegmatite, which could have had an unknown older age. Within the current radiometric context, however, the 48-m.y. age may date the emplacement of the Lemmon Rock leucogranite. More K-Ar support is found in the Redington Pass area. Marvin and others (1978) reported a 45.8-m.y. K-Ar age for muscovite in a sample of Wrong Mountain granite.

Discordant and relatively old K-Ar ages have been known from the two-mica granitic rocks since the work of Damon and others (1963; Table 1). A coarse muscovite from the Wrong Mountain granite yielded a 33.5-m.y. age. Muscovite from deformed Wilderness granite yielded K-Ar ages of 30.2 m.y. on muscovite versus 25.4 m.y. for biotite (Damon and others, 1963). Rb-Sr dates on the same sample reported by Livingston and others (1967) yielded 36.9 m.y. for muscovite as opposed to 25.4 m.y. for biotite. Another muscovite from deformed Wilderness granite at the same location yielded a 33-m.y. K-Ar age (Catanzaro and Kulp, 1964). Coarse-grained muscovite gave a 31.9-m.y. K-Ar age for a light band (Wilderness equivalent) in the mylonitic forerange gneisses as compared to 26.0 m.y. for fine-grained muscovite and 25.6 m.y. for fine-grained biotite from another sample at the same location. Recently, discordant K-Ar ages from the Wrong Mountain granite in Redington Pass were reported by Marvin and others (1978). Here, biotite gave an age of 21.9 m.y., and muscovite yielded a strongly discordant age of 35.1 m.y.

All of the relatively old and/or discordant ages reported from the Santa Catalina–Rincon–Tortolita complex are on coarse muscovites from Wilderness-type granitic material. Significantly, none of these ages is older than 50 m.y. The ages are distinctly older than the majority of K-Ar and fission-track ages in the complex, which are 20 to 30 m.y. (Table 1). We view these post–45-m.y. and pre–30-m.y.

muscovite ages as reduced ages that probably reflect the relatively retentive nature of coarse muscovites (Damon and others, 1963; Mauger and others, 1968). As a rule, these muscovites have had their ages reduced less than those for finer-grained micas. This is in opposition to the interpretation of Banks (1977 and this volume) that these ages represent contamination of the muscovites by excess Ar during what he considers a middle Tertiary event of batholithic intrusion.

As pointed out by Damon (1970), because all minerals have a measurable solubility for Ar in the presence of an external Ar pressure, excess environmental Ar can be detected by analyzing minerals in which K is a minor or trace component. For such minerals, the presence of significant amounts of excess environmental Ar yields highly discordant ages. Livingston and others (1967) analyzed plagioclase from mylonitic Wilderness granite and concluded that the plagioclase contained no more than 1.5×10^{-11} mol/g of excess Ar relative to muscovite and biotite. This amount of excess Ar would increase the apparent age of the muscovite or biotite by no more than 1.2 m.y. However, in order to place closer limits on the amount of excess environmental Ar, we have analyzed garnet containing only 0.04% K (Damon and others, 1980). This garnet contained only 3.16×10^{-12} mol/g of nonatmospheric ^{40}Ar of which no more than one-half could be excess environmental Ar. This amount would increase the age of muscovite or biotite by only about 0.1 m.y. Therefore, we conclude that the Santa Catalina part of the complex was open to the escape of Ar during the final elevated thermal history. Consequently, the nonatmospheric ^{40}Ar contained within K-bearing minerals of the complex was generated since that time or inherited from older minerals only partially degassed during the middle Tertiary thermal event that preceded final middle Tertiary cooling.

More convincing evidence for the Eocene igneous event is found in U-Th-Pb data recently reported from the Wilderness granite and associated aplite, alaskite, and pegmatite bodies. U-Th-Pb ages of 44 to 47 m.y. on "igneous-looking" monazite from a sample of Wilderness granite in the Santa Catalina main range were reported by Shakel and others (1977). Monazites from foliated two-mica mylonitic gneiss at the west end of the Santa Catalina forerange also yielded 44- to 47-m.y. U-Th-Pb ages (Shakel and others, 1977). It is interesting that the lower-intercept age reported by Catanzaro and Kulp (1964) for the highly discordant zircons from garnet-bearing two-mica mylonite gneiss (deformed Wilderness granite at Windy Point in the Santa Catalina main range) was 50 m.y. Catanzaro and Kulp (1964) emphasized the upper-intercept age of 1,660 m.y. and suggested that the 50-m.y. lower intercept was too old to represent the metamorphic event, which they believed was dated by K-Ar as 30 to 40 m.y. B.P. They thought that middle Tertiary episodic Pb loss from a Precambrian protolith might explain the data. In the context of our work, the 50-m.y. lower intercept probably dates the emplacement of the Wilderness granite. Catanzaro and Kulp included a picture of the zircons they dated. In the picture, there appear to be two populations present. About 10% of the zircons are stubby, opaque, and cloudy and perhaps could be older "inherited" zircons. The other 90% are clear, elongate, and euhedral zircons that might be younger igneous zircons formed during Eocene Wilderness granite crystallization. It is interesting that the actual analysis plots on the discordia line close to the 50-m.y. intercept about nine-tenths of the way down the discordia line toward the 50-m.y. lower intercept. If the source of the zircon contamination was Oracle Granite (as might be predicted by studies of Shakel and others, 1977; Shakel, 1978; and Rb-Sr data in Fig. 18), a discordia cord upper intercept at 1.45 b.y. would require a lower intercept *slightly* younger than 50 m.y. This younger lower-intercept age (interpreted by us to be age of emplacement) would be approximately concordant with our 47-m.y. Rb-Sr reference isochron.

In summary, field relationships require that Wilderness suite granites postdate Late Cretaceous–early Tertiary Leatherwood suite plutons but predate middle Tertiary Catalina suite plutons. Isotopic data from different methods are impressively concordant at 44 to 50 m.y. These include an 11-point whole-rock Rb-Sr isochron, two K-Ar dates of coarse muscovite, two U-Th-Pb dates on monazite, and one zircon sample dated by the U-Pb discordia method. Most of the dates are from the Wilderness granite, Lemmon Rock leucogranite, and related pegmatite phases in the Santa Catalina forerange.

However, one sample from the Derro Canyon granite and two from Wrong Mountain granite fall on our Rb-Sr reference isochron; this suggests that these plutons correlate with Wilderness granite in age as well as mineralogy and relative position within the intrusive sequence of the Santa Catalina–Rincon–Tortolita crystalline complex.

Middle Tertiary Quartz Monzonite (Catalina) Suite. Emplacement of one granite and three quartz monzonite plutons (designated the Catalina suite) in late Oligocene–early Miocene time marked the final event in the growth of the batholith component of the Santa Catalina–Rincon–Tortolita crystalline complex. By far, the greatest volume of magma emplaced during this time was that in the northwestern Santa Catalina Mountains and southern Tortolita Mountains where three coalescing plutons—the Reef of Rock granite and the Catalina and Tortolita quartz monzonites—form a small batholithic mass. The Catalina quartz monzonite forms a large, half-circle–shaped pluton in the northwestern Santa Catalina Mountains and an east-northeast–trending dikelike mass in the south-central Tortolita Mountains. The Tortolita quartz monzonite occupies a rectangular area with an east-northeast–trending long axis in the southern Tortolita Mountains and occurs as north-northwest–striking dikes in the western Santa Catalina Mountains. The Reef of Rock granite forms a jagged north-northeast–trending spine that borders the southeast margin of the Catalina quartz monzonite in the central Santa Catalina Mountains (Suemnicht, 1977). This granite is one of the youngest plutons of the Santa Catalina–Rincon–Tortolita crystalline complex. A fourth pluton, the Happy Valley quartz monzonite, is provisionally placed in the Catalina suite pending further work and appears as two stocklike masses on the eastern slopes of the Rincon Mountains. Together, Catalina suite plutons form about 15% of the batholithic rocks exposed in the complex.

Catalina suite plutons are mineralogically distinct from Wilderness and Leatherwood suites. Average modal analyses are reported in Table 5. Catalina suite plutons contain more quartz and more K-feldspar, less (but more sodic) plagioclase, and much less biotite than Leatherwood suite plutons. Both suites contain hornblende and sphene as important accessories. Catalina suite intrusions have similar quartz content, slightly more K-feldspar, slightly less (but more calcic) plagioclase, and similar amounts of biotite compared with Wilderness type plutons. Catalina plutons (with the exception of the northern mass of Happy Valley quartz monzonite) contain no muscovite compared with 1% to 7% in Wilderness plutons. Catalina suite plutons contain hornblende and sphene as common accessories and *no* garnet. The reverse is true for Wilderness suite plutons.

Upon casual inspection, Catalina quartz monzonite, the largest pluton of the Catalina suite, may easily be confused with Precambrian Oracle Granite. This confusion resulted in an incorrect age assignment for this rock initially by Tolman (1914, unpublished manuscript). This error was continued in many subsequent publications including the recent 1:500,000-scale Arizona State geologic map (Wilson and others, 1969). The mineralogic contrast between the two plutons was first observed by Wallace (1954), who assigned an older Precambrian age to the Oracle Granite on the basis of its intrusive contacts into Pinal Schist of older Precambrian age. A fossil horn coral found in a limestone inclusion by McCullough (1963) and Rb-Sr isotope data published by Hoelle (1976) established a Phanerozoic age for this intrusion. Subsequent isotopic results (Damon and others, 1963; Creasey and others, 1977; Shakel and others, 1977; this paper) firmly establish a late Oligocene age for this pluton. Quartz, plagioclase, K-feldspar, and biotite contents for Oracle Granite and Catalina quartz monzonite are very similar. The important mineralogic difference is in the accessory minerals. Catalina quartz monzonite contains hornblende and sphene in essentially all samples, but these minerals are absent from Oracle Granite.

Published modes of Catalina quartz monzonite are all from that part of the pluton in the western Santa Catalina Mountains (Table 5). The presumed analogue in the Tortolita Mountains has about 25% to 30% quartz, 30% to 35% K-feldspar, 25% to 30% plagioclase (An_{25-35}), 6% to 8% biotite, 1% hornblende, and 0.5% to 1% sphene. Fine- to medium-grained nonporphyritic border and coarser-

grained porphyritic main phases of Catalina quartz monzonite are present in both the Santa Catalina and Tortolita Mountains. The border phase (Table 5) is commonly present along outer margins of the Catalina intrusion and surrounds many of the larger inclusions within the Catalina pluton.

Within the small batholith of coalescing Catalina suite plutons in the western Santa Catalina and Tortolita Mountains, there is a compositional variation between plutons (Table 5). Catalina quartz monzonite contains less quartz, less (but more calcic) plagioclase, the same amount of K-feldspar, and more mafic minerals than Tortolita quartz monzonite. In turn, Reef of Rock granite contains more quartz, more K-feldspar, and less plagioclase than Tortolita quartz monzonite. Both plutons intrude Catalina quartz monzonite. Their overlapping isotopic ages (see below) suggest a differentiation continuum.

As discussed earlier, the Catalina quartz monzonite intrudes and postdates the Leatherwood quartz diorite (Suemnicht, 1977). The nature of the southern contact of the Catalina quartz monzonite with phases of the Wilderness granite has been much debated. All previously published opinions (McCullough, 1963; Creasey and others, 1977; Banks, 1977 and this volume) regard the contact as some type of metamorphic front. A new interpretation proposed in this paper is that the contact represents an intrusive contact of Catalina quartz monzonite into Lemmon Rock leucogranite border phase of the Wilderness granite. Much of the contact is occupied by a steeply inclined migmatite zone that contains an interleaved assemblage of metasedimentary rocks (quartzites, calc-silicate skarns, siliceous gneiss) and variably foliated intrusive rocks including Leatherwood quartz diorite, Lemmon Rock leucogranite, and Catalina quartz monzonite. The migmatite—which is interpreted by us to represent a screen of metamorphosed and highly *injected,* pre-Catalina intrusive and metasedimentary rocks—thins to the west. Here a fine- to medium-grained border phase of the Catalina quartz monzonite, similar to that described along the eastern margin of the pluton by Hoelle (1976) and Suemnicht (1977), sharply intrudes and contains inclusions of foliated Lemmon Rock leucogranite. This relationship persists for at least a 2-km length of Catalina-Wilderness contact. Both plutons contain numerous metasedimentary inclusions that locally obscure the intrusive relationships along the contact. In contrast to the conclusions of other workers (McCullough, 1963; Banks, this volume), thin sections and field observations along the Catalina-Wilderness contact in Cargodera Canyon indicate that foliated fabric in the metasedimentary inclusions, Catalina quartz monzonite, and Lemmon Rock leucogranite is mostly nonmylonitic. Our observations do not support the contentions of Creasey and others (1977) and Banks (1977 and this volume) that Cargodera Canyon represents a transition zone ("gneiss front") between mylonitic and nonmylonitic parts of a *single* pluton. In the Tortolita Mountains, Catalina quartz monzonite postdates the Leatherwood and Wilderness suites, as discussed above.

The youngest major pluton in the crystalline core of the complex is the Tortolita quartz monzonite. It is easily distinguished from the Catalina quartz monzonite by its finer grain size and nonporphyritic hypidiomorphic-granular texture. Wherever the two plutons are in contact, the Tortolita quartz monzonite clearly cuts the Catalina quartz monzonite (McCullough, 1963; Banks, 1976). In lower Cargodera Canyon, two large north-northwest–striking dikes of Tortolita quartz monzonite clearly crosscut and contain inclusions of Catalina quartz monzonite and Wilderness granite. These dikes were correlated by Banks (1976) with the main Tortolita pluton in the southern Tortolita Mountains 8 km to the west-northwest. We concur with Banks's correlation. In the southern Tortolita Mountains, the main pluton of Tortolita quartz monzonite occupies the entire southern third (about 70 km^2) of the mountain range. The contact between the Tortolita and Catalina plutons in the south-central Tortolitas was mapped by Budden (1975) as a mixed zone with many different phases present. More recent mapping by one of us (Keith) has indicated that the zone represents inclusions of quartz diorite that have been engulfed and injected by Catalina quartz monzonite and subsequently intruded by sheets of Tortolita quartz monzonite from the south (Fig. 4). Keith believes that the presence of K-feldspar porphyroblasts in and near the edges of the dioritic inclusions and the occurrence of biotitic "patches"

in the Catalina pluton suggest K metasomatism during intrusion of Catalina quartz monzonite. The Tortolita quartz monzonite and older rocks are locally intruded by pegmatite, lamprophyre, and granodiorite dikes which volumetrically are insignificant. At the southeast corner of the main Tortolita pluton, intrusions of Tortolita quartz monzonite into Catalina quartz monzonite have been recognized by Budden (1975) and Banks (1976, 1977, and this volume).

Another small pluton, the Reef of Rock granite, is exposed in the Santa Catalina Mountains, 2 km north of Mount Lemmon (Suemnicht, 1977). The granite intrudes and contains inclusions of Leatherwood quartz diorite and Catalina quartz monzonite (Suemnicht, 1977). Possible equivalents of the Reef of Rock granite intrude Tortolita quartz monzonite in the Tortolita Mountains where they have been mapped as a phase of the Tortolita pluton.

A possible fourth pluton of the Catalina suite is the Happy Valley quartz monzonite of the eastern Rincon Mountains (Drewes, 1974). Drewes (1974) mapped projections of the southernmost mass of Happy Valley quartz monzonite cutting Wrong Mountain granite (a Wilderness suite pluton). The northernmost mass contains muscovite (Miles, 1965) and may be a Wilderness suite pluton.

Plutons of the Catalina suite are the youngest set of intrusions in the batholithic sequence and mark its final consolidation. Two of the *youngest* plutons are intruded by northwest-striking dike swarms. Early Miocene K-Ar ages have been obtained from some of these dikes (Banks and others, 1978). The eastern part of the Catalina quartz monzonite is crosscut by northwest-striking rhyolite porphyry dikes. Tortolita quartz monzonite is crosscut by northwest-striking quartz latite and granodiorite dikes (Fig. 2). No dikes are known to crosscut the Happy Valley or Reef of Rock intrusions.

We have Rb-Sr geochemistry on two plutons of the Catalina suite, the Catalina and Tortolita quartz monzonites. Rb-Sr abundances for the two plutons (Fig. 19) do not overlap but are aligned along a similar trend, which is permissive of a differentiation continuum.

Isotopic analyses have been determined for main-phase quartz monzonites and correlative dike and aplite samples. We believe that data for both the Catalina and Tortolita plutons (including their dikes and aplites) are best explained by adherence to a reference isochron of ~26 m.y. (Fig. 20). The slope of the isochron is to a large degree governed by analyses of aplites, but we feel confident that the aplites sampled are comagmatic with the enclosing plutons. Samples that plot well above the reference isochron were collected near to and could have been easily contaminated by highly radiogenic wall rocks or inclusions. Rb-Sr abundances of dark inclusions (Fig. 21) in these young quartz monzonites suggest that a majority of the dark inclusions are from the Leatherwood suite of rocks.

The late Oligocene age suggested by the 26-m.y. Rb-Sr isochron is supported by abundant isotopic data. Single biotite K-Ar ages of 25.6 m.y. in the Santa Catalina Mountains and 28.0 m.y. in the Tortolita Mountains (Damon and others, 1963) for the Catalina pluton are semiconcordant with a single K-Ar biotite age of 23.8 m.y. and concordant K-Ar biotite-hornblende pairs of 23.9 m.y. (biotite) and 23.7 m.y. (hornblende), 24.7 m.y. (biotite) and 27.9 m.y. (hornblende), and 21.1 m.y. (biotite) and 21.6 m.y. (hornblende) for the Catalina quartz monzonite reported by Creasey and others (1977). The last concordant pair is from the Catalina quartz monzonite in the Tortolita Mountains. Similarly, biotite K-Ar ages from the Tortolita pluton of 24.5 m.y. in the Santa Catalina Mountains (Damon and others, 1963) and 22.7 m.y. in the Tortolita Mountains (Creasey and others, 1977) strongly overlap with those of the Catalina intrusion and suggest temporal equivalence. The notion of temporal equivalence is further supported by numerous fission-track ages of 30.0, 28.3, and 28.0 m.y. on sphene; 28.9, 27.1, and 25.9 m.y. on zircon; and 23.5, 20.8, and 21.7 m.y. on apatite for the Catalina quartz monzonite and 18.5 and 17.0 m.y. on apatite from the Tortolita quartz monzonite reported by Creasey and others (1977). With the exception of apatite, which represents final cooling of Catalina and Tortolita intrusions, the fission-track ages are all concordant with the K-Ar ages.

Any doubts about the age of the Catalina pluton were removed by the 27-m.y. U-Pb concordant

zircon age reported by Shakel and others (1977). The U-Pb data showed that Rb-Sr "isochrons" published earlier by Shakel and others (1972) and Hoelle (1976) probably involved erroneous assumptions regarding sample selection (see comments in Table 1).

In summary, field relationships indicate that plutons of the Catalina suite are younger than rocks of the Late Cretaceous–early Tertiary Leatherwood suite and Eocene Wilderness suite. Concordant K-Ar biotite ages and hornblende-biotite pairs, sphene and zircon fission-track ages, a U-Pb zircon age, and a poorly constrained Rb-Sr whole-rock isochron require a middle Tertiary age for quartz monzonites of the Catalina suite.

IMPLICATIONS OF PLUTONIC EPISODES FOR MYLONITIC DEFORMATION

Previous sections have detailed the emplacement of three suites of plutons from 75 to 20 m.y. ago. Plutons of *each* suite have been deformed to varying degrees by distinctive, gently inclined mylonitic foliation with conspicuous lineation that plunges east-northeast and west-southwest. At least three episodes or events of mylonitization (and probably more) are recorded in relationships where undeformed parts of younger plutons cut deformed parts of older plutons.

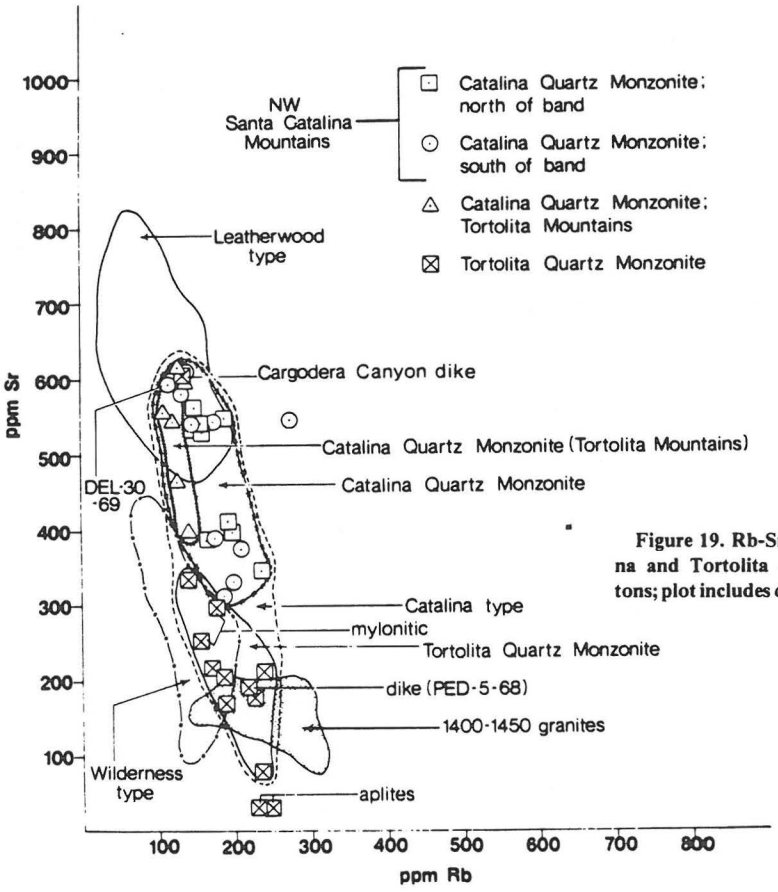

Figure 19. Rb-Sr abundances in Catalina and Tortolita quartz monzonite plutons; plot includes data from Hoelle (1976).

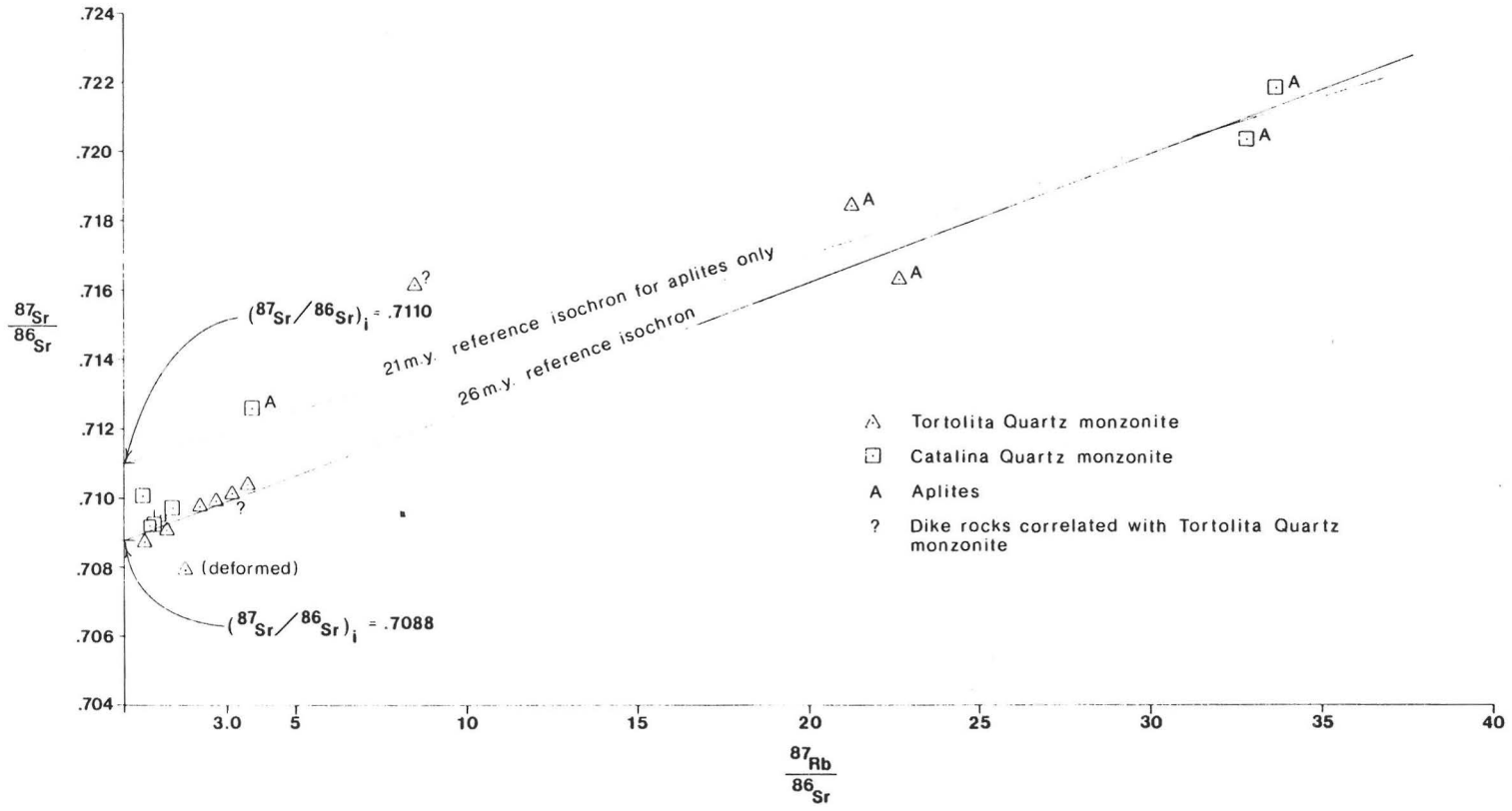

Figure 20. Rb-Sr isochron diagram for Catalina and Tortolita quartz monzonite plutons; plot includes data from Hoelle (1976); 26-m.y. reference isochron assumes Catalina and Tortolita quartz monzonite plutons are comagmatic.

The oldest mylonitic event is post–75 m.y. B.P. because it deforms Leatherwood quartz diorite. This fabric must be pre–50 m.y. because mylonitic foliation in Leatherwood is intruded in many places by dated 44- to 50-m.y.-old undeformed muscovite pegmatites east of Mount Lemmon (Hanson, 1966). In a well-exposed roadcut along the new paved-highway access to the Mount Lemmon ski area 2.5 km east-northeast of Mount Lemmon, several instructive relationships may be observed between mylonitic events in the Leatherwood quartz diorite and muscovite pegmatites of the Lemmon Rock leucogranite. Here, an older, coarser-grained mylonitic foliation is cut at a low angle by a younger, fine-grained, more intense mylonitic foliation. Two generations of pegmatites are present. The older generation consists of shallowly inclined sheets about 0.1 to 0.2 m thick which cut the older, coarser-grained mylonitic foliation but are conspicuously boudined where they cross the younger, fine-grained mylonitic foliation. The two foliation events and the shallowly inclined pegmatites are clearly crosscut by large, steeply inclined, undeformed pegmatite dikes that constitute 90% of the pegmatite exposed in the roadcut.

Similar relationships occur 20 km to the east-southeast of Mount Lemmon (Wilson, 1977; Ted Theodore, 1979, oral commun.) where undeformed pegmatite apophyses of the Wilderness pluton discordantly cut mylonite schist derived from Leatherwood. In addition, equigranular main-phase Wilderness granite may intrude mylonitic Leatherwood quartz diorite east of Green Mountain, about 12 km east-southeast of Mount Lemmon (Pilkington, 1962). The southern part of the Leatherwood pluton is continuously deformed along its east-southeast–trending margin for more than 20 km. As

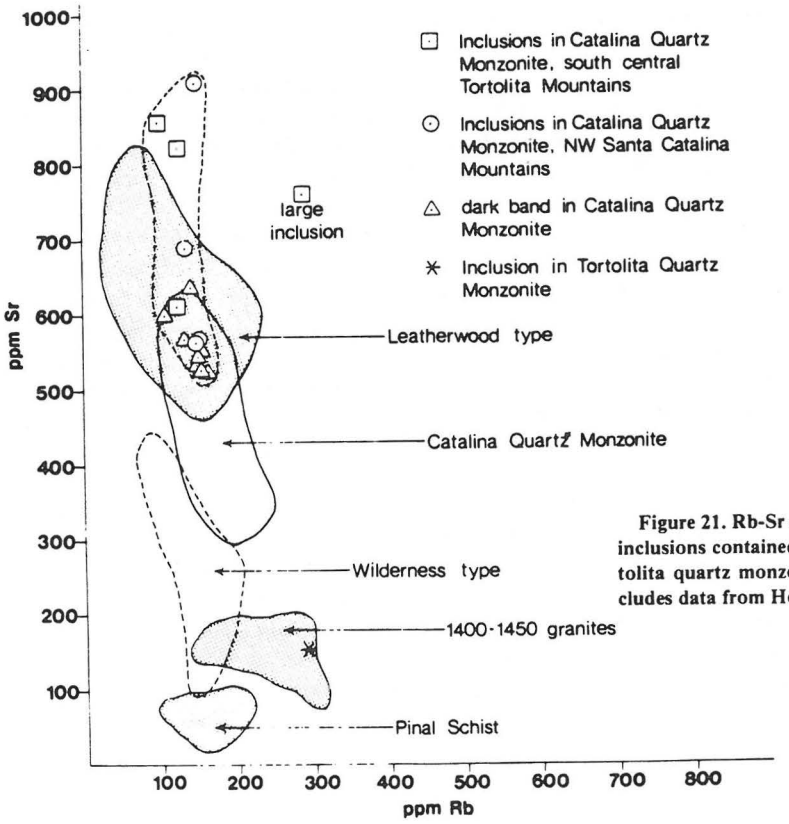

Figure 21. Rb-Sr abundances from dark inclusions contained in Catalina and Tortolita quartz monzonite plutons; plot includes data from Hoelle (1976).

such, mylonitic fabric in the Leatherwood constitutes a major pre–50 m.y. B.P. and post–75 m.y. B.P. mylonitic event in the Santa Catalina–Rincon–Tortolita crystalline complex.

Orientation of mineral lineation in mylonitic Leatherwood quartz diorite is distinct from that in main-range exposures of mylonitic Wilderness granite. Based on 116 measurements, mean lineation in Leatherwood quartz diorite exposures along the Oracle road 3 to 6 km northeast of Mount Lemmon is 16° N85°E (Tom Heidrick, 1979, written commun.). Lineation on low-angle mylonitic surfaces in the deformed Wilderness intrusion in the Windy Point and Spencer Peak areas about 5 and 15 km, respectively, southeast of Mount Lemmon is more northeasterly (about N35°E to N65°E). The difference in lineation orientation suggests that mylonitic foliation in the Leatherwood and Wilderness intrusions may have formed during two distinct episodes of cataclasis.

The next major mylonitic episode deformed the structurally lower parts of the Wilderness granite and its wall rocks in the Santa Catalina forerange. Analogous deformation may be represented by widespread mylonitic fabric in the mineralogically similar Wrong Mountain granite (Drewes, 1977) of the Rincon Mountains. This mylonitization deformed and therefore postdated the 44- to 50-m.y.-old muscovite granites but predated their cooling between 31 and 25 m.y. B.P. as defined by K-Ar and fission-track ages. Keith infers that relationships between deformed and undeformed pegmatites in the Santa Catalina forerange suggest that the mylonitic fabric exposed there formed during the emplacement of Wilderness equivalent pegmatites. Mylonitization in the forerange must have been completely over by the time of intrusion of an undeformed 21-m.y.-old trachyte dike (Shakel, 1974; Damon and others, 1980).

One of the above two episodes may be widespread throughout the northwestern Tortolita Mountains where the Chirreon Wash (Leatherwood suite) and Derrio Canyon (Wilderness suite) intrusions are strongly mylonitized—particularly so in the area of the Derrio Canyon granite sill sequence (Figs. 4 and 7). At least part of this deformation predated emplacement of the Catalina pluton as evidenced by large, strongly deformed and lineated inclusions of quartzite, Pinal Schist, stretched-pebble metaconglomerate, and Oracle Granite in relatively less-deformed Catalina quartz monzonite. Presence of mylonitic inclusions of Leatherwood quartz diorite in Catalina quartz monzonite in the Santa Catalina Mountains (Suemnicht, 1977) also indicates a mylonitic event that predated emplacement of the Catalina quartz monzonite.

In the southwestern Tortolita Mountains, the youngest episode of mylonitization clearly affects to varying degrees the Catalina quartz monzonite and the entire western half of the Tortolita quartz monzonite. This episode must postdate the two ~26-m.y.-old plutons but predate cooling of the mylonitic rocks between 17 and 20 m.y. B.P. as defined by fission-track apatite ages. An additional minimum age for this episode is provided by a series of northwest-trending dikes which discordantly intrude mylonitic foliation. One of these dikes which cuts mylonitic Chirreon Wash granodiorite has yielded a 24-m.y. K-Ar biotite date (Table 1). Thus, a significant mylonitic episode is bracketed very close to 25 m.y. B.P. In the South Mountains near Phoenix, Reynolds and Rehrig (this volume) have documented almost exactly the same age for mylonitic fabric that deforms a pluton which resembles phases of Tortolita quartz monzonite in rock type, texture, and style of mylonitic deformation.

In the Tortolita Mountains, several *events* of mylonitization are recognizable within the youngest *episode* of mylonitization. For example, near the mouth of Wild Burro Canyon, strongly mylonitized inclusions of Oracle Granite that were deformed during an earlier episode are included in the coarsely porphyritic phase of Catalina quartz monzonite. This phase in turn contains a younger, much weaker mylonitic foliation. These are both crosscut by low-dipping sheets of the granitic phase of Tortolita quartz monzonite which has been strongly mylonitized by a still-younger mylonitic event. This youngest mylonitic event may be related to a widespread set of shallow-dipping, relatively wide-spaced shears that cut older, more steeply inclined foliations (some of which are mylonitic) in the Chirreon and Catalina intrusions.

SUMMARY AND CONCLUSIONS

Various rocks within the Santa Catalina–Rincon–Tortolita crystalline complex can be correlated with rocks inside and locally outside of the complex by utilizing field relationships and lithologic, trace-element, and isotopic analyses. Deformed Precambrian, Paleozoic, Mesozoic, and Cenozoic rocks all occur within the complex, but its geology is *dominated* by a series of Late Cretaceous(?) through middle Tertiary plutonic and deformational episodes. Major plutonism was apparently episodic and produced three distinct ages and suites of intrusions. The Laramide (75 to 64 m.y. B.P.) quartz diorite and granodiorite (Leatherwood suite) were emplaced earliest. These were followed by Eocene (44 to 50 m.y. B.P.) muscovite granite, pegmatite, and alaskite (Wilderness suite). Finally, quartz monzonites (Catalina suite) were intruded in middle Tertiary time (27 to 25 m.y. B.P.). At least three episodes of mylonitic deformation occurred between 75 and 20 m.y. B.P. Although the plutonism was episodic, it cannot be definitively demonstrated that the mylonitic deformation was also episodic rather than part of a prolonged continuum. However, the close spatial and temporal association of mylonitization with plutonism suggests a genetic relationship between the two and therefore supports episodicity of mylonitization.

ACKNOWLEDGMENTS

This paper benefited greatly from conversations and communication with many geologists who unfortunately cannot all be mentioned. Discussions with colleagues D. W. Shakel, G. H. Davis, N. G. Banks, W. A. Rehrig, H. W. Peirce, P. J. Coney, E. J. McCullough, E. B. Mayo, S. C. Creasey, C. H. Thorman, T. G. Theodore, H. Drewes, P. Meyers, R. T. Budden, G. Suemnicht, P. Anderson, J. Hoelle, and C. W. Kiven particularly contributed to the development of concepts presented herein. We are especially grateful to E. J. McCullough, P. J. Coney, and G. H. Davis for their advice and encouragement. We also express appreciation to numerous students who have provided laboratory assistance during the past 18 yr. The quality of the manuscript was greatly improved by thoughtful reviews of N. G. Banks, S. C. Creasey, R. L. Armstrong, R. E. Zartmann, and M. Silberman. Unpublished K-Ar and Rb-Sr data which greatly influenced many of our geochronologic interpretations were generously provided by S. C. Creasey, R. F. Marvin, and H. Drewes of the U.S. Geological Survey, D. W. Shakel of Pima College, P. Anderson of the University of Arizona, and S. M. Soderman of the Oracle Ridge Mining Company. T. L. Heidrick of Gulf Minerals, Inc., kindly provided chemical data for the Leatherwood quartz diorite. Rb-Sr and K-Ar isotopic work performed at the Laboratory of Isotope Geochemistry, University of Arizona, was funded by National Science Foundation Grant EAR78-11535, Atomic Energy Commission contract AT(11-1)-689, and the state of Arizona. We thank J. LaVoie and R. DuPont of the Bureau of Geology and Mineral Technology and S. Harralson and B. Bible for their assistance in preparing this manuscript.

APPENDIX 1. NOMENCLATURE FOR PLUTONIC ROCKS IN THE SANTA CATALINA–RINCON–TORTOLITA CRYSTALLINE COMPLEX

INTRODUCTION

This appendix compares our preferred terminology* for what we believe are, in essence, plutonic rocks in the Santa Catalina–Rincon–Tortolita crystalline complex with nomenclature of other past and current workers. The discussion is arranged from the oldest to youngest rock unit. The number in parentheses that follows certain rock names corresponds to the plutons numbered in Figure 3. The subsections entitled "Location" designate the geographic area (also refer to Fig. 3) where *we* are using the preferred name. The subsections entitled "Comments" present historical notes and commentary about previous or current usages by other workers for the rock within the geographic area previously outlined.

The interested reader will quickly notice that all of our nomenclature lacks the term "gneiss." Although we recognize the presence of widespread areas of mylonite gneiss within the crystalline core of the Santa Catalina–Rincon–Tortolita complex, we are confident that in most cases, the igneous protolith that has been texturally modified by the mylonitization event(s) can be recognized. Future mapping in the complex should attempt to identify protoliths as closely as possible. Areas of mylonite overprint (textural modification of the protolith) should also be identified. The Mount Lemmon quadrangle mapped by Banks (1976) and Figure 3 of this paper are two approaches to the overprint problem. Banks (1976) enclosed the protolith symbol in parentheses to indicate areas where the protolith was strongly mylonitized. Figure 3 shows mylonitic or deformed areas by aligned linear patterns and areas of nonmylonitic or nondeformed igneous rocks by random patterns. These techniques avoid the impression imparted by previous maps (for example, see Wilson and others, 1969) that areas mapped as "gneiss" represent a unique rock unit. This in turn leads to the false generalization that the "gneiss" units are different from adjacent rocks and have a different origin. The emerging view instigated by Creasey and Theodore (1975), Banks (1976), Creasey and others (1977), and this paper is that the gneisses for the most part represent areas where the plutonic terrane is merely deformed. Thus, contacts between areas of mylonite gneiss and nonmylonitic counterparts are gradational as depicted in Figure 3.

MIDDLE PROTEROZOIC (1.7 TO 1.4 B.Y. B.P.) PLUTONIC ROCKS

Madera Diorite

Location. Exposures in Pinal Mountains and northern Dripping Spring Mountains, 60 km north of the Santa Catalina–Rincon–Tortolita complex.

Comments. Named by Ransome (1903) for exposures near Mount Madera in the Pinal Mountains. Intrusion in northern Tortolita Mountains, 6 km north of the crystalline core of the Santa Catalina–Rincon–Tortolita complex was questionably correlated with Madera Diorite by Banks and others (1978). Mylonitized diorites in the Santa Catalina forerange may correlate with Madera Diorite.

Johnny Lyon Granodiorite*

Location. Large half-moon–shaped exposure in Johnny Lyon Hills 20 km east of the Rincon Mountain part of the complex. Also widely exposed in the eastern Rincon Mountains in and east of Happy Valley according to Silver (1978).

Comments. Named by Silver (1955) for large exposure in western Johnny Lyon Hills and formally adopted by Cooper and Silver (1964). Silver (1978) indicated that exposures in the Happy Valley area of the eastern Rincon Mountains mapped by Drewes (1974) as Rincon Valley Granodiorite, are instead Johnny Lyon equivalent and recommended that the term "Rincon Valley Granodiorite" be discontinued for rocks in this area. Catanzaro and Kulp (1964) suggested that highly discordant zircons extracted from granitic gneiss at Windy Point in the Santa Catalina main range (viewed by us as mylonitically deformed Wilderness granite) were the same age (about 1,625 m.y.) as those extracted from Johnny Lyon Granodiorite by Silver and Deutsch (1963). We place more significance on the lower intercept age of 50 m.y. as the age of intrusion for Wilderness granite and consider the discordance to be due to contamination by older zircons of a possible 1,450-m.y. age (see discussion in text).

---

*The rock names that we prefer for current map usage within the complex are denoted by an asterisk the first time they are mentioned.

Plutons between 1,400 and 1,450 M.Y. Old

Oracle Granite*

Location. Large west-northwest–elongated exposure at Oracle, Arizona, and numerous scattered exposures north of the complex. Numerous mylonitic equivalents within the Santa Catalina and Tortolita parts of the complex are correlated with Oracle Granite by Tolman (1914, unpublished manuscript), Creasey and others (1977), Shakel and others (1977), and this paper.

Comments. Originally named by Tolman (1914, unpublished manuscript, as referred to by Moore and Tolman in their 1938 unpublished manuscript) for exposures at Oracle, Arizona. (The 1938 unpublished manuscript by B. N. Moore and C. F. Tolman is untitled and contains 131 single-spaced pages in elite-sized type. The manuscript is available for inspection at the Arizona Bureau of Geology and Mineral Technology, 845 N. Park Avenue, Tucson, Arizona 85719.) First published reference is Peterson (1938). Name has been subsequently retained for rock in type area by all subsequent workers (for example, Banerjee, 1957; Creasey, 1967). Mylonitic equivalents have recently been mapped in the Santa Catalina forerange by Creasey and Theodore (1975), Banks (1976), Creasey and others (1977). This correlation was confirmed by U-Pb studies reported by Shakel and others (1977). Previous workers had included these mylonitic gneisses as dark bands in the Catalina gneiss or forerange banded gneiss complex and assigned various names to some of the larger bands (for example, Peterson, 1968; Shakel, 1974).

Ruin Granite

Location. Widespread exposures north and northwest of Globe, Arizona, 100 km north of the complex.

Comments. Named by Ransome (1903) for exposures in Ruin Basin 20 km northwest of Globe. Oracle Granite and Ruin Granite, if not the same rock, are the same age (Livingston and others, 1967; Silver, 1968).

Continental Granodiorite*

Location. Large north-trending exposure on west side of northern Santa Rita Mountains 20 km south of the complex. Mapped as a widespread unit by Drewes (1974, 1977) throughout Rincon and Tanque Verde parts of the complex.

Comments. Named by Drewes (1968) for exposures in the northern Santa Rita Mountains where the rock is predominantly porphyritic biotite granodiorite and quartz monzonite with small areas of hornblende-bearing granodiorite and quartz monzonite. Drewes assigned an imprecise age of 1,450 to 1,700 m.y. to the Continental Granodiorite in its type area in the northern Santa Rita Mountains. This age was based on what he regarded as equivocal ages from discordant K-Ar, Rb-Sr, and Pb-α data ranging from 55 m.y. to 1,450 m.y. on coarsely porphyritic samples (see Table 1). Drewes (1976b) regarded all five ages as reduced ages and assigned a possible true age of 1,600 to 1,700 m.y. Field and U-Pb studies reported by Silver (1978) revealed that at least two intrusive phases are present, "one 1,430 m.y. old and the other more than 1,600 m.y. old" (Silver, 1978, p. 162). Most of the Continental Granodiorite of Drewes is coarsely porphyritic. This fact combined with two imprecise 1,360- and 1,450-m.y. Pb-α ages reported by Drewes (1968) and the 1,430-m.y. U-Pb age reported by Silver (1968) indicate that most of the Continental Granodiorite in the type area is probably of the 1,400- to 1,450-m.y.-old pluton generation which has extensively intruded the Johnny Lyon Granodiorite and/or rocks of similar age (1,600 m.y.). For the above reasons, we suggest that the term "Continental Granodiorite" be restricted in the Santa Rita, northern Empire, and Rincon Mountains to coarsely porphyritic biotite quartz monzonite and its mylonitic equivalents that can be shown to have a 1,400- to 1,450-m.y. ancestry. "Continental Granodiorite" in this sense is correlative to "Oracle Granite" of the Santa Catalina and Tortolito parts of the complex.

Rincon Valley Granodiorite*

Location. Several large outcrop areas mapped by Drewes (1974, 1977) on both east and west sides of the Rincon Mountains, adjacent to but not within the crystalline core of the complex. As used by us, "Rincon Valley Granodiorite" is restricted to exposures in Rincon Valley on the southwest side of the Rincon Mountains.

Comment. Exposures in Rincon Valley were originally referred under the term "Rincon granite" by Moore and Tolman (1938, unpub. manuscript). Referred to as Rincon Valley Granite by Moore and others (1949) and Acker (1958),who assigned a Cretaceous-Tertiary (Laramide) age to the rock. Renamed Rincon Valley Granodiorite, assigned a middle Proterozoic age on the basis of K-Ar radiometric data, and extended to outcrops in the eastern Rincon Mountains by Drewes (1974, 1977). Exposures on the east side of the Rincon Mountains are probably Johnny Lyon Granodiorite as suggested by Silver (1978). Exposures in Rincon Valley are also petrographically similar to Johnny Lyon Granodiorite, but it is not clear whether they are from the same pluton. Hence, we suggest "Rincon Valley Granodiorite" be limited to Rincon Valley exposures pending further work. The coarsely porphyritic quartz monzonite, which was mapped by Drewes (1977) as Rincon Valley Granodiorite(?) northwest of Saguaro

National Monument in the Tanque Verde Mountains, mineralogically and texturally resembles the 1,400- to 1,450-m.y.-old granitic suite. Three K-Ar ages of 1,380, 1,390, and 1,400 m.y. and one 1,400-m.y. Rb-Sr model age are essentially concordant and are alternatively interpreted by us as an emplacement age. Also, the single Rb-Sr analysis reported by Marvin and Cole (1978) plots very near the composite 1,380-m.y. Rb-Sr isochron for Ruin Granite and Oracle Granite of the 1,400- to 1,450-m.y.-old granitic clan (Fig. 14).

POST-PALEOZOIC BATHOLITHIC ROCKS

Laramide Quartz Diorite–Granodiorite (Leatherwood) Suite

Rice Peak granodiorite porphyry* (1)

Location. Two stocklike masses intruding Apache Group rocks in the northern Santa Catalina Mountains between the Mogul and Geesman faults.

Comments. Described under unnamed "andesite" by Moore and Tolman (1938, unpub. manuscript) and Moore and others (1949). Eastmost mass shown as Laramide volcanics on the "Arizona Highway Geologic Map" compiled by Cooley (1967). Mapped as "meta-diorite" by Wallace (1954) and as "granodiorite porphyry" by Creasey (1967) and Suemnicht (1977). Granodiorite porphyry at San Manuel mapped as same rock by Creasey (1967). Waag (1968) and Creasey and Theodore (1975) suggested that the rocks we call Rice Peak granodiorite and Leatherwood quartz diorite may be closely related if not the same rock.

Leatherwood quartz diorite* (2)

Location. Subcircular stocklike mass in central Santa Catalina Mountains continuous with and gradational into several mylonitized sills in the northeast Santa Catalina Mountains. May be present in Rincon Mountains although it is not recognized by current mapping (Drewes, 1974, 1977).

Comment. Originally named by Tolman in an unpublished 1914 manuscript for exposures near the Leatherwood Mine group in the north-central Santa Catalina Mountains. Referred to as unnamed "quartz diorite and related schistose rock" by Moore and others (1949) and is accompanied by map symbology "Tld" and "Tldp." Name was first used in print by Bromfield (1952) and subsequently used by Peirce (1958), DuBois (1959a, 1959b), Wood (1963), Hanson (1966), Braun (1969), Matter (1969), Banks (1976), Creasey and others (1977), Suemnicht (1977), and Banks (this volume). Included within "TKm" unit of Cooley (1967) (see comment under Wilderness granite for more discussion). Pilkington (1962) and Waag (1968) mapped the schistose rock as quartz latite porphyry which Waag (1968) correlated with Leatherwood quartz diorite. Creasey and Theodore (1975) mapped the unit as unnamed quartz diorite but acknowledged the local use of the term "Leatherwood."

Chirreon Wash granodiorite* (3)

Location. East-elongated intrusion in the north-central Tortolita Mountains.

Comments. Mapped as a composite granodiorite, quartz diorite, monzodiorite, and diorite intrusion under the heading "quartz monzonite of Samaniego Ridge and related rocks" by Banks and others (1977). Named granodiorite of Chirreon Wash by Banks and others (1978) and adopted here as Chirreon Wash granodiorite.

Eocene Muscovite Granite (Wilderness) Suite

Derrio Canyon granite* (4) and Related Pegmatites

Location. Sheetlike mass of muscovite-garnet granite and related pegmatite dikes and sheets in the northwest to north-central Tortolita Mountains.

Comments. Main mass mapped as mylonitic "quartz monzonite of Samaniego Ridge" by Banks and others (1977). Pegmatite, aplite, and alaskite apophyses which extend eastward into and intrude Chirreon Wash granodiorite mapped under the heading "quartz monzonite of Samaniego Ridge" as a "pegmatite complex" by Banks and others (1977). Banks (this volume) refers to the body that is co-extensive with our "Derrio Canyon granite" as Cottonwood Canyon gneiss and infers that it was metamorphically derived from the Chirreon Wash granodiorite.

Wilderness granite* and Related Lemmon Rock leucogranite* (5)

Location. Large sill-like or laccolithic mass which extends westward from upper Sabino Canyon (4 km south of Mount Lemmon) through the Wilderness of Rocks, 3 km south of Mount Lemmon to Romero Pass and Romero Canyon. Mylonitized varieties extend southwesterly and south into the Santa Catalina forerange where they are a main component of the forerange mylonitic gneiss complex. A related assemblage of pegmatites, aplites, and

alaskites (Lemmon Rock leucogranite) occurs along the north margin of the pluton. Wilderness granite includes biotite-rich phases (for example, a biotite-rich phase in the Spencer Campground area about 5 km east-southeast of Mount Lemmon). Wilderness pluton extends eastward from upper Sabino Canyon through Molino Canyon (9 km southeast of Mount Lemmon) to the Bellota Ranch region (15 km southeast of Mount Lemmon). East of Bellota Ranch, muscovite granite outcrops that are continuous with Wilderness exposures referred to as Youtcy granite (see below) may in fact be the eastward extension of the Wilderness intrusion.

Comments. The area for which we are using the term "Wilderness Granite" contains a subarea (Santa Catalina main range) composed mainly of granitic rock referred under the term "Catalina batholith" by Moore and Tolman (1938, unpub. manuscript). Mylonitic varieties in the Santa Catalina forerange were referred under the term "Catalina gneiss." The contact between the two units was originally mapped by Tolman (1911 and 1912) and has appeared on most subsequent pre-1976 regional maps (beginning with the 1924 Arizona state geologic map by Darton and others) as a west-northwest–trending, solid-line contact. Interestingly, the map contained in the 1949 open-file report by Moore and others carries the notation "scratch contact" for the west-northwest–trending contact. The text contains the admonition, "it should be noted that in general there is no distinct boundary between the two kinds of rocks" (p. 12). Moore and others (1949) included all exposures in the Santa Catalina main range and forerange under the umbrella term "Santa Catalina granitic complex," which consisted of three subdivisions: (1) a gneissic variety in the forerange south of the west-northwest–trending contact which contained a leucocratic, medium- to coarse-grained rock resembling a sheared granite (mostly our deformed Wilderness granite), and a porphyritic, mesocratic, coarse-grained rock resembling a sheared granite (mostly the deformed Oracle Granite of Creasey and others, 1977; Banks, 1976 and this volume; this paper); (2) a granitic gneiss in the Santa Catalina main range (equivalent to mylonitic Wilderness granite); and (3) a muscovite granite in the Santa Catalina main range (equivalent to nonmylonitic, undeformed Wilderness granite). Peirce (1958) mapped the granitic gneisses of the main range near Mount Lemmon as unnamed remobilized Precambrian granite. DuBois (1959a, 1959b) included all gneissic varieties of the Santa Catalina main range and forerange under the term "Catalina gneiss." This usage was adopted by Pilkington (1962), McCullough (1963), Mayo (1964), Hanson (1966), Pashley (1966), Peterson (1968), Waag (1968), Matter (1969), Sherwonit (1974), and Shakel (1972, 1974). As did Bromfield (1952), these workers informally recognized textural differences between the forerange gneisses and main range gneisses by informal terms such as forerange banded gneiss and main range granitic gneiss. Some of the larger leucocratic layers of the forerange gneisses were given various names by Peterson (1958) and Shakel (1974). All of the above workers believed that the gneisses were derived metamorphically from a sedimentary protolith generally thought to be older Precambrian in age.

"Catalina gneiss" nomenclature as originally envisioned by DuBois (1959a, 1959b) reached its maximum usage on the 1:1,000,000 "Arizona Highway Geologic Map" compiled by Cooley (1967). On this map all gneissic rocks in the Santa Catalina main range and forerange are designated "TKm," which is captioned "mainly schist and gneiss, including the Catalina Gneiss." This map does not show the Tolman contact discussed above. The "TKm" unit of Cooley (1967) includes *all* of the following units shown in Figure 3 of this paper: Leatherwood quartz diorite, Wilderness granite; Wrong Mountain granite, and mylonitic Oracle Granite and Continental Granodiorite.

Comparatively undeformed varieties of muscovite granite in the Santa Catalina main range were renamed "Wilderness granite" for exposures in the Wilderness of Rocks 3 km south of Mount Lemmon by Doug Shakel around 1972 (1975, oral commun.). Name first appeared in print in Budden (1975). Budden's Wilderness granite is co-extensive with the "TKg" unit outlined on the 1969 Arizona state geologic map by Wilson and others. Unit was redesignated "quartz monzonite of Samaniego Ridge" by Creasey and Theodore (1975) and Banks (1976, 1977). These workers dissolved Tolman's long-standing contact and mapped large sill-like apophyses of deformed Samaniego quartz monzonite into the Santa Catalina forerange. Rocks mapped as quartz monzonite of Samaniego Ridge in the Santa Catalina main range and forerange were regarded by Creasey and others (1977) as a metamorphic differentiate of a porphyritic sphene-bearing hornblende-biotite quartz monzonite on Samaniego Ridge in the northwest Santa Catalina Mountains, 5 km northwest of Mount Lemmon (see discussion under Catalina quartz monzonite). The term "Wilderness granite" has been continued by Shakel and others (1977), Shakel (1978), and this paper because of textural and mineralogic differences between rocks on Samaniego Ridge and in the Wilderness of Rocks. Alaskite and pegmatite unit has been informally referred to as "Lemmon Rock intrusive" by Hoelle (1976) and "Lemmon Rock leucogranite" by Shakel (1978). Banks (this volume) has named the area co-extensive with the "Santa Catalina granitic complex" of Moore and others (1949) the "gneiss of Windy Point," which includes all of our Wilderness and Wrong Mountain granite.

Espiritu Canyon granite* (6) and Associated Aplites

Location. East-northeast–elongated pluton exposed on the east end of the Tanque Verde Mountains.

Comments. Named by Thorman and Drewes (1978) for exposures 3 km northeast of Mica Mountain in the

Tanque Verde–Rincon Mountains and assigned a Tertiary age. Southwest one-half of pluton mapped by Drewes (1977) as Wrong Mountain Quartz Monzonite and assigned an older Precambrian age. Thorman and Drewes (1978) view Espiritu Canyon pluton as a Tertiary remobilization of Precambrian Wrong Mountain Quartz Monzonite. Redesignated as quartz monzonite of Samaniego Ridge by Banks (this volume), who shows it to be undeformed and have gradational contacts with gneiss of Windy Point (Wrong Mountain quartz monzonite of Drewes, 1977). In our view, the Espiritu Canyon pluton may be an undeformed variety of Wrong Mountain granite. The two bodies may be part of a single Eocene muscovite granite pluton.

Wrong Mountain granite* (7)

Location. Large sheetlike laccolithic mass widespread throughout the Tanque Verde and Rincon Mountains.

Comments. Named Wrong Mountain Quartz Monzonite by Drewes (1977) for exposures at Wrong Mountain 3 km south of Rincon Peak in the Rincon Mountains and assigned an older Precambrian age. It is a major map unit of Drewes (1974, 1977) and Thorman and Drewes (1978) throughout the Rincon and Tanque Verde Mountains. Considered by Drewes (1977) as the leucocratic component of formational rank in his proposed "Santa Catalina Group" terminology, which is equivalent to Catalina gneiss terminology of DuBois (1959a, 1959b) for the Santa Catalina Mountains. If the Wrong Mountain mass is instead an Eocene pluton as proposed here, the Santa Catalina Group terminology as proposed by Drewes (1977) no longer has any useful meaning and should be discontinued. The entire unit has been included under "gneiss of Windy Point" nomenclature of Banks (this volume).

Youtcy granite* (8)

Location. As provisionally used by us, "Youtcy granite" applies to an igneous body of undetermined shape and size underlying the Youtcy Ranch area in Redington Pass. This body may be an undeformed extension of "Wilderness granite" farther west.

Comments. Name originally given by Tolman and Moore (1938, unpub. manuscript) to nongneissic exposures of muscovite granite around Youtcy Ranch in Redington Pass. Included as nongneissic component of the Santa Catalina granitic complex by Moore and others (1949). Shown on the map in Bromfield (1952) as "Catalina granite." An extension of the Youtcy mass in the Korn Kob mine area north of Redington Pass was mapped as "Catalina granite" by Wilson (1977). Entire area assigned to the Youtcy granite was mapped as quartz monzonite of Samaniego Ridge by Creasey and Theodore (1975) and Creasey and others (1977). Redesignated "quartz monzonite of Youtcy Ranch" by Thorman and Drewes (1978), who showed continuous exposure into but no contact with "quartz monzonite of Samaniego Ridge west and southwest of the Youtcy ranch. Thorman and Drewes (1978) considered the Youtcy pluton to be a remobilized phase of the "quartz monzonite of Samaniego Ridge" (in this area, equivalent to our Wilderness granite).

Middle Tertiary Quartz Monzonite (Catalina) suite

Catalina quartz monzonite* (9)

Location. Large half-circle–shaped exposure in the northwest Santa Catalina Mountains. Large east-northeast–trending elongate mass in the south-central Tortolita Mountains.

Comments. Originally mapped as Oracle Granite of older Precambrian age by Tolman [unpub. 1914 manuscript, cited in 1938 unpub. manuscript by Moore and Tolman (see comments on Oracle Granite)]. Similar treatment and citation is given by Moore and others (1949) and Bromfield (1952). Renamed Samaniego granite by Wallace (1954) on the basis of mineralogic differences of rocks exposed in the vicinity of Samaniego Ridge 5 km northwest of Mount Lemmon from Oracle Granite in the type area. Wallace retained the Precambrian age. Renamed Catalina granite by McCullough (1963), who assigned a post-Paleozoic age to the body based on a rugose coral in a carbonate inclusion. Eastern contact of Catalina quartz monzonite with Oracle Granite was first recognized by Hoelle about 1974 and more precisely located by the mapping of Banks (1976) and Suemnicht (1977). Appeared as Precambrian granite on the Arizona state geologic map by Wilson and others (1969), which used Tolman's mapping. "Catalina granite" nomenclature continued by Shakel and others (1972), Budden (1975), and Hoelle (1976), who all assigned a Late Cretaceous age to the body on the basis of improperly interpreted Rb-Sr isotopic data (see Table 1). Shown as a Laramide intrusion ("Li") on the "Arizona Highway Geologic Map" compiled by Cooley (1967). Renamed quartz monzonite of Samaniego Ridge by Banks (1976). Samaniego term was extended by Creasey and Theodore (1975), Banks (1976), Creasey and others (1977), Banks and others (1978) to include many presumed Phanerozoic plutonic bodies in the Tortolita, Durham-Suizo, southwest Tortilla, and Santa Catalina ranges. "Catalina granite" term was continued for the body in the northwest Santa Catalina Mountains by Suemnicht (1977), Shakel and others (1977), and Shakel (1978). Banks (this volume) has discontinued the Samaniego nomenclature for plutons in the Tortolita Mountains. As used by Banks (this volume), "quartz

monzonite of Samaniego Ridge" is restricted to exposures in northwest Santa Catalina Mountains (equivalent to our Catalina quartz monzonite) and exposures around Youtcy Ranch in Redington Pass and Espiritu Canyon (in our view probable Wilderness and Wrong Mountain equivalents, respectively) northeast of Mica Mountain in the Tanque Verde Mountains. The east-northeast–trending mass in the south-central Tortolita Mountains, which is correlated by us with the Catalina quartz monzonite body in the northwest Santa Catalina Mountains, is designated by Banks (this volume) as "quartz monzonite of Wild Burro Canyon." On the basis of impressively similar texture, modal mineralogy, Rb-Sr trace-element data, and Sr isotopes of Tortolita exposures with the Catalina quartz monzonite in the northwest Santa Catalina Mountains, we believe that the Wild Burro Canyon term seems inappropriate.

Tortolita quartz monzonite* (10)

Location. Large east-northeast–elongated pluton in the southern Tortolita Mountains and large northwest-trending dikes in the western Santa Catalina Mountains.

Comments. Originally named Tortolita granite by Moore and Tolman (1938, unpub. manuscript) for exposures in the southwest Tortolita Mountains. Included by Moore and others (1949) as a pluton member of the "Santa Catalina granitic complex." Mapped by Budden (1975) as Tortolita granodiorite and later as quartz monzonite of the Tortolita Mountains by Banks and others (1976), Creasey and others (1977), and Banks and others (1977). Dike exposures in Santa Catalina Mountains originally mapped as "Cargadero [Cargodera] Canyon granite" by McCullough (1963) and later as quartz monzonite of the Tortolita Mountains by Banks (1976).

Reef of Rock granite* (11)

Location. North-northeast–trending dikelike mass of leucocratic granite along Reef of Rock ridge 2 km north of Mount Lemmon. Scattered dikes of biotite granite which intrude Tortolita quartz monzonite (but not differentiated from Tortolita quartz monzonite during reconnaissance mapping) in the southwest Tortolita Mountains may equate with Reef of Rock granite.

Comments. Exposures at Reef of Rock originally mapped and named "Mount Lemmon granite" by Moore and Tolman (1938, unpub. manuscript), who indicated the body intruded Oracle Granite (Catalina quartz monzonite) and Leatherwood quartz diorite. Included by Moore and others (1949) as a nongneissic granite within the "Santa Catalina granitic complex." Shown as "Catalina granite" on the maps of Bromfield (1952), Peirce (1958), Hanson (1966), and Waag (1968). Shown on the 1924 (Darton and others) and 1969 (Wilson and others) Arizona state maps as "Kg" and "TKg," respectively. Renamed "Reef granite" by Budden (1975). Included within the quartz monzonite of Samaniego Ridge unit of Banks (1976), Creasey and others (1977), and Banks (this volume). Renamed "Reef of Rock granite" by Suemnicht (1977), who showed the rock to be a distinct intrusive phase into Catalina quartz monzonite and Leatherwood quartz diorite.

Happy Valley quartz monzonite (12)

Location. Two stocklike masses within the eastern Rincon Mountains.

Comments. Named "Happy Valley quartz monzonite" by Miles (1965) for exposures near Barney Ranch south of Lechequilla Peak (8 km east of Mica Mountain) in the eastern Rincon Mountains. Exposures near Barney Ranch referred to as granodiorite of Happy Valley by Drewes (1974, 1977), who also mapped a large mass to the south in the Little Rincon Mountains (8 km east of Rincon Peak) under the same name. Northern mass is mineralogically similar to (Table 5) and may belong to the muscovite granite (Wilderness) suite.

REFERENCES CITED

Acker, C. J., 1958, Geologic interpretations of a siliceous breccia in the Colossal Cave area, Pima County, Arizona [M.S. thesis]: Tucson, University of Arizona, 50 p.

Banerjee, A. R., 1975, Structure and petrology of the Oracle Granite, Pinal County, Arizona [Ph.D. dissert.]: Tuscon, University of Arizona, 112 p.

Banks, N. G., 1976, Reconnaissance geologic map of the Mount Lemmon quadrangle, Arizona: U.S. Geological Survey Map MF-747.

——1977, Geologic setting and interpretation of a zone of middle Tertiary igneous-metamorphic complexes in south-central Arizona: U.S. Geological Survey Open-File Report 77-376.

——1980, Geology of a zone of metamorphic core complexes in southeastern Arizona: Geological Society of America Memoir 153 (this volume).

Banks, N. G., and others, 1972, Chronology of intrusion and ore deposition at Ray, Arizona: Part I, K-Ar ages: Economic Geology, v. 67, p. 864–878.

Banks, N. G. and others, 1977, Reconnaissance geologic map of the TortoMountains quadrangle: U.S. Geological Survey Miscellaneous Field Studies Map MF-864.

——1978, Radiometric and chemical data for rocks of the Tortolita Mountains 15′ quadrangle, Pinal County, Arizona: Isochron/West, no. 22, p. 17–21.

Blake, W. P., 1908a, Geological sketch of the region of Tucson, Arizona, *in* MacDougal, D. T., ed., Botanical features of North American deserts: Carnegie Institution of Washington Publication 99, p. 45–68.

——1908b, Note upon the Santa Catalina gneiss, Arizona: Science, n.s., v. 28, p. 379–380.

Braun, E. R., 1969, Geology and ore deposits of the Marble Peak area, Santa Catalina Mountains, Pima County, Arizona [M.S. thesis]: Tucson, University of Arizona, 75 p.

Bromfield, C. S., 1950, Geology of the Maudina Mine area, northern Santa Catalina Mountains, Pinal County, Arizona [M.S. thesis]: Tucson, University of Arizona, 63 p.

——1952, Some geologic features of the Santa Catalina Mountains, *in* Guidebook for field trip excursions in southern Arizona: Arizona Geological Society Digest, v. 5, p. 51–55.

Bryant, D. L., 1968, Diagnostic characteristics of the Paleozoic formations of southeastern Arizona: Arizona Geological Society Guidebook III, p. 33–49.

Budden, R. T., 1975, The Tortolita–Santa Catalina Mountain complex [M.S. thesis]: Tucson, University of Arizona, 133 p.

Catanzaro, E. J., and Kulp, J. L., 1964, Discordant zircons from the Little Belt (Montana), Beartooth (Montana), and Santa Catalina (Arizona) Mountains: Geochimica et Cosmochimica Acta, v. 28, p. 87–124.

Coney, P. J., 1979, Tertiary evolution of Cordilleran metamorphic core complexes, *in* Armentrout, J. W., and others, eds., Cenozoic paleogeography of western United States: Society of Economic Paleontologists and Mineralogists, Pacific Section Symposium III, p. 15–28.

——1980, Cordilleran metamorphic core complexes: An overview: Geological Society of America Memoir 153 (this volume).

Cooley, M. E., 1967, Arizona highway geologic map: Arizona Geological Society, scale 1:1,000,000.

Cooper, J. R., and Silver, L. T., 1964, Geology and ore deposits of the Dragoon quadrangle, Cochise County, Arizona: U.S. Geological Survey Professional Paper 416, 196 p.

Creasey, S. C., 1965, Isotopic age of fresh and altered igneous rocks associated with copper deposits, southeastern Arizona [abs.]: Geological Society of America Special Paper 87, p. 39.

——1967, General geology of the Mammoth quadrangle, Pima County, Arizona: U.S. Geological Survey Bulletin 1218, 94 p.

Creasey, S. C., and Kistler, R. W., 1962, Age of some copper-bearing porphyries and other igneous rocks in southeastern Arizona, *in* Geological Survey research, 1962: U.S. Geological Survey Professional Paper 450-D, p. D1–D5.

Creasey, S. C., and Theodore, T. G., 1975, Preliminary reconnaissance geologic map of the Bellota Ranch quadrangle, Pima County, Arizona: U.S. Geological Survey Open-File Report 75-295.

Creasey, S. C., and others, 1977, Middle Tertiary plutonism in the Santa Catalina and Tortolita Mountains, Arizona: U.S. Geological Survey Journal of Research, v. 5, p. 705–717.

Damon, P. E., 1968, Application of the potassium-argon method to the dating of igneous and metamorphic rocks within the Basin-Ranges of the Southwest: Arizona Geological Society Guidebook III, p. 7–20.

——1970, A theory of "real" K-Ar clocks: Eclogae Geologicae Helvetiae, v. 63, p. 69–76.

Damon, P. E., and Giletti, B. J., 1961, The age of basement rocks of the Colorado Plateau and adjacent areas, *in* Kulp, J. L., ed., Geochronology of rock systems: New York Academy of Science Annals, v. 91, p. 443–453.

Damon, P. E., and Mauger, R. M., 1966, Epeirogeny-orogeny viewed from the Basin and Range Province: Society of Metallogenetic Engineers Transactions, v. 235, p. 99–112.

Damon, P. E., Livingston, D. E., and Erickson, R. C., 1962, New K-Ar dates for the Precambrian of Pinal, Gila, Yavapai and Coconino Counties, Arizona: New Mexico Geological Society, 13th Field Conference Guidebook, p. 56–57.

Damon, P. E., Erickson, R. C., and Livingston, D. E., 1963, K-Ar dating of Basin and Range uplift, Catalina Mountains, Arizona: Nuclear Geophysics, National Academy of Sciences/National Research Council Publication 1075, p. 113–121.

Damon, P. E., and others, 1969, Correlation and chronology of ore deposits and volcanic rocks, *in* Annual progress report no. 1969 C00-689 to U.S. Atomic Energy Commission: Tucson, Geochronology Labs., University of Arizona, 90 p.

——1980, New Rb-Sr and K-Ar data for the Santa Catalina–Rincon–Tortolita metamorphic core complex: Isochron/West (in press).

Darton, N. H., Lausen, C., and Wilson, E. D., 1924, Geologic map of the State of Arizona: Arizona Bureau of Mines and U.S. Geological Survey, scale 1:500,000.

Davis, G. A., and others, 1980, Mylonitization and detachment faulting in the Whipple-Buckskin-Rawhide Mountains terrane, southeast California

and western Arizona: Geological Society of America Memoir 153 (this volume).

Davis, G. H., 1975, Gravity-induced folding off a gneiss dome complex, Rincon Mountains, Arizona: Geological Society of America Bulletin, v. 86, p. 979–990.

——1977a, Characteristics of metamorphic core complexes, southern Arizona: Geological Society of America Abstracts with Programs, v. 9, p. 944.

——1977b, Reply *to* Discussion *on* Gravity-induced folding off a gneiss dome complex, Rincon Mountains, Arizona: Geological Society of America Bulletin, v. 88, p. 1212–1216.

——1978, Third day, road log from Tucson to Colossal Cave and Saguaro National Monument: New Mexico Geological Society, 29th Field Conference Guidebook, p. 77–87.

——1979, Laramide folding and faulting in southeastern Arizona: American Journal of Science, v. 279, p. 543–569.

——1980, Structural characteristics of metamorphic core complexes, southern Arizona: Geological Society of America Memoir 153 (this volume).

Davis, G. H., and Coney, P. J., 1979, Geological development of Cordilleran metamorphic core complexes: Geology, v. 7, p. 120–124.

Davis, G. H., and Frost, E. G., 1976, Internal structure and mechanism of emplacement of a small gravity-glide sheet, Saguaro National Monument (east), Tucson, Arizona: Arizona Geological Society Digest, v. 10, p. 287–304.

Davis, G. H., and others, 1975, Origin of lineation in the Catalina-Rincon-Tortolita gneiss complex, Arizona: Geological Society of America Abstracts with Programs, v. 7, p. 602.

Drewes, H., 1968, New and revised stratigraphic names in the Santa Rita Mountains of southeastern Arizona: U.S. Geological Survey Bulletin 1274-C, p. 1–15.

——1974, Geologic map and sections of the Happy Valley quadrangle, Cochise County, Arizona: U.S. Geological Survey Map I-832, scale 1:48,000.

——1976a, Laramide tectonics from Paradise to Hells Gate, southeastern Arizona: Arizona Geological Society Digest, v. 10, p. 151–167.

——1976b, Plutonic rocks of the Santa Rita Mountains, southeast of Tucson, Arizona: U.S. Geological Survey Professional Paper 915, 76 p.

——1977, Geologic map and sections of the Rincon Valley quadrangle, Pima County, Arizona: U.S. Geological Survey Map I-998, scale 1:48,000.

Drewes, H., and Thorman, C. H., 1978, New evidence for multiphase development of the Rincon metamorphic core complex east of Tucson, Arizona: Geological Society of America Abstracts with Programs, v. 10, p. 103.

DuBois, R. L., 1959a, Geology of the Santa Catalina Mountains: Arizona Geological Society Guidebook II, p. 106–116.

——1959b, Petrography and structure of a part of the gneissic complex of the Santa Catalina Mountains: Arizona Geological Society Guidebook II, p. 117–127.

Eberly, L. D., and Stanley, T. B., 1978, Cenozoic stratigraphy and geologic history of southwestern Arizona: Geological Society of America Bulletin, v. 89, p. 921–940.

Erickson, R. C., 1962, Petrology and structure of an exposure of the Pinal Schist, Santa Catalina Mountains, Arizona [M.S. thesis]: Tucson, University of Arizona, 71 p.

Frost, E. G., 1977, Mid-Tertiary, gravity-induced deformation in Happy Valley, Pima and Cochise Counties, Arizona [M.S. thesis]: Tucson, University of Arizona, 86 p.

Giletti, B. J., and Damon, P. E., 1961, Rubidium-strontium ages of some basement rocks from Arizona and northwestern Mexico: Geological Society of America Bulletin, v. 72, p. 639–644.

Hanson, H. S., 1966, Petrography and structure of the Leatherwood quartz diorite, Santa Catalina Mountains, Pima County, Arizona [Ph.D. dissert.]: Tucson, University of Arizona, 104 p.

Hayes, P. T., 1970, Cretaceous paleogeography of southeastern Arizona and adjacent areas: U.S. Geological Survey Professional Paper 658-B, 42 p.

Hayes, P. T., and Drewes, H., 1968, Mesozoic sedimentary and volcanic rocks of southeastern Arizona, *in* Titley, S. R., ed., Southern Arizona guidebook III: Tucson, Arizona Geological Society, p. 49–58.

——1978, Mesozoic depositional history of southeastern Arizona: New Mexico Geological Society, 29th Field Conference Guidebook, p. 201–208.

Hernon, R. M., 1932, Pegmatite rocks of the Catalina-Rincon Mountains, Arizona [M.S. thesis]: Tucson, University of Arizona, 65 p.

Higgins, M. E., 1971, Cataclastic rocks: U.S. Geological Survey Professional Paper 687, 97 p.

Hoelle, J. L., 1976, Structural and geochemical analysis of the Catalina granite, Santa Catalina Mountains, Arizona [M.S. thesis]: Tucson, University of Arizona, 79 p.

Johnson, J. P., 1972, K-Ar dates on intrusive rocks and alteration associated with the Lakeshore porphyry copper deposit, Pinal County, Arizona: Isochron/West, no. 4, p. 29–30.

Keith, S. B., 1978, Paleosubduction geometries inferred from Cretaceous and Tertiary magmatic patterns in southwestern North America: Geology, v. 6, p. 515–521.

Livingston, D. E., 1969, Geochronology of older Precambrian rocks in Gila County, Arizona [Ph.D. dissert.]: Tucson, University of Arizona, 224 p.

Livingston, D.E., and Damon, P. E., 1968, The ages of

stratified Precambrian rock sequences in central Arizona and northern Sonora: Canadian Journal of Earth Sciences, v. 5, p. 763–772.

Livingston, D. E., and others, 1967, Argon 40 in cogenetic feldspar-mica mineral assemblages: Journal of Geophysical Research, v. 72, p. 1362–1375.

Marvin, R. F., and Cole, J. L., 1978, Radiometric ages: Compilation A, U.S. Geological Survey: Isochron/West, no. 22, p. 3–14.

Marvin, R. F., and others, 1973, Radiometric ages of igneous rocks from Pima, Santa Cruz, and Cochise Counties, southeastern Arizona: U.S. Geological Survey Bulletin 1379, 27 p.

Marvin, R. F., Naeser, C. W., and Mehnert, H. H., 1978, Tabulation of radiometric ages—including unpublished K-Ar and fission track ages—for rocks in southeastern Arizona and southwestern New Mexico: New Mexico Geological Society, 29th Field Conference Guidebook, p. 243–257.

Matter, P., 1969, Petrochemical variations across some Arizona pegmatites and their enclosing rocks [Ph.D. dissert.]: Tucson, University of Arizona, 173 p.

Mauger, R. L., Damon, P. E., and Livingston, D. E., 1968, Cenozoic argon ages on metamorphic rocks from the Basin and Range Province: American Journal of Science, v. 266, p. 579–589.

Mayo, E. B., 1964, Folds in gneiss beyond North Campbell Avenue, Tucson, Arizona: Arizona Geological Society Digest, v. 7, p. 123–145.

McCullough, E. J., Jr., 1963, A structural study of the Pusch Ridge–Romero Canyon area, Santa Catalina Mountains, Arizona [Ph.D. dissert.]: Tucson, University of Arizona, 67 p.

Miles, C. H., 1965, Metamorphism and hydrothermal alteration in the Lecheguilla Peak area of the Rincon Mountains, Cochise County, Arizona [Ph.D. dissert.]: Tucson, University of Arizona, 98 p.

Moore, B. N., and others, 1949, Geology of the Tucson quadrangle, Arizona: U.S. Geological Survey Open-File Report, 20 p.

Pashley, E. F., 1966, Structure and stratigraphy of the central, northern, and eastern parts of the Tucson Basin, Arizona [Ph.D. dissert.]: Tucson, University of Arizona, 273 p.

Peirce, F. L., 1958, Structure and petrology of part of the Santa Catalina Mountains [Ph.D. dissert.]: Tucson, University of Arizona, 86 p.

Peirce, H. W., 1976, Elements of Paleozoic tectonics in Arizona: Arizona Geological Society Digest, v. 10, p. 37–58.

Peterson, D. W., 1961, AGI data sheet 22: Geotimes, v. 5, no. 6, p. 30–36.

Peterson, N. C., 1938, Geology and ore deposits of the Mammoth mining camp area, Pinal County, Arizona: University of Arizona, Arizona Bureau of Mines Bulletin 144, 63 p.

Peterson, R. C., 1968, A structural study of the east end of the Catalina Forerange, Pima County, Arizona [Ph.D. dissert.]: Tucson, University of Arizona, 105 p.

Pilkington, H. D., 1962, Structure and petrology of a part of the east flank of the Santa Catalina Mountains, Pima County, Arizona [Ph.D. dissert.]: Tucson, University of Arizona, 120 p.

Ransome, F. L., 1903, Geology and ore deposits of the Globe-Miami district, Arizona: U.S. Geological Survey Professional Paper 342, 151 p.

——1916, Some Paleozoic sections of Arizona and their correlation: U.S. Geological Survey Professional Paper 98-K, p. 144–145.

Rehrig, W. A., and Reynolds, S. J., 1980, Geologic and geochronologic reconnaissance of a northwest-trending zone of metamorphic core complexes in southern and western Arizona: Geological Society of America Memoir 153 (this volume).

Reynolds, S. J., and Rehrig, W. A., 1980, Mid-Tertiary plutonism and mylonitization, South Mountains, central Arizona: Geological Society of America Memoir 153 (this volume).

Rose, A. W., and Cook, D. R., 1965, Radioactive age dates of porphyry copper deposits in the western United States [abs.]: Geological Society of America Special Paper 87, p. 139.

Scarborough, R. B., and Peirce, H. W., 1978, Late Cenozoic basins of Arizona: New Mexico Geological Society, 29th Field Conference Guidebook, p. 253–259.

Shafiqullah, M., Damon, P. E., and Peirce, H. W., 1976, Late Cenozoic tectonic development of Arizona Basin and Range Province [abs.]: International Geological Congress, 25th, Sydney, v. 1, p. 99.

Shafiqullah, M., and others, 1978, Mid-Tertiary magmatism in southeastern Arizona: New Mexico Geological Society, 29th Field Conference Guidebook, p. 231–242.

Shakel, D. W., 1972, "Older" Precambrian gneisses in southern Arizona: International Geological Congress, 24th, Montreal, section 1, p. 278–287.

——1974, The geology of layered gneisses in part of the Santa Catalina forerange, Pima County, Arizona [M.S. thesis]: Tucson, University of Arizona, 233 p.

——1978, Supplemental road log number 2: Santa Catalina Mountains via Catalina Highway: New Mexico Geological Society, 29th Field Conference Guidebook, p. 105–111.

Shakel, D. W., Livingston, D. E., and Pushkar, P. D., 1972, Geochronology of crystalline rocks in the Santa Catalina Mountains near Tucson, Arizona: A progress report: Geological Society of America Abstracts with Programs, v. 4, p. 408.

Shakel, D. W., Silver, L. T., and Damon, P. E., 1977, Observations on the history of the gneissic core complex, Santa Catalina Mountains, southern Ari-

zona: Geological Society of America Abstracts with Programs, v. 9, p. 1169–1170.

Sherwonit, W. E., 1974, A petrographic study of the Catalina gneiss in the forerange of the Santa Catalina Mountains [M.S. thesis]: Tucson, University of Arizona, 165 p.

Shride, A. F., 1967, Younger Precambrian geology in southern Arizona: U.S. Geological Survey Professional Paper 566, 89 p.

Silver, L. T., 1955, The structure and petrology of the Johnny Lyon Hills area, Cochise County, Arizona [Ph.D. dissert.]: Pasadena, California Institute of Technology, 407 p.

——1968, Precambrian batholiths of Arizona [abs.]: Geological Society of America Special Paper 121, p. 558–559.

——1978, Precambrian formations and Precambrian history in Cochise County, southeastern Arizona: New Mexico Geological Society, 29th Field Conference Guidebook, p. 157–164.

Silver, L. T., and Deutsch, S., 1963, Uranium-lead isotopic variations in zircons: A case study: Journal of Geology, v. 71, p. 721–758.

Streckeisen, A., 1976, To each plutonic rock its proper name: Earth-Science Reviews, v. 12, p. 1–33.

Suemnicht, G. A., 1977, The geology of the Cãnada del Oro headwaters, Santa Catalina Mountains, Arizona [M.S. thesis]: Tucson, University of Arizona, 108 p.

Thorman, C. H., 1977, Discussion *on* Gravity induced folding off a gneiss dome complex, Rincon Mountains, Arizona: Geological Society of America Bulletin, v. 88, p. 1211–1212.

Thorman, C. H., and Drewes, H., 1978, Mineral resources of the Rincon Wilderness study area, Pima County, Arizona: U.S. Geological Survey Open-File Report 78-596, 58 p.

Titley, S. R., 1976, Evidence for a Mesozoic linear tectonic pattern in southeastern Arizona: Arizona Geological Society Digest, v. 10, p. 71–102.

Waag, C. J., 1968, Structural geology of the Mount Bigelow–Bear Wallow–Mount Lemmon area, Santa Catalina Mountains, Arizona [Ph.D. dissert.]: Tucson, University of Arizona, 133 p.

Wallace, R. M., 1954, Structures of the northern end of the Santa Catalina Mountains, Arizona [Ph.D. dissert.]: Tucson, University of Arizona, 45 p.

Wilson, E. D., Moore, R. T., and Cooper, J. R., 1969, Geologic map of Arizona: Arizona Bureau of Mines and U.S. Geological Survey, scale 1:500,000.

Wilson, J. R., 1977, Geology, alteration, and mineralization of the Korn Kob Mine area, Pima County, Arizona [M.S. thesis]: Tucson, University of Arizona, 103 p.

Wood, M. M., 1963, Metamorphic effects of the Leatherwood quartz diorite, Santa Catalina Mountains, Pima County, Arizona [M.S. thesis]: Tucson, University of Arizona, 68 p.

MANUSCRIPT RECEIVED BY THE SOCIETY JUNE 21, 1979

MANUSCRIPT ACCEPTED AUGUST 7, 1979

[Section 7]

Santa Catalina Mountains
Lithology and Geochemistry

Schist control sample (Figure 5-20). Indeed uranium contents of "modified" schist samples show little departure from uranium values typical of Pinal Schist phyllite lithologies throughout southeast Arizona (Figure 5-22). For these samples, we conclude that contents of uranium, thorium, and chromium, were unchanged during metamorphisms.

Santa Catalina Traverse

Geologic Setting

One of the best examples of core-complex plutonic, metamorphic and mylonitic phenomena is spectacularly exposed in the Santa Catalina Mountains of southeast Arizona. Numerous workers have studied various aspects of the geology of the mountain range (see summaries and references in Keith and others, 1980; Davis, 1980; Banks, 1980; Shakel, 1978; Creasey and others, 1977). The following discussion of the geology of the range is based on the synthesis and interpretation of Keith and others (1980).

The plutonic geology of much of the Santa Catalina Mountains (see also Appendix D) can be viewed in terms of a stacked sill complex that consists of five major lithologic pseudo-stratigraphic assemblages which have gently inclined tabular forms and boundaries, (see Figure 5-23). The five assemblages are described below from structurally lowest to highest levels.

Seven Falls Foliated Biotite Granite. A leucocratic foliated biotite granite named the Seven Falls Gneiss by Petersen (1968) is exposed at the lowest structural level of the Wilderness stacked sill complex. We hereafter refer to this unit as the Seven Falls foliated granite. Chemical analyses and modal data for the Seven Falls foliated granite are presented in Tables 5-4 and 5-5 respectively.

Forerange banded gneiss complex. A banded gneiss complex overlies the Seven Falls foliated granite throughout the Santa Catalina forerange. This gneiss complex consists of alternating light-and dark-colored lithologies which are interlayered on a wide variety of scales. The dark components are rich in biotite (20%) and are predominantly composed of mylonitically deformed Oracle Granite (1.45 b.y. B.P. emplacement age). Keith and others (1980) have interpreted most of the light-colored components of the gneiss complex as sills of Eocene Wilderness that were injected in lit-par-lit fashion into darker phases of 1.45 b.y. B.P. Oracle Granite. Petrographic data (Sherwonit, 1974; see Table 5-4) indicate that Wilderness equigranular biotite granite sills which are structurally low in the banded gneiss complex are more biotite-rich than those higher in the banded gneiss complex.

TABLE 1

AVERAGE CHEMICAL COMPOSITION OF COMPONENTS

WITHIN THE WILDERNESS GRANITE STACKED SILL COMPLEX

increasing structural level ——————————→

Element[3] or Element Oxide[4]	Seven Falls Foliated granite	n[1]	MAIN RANGE SILL — Lower Portion: Foliated biotite granite	n	MAIN RANGE SILL — Upper Portion: Two-mica granite	n	Lemmon Rock leucogranite	n	Garnet schlieren	n
SiO_2	64.88	1	70.6	1	74.06	13	75.2	2	70.63	1
AL_2O_3	16.6	1	14.5	1	14.67	13	13.1	2	13.5	1
Fe_2O_3	.81	1	1.01[2]	1	.50	10	.29	4	1.51	1
FeO	1.42	1	.68[2]	1	.39	10	.195	4	1.39	1
MgO	.59	1	.32	1	.19	13	.06	2	.17	1
CaO	3.14	1	1.81	1	1.3	13	.44	5	.25	1
Na_2O	5.61	1	3.51	1	3.92	13	4.04	2	2.08	1
K_2O	2.09	1	4.23	1	3.62	13	4.48	5	1.92	1
P_2O_5	.14	1	.10	2	.041	13	.09	2	.03	1
U	.90	1	.90	2	1.37	14	3.5	2	28.5	1
Th	6	1	6.5	2	<4.8[2]	14	<2.5[2]	2	50	1
Sc	4	1	5	2	3.3	14	<5.0	2	9	1
Ti	2200	1	2050	2	770	15	110	4	280	1
Mn	350	1	345	2	470	15	1980	5	34,000	1
Y	10	1	11.5	2	7.6	14	8.5	2	270	1
Ce	76	1	52	2	<37	14	<25	2	53	1
Nb	<4	1	4	2	<8.5	14	<72	2	24	1
Ba	1100	1	2050	2	1375	15	482	2	21	1
Li	27	1	14.5	2	26	14	128	2	32	1
V	35	1	21.5	2	7.	14	2	1	<2	1
Cu	7	1	9	2	15.	15	19.5	2	4	1
Zn	72	1	81.5	2	65.	15	155.	5	260	1
Cr	6	1	6.5	2	7.	14	19.5	2	5	1
Ni	4	1	6	2	<4.5	14	12	2	<4	1
Be	2	1	1	2	2.1	14	7.5	2	2	1
Rb			70	1	121	12	378	7		
Sr	760	1	490	2	320	25	28.3	7	10	1

Notes:
1) n= number of samples
2) Less than sign (<) indicates some samples for the element in question were below the detection limit for that element.
3) Element analytical values are in ppm.
4) Element oxide values are in weight percent.

Pegmatitic Wilderness phases contain muscovite only in the upper two-thirds of the banded gneiss complex and are more biotite-rich in the lower third. We believe the forerange banded gneiss complex extends northward beneath a large higher-level sill of Wilderness granite in the Santa Catalina main range as a large, tabular, highly injected sheet (refer to Figure 5-23).

Main Range Wilderness Granite Sill. A batholithic, laccolithic sill of Eocene wilderness granite overlies the banded gneiss complex. This 2.5 km-thick intrusion exhibits an asymmetrical laccolithic geometry. The Wilderness laccolithic sill is composed of equigranular granite and interlayered pegmatite, aplite, and alaskite. Throughout most of the laccolithic sill, the equigranular granite contains biotite, muscovite, and garnet. However, near the base of the laccolith, the equigranular granite contains biotite and sparse garnet, but no muscovite. We will refer to the gradational zone between the main two-mica phase and the structurally lower, biotite-only phase as the "muscovite-in boundary". Pegmatites, aplite, and alaskite within the Wilderness main range laccolith generally contain muscovite and garnet. Modal analyses and average chemical data for the main range laccolithic sill are presented in Tables 5-4 and 5-5 respectively.

Lemmon Rock Leucogranite. Late-stage pegmatite, aplites, and leucogranites are especially abundant near the top of the main range Wilderness laccolith. In many places, alasko-pegmatitic rocks form a leucogranite "cap" named Lemmon Rock leucogranite by Shakel (1978). This "cap" grades downward into the main range laccolithic sill of equigranular two-mica granite and intrudes upward into the late Cretaceous Leatherwood quartz diorite and younger Precambrian Apache Group. Garnet is locally abundant and in places forms spectacular "railroad track" bands of garnet schlieren. Representative modes and chemical analyses of the Lemmon Rock leucogranite and the lithologically unusual garnet schlieren leucogranite are presented in Tables 5-4 and 5-5 respectively.

Sedimentary "cover" and Leatherwood Quartz Diorite. The uppermost of the five major pseudostratigraphic assemblages is composed of Precambrian Apache Group sedimentary rocks, Precambrian diabase, Paleozoic sedimentary rocks, and sill-like apophyses of Late Cretaceous Leatherwood quartz diorite which

have chiefly intruded between the Apache Group and Paleozoic sedimentary rocks. The sedimentary rocks are highly metamorphosed directly above their contact with the underlying Wilderness granite laccolith and adjacent to the quartz diorite sills; they are less metamorphosed up structural section to the north.

Mylonitic Deformation

Rocks in five major pseudostratigraphic assemblages locally exhibit a gently inclined mylonitic foliation. The banded gneiss complex of the forerange, and the lower half of the Wilderness granite laccolith are generally mylonitic; rocks higher in the mountain range are generally not mylonitic (see Figure 5-23). In the context of this project, James DuBois has examined many thin-sections of mylonitic and undeformed phases of Wilderness granite, (see Appendix E), and has established the following generalized deformation sequence in muscovite-bearing, equigranular phases of the Wilderness pluton:

1) quartz recrystallizes, becoming amoeboid;
2) quartz becomes finer-grained and feldspars become somewhat rounded;
3) quartz forms streaked lenses, and coarse green muscovite begins to break down to fine-grained, white muscovite; fine-grained biotite also develops; feldspars become cracked both parallel to and perpendicular to the foliation with quartz filling the fractures;
4) biotite forms foliated laminae through the rock which are wrapped around feldspar grains; feldspars become more rounded; pressure solution deposits of quartz form adjacent to feldspars, forming small augen; and
5) total rounding of feldspars takes place; biotite becomes very fine-grained and layers of biotite form continuous, millimeter-scale bands through the rock; magnetite and sphene appear intergrown with the biotite; chlorite develops on the biotite.

This general sequence mainly applies to the muscovite-stable, equigranular phases of Wilderness granite above the "muscovite-in" boundary in Figure 5-23.

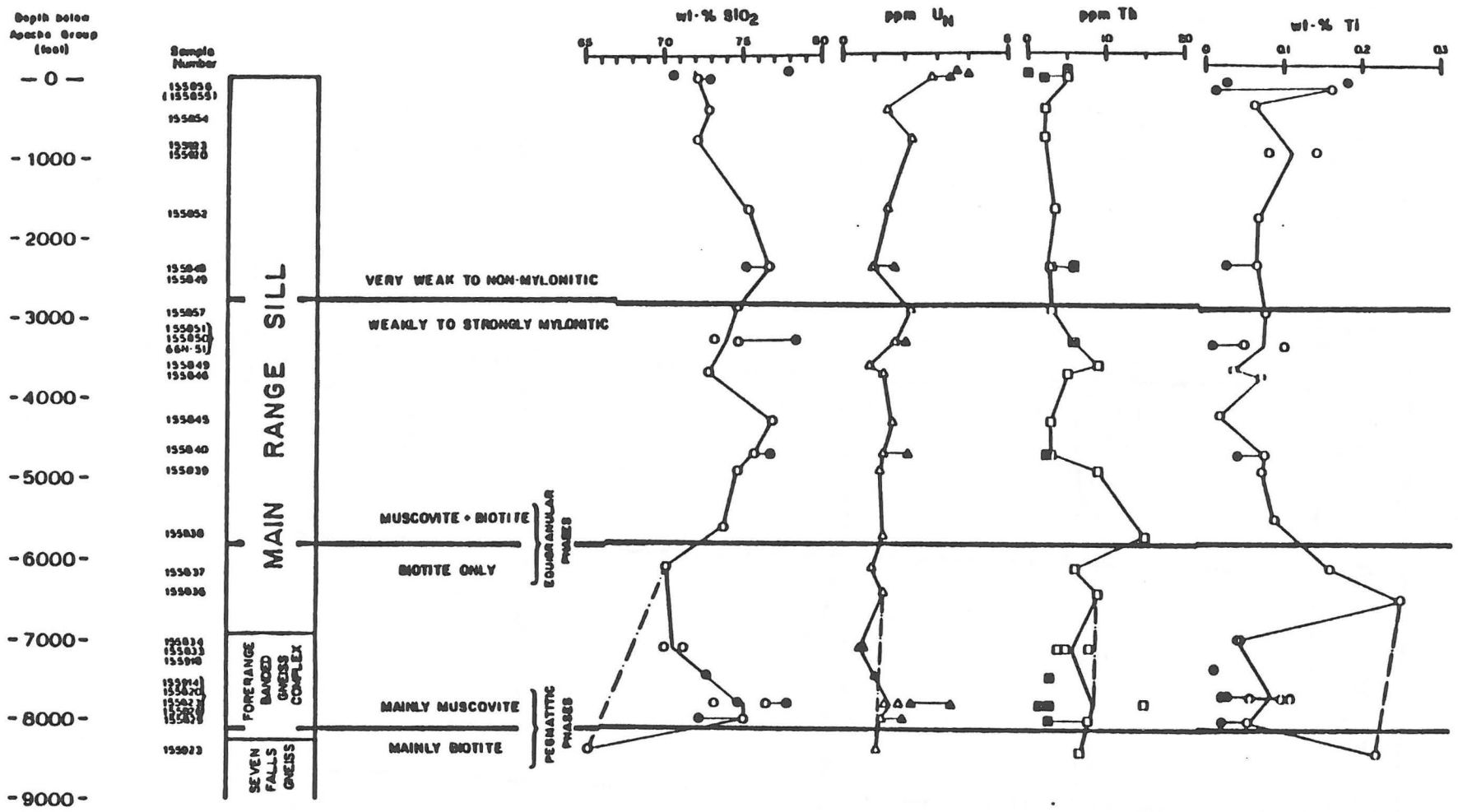

Figure 5-24. Selected major element oxides and trace elements plotted as a function of structural position in the Wilderness granite stacked sill complex, Santa Catalina Mountains, Arizona. Lower horizontal line represents the transition between muscovite- and biotite-bearing pegmatitic phases. Middle horizontal line represents the transition between biotite-bearing and muscovite-biotite-bearing equigranular phases. Upper horizontal line represents the transition between mylonitic and nonmylonitic structural levels of the complex. Equigranular phases are depicted by open symbols and pegmatitic phases are depicted by shaded symbols. Thin horizontal lines connect data points of equigranular and pegmatitic phases that were collected at the same locality.

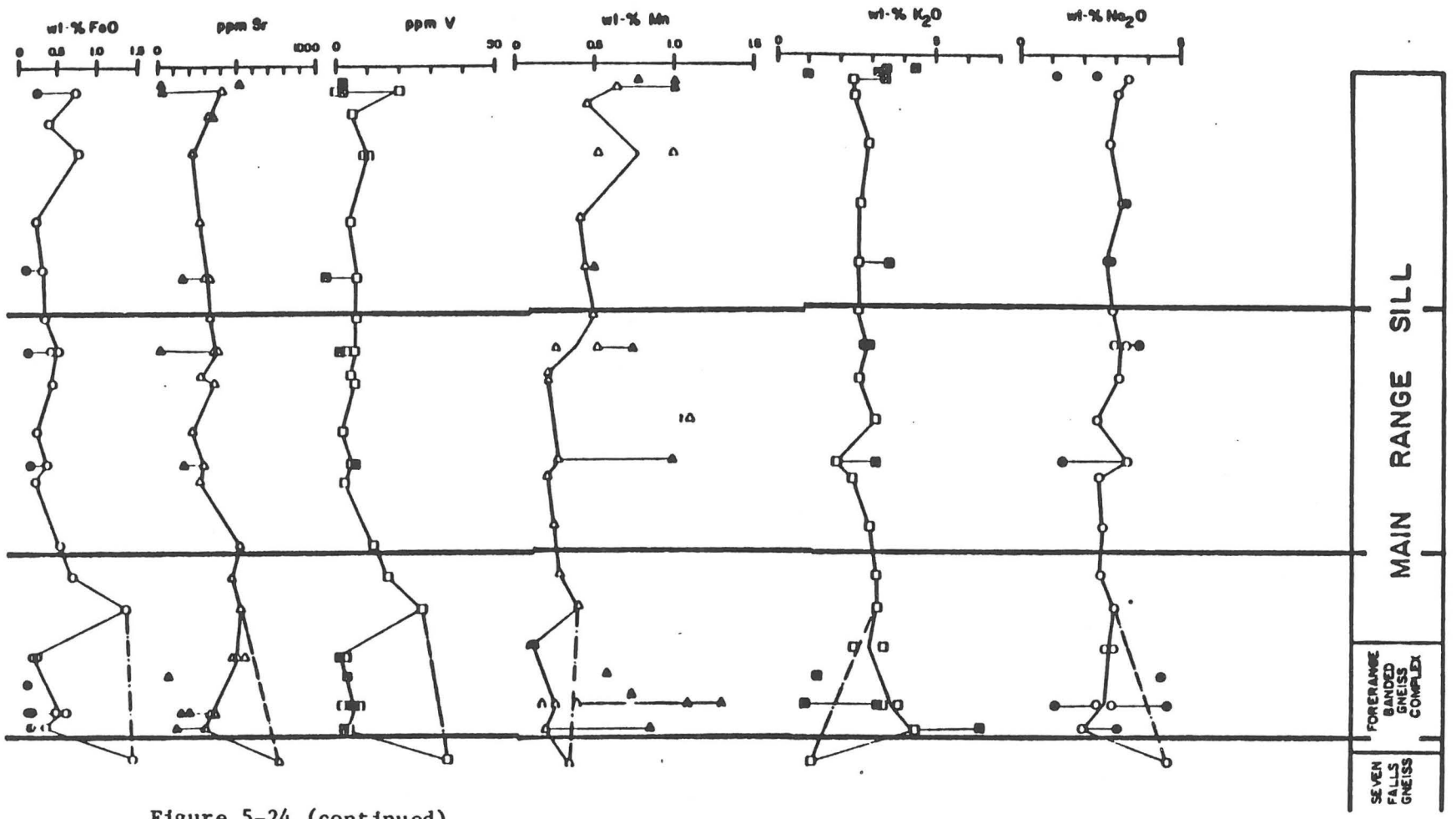

Figure 5-24 (continued)

Mylonitically deformed Oracle Granite in the Santa Catalina forerange banded gneiss complex comprises the distinctive mesocratic augen gneisses (informally referred to as 'dark bands'). Where the coarse-grained augen gneiss is concordantly interlayered with the Wilderness leucocratic component, contacts are commonly marked by a zone of mylonite schist. Some of the leucocratic sills or light bands are completely encased in a sheath of mylonitic schist. Zones of mylonitic schist may vary from one to several meters in thickness; away from the contact, they progressively grade into coarse-grained augen gneiss. In thicker exposures of augen gneiss, there are comparatively non-rounded, rectangular 'box car' crystals of potassium feldspar; these are typical of undeformed Oracle Granite. Biotite is the only mica present in the dark component of the forerange banded gneiss. However, muscovite becomes common and locally is the dominant mica in areas of mylonitic Oracle Granite that are intruded by equigranular muscovite-bearing Wilderness phases. K-feldspar augen in the deformed Oracle Granite are enveloped by a fine-grained matrix of feldspar and quartz. Foliation surfaces are undulatory and contain alligned aggregates of biotite and recrystallized quartz. Elongate aggregates of quartz with sutured boundaries or with ribbon textures are common within the plane of foliation and are expressed as a rod-like lineation which resembles "hot" slickensides.

Geochemistry

Our detailed sampling in the Santa Catalina Mountains was designed to evaluate several unresolved geochemical questions. In the forerange banded gneiss complex, we were interested in how the geochemistry of the Oracle Granite was affected by mylonitization and/or lit-par-lit intrusion of Wilderness Granite sills. Our sampling within phases of the Wilderness Granite was meant to evaluate the geochemical effects of three processes: 1) magmatic differentiation; 2) partitioning of elements between co-existing equigranular granite and late stage, water-rich, pegmatitic phases; and 3) mylonitization. We also collected samples of metasedimentary rocks (see Appendix E) near the top of the Wilderness laccolith to examine how (or if) they were geochemically modified by the adjacent intrusion.

On Figure 5-24, selected geochemical data are plotted as a function of structural position in the Wilderness Granite stacked sill complex. Sample localities are shown in Figure 5-23. The data indicate that distinct geochemical changes occur vertically in the pluton. Rocks in lower structural levels have low contents of SiO_2, K_2O, and MnO, and high contents of CaO, FeO, Fe_2O_3, V, TiO_2, and Sr relative to rocks in upper structural levels. Intriguingly, variation patterns of Na_2O and K_2O are virtually mirror

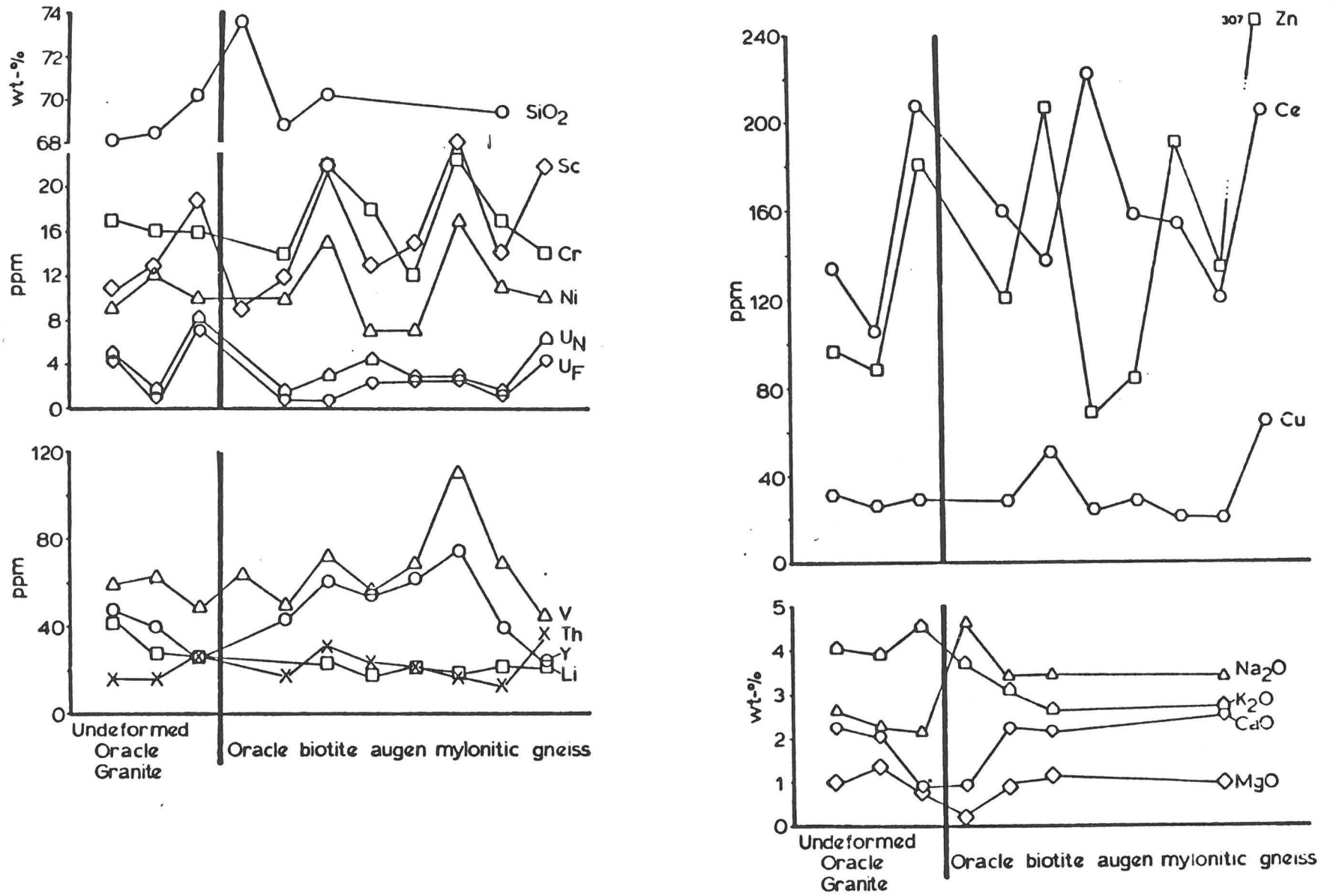

Figure 5-25. Gains and losses for selected major element oxides and trace elements for undeformed (nonmylonitic) samples of Oracle Granite versus mylonitic counterparts in the Santa Catalina forerange, Arizona

images of one another; that is, parts of the pluton which are relatively sodium-rich are potassium-poor, and vice-versa. Uranium contents show a tendency to increase upwards towards the top of the pluton. These variation patterns are interpreted by us to reflect progressive differentiation of the Wilderness intrusion.

Comparison of analyses of co-existing equigranular granite and coarse-grained pegmatites indicate how different elements were partitioned between the magma (which ultimately crystallized to form equigranular granite) and its water-saturated phases (which solidified into aplite and pegmatite). Pegmatic phases at any given structural level in the Wilderness pluton are consistently enriched in Mn and Nb, and depleted in Si and K as compared to co-existing equigranular counterparts. Conversely, equigranular phases are consistently enriched in Ti, V, Li, Ba, Sr, Mg, Ca, Ce, Zn, and Fe relative to cospatial pegmatites. Sodium contents reveal no systematic partitioning between equigranular and pegmatitic phases. Uranium is strongly enriched in the pegmatites relative to equigranular phases; this affirms uranium's affinity for hydrous fluids. In contrast, thorium is relatively enriched in the equigranular phases.

Geochemistry of rocks in the forerange banded gneiss complex reflects the combined results of plutonism, metamorphism, contact metasomatism, and mylonitization. In order to evaluate the relative effects of these processes, we have plotted geochemical analyses of light-colored (Wilderness Granite) components of the forerange banded gneiss within the overall differentiation framework of the entire Wilderness stacked sill complex (Figure 5-24). When compared to the overall differentiation trend, Wilderness components of the forerange banded gneiss commonly exhibit a distinct departure. In particular, Wilderness phases of the banded gneiss are strongly depleted in Na, Ti, Zn, V, Sr, Ca, Fe, Mg, and Al relative to the overall differentiation trend. These phases are strongly enriched in SiO_2 and K_2O relative to the predicted differentiation trend. No systematic depletions or enrichments are exhibited by analyses of Cu, Ba, Y, and importantly, U or Th. Dark components of the forerange banded gneiss (mylonitic Oracle Granite) are markedly depleted in K_2O and enriched in Na_2O compared to nonmylonitic control data from outside of the Santa Catalina forerange (See Figure 5-25). In contrast, contents of uranium, thorium and most other elements are similar for samples of

nonmylonitic and mylonitic Oracle Granite; these data indicate that only the alkali elements (Na and K) were sufficiently mobile during mylonitization to undergo detectable geochemical changes (See Figure 5-25).

Mylonitic samples of Wilderness Granite from the main range laccolithic sill are not markedly displaced from the inferred, overall differentiation trend (See Figure 5-24). This documents that mylonitization of the main range Wilderness laccolithic sill did not result in any major geochemical changes.

Geochemical Comparison of Mylonitic Rocks From the Tortolita and Santa Catalina Complexes

It is instructive to compare the geochemical changes that accompanied mylonitization in the Tortolita Mountains against those in the Santa Catalina Mountains. Table 5-6 summarizes the gains and losses undergone by rocks during mylonitization in both mountain ranges. In general, mylonitization was accompanied by gains of SiO_2 and losses of Li, Fe, P_2O_5, V, Mn, and possibly Ti. Contents of U, Th, Rb, Ba, Cr, and Y were unchanged by mylonitization. However, the interrelationship between potassium and sodium contents is provocative. In the northeast Tortolita Mountains, loss of potassium in mylonitic Oracle Granite is accompanied by probable potassium gain in the adjacent recrystallized Pinal Schist band. Gain of sodium in the muscovite-bearing, mylonitic Oracle Granite is matched by sodium loss in the adjacent recrystallized Pinal Schist. Similarly, in the Santa Catalina forerange, gains of sodium and losses of potassium in mylonitic Oracle Granite are complemented respectively by sodium loss and potassium gain in the leucocratic injection sheets of Wilderness Granite.

Conclusions and Speculations

Based on detailed sampling of mylonitic and metamorphic rocks in the Tortolita and Santa Catalina complexes, we offer some general conclusions regarding how mylonitization and metamorphism has affected protolith geochemistry. Geochemical data from both complexes suggests that <u>intense</u> mylonitization of various interlayered lithologies was accompanied by the addition of silica. This may indicate that mylonitization occurred in the presence of a silica-rich fluid. Mylonitization evidently resulted in depletion of Fe, Ti, P_2O_5, V, and Mn. Perhaps the silica rich fluid scavanged the deforming rock for these elements. The data may indicate that Na and K were exchanged between adjacent lithologies during

TABLE 5-6:

COMPARISON OF GAINS AND LOSSES IN MYLONITIC ROCKS

FROM THE SANTA CATALINA AND TORTOLITA COMPLEXES

	TORTOLITA COMPLEX			SANTA CATALINA COMPLEX		
Element or Element Oxide	Recrystallized Pinal Schist	Chloritic Mylonitic Oracle Granite	Muscovitic Mylonitic Oracle Granite	Mylonitic Oracle Granite Forerange	Mylonitic Wilderness Granite Forerange	Mylonitic Wilderness Granite Mainrange
SiO_2	+++[1]	+++[1]	+++[1]	+?[1]	+++[1]	0[1]
FeO	-	-	---		---	0
MgO	--	0	—	0	---	0
CaO	0	--	---	0	--	0
Na_2O	—	0	++	++	--	0
K_2O	+?	0	—	--	++	0
P_2O_5	---	---	---	0	---	0
Mn	---		--	0	-	0
Ti	—?		---	+?	---	0
U	0		0	0	0	0
Th	0		0	0	0	0
Y	0		--	0?	0	0
Ce	0		---	0	--	0
Ba	0		++	0	0	0
Li	--		---	0	--	0
V	--		---	0?	---	0
Cu	—?		—?	0	0	0
Zn	—		—	0	—	0
Cr	0		-	0	++	0
Ni	-		--	0	0	0
Rb	0	0	0	0	0	0
Sr	0	0	+++	0	—	0

Note: [1] Symbols in column are defined as follows: +++ = large gain; ++ = gain; + = slight gain; 0 = no change; - = slight loss; -- = loss; and --- = large loss.

intense mylonitization.

In contrast, areas where a single rock type experienced only moderate to weak mylonitization, the data reveal no systematic geochemical changes due to mylonitization. Thus, in these areas (such as the main range sill of Wilderness Granite in the Santa Catalina main-range), mylonitization was fundamentally isochemical. Local ultramylonite bands in the Wilderness pluton, however, contain numerous prominant bands of ribbon quartz. Thus, zones of strong mylonitization in homogeneous granitic rocks may have undergone silica addition and iron, phosphorous, vanadium, and manganese depletion. At present, we have no chemical data to confirm this speculation.

In all types, uranium and thorium contents were not affected by mylonitization, possibly because both elements are largely tied up in refractory accessory minerals that resist mylonitization. A partial test of this hypothesis is provided by comparison of fluorometric and neutron-activation uranium analyses for some moderately to highly uraniferous rocks (Table 5-7). The table indicates that uranium values determined by neutron activation are consistently higher than those determined by fluorimetry. This is probably due to the fact that some uranium was not taken into solution during the acid-leach phase of fluorimetry. In effect, fluorimetric analyses may reflect only the loosely held or acid-leachable uranium; it is this uranium that would most likely be redistributed by mylonitization. Uranium which is detected by neutron activation but not fluorimetry may largely reside in refractory accessory minerals; this uranium would be relatively immobile during mylonitization. The high ratio of neutron activation/fluorimetric analyses for many of the Tortolita and Santa Catalina samples may indicate that most uranium is indeed tied up in refractory accessory minerals. Therefore, mylonitization in the Santa Catalina and Tortolita complexes had little effect on uranium contents. However, for increased credibility, this preliminary conclusion must await testing by detailed sampling of mylonitic and nonmylonitic phases of highly uraniferous protoliths.

TABLE 5-7:

COMPARISON OF URANIUM CONTENTS IN SELECTED ROCK TYPES FROM THE SANTA CATALINA AND TORTOLITA COMPLEXES BY ANALYTICAL METHOD

Rock Type	Sample Number	Uranium By Neutron Activation (ppm)	Uranium By Fluorometric (ppm)
Eocene-Oligocene alkali-calcic suite			
Catalina quartz monzonite	155882	1.7	1.1
Tortolita quartz monzonite	155887	2.1	0.76
Tortolita quartz monzonite	155885	2.7	0.86
Aplite in Tortolita quartz monzonite	155886	6.7	3.5
Reef Granite	155857	33.1	0.33
Reef Granite	155858	11.7	0.25
Mid-Cretaceous to mid-Eocene peraluminous 2-mica suite			
Derrio Ganyon granite	155912	1.1	0.46
Derrio Canyon granite	155877	0.8	0.25
Wilderness granite sill complex			
Seven Falls granitic gneiss	155923	0.9	0.5
Biotite granite (lower main-range sill)	155836	1.1	0.45
2-mica granite (upper main-range sill)	155840	1.05	0.25
Lemmon Rock leucogranite	155865	3.60	2.19
Garnet schlieren in Lemmon Rock leucogranite	155868	28.50	0.64
Mid-Cretaceous to late Cretaceous calc-alkalic suite			
Leatherwood quartz diorite	155864	4.2	0.87
Leatherwood quartz diorite	155869	5.0	1.7
Chirreon Wash granodiorite	155864	3.6	2.3
Chirreon Wash granodiorite	155873	4.2	2.4
Chirreon Wash granodiorite (mylonitic)	155896	3.5	1.8
1400 m.y. granitoids			
Oracle Granite	155844	4.9	4.4
Oracle Granite (mylonitic)	155892	4.8	2.42
Oracle Granite (mylonitic)	155889	4.00	0.91
1700 m.y. Pinal Schist			
Pinal Schist (unmodified)	155902	3.5	1.98
Pinal Schist (modified)	155895	4.00	1.99